

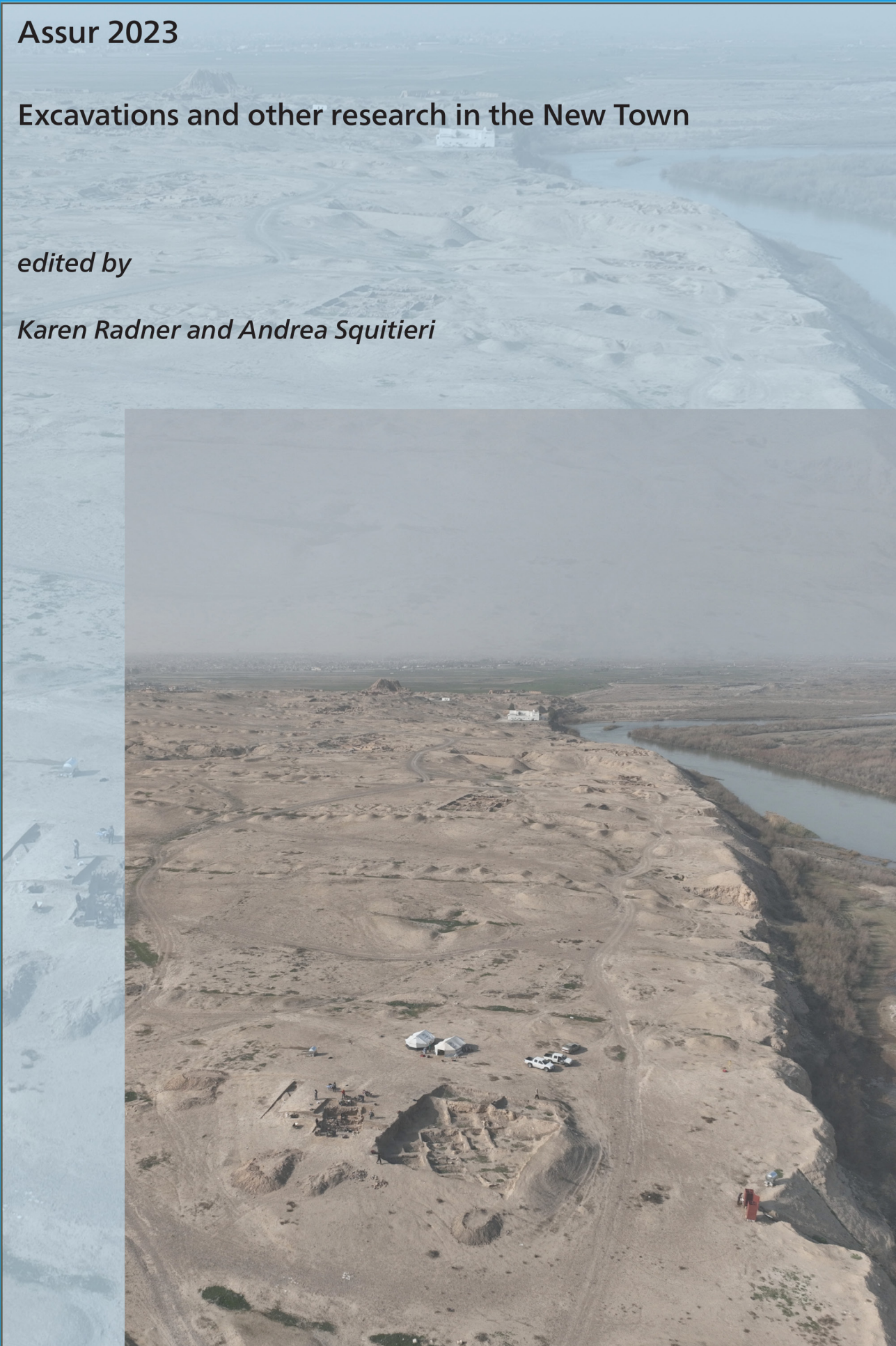
Exploring Assur

Assur 2023

Excavations and other research in the New Town

edited by

Karen Radner and Andrea Squitieri



EXPLORING ASSUR
VOLUME 1

Exploring Assur

edited by

Karen Radner and F. Janoscha Kreppner

Assur 2023
Excavations and other research in the New Town

edited by

Karen Radner and Andrea Squitieri



PEWE-VERLAG
2024

Gedruckt mit Unterstützung der Deutschen Forschungsgemeinschaft (Gottfried Wilhelm Leibniz-Preis 2022)

Die Pdf-Datei darf unter folgender Lizenz verbreitet werden:



Bibliografische Information der Deutschen Nationalbibliothek

Die Deutsche Nationalbibliothek verzeichnet diese Publikation in der Deutschen Nationalbibliografie; detaillierte bibliografische Daten sind im Internet über <http://dnb.dnb.de> abrufbar.

© PeWe-Verlag – Gladbeck 2024

Alle Rechte, insbesondere das Recht der Vervielfältigung und Verbreitung sowie der Übersetzung, vorbehalten. Kein Teil des Werkes darf in irgendeiner Form durch Fotokopie, Mikrofilm usw. ohne schriftliche Genehmigung des Verlages reproduziert oder unter Verwendung elektronischer Systeme verarbeitet, vervielfältigt oder verbreitet werden.

Layout und Prepress: PeWe-Verlag, Gladbeck

Umschlaggestaltung: PeWe-Verlag, Gladbeck

Umschlagabbildung: Dronenfoto der Neustadt von Assur im Februar 2023 (Jens Rohde für das Assur Excavation Project)

Druck und Bindung: Hubert & Co – eine Marke der Esser bookSolutions GmbH

Gedruckt auf alterungsbeständigem Papier

Printed in Germany

ISBN: 978-3-935012-66-9

Table of contents

Preface	11
A. Introduction (<i>Karen Radner</i>)	13
B. The Andrae House, a monument in its own right: a brief history of the building and its use (<i>Karen Radner & Jana Richter</i>)	18
B1. A brief sketch of the Andrae House's fortunes from 1903 to 2023	18
B2. Andrae's original building	28
B3. The Andrae House in the service of local government	55
B4. The Andrae House after the SBAH refurbishment	55
B5. The Andrae House today	58
C. Remote sensing and coring in the New Town of Assur	65
C1. Topographic survey and drone mapping (<i>Jens Rohde & Andrea Squitieri</i>)	65
C2. Geophysical prospecting in Assur, 2023	67
C2.1 Magnetometer prospecting at Assur, 2023 (<i>Jörg Fassbinder, Jean-Jacques Herr, Marco Wolf & Lena Ruider</i>)	67
C2.1.1 The data of the 1989 magnetometer survey at Assur	68
C2.1.2 Resuming magnetometer prospecting at Assur in 2023	68
C2.1.3 First results of the 2023 magnetometer prospecting in the New Town of Assur	70
C2.1.3.1 The urban layout of the New Town of Assur	72
C2.1.3.2 Some glimpses into the architecture of the New Town	74
C2.1.3.3 Thoughts on the pyrotechnological installation	79
C2.1.4 Conclusions	79
C2.2 Electrical Resistivity Tomography (ERT) prospecting in the New Town of Assur, 2023 (<i>Jörg Fassbinder & Marco Wolf</i>) ..	81
C3. Geoarchaeological coring in the New Town of Assur, 2023 (<i>Mark Altaweel</i>)	81
C3.1 The scope of the 2023 work	83
C3.2 The cores and their description	83
C3.3 Discussion and preliminary results	87
C4. Soil and sediment magnetism in Assur, 2023 (<i>Andreas Stele, Sandra Hahn, İnci Nurgül Özdoğru & Jörg Fassbinder</i>)	88
C4.1 Approach and methodological background	88
C4.2 Results and discussion	89
C4.3 Conclusions	92
D. Excavating in the New Town of Assur in 2023	93
D1. The 2023 work plan and its implementation (<i>Karen Radner & Andrea Squitieri</i>)	93
D1.1 A new digital documentation system for Assur	95
D1.2 A sampling strategy for Assur: objectives and methods in 2023	96
D1.2.1 Sampling floors	96
D1.2.2 Sampling human burials	97

D1.3	First radiocarbon dates from the 2023 excavations	98
D2.	Excavating Trench NT1 2023 in the New Town of Assur (<i>F. Janoscha Kreppner, Jens Rohde & Andrea Squitieri</i>)	104
D2.1	The relative stratigraphy	104
D2.2	The trench surface, the topsoil and NT1 2023 Phase 9	105
D2.3	NT1 2023 Phase 8: the chamber tomb (= Grave 1)	105
D2.3.1	The main entrance	109
D2.3.2	The main corridor	110
D2.3.3	The northern chamber	111
D2.3.3.1	The walls and the vault	111
D2.3.3.2	Subdivisions 5 to 8 and the northern corridor	112
D2.3.3.3	The floor deposits	113
D2.3.3.4	The upper deposits	114
D2.3.4	The southern chamber	115
D2.3.4.1	The walls and the vault	115
D2.3.4.2	Subdivisions 1 to 4 and the southern corridor	115
D2.3.4.3	The floor deposits	116
D2.3.4.4	The upper deposits	118
D2.4	NT1 2023 Phase 7	118
D2.5	NT1 2023 Phase 6: Graves 3 and 4	119
D2.5.1	Grave 3	119
D2.5.2	Grave 4	121
D2.6	NT1 2023 Phase 5: Building A	122
D2.6.1	Room 1	122
D2.6.2	Room 2	125
D2.6.3	Room 3	126
D2.7	NT1 2023 Phase 4: Building B	127
D2.7.1	The walls	127
D2.7.2	Unroofed Area 4	127
D2.7.2.1	The floor and its substructure	127
D2.7.2.2	The occupation levels	127
D2.7.2.3	The upper deposits	130
D2.8	NT1 2023 Phase 3: Grave 5	130
D2.9	NT1 2023 Phase 2	132
D2.10	NT1 2023 Phase 1 and the virgin soil	135
D3.	Excavating a sondage linked to the 2002 SBAH trench (<i>Karen Radner, Andrea Squitieri & Jens Rohde</i>)	136
D3.1	“Room 6”	137
D3.2	“Room 5”	138
E.	Pottery from Assur, 2023	140
E1.	From Late Bronze Age to the early Islamic period: the pottery repertoire of the 2023 excavations of Assur (<i>F. Janoscha Kreppner, Jana Richter & Andrea Squitieri</i>)	140
E1.1	Registration and workflow	140
E1.2	Pottery from the Parthian chamber tomb (= Grave 1)	141
E1.3	Pottery from Grave 3	143
E1.4	Pottery from Building A	143
E1.5	Pottery from Building B	145
E1.6	Pottery from Grave 5	147
E1.7	Pottery from the deep sounding below Grave 5	149
E1.8	Pottery from the sondage linked to the 2002 SBAH trench ..	149

E2.	First steps towards a fabric classification for Assur: portable X-ray fluorescence (p-XRF) and petrographic analyses on the 2023 pottery (<i>Michaela Schauer & Silvia Amicone</i>)	150
E2.1	Methodology and dataset	150
E2.2	Results of the p-XRF analysis	153
E2.3	Results of the petrographic analysis	156
E2.4	Discussion	157
F.	Small finds from Assur, 2023 (<i>Andrea Squitieri</i>)	160
F1.	Introduction	160
F2.	Finds from the trench surface and the topsoil	160
F3.	Finds from NT1 2023 Phase 9	161
F4.	Finds from NT1 2023 Phase 8 (chamber tomb = Grave 1)	162
F4.1	Finds from within the chamber tomb's walls	162
F4.2	Finds from the northern chamber and the main corridor	163
F4.3	Finds from the southern chamber	165
F4.4	Finds from the upper deposits	169
F5.	Finds from NT1 2023 Phase 6: Grave 3 and Grave 4	170
F6.	Finds from NT1 2023 Phase 5	172
F6.1	The stamp seal AS 261432:011:028 (<i>Veronica Hinterhuber</i>)	173
F7.	Finds from NT1 2023 Phase 4: Building B	174
F8.	Finds from NT1 2023 Phase 3: Grave 5	178
F9.	Finds from NT1 2023 Phase 2	179
F10.	Finds from NT1 2023 Phase 1	179
F11.	Finds from NT1 2023 arranged by main categories	180
F11.1	Stone tools	180
F11.2	Loom weights	180
F11.3	Personal ornaments	180
F11.4	Figurines	180
F12.	Finds from the sondage linked to the 2002 SBAH trench	180
F12.1	Room 5	180
F12.2	Room 6	182
F13.	Finds from cleaning the 2002 SBAH trench	182
F14.	Surface finds without stratigraphic context	183
G.	Epigraphic finds from Assur, 2023	184
G1.	Cuneiform inscriptions from excavation and surface (<i>Karen Radner</i>)	184
G1.1	Bricks with royal inscriptions unearthed during the 2023 excavations	184
G1.2	Bricks with royal inscriptions found on the surface	187
G1.3	An inscribed stone block from the Aššur temple	192
G1.4	Appendix A: A brick with an incised gaming board	194
G1.5	Appendix B: A brick with an inscription of Aššur-nerari I, now in Munich	194
G1.6	Appendix C: A brick with an inscription of Tukulti-Ninurta from Kar-Tukulti-Ninurta	195
G2.	The Aramaic inscription on the sarcophagus of Grave 3 from Assur (<i>Holger Gzella</i>)	196
G2.1	Script and language	196
G2.2	Text, translation, and notes	198
G2.3	Historical implications	198

H. Plant remains from Assur, 2023	200
H1. Introducing the contexts and periods concerned (<i>Karen Radner & Andrea Squitieri</i>)	200
H2. Wood identification from charcoal remains (<i>Katleen Deckers</i>)	201
H3. Plant identification from light fraction flotation samples (<i>Claudia Sarkady</i>)	202
H3.1 Methodology: collection and preparation of the samples in the lab	202
H3.2 Cereals	203
H3.2.1 Barley (<i>Hordeum vulgare</i>)	203
H3.2.2 Wheat	206
H3.2.2.1 Emmer (<i>Triticum dicoccum</i>)	206
H3.2.2.2 Einkorn (<i>Triticum monococcum</i>)	207
H3.2.2.3 Bread wheat (<i>Triticum aestivum</i>)	207
H3.2.3 Threshing residues (“chaff”)	207
H3.2.4 Indeterminate wheat	207
H3.2.5 Indeterminate cereals	207
H3.3 Cultivated pulses	208
H3.3.1 Lentil (<i>Lens culinaris</i>)	208
H3.3.2 Pea (<i>Pisum sativum</i>)	208
H3.3.3 Indeterminate legumes	208
H3.4 Olive	209
H3.5 Wild plants	209
H3.5.1 Aizoaceae, noon flower family	209
H3.5.2 Amaranthaceae, foxtail family	209
H3.5.3 Asteraceae or Compositae, sunflower family	209
H3.5.4 Boraginaceae, forget-me-not family	209
H3.5.5 Brassicaceae, mustard family	210
H3.5.6 Caryophyllaceae, carnation or pink family	210
H3.5.7 Cistaceae, cistus family	210
H3.5.8 Hyacinthaceae, hyacinth family	211
H3.5.9 Fabaceae, wild legume family	211
H3.5.10 Lamiaceae, labiate family	212
H3.5.11 Malvaceae, mallow family	212
H3.5.12 Papaveraceae, poppy family	213
H3.5.13 Plantaginaceae, plantain family	213
H3.5.14 Poaceae, grass family	213
H3.5.15 Polygonaceae, knotweed family	214
H3.5.16 Rosaceae, rose family	214
H3.5.17 Rubiaceae, bedstraw family	214
H3.5.18 Scrophulariaceae, figwort family	214
H3.5.19 Thymelaeaceae, daphne family	214
H3.5.20 Valerianaceae, valerian family	215
H3.6 Vitaceae, grape family	215
H3.7 Zygophyllaeae, caltrop family	215
H3.8 Indeterminate seeds	215
H3.9 Indeterminate stems	215
H3.10 Indeterminate husk fragments	216
H3.11 Varia	216
H3.12 Preliminary overall assessment	216
H3.13 Evaluation according to stratigraphic contexts (<i>Andrea Squitieri & Karen Radner</i>)	216

I. Calcinated textile fragments from Grave 3: a preliminary report (<i>Annette Paetz gen. Schieck</i>)	220
I.1 Preservation conditions	220
I.2 Textile qualities	221
I.3 First conclusions	223
J. First conclusions (<i>Karen Radner & F. Janoscha Kreppner</i>)	224
Bibliography	229

Preface

Karen Radner

To Grant Frame, in admiration

The 2023 field season at Assur saw the first of a series of excavations in the New Town that my 2022 Gottfried Wilhelm Leibniz Award funds. I am grateful to Laith Majeed Hussein, the chairman of the State Board of Antiquities and Heritage, and SBAH's head of excavations, Ali Obeid Shalgham, for their trust and support, as well as to all the many other SBAH members who enable our work. A special debt of gratitude is reserved for SBAH Salaheddin and its directors, Salim Abdullah Ali and Muthanah Ahmed Issa, as well as Amr Mohammad Jasim, the head of its Sherqat branch, and his colleagues Sakhar Mohammad Ajaj and Omar Laith Allawi. Among the local staff, I want to single out Ahmed Khidr Ahmed, known as "Arabi", who served as the mission's driver and mechanic, Bashir Atiah Khalifa, who not only was the mission's cook but also freely shared his medical expertise as Sherqat's most-sought-after healer, and Mahjub Mohammad Jar, one of the last remaining "Sherqatis" who generously passed on his know how to the novice excavation workmen from Sherqat and Sdera. The success of the 2023 field season owes everything to Salim Abdullah Ali's and his team's determination to protect the site that they so dearly love and to resume its archaeological exploration.

I am deeply indebted to Peter Miglus for his advice and the encouragement with which he accompanied the project's genesis; I would not have embarked on this adventure without his blessings. I benefitted greatly from his and Stefan Maul's generosity as the joint heads of the Nineveh mission of the University of Heidelberg, who not only shared their experiences of working in northern Iraq but also housed me at various times in their excavation house in Mosul before we had a base in Sherqat. My gratitude also belongs to Margarethe van Ess and Simone Mühl of the Orient-Abteilung of the German Archaeological Institute who helped me set up the project and were instrumental in liaising with SBAH, especially in December 2021 when the idea to work in Assur first took shape.

Above all, I am tremendously grateful to F. Janoscha Kreppner who did not hesitate to join me on this ambitious project as the co-director of the Assur Excavation

Project despite his heavy work burden at the University of Münster. My co-editor for this volume, Andrea Squitieri, was as ever his cheerful but merciless self, especially when marshalling the contributors to this inaugural volume of the series *Exploring Assur* and thus enabling us to complete it before the beginning of the second field season on 5 February 2024. I am very happy that after two years with the Heidelberg Nineveh mission, the Leibniz Award allowed me to bring him back to LMU Munich, as well as hire Jana Richter and Jens Rohde for the duration of the DFG funding, which will end in January 2030. They constitute the core team of the Assur Excavation Project.

Most members of the team we assembled have worked together since the early days of the Peshdar Plain Project, which has been exploring the Dinka Settlement Complex in the Autonomous Kurdish Region of Iraq since 2015. My heartfelt thanks go to Mark Altaweel for his willingness to join the team even though the schedule of the British academic year made it very difficult for him. Despite being able to rely on a seasoned team, relocating to central Iraq brought many challenges, not least because of the inclement climatic conditions that led to the decision to work in February and March 2023. While it was still very cold in February, with temperatures frequently below zero during the night, the balmy March weather was occasionally interrupted by very strong storms that drenched the excavation and muddied the Tigris for days, seriously inhibiting both the dig and the floatation work. We were fortunate to have a comfortable home and work environment in the shape of the newly restored Andrae House and take the opportunity to thank Kamal Raheed Raheem who oversaw this huge project. Once having completed the renovations, he kindly agreed to join the mission as head of logistics, and it is impossible to imagine working in Assur without his unfailing support, but especially his good sense and eternal optimism. These are qualities that are badly needed in a place whose recent history is as troubled as that of Sherqat.

As ever, our publisher Peter Werner patiently and meticulously oversaw the production of the volume. I am

pleased to continue the excellent collaboration that we started in 2016 with the publication of the first volume of the series *Peshdar Plain Project Publications*. At LMU Munich, I am grateful to Denise Bolton for proofreading the entire volume at short notice.

Finally, I offer my heartfelt thanks to the institutions that provided the funding for our work: in addition to the German Research Foundation (DFG), which supports the project through the Leibniz Award, funding was made available by the Bavarian Academy of Sciences, the Bavarian State Ministry for Science and Art and the Austrian Embassy in Baghdad as well as LMU Munich through the generous endowment of the Alexander von Humboldt Chair for the Ancient History of the Near and Middle East which I have held since 2015. It was a great honour to present the results of our first season at Assur at the Chai Talk at Al-Mada House in Baghdad (9 June 2023) and a lecture at the Mosul Heritage House in Mosul (11 June 2023), both co-organised by the Goethe Institute Iraq, at the 551. Stiftungsfest of LMU Munich (30 June

2023) and as a Leibniz Lecture organised by the DFG at the DAAD-University of Cambridge Research Hub for German Studies in Cambridge (14 November 2023).

I dedicate this inaugural volume of the series *Exploring Assur* as a small token of my gratitude and respect to my old friend Grant Frame, one of the world's leading experts in the history of the long-lived kingdom of Assyria but also its eventual nemesis, the Neo-Babylonian Empire. We first met in Helsinki in 1997 and have worked closely together since 2007 when he asked me to join the Editorial Board of the series *Royal Inscriptions of the Neo-Assyrian Period* (RINAP). In the past years, we have also co-edited the *Royal Inscriptions of the Neo-Babylonian Empire* (RINBE) series, and with the Leibniz Award funding, we recently embarked on the next legs of completing and updating A. Kirk Grayson's monumental *Royal Inscriptions of Mesopotamia* (RIM) project, with our new publication enterprises *Royal Inscriptions of the Kassites and Kudurrus* (RIKK) and *Royal Inscriptions of Assyria* (RIA). Thank you, Grant, for your friendship, humour and generosity.

A. Introduction

Karen Radner

On 7 April 2022, the Iraqi State Board of Antiquities and Heritage headed by Dr Laith Majeed Hussein granted permission to a research project with the title “Excavations and Geophysical Exploration in Assur as well as Restoration of the Andrae House”, jointly headed by Karen Radner (LMU Munich) and F. Janoscha Kreppner (University of Münster). We are immensely grateful to Dr Laith and SBAH’s head of excavations, Ali Obeid Shalgham, for their trust and support, as well as to all the many other SBAH members who enable our work (**Fig. A1**). Funding for the project is provided by the German Research Foundation (DFG) through a 2022 Gottfried Wilhelm Leibniz Award. According to the agreement with SBAH, the work programme consists of three parts:

1. The restoration of the excavation house originally used by Walter Andrae, severely damaged in late 2016 as the result of ISIS occupation and its capture through Iraqi state forces;

2. the geophysical prospection of Assur employing magnetometer and electrical resistivity tomography (ERT); and
3. archaeological excavations focused on the southern part of the city (“New Town”).

We are grateful for the logistic and legal support of Kamal Rasheed Raheem and Goran Omar Muhammad who travelled from Sulaymaniyah to Baghdad to assist us in the negotiations with SBAH in April 2022. That our old friends Zuhair Rajab Abdullah al-Samarraee and Anmar Abdullilah Fadhil joined us at SBAH to lend support to our application was immensely touching.

After receiving the license, we travelled to Sherqat on 8 April 2022 to meet with the local SBAH representatives, headed by Salim Abdullah Ali (**Fig. A2**). As a first step towards the new collaboration, it was agreed that I would dedicate some funds to the renovation of the SBAH office building outside the ruins of Assur (**SB1**) so that it could

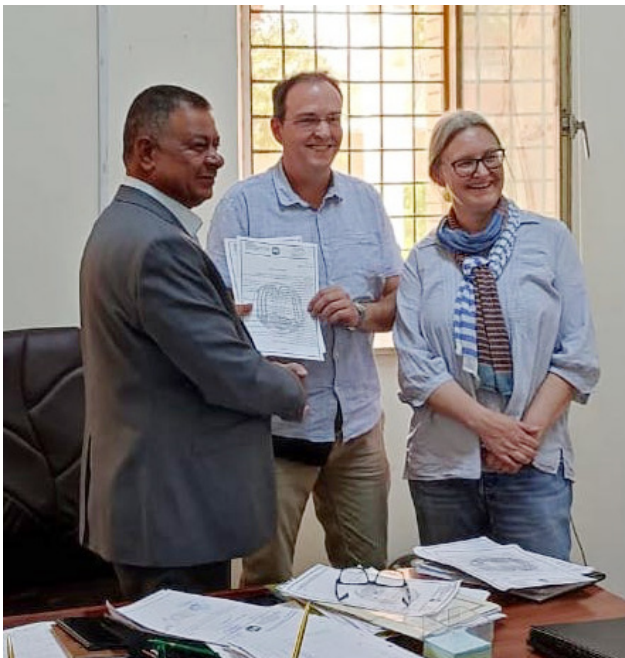


Fig. A1: Ali Obaid Shalgham, the head of the SBAH excavation unit, presents the signed and stamped excavation license to Karen Radner and F. Janoscha Kreppner. Photo by Goran Omar Muhammad (7 April 2022).



Fig. A2: Meeting the SBAH representatives of Salaheddin province and the Sherqat office in the SBAH building at Assur. From left to right, Muthanna Ahmed Issa, F. Janoscha Kreppner, Omar Basharaty, Salim Abdullah Ali, Karen Radner, Sakhar Mohammad Ajaj and Jan Heiler. Photo by Omar Leith Allawi (8 April 2022).

house the team in spring 2023. This work started soon after on 13 April 2023 and was completed by the end of June. In addition to rewiring the building, secure storage facilities were constructed on the roof as well as in the courtyard of the office building, where additional outside sanitary facilities with a shower and a toilet were built. The renovation work was supervised by Kamal Rasheed Raheem and I was able to inspect it personally during a visit on 4 July 2023 while on excavation in Gird-i Rostam (Penjween district, province of Sulaymaniyah, co-directed with Dan Potts of New York University).

Spurred on by the successful realisation of the refurbishment of the SBAH office building, I then decided to change my initial plans concerning the renovation of the ruined excavation house originally occupied by Walter Andrae and his team. Originally, this large-scale enterprise was meant to start during the excavation campaign scheduled for February and March 2023. Now, it was agreed that Kamal Rasheed Raheem would supervise the project which was meant to start as soon as the International Council on Monuments and Sites (ICOMOS) had authorised the renovation plans submitted by SBAH to the UNESCO World Heritage Centre. Authorisation was granted on 12 September 2022, and work began soon after. Akam Omar Ahmed Al-Qaradaghi, head conservator of

the Sulaymaniyah Archaeological Museum, kindly agreed to join the project, having previously overseen the restoration of the Tabira Gate, which ISIS had destroyed, in a project led by Tobin Hartnell of the American University of Sulaymaniyah.

On 5 November 2022, while working at Khorsabad as the epigraphist of the team headed by Pascal Butterlin (Université Paris 1 Panthéon-Sorbonne), I was able to meet with Raheem and Ali to discuss progress. As the renovation work was advancing smoothly, it was decided that rather than the SBAH office building, the Andrae House should accommodate the team in the spring season. This was a key development as it allowed me to substantially increase the size of the team (**Fig. A3**). The building work was completed in January 2023, and the Andrae House was then supplied with basic furnishings, including a generator, kerosene heaters, a full kitchen unit, beds, and some tables and chairs. The furniture and equipment for the workrooms were only procured at the beginning of the spring campaign, while the fitting of purpose-built metal shelves continued until the end of March. The refurbishment of the excavation house was completed with the installation of solar panels on the roof of the south wing and a photovoltaic system housed in the west wing in August 2023 (**SB5**).



Fig. A3: The team on the roof of the southeastern part of the excavation house. Drone photo by Jens Rohde (17 February 2023).

with the associated processing of the pottery and small finds. Ellen Coster, Veronica Hinterhuber, Susanne Weber and Tarik Willis joined the team on 17 February 2023, and later on 9 March 2023, Hero Salih Ahmed from Sulaymaniyah. The field team included 15 workers from Sherqat and Sdera, including Mahjub Mohammad Jar as an expert excavator (“Sherqati”).

The fourth stage lasted from 25 to 30 March 2023, during which time the final documentation was completed, and the handover of the samples and finds selected by SBAH for the Iraq Museum was prepared. The team left Iraq on 31 March 2023.

Joint heads of mission:

- Karen Radner (LMU Munich); 12 February–31 March 2023;
- F. Janoscha Kreppner (University of Münster); 8 February–31 March 2023.

SBAH archaeologists:

- Salim Abdullah Ali (SBAH Salaheddin), as principal representative (**Fig. A5**);
- Amr Mohammad Jasim (SBAH Sherqat), as representative;



Fig. A5: F. Janoscha Kreppner, Kamal Rasheed Raheem, Salim Abdullah Ali, and Karen Radner in front of the map of Assur in the SBAH office building. Photo by Sakhar Mohammad Ajaj.

- Sakhar Mohammad Ajaj (SBAH Sherqat), as representative;
- Muthanna Ahmed Issa (SBAH Salaheddin);
- Omar Laith Allawi (SBAH Sherqat).

Local logistics:

- Kamal Rasheed Raheem (Sulaymaniyah Directorate of Antiquities and Heritage; retired), as head of logistics (**Fig. A5**);
- Ahmed Khidr Ahmed, known as “Arabi” (SBAH Sherqat), as driver;
- Hussein Abdallah (SBAH Sherqat), as house guard;
- Ali Hussein (SBAH Sherqat), as house guard;
- Bashir Atiah Khalifa (SBAH Sherqat), as cook;
- Ali Hussein Abdallah, as assistant cook (8 February–16 March 2023);
- Omar Hussein Abdallah, as assistant cook (17 February–31 March 2023);
- Ali Saad, as janitor.

Archaeological team:

- Mark Altaweel (University College London); 12 February–19 February 2023;
- Ellen Coster (University of Münster); 17 February–31 March 2023;
- Jörg Fassbinder (LMU Munich); 12 February–26 February 2023;
- Christoph Forster (Datalino; www.datalino.de); 12 February–2 March 2023;
- Cajetan Geiger (Bochum University); 8 February–2 March 2023;
- Jan Heiler (Heidelberg University & LMU Munich); 8 February–31 March 2023;
- Jean-Jacques Herr (LMU Munich & Archaios; <https://www.archaios.fr>); 8 February–26 February 2023;
- Veronica Hinterhuber (LMU Munich); 17 February–31 March 2023;
- Akam Omar Ahmed Al-Qaradaghi (seconded from Sulaymaniyah Directorate of Antiquities and Heritage for find restoration); 8 February–31 March 2023;
- Jana Richter (LMU Munich); 8 February–31 March 2023;
- Jens Rohde (University of Münster & LMU Munich); 8 February–31 March 2023;
- Lena Ruider (LMU Munich); 12 February–26 February 2023;
- Hero Salih Ahmed (seconded from Sulaymaniyah Directorate of Antiquities and Heritage for pottery processing); 9 March–31 March 2023;
- Andrea Squitieri (Heidelberg University & LMU Munich); 8 February–31 March 2023;
- Susanne Weber (LMU Münster); 17 February–31 March 2023;

- Tarik Willis (University of Münster); 17 February–31 March 2023;
- Marco Wolf (LMU Munich); 12 February–26 February 2023.

Local excavation staff (Fig. A6):

- Abu Hais Sa'la, as site guard;
- Issa Ibrahim Atiyah, as site guard;
- Mahjub Mohammad Jar, as foreman (“Sherqati”);
- 14 workers from Sherqat and Sdera.

In addition to the many people working on-site in Assur, various researchers and research teams are processing and analysing finds and samples (§D1) collected during this first field season:

- Animal remains: Joris Peters (LMU Munich);
- Human DNA analysis: Johannes Krause, Philipp Stockhammer and the team of the Max-Planck-Institut für evolutionäre Anthropologie, Leipzig;
- Material studies: Silvia Amicone and the Competence Center Archaeometry – Baden Wuerttemberg (University of Tübingen): §E2;
- Palaeobotanical analysis: Claudia Sarkady and the Archäobotanisches Labor Eggstädt: §H3;
- Physical anthropology: Rafał Fetner (University of Warsaw);
- Radiocarbon dating: Curt-Engelhorn-Zentrum Archäometrie, Reiss-Engelhorn-Museen, Mannheim: §D1.3;

- Sedimentology: Eileen Eckmeier (University of Kiel) and Andreas Stele (Bayerisches Landesamt für Denkmalpflege): §C4;
- Textile analysis: Annette Paetz gen. Schieck and the Deutsches Textilmuseum Krefeld: §I;
- Wood analysis from charcoals: Katleen Deckers (University of Tübingen, within the context of the ERC project “Climate, Landscape, Settlement and Society: Exploring Human-Environment Interaction in the Ancient Near East” (CLaSS) led by Dan Lawrence (Durham University): §H2;
- XRF analysis: Michaela Schauer (LMU Munich): §E2.

We are very lucky that some of them have been able to produce reports of their work already for this first publication of the Assur Excavation Project, in addition to the reports on the mapping campaign (§C1), the geophysical prospection (§C2), the coring work (§C3) and the excavation (§D), as well as first assessments of the pottery (§E1), the small finds (§F) and the epigraphic finds (cuneiform: §G1; alphabetic: §G2, by Holger Gzella). We are extremely grateful to Dr Laith Majeed Hussein and his SBAH team in Baghdad for enabling us to export the various kinds of samples that underpin the analyses. The return of the leftovers of these samples was formally accepted by SBAH in Baghdad on 23 October 2023.



Fig. A6: The excavation team on the day before the beginning of Ramadan, with the foreman (“Sherqati”) Mahjub Mohammad Jar kneeling to the right of the table. Drone photo by Jens Rohde (22 March 2023).

B. The Andrae House, a monument in its own right: a brief history of the building and its use

Karen Radner & Jana Richter²

120 years ago, the so-called Andrae House was built in the middle of the ruins of the ancient city of Assur to provide a base for the excavations of the Deutsche Orient-Gesellschaft headed by Walter Andrae, a trained architect who oversaw most of the construction himself from 1903 onwards. According to Iraqi law, a building receives heritage status when its age exceeds a hundred years.³ Following this definition, the Andrae House itself is a monument within the archaeological site of Assur, and it is consequently part of the dossier submitted to UNESCO when Assur was included in the World Heritage List in 2003, as only the second property in Iraq after Hatra (1985).

In fulfilment of the research permit issued by the Iraqi State Board of Antiquities and Heritage in April of 2022, and as a practical preparation for the first season of new excavations in February and March of 2023, the work programme at the onset of the new project encompassed the repair and restoration of the dilapidated Andrae House. Among the locals of Sherqat, the building is commonly referred to as the “German House” (*al-bayt al-almānī*), “Walter’s Palace” (*qaṣr Fālṭr*), “Andrae’s Palace” (*qaṣr Andrayh*) or simply “The Palace” (*al-qaṣr*), and considered a landmark worthy of pride and protection. It has been the subject of a 2020 book written by local historian and retired director of the SBAH Sherqat office Mohammad Ajaj Jarjis, published under the title *Qaṣr Andrayh: maqarr bi’ta at-tanqīb al-almāniya fī Āšūr* (which translates as *Andrae’s*

Palace: the headquarters of the German excavation mission in Assur). But despite the popular emphasis on continuity and preservation, archival materials in the possession of the Deutsche Orient-Gesellschaft, kept in the photo archive of the Vorderasiatisches Museum and the central archive of Staatliche Museen zu Berlin, attest to extensive changes within and around the building during its existence, as the present contribution aims to highlight.

B1. A brief sketch of the Andrae House’s fortunes from 1903 to 2023

Overlooking the Tigris from its position on the eastern edge of the site and close enough to the old quay wall originally constructed by Adad-nerari I of Assyria (1305-1274 BC) to offer easy access to riverine traffic and transport (**Fig. D1.1**), the house served as Walter Andrae’s permanent residence and base for all his work in Assur. For the twelve years from 1903 to 1914, Andrae lived in the house, interrupted only by two nine-month-long trips to Germany in 1908 and 1912 and a shorter health-related stay in Baghdad over the summer of 1909.⁴

After the German excavation was closed down just before World War I began in 1914, the Ottoman police authority took over the former expedition house as their local headquarters (*qishla*), and the building served in that function until 1920. Following the Iraqi Revolt of 1920 against the proposed British Mandate of Mesopotamia and the subsequent creation of the Kingdom of Iraq under British Administration (“Mandatory Iraq”), the house became the administrative headquarters of the Sherqat district.

After 1929, once the district headquarters had been moved to the town centre of Sherqat, the house stood empty and was handed over to Sheikh Ajil Al-Yawar as a source of reusable building materials. He had the doors

² The authors wish to thank Mohammad Ajaj Jarjis, Sakhar Mohammad Ajaj and Kamal Rasheed Raheem for sharing their knowledge about the house with us, Peter Miglus for information on the 2000 restorations and Helen Gries for help with Andrae’s photographs and paintings. We are very grateful to Daniel Schwemer and Joachim Marzahn of the Deutsche Orient-Gesellschaft, to Alrun Gutow and Olaf Teßmer of the photo archive of the Vorderasiatisches Museum, and to Beate Ebel-Borchert of the central archive of Staatliche Museen zu Berlin for their permissions and support of our archival research. High-resolution scans of Andrae’s excavation photos were provided by Alrun Gutow, and Michaela Hussein-Wiedemann digitised the ground plan sketches from Andrae’s letters, and we wish to thank them for their speed and diligence.

³ Jarjis 2020, 35.

⁴ Andrae 1908b, 25; 1909a, 38; 1909b, 45; 1913, 43; Jordan 1909, 44; 1912, 26; Koldewey 1909, 17 (quoting reports by Julius Jordan).

and windows removed for installation at his own house, which was constructed during the years 1929-1931, and also some of the stone walls dismantled for gypsum extraction.⁵ After that, the Andrae House was left in ruins for decades, with many of the remaining ceilings and walls collapsing.

In 1978, it was decided that the State Board of Antiquities and Heritage (SBAH) of Iraq was to resume archaeological research in Assur. The Andrae House was renovated and enlarged to serve as a base for all Iraqi and foreign missions working at the site. Among others, it housed the German teams led by Reinhard Dittmann in 1986-1989, by Barthel Hrouda in 1989-1990 and by Peter Miglus in 2000-2001.⁶ At that time, the house was also turned into the headquarters of the SBAH's Sherqat office. It continued to serve as such until 2008 when a new purpose-built building was constructed outside of the fortification wall at the main entrance to the site, near the Tabira Gate.⁷ Importantly, the new SBAH office building's power and water supplies were connected to the modern town, unlike the Andrae House, which used a generator and an ancient well that had been put back to use in Andrae's time; today, this well is dry.

In 2015, an ISIS terrorist cell took possession of the vacant building and subsequently used it as a military barracks to operate in the Sherqat region. When the Iraqi armed forces attacked late in 2016, the terrorists stripped the building of everything of value, including all furniture, doors, windows, electricity cables and water pipes, and smeared the walls with offensive and obscene graffiti. The Iraqi aerial attacks leading to the recapture of the house resulted in severe damage to the roof of the Great Hall (SB4) and sadly also the destruction of one of the mature palm trees in the courtyard. Once the fighting was over, the staff of SBAH's Sherqat office provisionally cleared and cleaned the house but otherwise had to leave it in ruins. The shell of the building stood empty until September 2022.

In May 2022, Karen Radner received the Gottfried Wilhelm Leibniz Award of the German Research Foundation (DFG) and was in a position to use some of its funds for the restoration of the Andrae House, as part of the fulfilment of the stipulations of the research permit issued by SBAH in April 2022. Her longtime research partner Kamal Rasheed Raheem, the recently retired head of the Sulaymaniyah Directorate of Antiquities and Heritage, had overseen the restoration of several similar buildings from



Fig. B1.1: The excavation house from the south, before and after restoration. Photos by Akam Omar Ahmed Al-Qaradaghi.

the early 20th century in Sulaymaniyah. Having worked in Assur as a recently graduated SBAH employee in 1980, he agreed to supervise the restoration of the Andrae House. The sculptor and conservator Akam Omar Ahmed Al-Qaradaghi, also from Sulaymaniyah, was recruited to provide further expertise in restoring the historic building using traditional construction methods. He documented the ongoing restoration process, which resulted in a photograph exhibition that was installed in one of the rooms of the west wing in February 2023 (**Figs. B1.1-17, B4.11**).

The involvement of Kamal Rasheed Raheem and Akam Omar Ahmed Al-Qaradaghi was made possible through the generous support of the Bavarian Academy of Sciences, which had previously sponsored Barthel Hrouda's work in Assur in 1989-90. The restoration started in September 2022 in close collaboration with the SBAH Sherqat office and was completed in January 2023. In February and March 2023, the building housed the team for the first season of the new excavations and in November 2023, after solar panels and a photovoltaic system had been installed, a smaller team stayed there again to work on the pottery.

⁵ Jarjis 2020, 30.

⁶ Dittmann 1990; Hrouda 1991; Miglus 2000.

⁷ Jarjis 2020, 35.



Fig. B1.3: The southeastern corner of the excavation house with the dining room, as seen from the bank of the Tigris, before and after restoration. Photos by Akam Omar Ahmed Al-Qaradaghi.



Fig. B1.2: The eastern gate as seen from the bank of the Tigris, before and after restoration. Photos by Akam Omar Ahmed Al-Qaradaghi.



Fig. B1.5: The courtyard's southeastern corner, before and after restoration. Photos by Akam Omar Ahmed Al-Qaradaghi.



Fig. B1.4: The courtyard's southwestern corner with the western gate, before and after restoration. Photos by Akam Omar Ahmed Al-Qaradaghi.



Fig. B1.7: The western gate as seen from inside the excavation house, before and after restoration. Photos by Akam Omar Ahmed Al-Qaradaghi.



Fig. B1.6: The façade of the southeastern block of the excavation house, before and after restoration. Photos by Akam Omar Ahmed Al-Qaradaghi.



Fig. B1.9: The courtyard as seen from the roof of the north wing, before and after restoration. Photos by Akam Omar Ahmed Al-Qaradaghi.



Fig. B1.8: The eastern gate as seen from inside the excavation house, before and after restoration. Photos by Akam Omar Ahmed Al-Qaradaghi.



Fig. B1.11: Inside the southern part of the west wing, before and after restoration. Photos by Akam Omar Ahmed Al-Qaradaghi.



Fig. B1.10: The courtyard with the southern part of the east wing as seen from the roof of the north wing, before and after restoration. Photos by Akam Omar Ahmed Al-Qaradaghi.



Fig. B1.13: The ground-floor corridor of the north wing, before and after restoration. Photos by Akam Omar Ahmed Al-Qaradaghi.



Fig. B1.12: Inside the storage room in the south wing, before and after restoration. Photos by Akam Omar Ahmed Al-Qaradaghi.



Fig. B1.14: The bathroom on the north wing's ground floor, before and after restoration. Photos by Akam Omar Ahmed Al-Qaradaghi.



Fig. B1.15: The second-floor corridor of the north wing, before and after restoration. Photos by Akam Omar Ahmed Al-Qaradaghi.



Fig. B1.17: Inside the office room on the north wing's second storey, before and after restoration. Photos by Akam Omar Ahmed Al-Qaradaghi.



Fig. B1.16: The office room on the north wing's second storey, before and after restoration. Photos by Akam Omar Ahmed Al-Qaradaghi.

B2. Andrae's original building

It was not Walter Andrae but his mentor Robert Koldewey who selected the site for the construction of the house and under whose direction the building activities commenced in August 1903. The starting date of construction works is evidenced by the first house-related expenses entered into the accounting book of the Assur excavation for this month.⁸ A significant consideration at the time concerned the potential ramifications of erecting the structure at a location where it might obstruct future excavation works.⁹ Fortunately, these concerns turned out to be unwarranted.

The archaeological excavations began on 18 September 1903,¹⁰ some six weeks before Walter Andrae himself arrived at Assur at the end of October.¹¹ He and the other members of the expedition were able to move into the house on 20 November 1903,¹² just three months after the start of its construction and at a time when the wall plaster had not yet fully dried.¹³ A photograph shows the campsite on the very day when the team moved into the house (**Fig. B2.1**). At least one tent stayed in use for some time, as another photograph taken on 19 January 1904 demonstrates (**Fig. B2.2**).¹⁴

The beginning of the house's construction is documented in a series of photographs (**Figs. B2.3-4**).¹⁵ When the team took up residence in the building, the nascent structure comprised a single rectangular two-storey building at the eastern border of a square courtyard (**Fig. B2.2**). Until today, the excavation house features a rectangular architectural layout oriented in a northwest-southeast direction, where the rooms surround and open towards a spacious central courtyard. In its original design, the principal entrance led through the northern wall into the building. The east wing, which constitutes the oldest part of the house, was originally the only section to feature

two floors, with the private bedrooms for Andrae and his assistants located on the upper storey.

In the next phase of development, several additional structures were erected around the excavation house. To its south, a complex of smaller buildings housed the warden (German "Aufseher") with his wife who took care of the expedition's laundry and baked their bread and offered accommodation for the four specially trained excavation workers and their families (**Fig. B2.6**).¹⁶ Having previously worked at Koldewey's excavations in Babylon, these workers joined the expedition from Hillah. They trained the first generation of local excavators whose skills in recognising mud-brick structures eventually became so famous in Iraq that any specialist excavation worker is called "Sherqati".

A photograph from the last day of February 1904 (**Fig. B2.7**) is the earliest evidence of the dwellings to the south of the main building, showing that these were initially built without an enclosure wall. During the following days, construction began of a two-storey building in the area northwest of the excavation house, completed no later than in mid-March 1904 (**Fig. B2.8**). This structure, which is today known as "Umyan's House" (*bayt 'Umyān*) housed the cook and his wife, and the expedition treasurer Shaul Selman (also known as Saul Salomon) who had joined Andrae's new excavation in Assur from Hillah that same spring.¹⁷ Although in ruins, it has survived in its substance until today.

During February and March 1904, the excavation house underwent further development with the addition of three more living rooms in the northeastern corner of the second floor (**Figs. B2.9-10**). For the final stages of the house's initial construction, Andrae notes the establishment of a stable and a blacksmith workshop (**Figs. B2.11-12**), which was established in the western portion of the building. This forge was pivotal for assembling and keeping in good repair the rail lines and coal trolleys used for transporting and depositing the excavated soil. Finally, storage areas that had initially been created along the northern and southern walls of the courtyard as mere spaces covered by wooden roofs were now turned into closed rooms, and a large hall was built along the western courtyard wall to provide storage for larger-sized archaeological finds.¹⁸

By spring 1904, all these steps had been completed, as documented by the final report with a floor plan and photographs that Andrae submitted to the Deutsche Orient-

8 SMB-ZA, III/DOG II 1.4.4.5 Conten Assur 1903-1908.

9 Koldewey 1903, 16.

10 Koldewey 1903, 18.

11 Andrae 1904a, 10.

12 Andrae 1904b, 43.

13 Andrae 1988, 153.

14 Also Andrae 1904b, 47 (from 1 December 1903).

15 These two photographs from a "Babylon" film roll are not listed in the Assur photo register. They are dated to the year "03" and signed with Koldewey's, not Andrae's characteristic initials in their bottom right corners. This suggests that the photographs were taken by Koldewey before Andrae arrived at Assur. The assumption that they document an early building stage of the east wing is based on the distributions of doors and windows, which match later views of the excavation house, e.g. in Ass Ph 2256 (**Fig. B2.5**), taken in February 1907.

16 Andrae 1904c, 17.

17 Andrae 1904c, 29; 1904e, 27; 1988, 73-74.

18 Andrae 1904c, 31-32.



Fig. B2.1: The initial tent camp on the site of Assur on 20 November 1903. Ass Ph 85 (© Staatliche Museen zu Berlin [= SMB], Vorderasiatisches Museum [= VAM], Deutsche Orient-Gesellschaft [= DOG]; photo by Walter Andrae).



Fig. B2.2: View of the Assur expedition house from the northwest on 19 January 1904. Detail of Ass Ph 123 (© SMB, VAM, DOG; photo by Walter Andrae).



Fig. B2.3: Construction of the east wing of the expedition house in 1903. Bab Ph 487 (© SMB, VAM, DOG; photo by Robert Koldewey).



Fig. B2.4: Preparing building materials at the construction site of the expedition house in 1903. Bab Ph 488 (© SMB, VAM, DOG; photo by Robert Koldewey).



Fig. B2.5: A large door socket stone brought in from the excavation is pictured in the courtyard of the expedition house on 5 February 1907, with the ground floor of the east wing visible in the background. Ass Ph 2256 (© SMB, VAM, DOG; photo by Walter Andrae).

Gesellschaft.¹⁹ Two of his letters written in February and March 1904 contain sketches of the house's ground plan (Figs. B2.13-14).²⁰ In a letter to DOG chairman James Simon from 29 May 1904, Andrae mentions that the workmen who had been preparing the gypsum plaster at the house's construction site were now employed as rail navigators in the excavation.²¹

Photographs dating to May 1904 picture the house's interior and exterior from different perspectives (Figs. B2.15-19). They show that the supplementary buildings south of the main house had now been connected to the complex by an enclosing wall, whereas Shaul Selman's



Fig. B2.6: A view from the rooftop of the expedition house across the southern appended buildings, taken on 2 April 1904. Ass Ph 179 (© SMB, VAM, DOG; photo by Walter Andrae).

and the cook's house remained free-standing to its north-west (Figs. B2.18-19).

Throughout all of Andrae's years at Assur, the primary entrance of the main house led through the arched gate positioned in the centre of the north wing, as evidenced by several photographs (Figs. B2.18 and B2.20-21). While this was possibly the only permanent point of access to the house, Andrae's floor plan sketch (Fig. B2.13) shows that a second door in the southern façade existed at least during the time when the west wing of the building was under construction. There is no indication that the enclosure with the dwellings to the south of the excavation house (Figs. B2.22-23) ever had a direct connection to the main building; rather, its south wall was used as a part of a separate enclosed compound.

Pictures taken in October 1904 first attest to the creation of a walled garden on the river slope east of the excavation house (Figs. B2.24-25). During November 1904, facilities to store and document archaeological finds were constructed along the western side of the courtyard, thus closing up the remaining gap between the north wing of the house (Fig. B2.26) and the blacksmith workshop in the southwestern corner of the courtyard (Fig. B2.27). Andrae describes this newly added part of the building

19 Andrae 1904e, 25-28. The architectural drawing by Ernst Herzfeld that Andrae mentions in his summary report was not included in the published article.

20 Walter Andrae to Robert Koldewey, 22 February 1904 (SMB-ZA, III/DOG II 1.2.10.9); Andrae to Koldewey, 29 March 1904 (SMB-ZA, III/DOG II 1.2.10.9).

21 Walter Andrae to James Simon, 29 May 1904 (SMB-ZA, IV/NL Bode 0497).

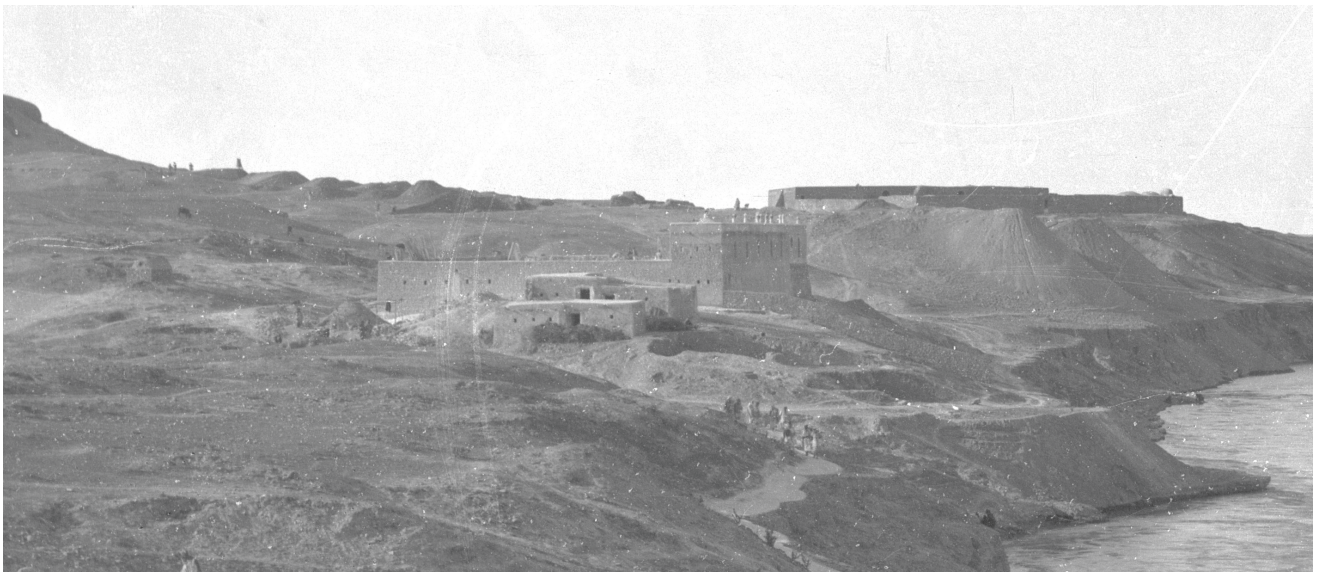


Fig. B2.7: The expedition house from the southeast on 29 February 1904. Detail of Ass Ph 160 (© SMB, VAM, DOG; photo by Walter Andrae).



Fig. B2.8: View of the expedition house from the southeast on 13 March 1904. Detail of Ass Ph 168 (© SMB, VAM, DOG; photo by Walter Andrae).



Fig. B2.9: Construction of the living rooms in the north wing. Ass Ph 162, taken on 2 March 1904 (© SMB, VAM, DOG; photo by Walter Andrae).

as an “open hall”,²² and photographs from 1904 and 1905 show that whereas the two entrances leading to the forge were closed with wooden lattice doors (Figs. B2.27-28), the rest of the west wing had open arched gates (Figs. B2.27 and B2.29). The presence of this type of entrance identifies a photograph (Fig. B2.30), which documents a life-sized statue, as a picture taken inside this hall. It shows the hall's vaulted stone-built interior walls to be unplastered, in contrast to the smaller storage rooms on the ground floor of the north wing (Fig. B2.29). A photograph of a view towards the south, with the meteorological station set up in the centre of the picture, provides a good impression of the composite character of the west wing, with its different roof constructions attesting to the subsequent phases of construction of that part of the house (Fig. B2.31).

In the course of the building work undertaken in November 1904, a fourth room was added on the second floor of the north wing (Fig. B2.26). A lively scene captured in a photograph from late November 1904 (Fig. B2.32) likely documents this work: two workmen prepare the gypsum plaster while two others carry the freshly mixed material in their bare hands to the construction site.

²² Andrae 1905, 36.



Fig. B2.10: View of the expedition house from the northwest on 11 May 1904. Detail of Ass Ph 189 (© SMB, VAM, DOG; photo by Walter Andrae).

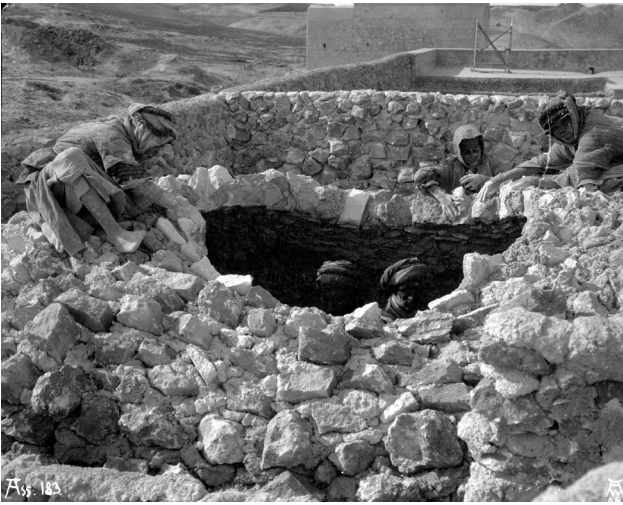


Fig. B2.11: Building the roof of the blacksmith workshop in the west wing on 15 April 1904. Ass Ph 183 (© SMB, VAM, DOG; photo by Walter Andrae).



Fig. B2.12: View into the blacksmith workshop, during the construction of its forge on 11 May 1904. Ass Ph 184 (© SMB, VAM, DOG; photo by Walter Andrae).

In preparation for the winter, Andrae also built stables and a henhouse,²³ although we have not been able to pinpoint the latter's exact location. The domed and perforated cube-like building visible in some photos in the

southern part of the courtyard is not a henhouse, as we thought at one point, but a shelter in which large, porous ceramic jars filled with water (Arabic *ḥebb*) were stored and cooled.²⁴ The expedition initially relied only on the Tigris for its fresh water supply: water was first collected from the river in waterskins and then decanted into water jars, which were carried up to the water shelter in the excavation house's courtyard, at first with the help of a donkey and later a horse.²⁵ This way of procuring drinking water was so common at the time, even in Baghdad's shops and urban residences,²⁶ that Andrae simply refers to "the hebbes" when writing to Koldewey.²⁷ Some of these water vessels are pictured on pot stands in front of the excavation house's water shelter in the background of a photograph (Fig. B2.33). With its domed roof and perforated walls, the shelter was well-ventilated and shady, and its bitumen-plastered floor made sure that it remained structurally sound despite the water habitually sloshing around. The shelter was already included in Andrae's floor plan sketch of early 1904 (Fig. B2.13) but is first clearly visible in photographs taken from several directions around Christmas 1905 on the occasion of the first snow-fall experienced by the expedition (Figs. B2.34-37).

Those same photographs also clarify the ways of access to the first floor of the excavation house, as they were taken towards the south (Fig. B2.35), northeast (Fig. B2.36) and northwest (Fig. B2.29). The upper storey could be reached in three ways, either by a set of external stairs in the courtyard in the northeastern corner or via two sets of internal stairways located in the building's southern corners (in the southeast: Figs. B2.33 and B2.35; in the southwest: Fig. B2.27). Once on the first floor, it was possible to access all its parts as they were connected through a circular route that led from wing to wing across the roofs and through an entrance on the north wing.

The four main wings of the Andrae House remained unchanged from 1905 to 1907, as a comparison between the photograph series Ass Ph 1086-1090 (Figs. B2.34-37) with Ass Ph 2438-2440 (Figs. B2.38-40) shows. The year 1907 saw a grain mill installed in the centre of the courtyard

²³ Andrae 1905, 36.

²⁴ Called "Brunnenhäuschen" in a letter from Andrae to Koldewey, 22 February 1904 (SMB-ZA, III/DOG II, 1.2.10.9).

²⁵ Andrae 1988, 157; letter from Andrae to Koldewey, 12 July 1905 (SMB-ZA, III/DOG II, 1.2.10.10).

²⁶ Krotkoff 1972, 94; Reuther 1910, 24-25.

²⁷ Letter from Andrae to Koldewey, 22 February 1904 (SMB-ZA, III/DOG II, 1.2.10.9).

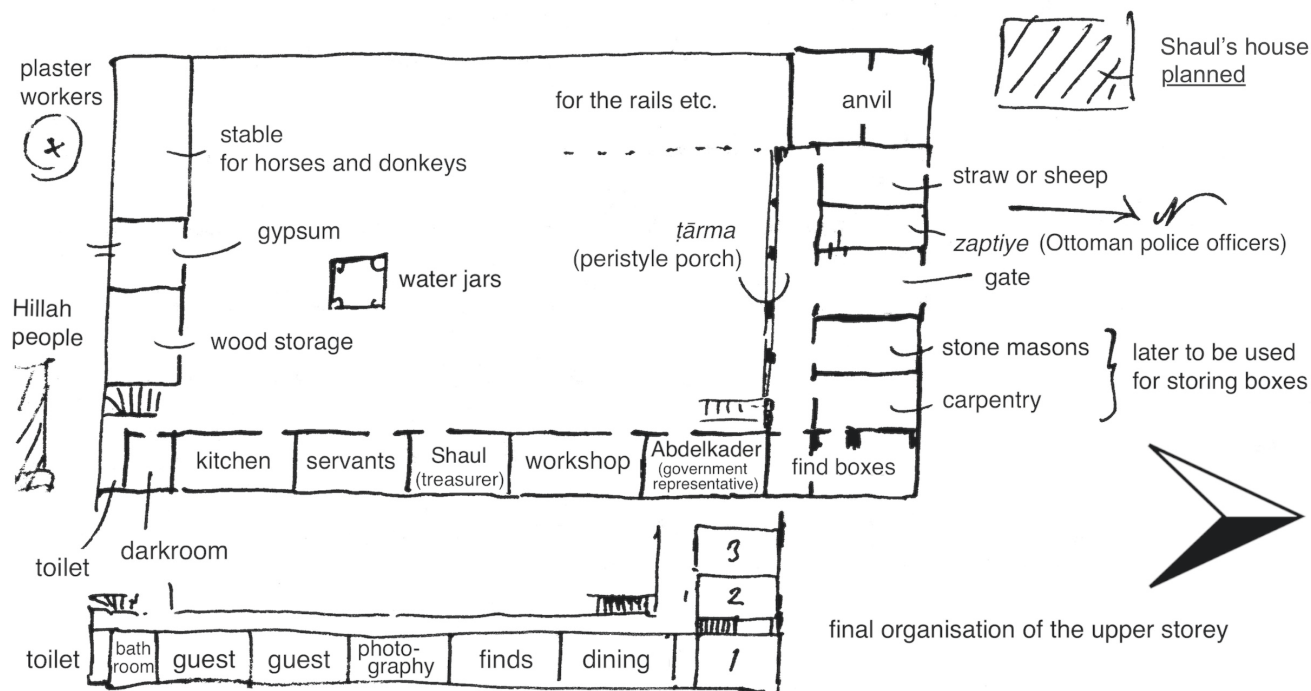
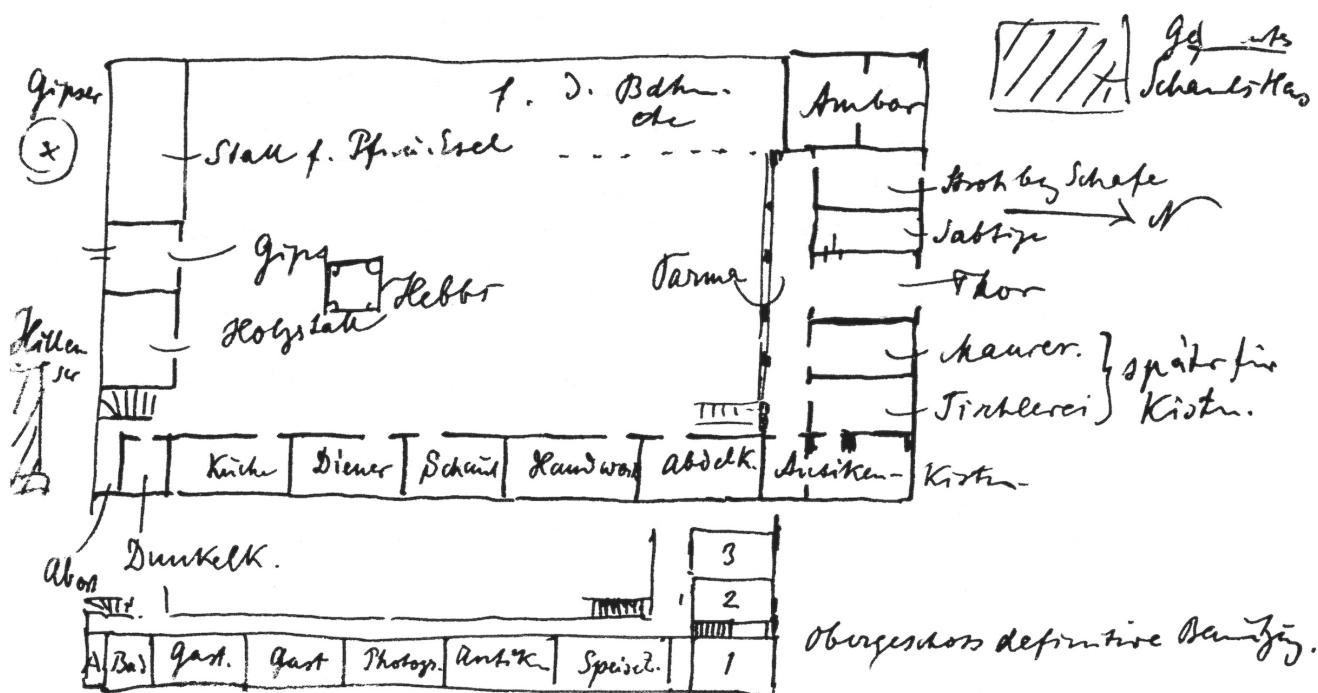


Fig. B2.13: Sketch plan of the rooms on the ground floor and the first floor of the expedition house, as sketched by Walter Andrae in a letter to Robert Koldewey on 22 February 1904 (SMB-ZA, III/DOG II 1.2.10.9). Top: Andrae's original, bottom: with translated labels and a north arrow, prepared by Jana Richter.

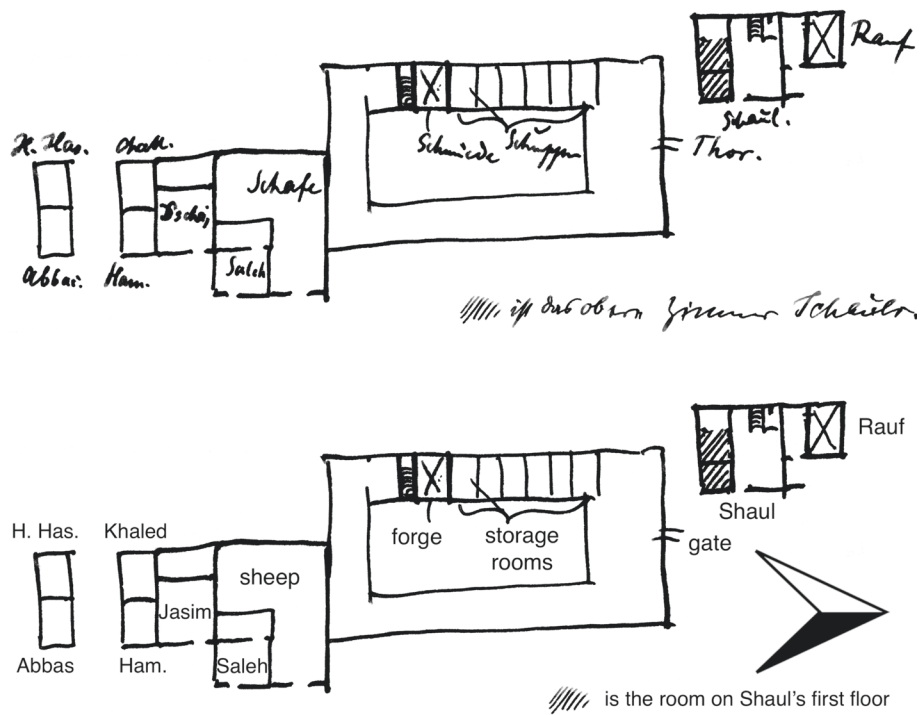


Fig. B2.14: Sketch plan of the surrounding buildings and newly added rooms in the west wing of the expedition house, as sketched by Walter Andrae in a letter to Robert Koldey on 29 March 1904 (SMB-ZA, III/DOG II 1.2.10.9). Top: Andrae's original, bottom: with translated labels and a north arrow, prepared by Jana Richter.



Fig. B2.15: View of the courtyard on 11 May 1904 after delivery of rail components by donkey caravan, looking north. Ass Ph 196 (© SMB, VAM, DOG; photo by Walter Andrae).



Fig. B2.16: View of the north wing of the expedition house on 11 May 1904, looking northwest across Shaul Selman's house towards the ziggurat of the Aššur temple. Ass Ph 197 (© SMB, VAM, DOG; photo by Walter Andrae).



Fig. B2.17: View of the northern façade of the expedition house on 11 May 1904, with Shaul Selman's house on the right. Ass Ph 198 (© SMB, VAM, DOG; photo by Walter Andrae).



Fig. B2.18: View of the expedition house and Shaul Selman's house from the northeast, taken on 11 May 1904. Ass Ph 199 (© SMB, VAM, DOG; photo by Walter Andrae).



Fig. B2.19: View of the expedition house with surrounding buildings on 21 May 1904, looking northeast. Ass Ph 212 (© SMB, VAM, DOG; photo by Walter Andrae).

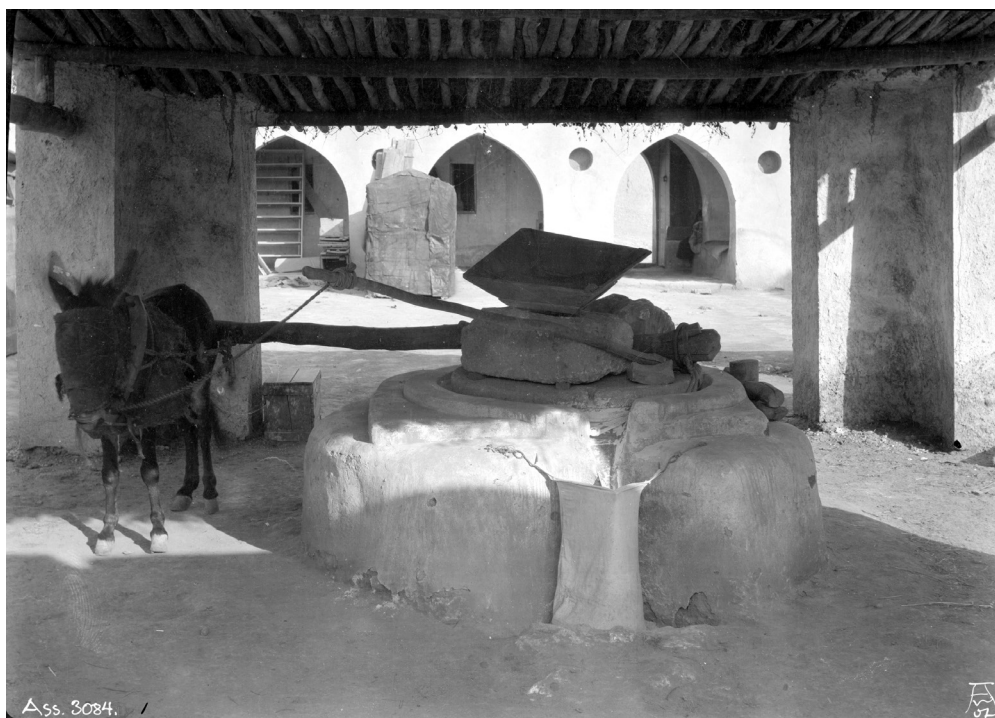


Fig. B2.20: The donkey-driven mill in the courtyard of the excavation house on 14 November 1907, looking north. Ass Ph 3084 (© SMB, VAM, DOG; photo by Walter Andrae).



Fig. B2.21: The excavation house with front garden and surrounding buildings, looking south. Detail of a photo taken at some point after April 1912. Ass Ph 6184 (© SMB, VAM, DOG; photographer unknown).



Fig. B2.22: A view across the snow-covered dwellings south of the excavation house on 26 January 1911. Ass Ph 5494 (© SMB, VAM, DOG; photo by Conrad Preußer).



Fig. B2.23: A view across the dwellings south of the excavation house, with the workmen's village in the background. Photo taken at some point after April 1912. Ass Ph 7045 (© SMB, VAM, DOG; photographer unknown).



Fig. B2.24: The excavation house as seen from the river bank on 6 October 1904, looking southwest. Detail of Ass Ph 290 (© SMB, VAM, DOG; photo by Walter Andrae).



Fig. B2.25: The excavation house as seen from the river bank on 6 October 1904, looking southwest. Detail of Ass Ph 291 (© SMB, VAM, DOG; photo by Walter Andrae).



Fig. B2.26: View of the courtyard in December 1904 after the arrival of a caravan delivering food provisions, looking north. Ass Ph 376 (© SMB, VAM, DOG; photo by Walter Andrae).



Fig. B2.27: View across the courtyard on 11 March 1905, as a large wooden find chest is being prepared, looking southwest. Ass Ph 512 (© SMB, VAM, DOG; photo by Walter Andrae).

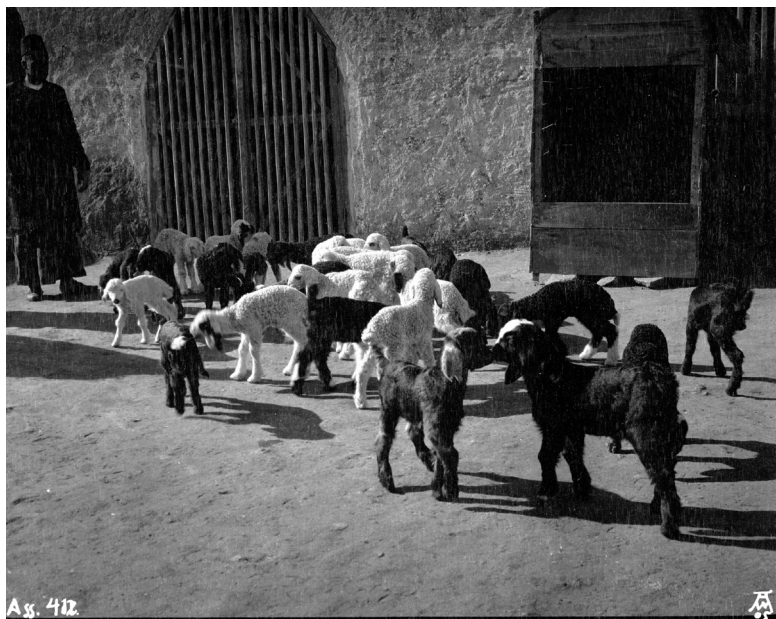


Fig. B2.28: Lambs playing in the courtyard in front of the west wing on 31 January 1905. Ass Ph 411 (© SMB, VAM, DOG; photo by Walter Andrae).

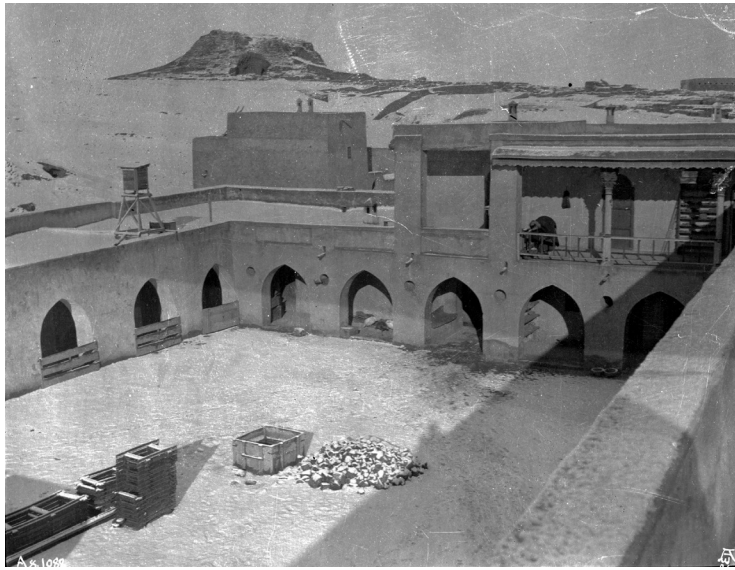


Fig. B2.29: Looking northwest across the snow-covered courtyard on 26 December 1905. Ass Ph 1088 (© SMB, VAM, DOG; photo by Walter Andrae).



Fig. B2.30: A basalt statue (Ass 7332) inside the find storage room on 6 January 1906. Ass Ph 1103 (© SMB, VAM, DOG; photo by Walter Andrae).



Fig. B2.31: The weather station on top of the west wing on 21 April 1905, looking south. Ass Ph 593 (© SMB, VAM, DOG; photo by Walter Andrae).



Fig. B2.32: Workers mixing plaster in the courtyard of the excavation house during the final days of November 1904. Ass Ph 350 (© SMB, VAM, DOG; photo by Walter Andrae).



Fig. B2.33: Large door socket stones from the excavation are pictured in the courtyard on 5 February 1907, with the water shelter and the south wing of the excavation house visible in the background. Ass Ph 2255 (© SMB, VAM, DOG; photo by Walter Andrae).

(**Fig. B2.20**).²⁸ In 1908, another living room was added to the north wing's upper storey,²⁹ thereby completing the northern façade. It is first shown in a famous autochrome photograph from February 1910 (**Fig. B2.41**),³⁰ and again in the pictures taken when the expedition experienced snowfall for the second time in early 1911 (**Figs. B2.42-43**). This harsh winter also necessitated further building work on the mill in the courtyard, which was turned into a closed one-room building during that time.³¹

The latest depictions of the expedition house date to an unspecified time in 1912 or later, towards the end of Andrae's time at Assur, and can be found in the backgrounds of the photographs Ass Ph 6184 (**Fig. B2.21**) and Ass Ph 6429a (**Fig. B2.44**). On the one hand, they show ongoing construction to the west of the main building where additional small houses share an enclosure wall with it (**Fig. B2.44**). Most of these western buildings existed already in mid-1910 (**Fig. B2.45**) but they had not yet been combined into the enclosed compound shown in a photograph

from August 1911 (**Fig. B2.46**). On the other hand, these late images show a low, roofed structure on top of the east wing (**Fig. B2.44**). Its construction is probably captured in the photograph of August 1911, which shows four short parallel walls delimiting some small and at that time still unroofed compartments on top of that wing (**Fig. B2.46**).

Photographs and paintings from the years 1909, 1911, and 1912 show expansive gardens not only to the east of the house, towards the Tigris but also to the building's north. The riverside garden³² (**Figs. B2.47-50**) was enclosed by a wall early on (**Fig. B2.24**), but as shown in an oil painting of Andrae's (**Fig. B2.51**),³³ the northern garden started as an open planted area and was only later, in

1909, turned into an enclosed garden (**Figs. B2.21, B2.46, B2.48**). The region's unreliable rainfall could severely impede agricultural productivity and the local availability of food supplies. Faced with such uncertainties that were further compounded by locusts and other pests, Andrae opted to mitigate provisioning risks by making the expedition as independent as possible from purchasing food supplies. We have already mentioned the construction of a henhouse in 1904 and a grain mill in 1907. Moreover, the expedition's meat and dairy were sourced from the expedition-owned herd comprising around 150 sheep and goats.³⁴ Seen in this context, Andrae's deliberate cultivation of an increasingly large area surrounding the house with soil taken from the excavation clearly transcends mere aesthetic and recreational considerations. In addition to enhancing the visual appeal of the house and creating a pleasant environment, the gardens also provided the expedition with a sustainable source of home-grown produce. The conscientious planning undertaken by Andrae reflected a proactive response to the uncertainties inherent in the local agricultural landscape, ensuring a

28 Andrae's comment about having brick masons and excavation workmen do "repairs and a few additions" could be related to this, and would then date the building of the mill to September/October 1907 (Andrae 1908a, 31).

29 Koldewey 1909, 17 (quoting reports by Julius Jordan).

30 On the pioneering autochrome photographs taken in Assur, see Marzahn 1998.

31 Andrae 1911, 53 (with a photograph taken by Julius Jordan).

32 Andrae/Boehmer 1989, pl. 90.

33 Inventory no. VAK 00019; it currently hangs in VAM curator Helen Gries' office.

34 Andrae 1904e, 75.

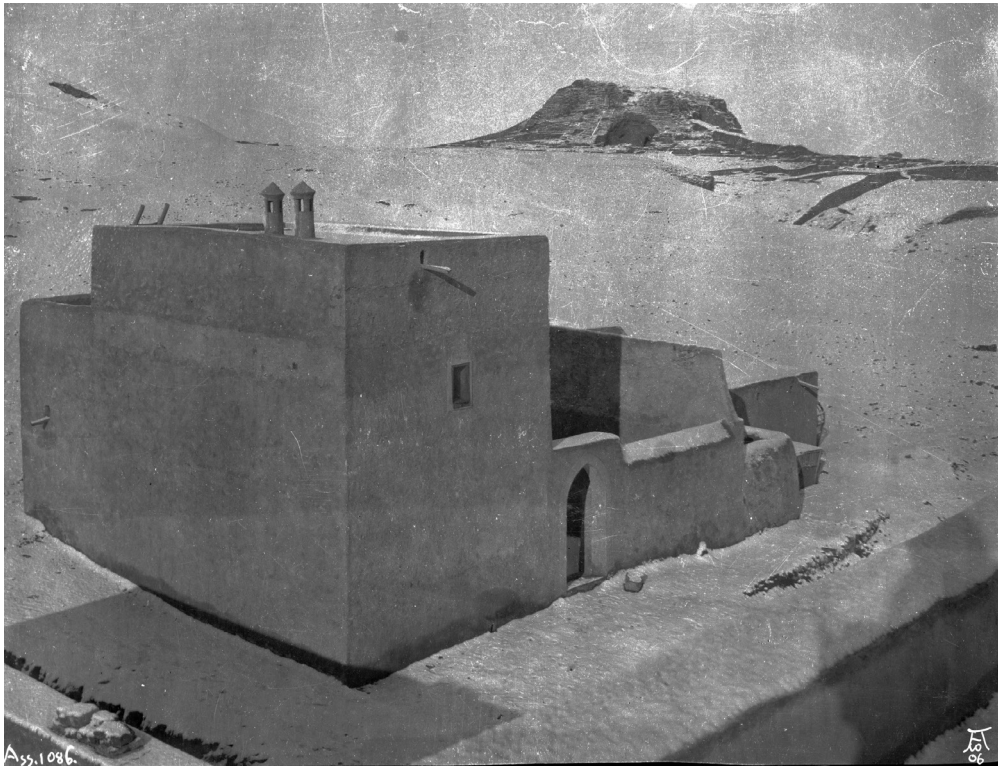


Fig. B2.34: Looking northwest from the excavation house onto Shaul Selman's snow-covered house on 26 December 1905. Ass Ph 1086 (© SMB, VAM, DOG; photo by Walter Andrae).

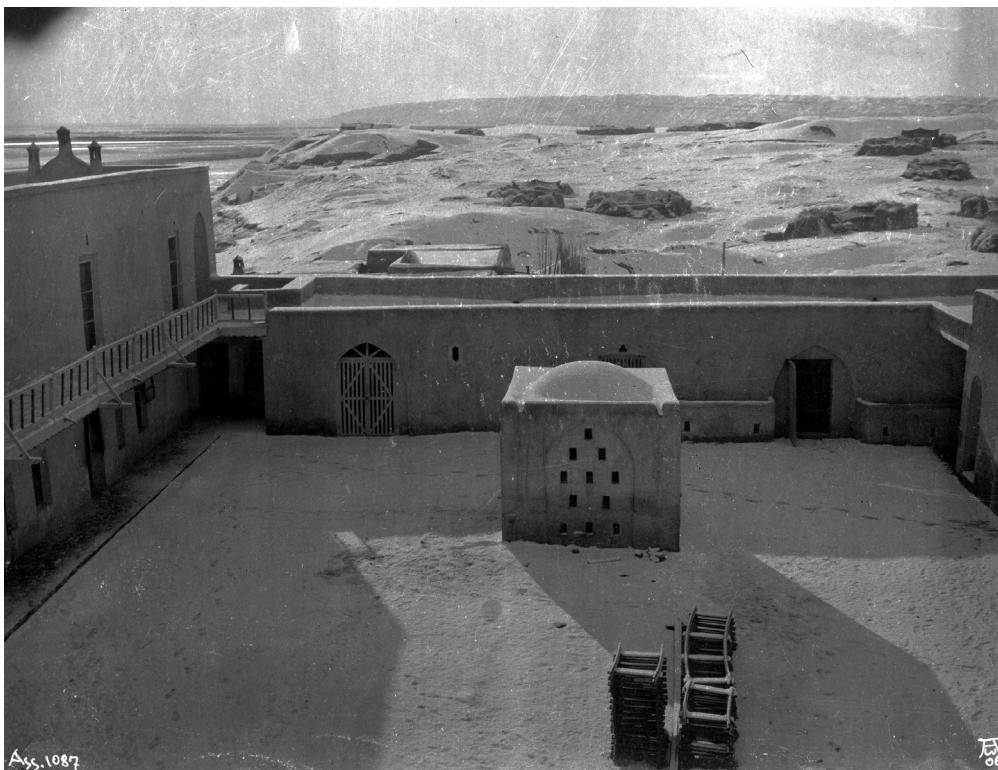


Fig. B2.35: Looking south across the snow-covered courtyard on 26 December 1905. Ass Ph 1087 (© SMB, VAM, DOG; photo by Walter Andrae).



Fig. B2.36: Looking northeast across the snow-covered courtyard on 26 December 1905. Ass Ph 1089 (© SMB, VAM, DOG; photo by Walter Andrae).



Fig. B2.37: A view from the rooftop of the expedition house across the snow-covered southern appended buildings, taken on 26 December 1905. Ass Ph 1090 (© SMB, VAM, DOG; photo by Walter Andrae).



Fig. B2.38: Looking northwest across the courtyard on 30 April 1907, as locust swarms plague the excavation house. Ass Ph 2438 (© SMB, VAM, DOG; photo by Walter Andrae).



Fig. B2.39: Looking from the excavation house northwest towards Shaul Selman's house on 30 April 1907, as locust swarms plague the site. Ass Ph 2439 (© SMB, VAM, DOG; photo by Walter Andrae).



Fig. B2.40: Looking south from the portico onto the courtyard on 30 April 1907, as locust swarms surround the excavation house. Ass Ph 2440 (© SMB, VAM, DOG; photo by Walter Andrae).



Fig. B2.41: Expedition members in front of the living rooms in the north wing. Black-and-white print (Ass Ph 7044) of an older autochrome photo (LumA 48), which Walter Andrae took on 7 February 1910 (cf. Marzahn 1998, 238; exact date established from the excavation photo register by Jana Richter).



Fig. B2.42: Looking northwest across the snow-covered courtyard on 26 January 1911. Ass Ph 5493 (© SMB, VAM, DOG; photo by Conrad Preußner).



Fig. B2.43: The snow-covered excavation house as seen from the river bank on 30 January 1911, looking southwest. Detail of Ass Ph 5496 (© SMB, VAM, DOG; photo by Conrad Preußner).



Fig. B2.44: The excavation house with neighbouring buildings, as seen from the southwest at a date later than April 1912. Detail of Ass Ph 6429a (© SMB, VAM, DOG; photographer unknown).

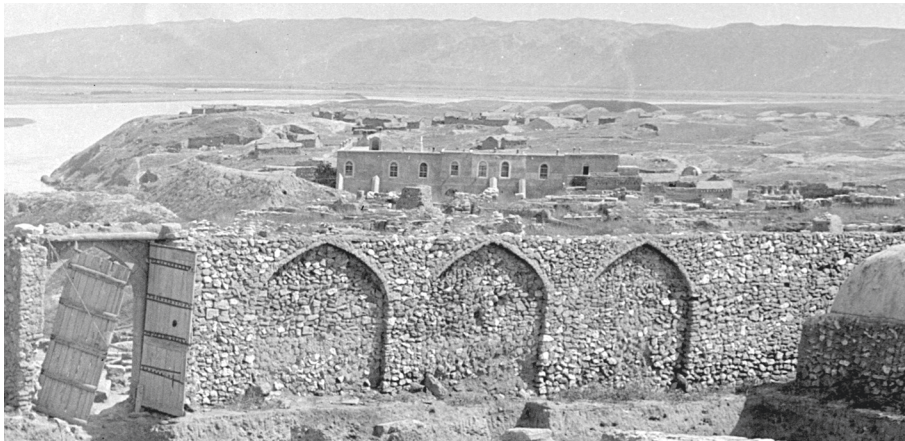


Fig. B2.45: The excavation house with neighbouring buildings, as seen from the Ottoman fortress to its north on 27 May 1910. Detail of Ass Ph 5126 (© SMB, VAM, DOG; photo by Conrad Preußner).



Fig. B2.46: The expedition house with neighbouring buildings behind heaps of excavated soil, as seen from the north on 17 August 1911. Detail of Ass Ph 5752 (© SMB, VAM, DOG; photo by Conrad Preußner).



Fig. B2.47: A view of the garden on the riverside on 20 September 1909, looking southwest. Ass Ph 4618 (© SMB, VAM, DOG; photo by Walter Andrae).



Fig. B2.48: The expedition boat in front of the house, as seen from the Tigris on 20 September 1909. Ass Ph 4620 (© SMB, VAM, DOG; photo by Walter Andrae).



Fig. B2.49: A view of the garden on the riverside on 20 September 1909, looking northwest. Ass Ph 4622 (© SMB, VAM, DOG; photo by Walter Andrae).



Fig. B2.50: Inside the riverside garden on 30 April 1910, looking south. Luma 69 (© SMB, VAM, DOG; photo by Walter Andrae). For this autochrome photo see Marzahn 1998, 238.



Fig. B2.51: Assur in springtime, depicting a view from the Aššur temple excavations southwards onto the Tigris and the expedition house. Oil painting by Walter Andrae, 1909. VAK 00019 (© SMB, VAM; photo by Olaf M. Teßmer).



Fig. B2.52: Mudbrick houses next to the partially stone-built homes of the specialist workers that joined the expedition from Hillah, as seen from the river on 20 September 1909. Detail of Ass Ph 4619 (© SMB, VAM, DOG; photo by Walter Andrae).

degree of self-sufficiency and resilience against external factors impacting food security.

The excavation workers were mainly recruited from the Jaboor tribe, from both sides of the Tigris.³⁵ At the time, the majority of them had already given up herding and were therefore willing to move their tents to locations close to their new place of work. As a result, an extended campsite developed within the ruins of Assur. After having been moved several times for the sake of making space for the excavation,³⁶ this camp was turned into a more permanent village of mudbrick houses (**Fig. B2.45** and **Fig. B2.52**), and other such buildings can be seen in various photographs showing the excavation.³⁷

B3. The Andrae House in the service of local government

After Walter Andrae had left Assur in 1914 and before SBAH started its restorations in 1978, the building underwent several architectural changes.

Firstly, the creation of an entrance door in the middle of the south wing provided direct access to the large room in the southwestern corner of the building (room no. 22 in **Fig. B5.1**; cf. **Fig. B4.1**). Secondly, the galleries on the first floor of the north wing were turned into closed corridors. Thirdly, and possibly as a result of Sheikh Ajil al-Yawar using the building as a quarry (**SB1**), the east wing was split into two independent sections, with a northern and a southern group of rooms now separated by a central gateway that led from the courtyard towards the Tigris (situated between rooms no. 8 and no. 16 in **Fig. B5.1**). This entrance is still in use today.

B4. The Andrae House after the SBAH refurbishment

The restoration project undertaken by the State Board of Antiquities and Heritage in 1978 aimed for a careful repair and stabilisation of the original building substance of the Andrae House wherever it had survived. However, the ruinous state of the building required the SBAH team to construct entire stretches of walls anew. In the affected areas, internal changes were frequently introduced to the original room structure to better accommodate the anticipated work activities, as the house was now meant to

combine the functions of a periodically used excavation house with that of a permanently occupied SBAH office building.

Three major additions were made to the building's ground plan:³⁸ Firstly, a new room was attached to the outside of the southern part of the east wing, to create a dining hall that overlooks the Tigris and that is directly connected to the existing kitchen (visible behind the trees in **Fig. B4.7**). Secondly, the roof of the northern part of the east wing was extended southwards right up to the courtyard gate, thus forming a much longer room on the ground floor (compare **Fig. B4.1** to **Fig. B5.1**). Thirdly, a room was added to the building in the northeastern corner of the courtyard which also resulted in an increase in office space on the first floor of the north wing (compare **Fig. B4.2** to **Fig. B4.3**). In the absence of a corridor connecting the northern and southern parts of the building, both were equipped with additional staircases leading up to the first floor. In addition, the courtyard façade of the southeastern corner was lined with natural stone (**Fig. B4.4**). All these new elements are still present today.

The Iraqi documentation explicitly lists a few cases where it was possible to preserve the old roofs after consolidation, as opposed to most cases where new roofs had to be constructed and were built using reinforced concrete. According to this distinction, the oldest preserved parts of the house were Andrae's former blacksmith workshop in the southern part of the west wing, as well as the bedrooms in the southeastern and the northeastern corners of the building.³⁹

The latter includes the corner room known as "Andrae's Office". The SBAH team was responsible for installing the wide window panes and especially the balcony overlooking the Tigris on its eastern side, new features that had not been part of the house in Walter Andrae's time. Photographs from the construction site of 1978 (**Figs. B4.5-6**) show the base plate and short stubs of reinforcing bars, indicating that the balcony was added only during this time.

A photograph that Jörg Fassbinder took in April 1989 (**Fig. B4.7**), during the geophysical survey initiated by Barthel Hrouda, shows that same balcony at a time when the area between the house and the Tigris still preserved the terraced topography of Andrae's riverside garden although it was no longer used to grow vegetables and its enclosing walls were gone. At that time, several trees were growing on the lower terrace along the river slope. A

35 Andrae 1904b, 46.

36 Andrae 1904d, 70.

37 E.g. in the photographs Ass Ph 2292, 3781, 4324, and 4611.

38 Jarjis 2020, figs. 2-3 show the situation before these additions, and Jarjis 2020, figs. 8-9 afterwards.

39 Jarjis 2020, 32.

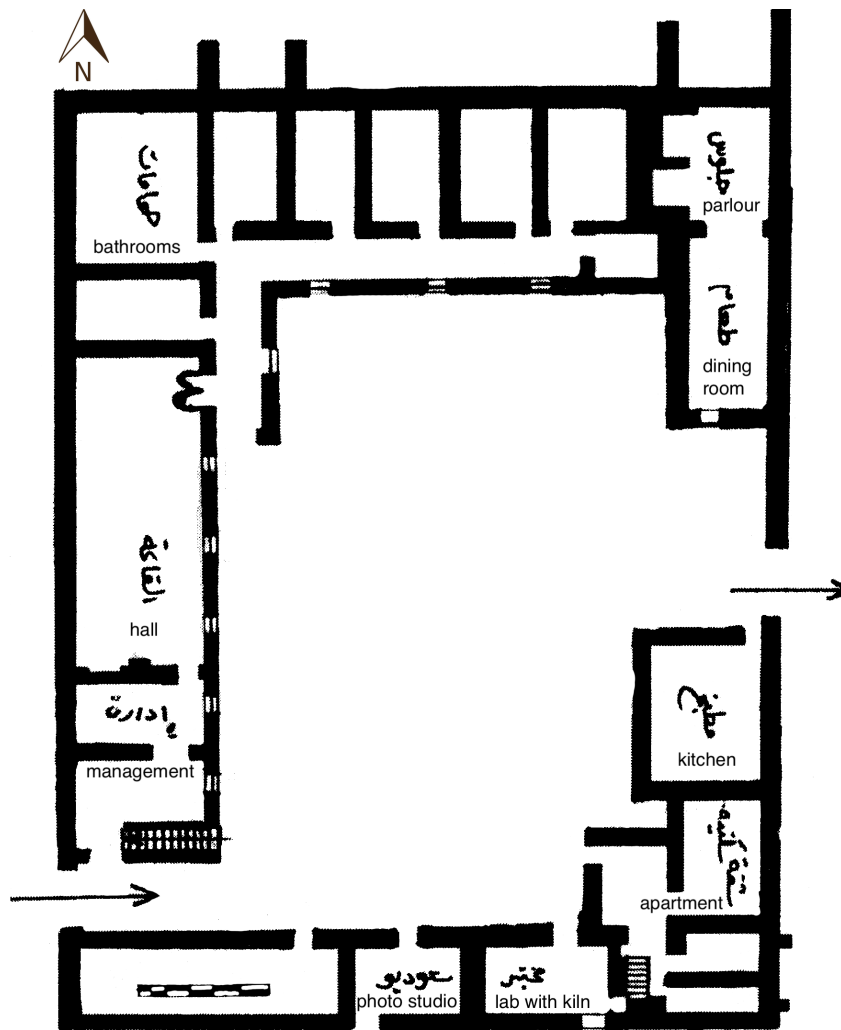


Fig. B4.1: Ground plan of the excavation house before the 1978 SBAH renovations: ground floor. Reproduced from Jarjis 2020, 47, with English annotations prepared by Jana Richter based on information from Jarjis 2020, 23.

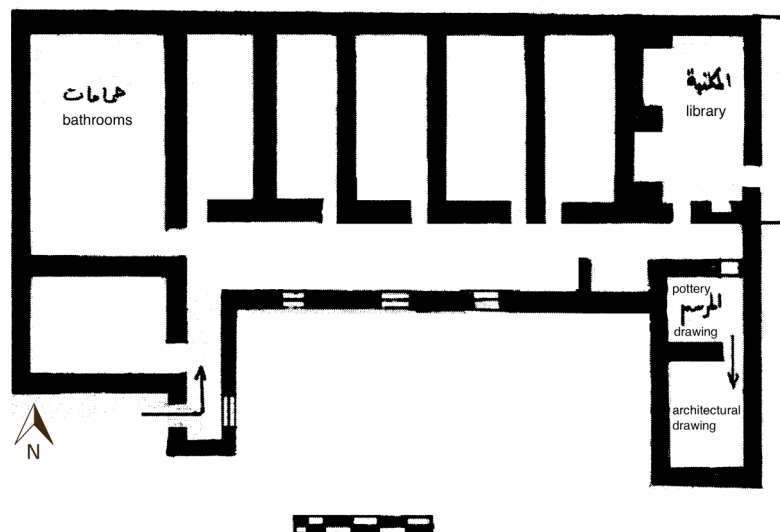


Fig. B4.2: Ground plan of the excavation house before the 1978 SBAH renovations: first floor of the north wing. Reproduced from Jarjis 2020, 49, with English annotations prepared by Jana Richter based on information from Jarjis 2020, 25.

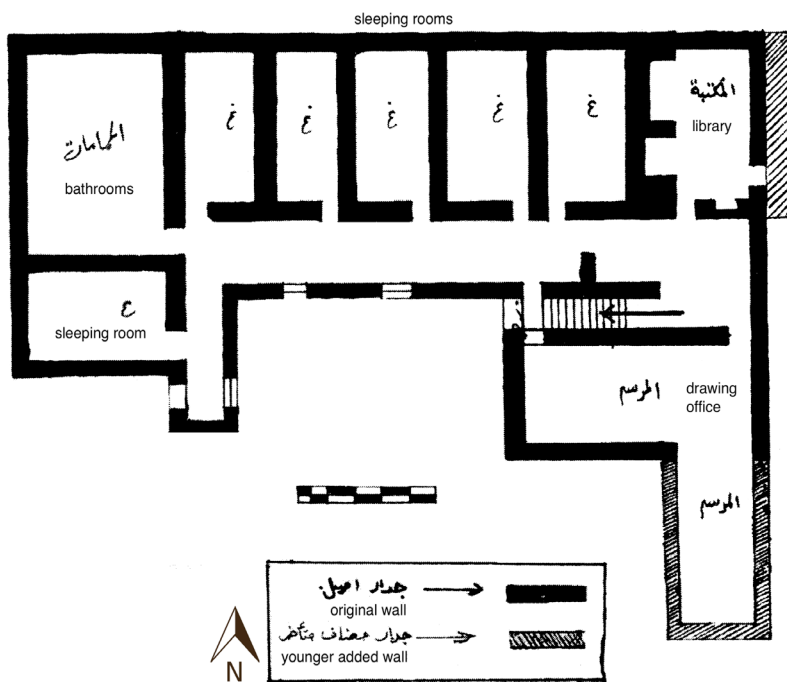


Fig. B4.3: Ground plan of the excavation house after the 1978 SBAH renovations: first floor of the north wing. Reproduced from Jarjis 2020, 61, with English annotations prepared by Jana Richter.



Fig. B4.4: View of the stone-lined façade of the southeastern corner of the excavation house as seen from the courtyard in November 2023. Photo by Andrea Squitieri.

comparison with a photograph taken in the spring of 2023 (**Fig. B5.6**) shows that only one of them survives today.

As part of the SBAH refurbishments, the inner courtyard, which had been purely functional in Andrae's times, was turned into a garden. A lawn was created and trees and shrubs were planted, while the path connecting the western and eastern wings was lined with climbing plants

that were grown over an overhead trellis to provide shade. Jörg Fassbinder's 1989 photos show the pleasant results (**Fig. B4.8-B4.9**).

Inside the house, it is striking that several of the building parts with reportedly authentic roofs also feature deep arched niches set into thick walls. Most probably, these are blocked entrances that had formerly connected storage rooms or led to the courtyard (**Fig. B4.10**). When using the presence of these niches as a criterion for determining the original parts of the building, it becomes clear that even today, every wing includes at least a few metres of authentic old walls. While not one complete wing of the original construction has survived, neither is there any area that the SBAH team needed to build from scratch.

Some of the oldest preserved architectural elements are found in what is today known as the "heritage part" in the west wing of the building. However, it is worth emphasising that its largest room, the so-called Great Hall (**Fig. B4.11**; room no. 13 in **Fig. B5.1**), differs in its representative character very substantially from the semi-open, unplastered find storage that Andrae had constructed in 1903-1904 and used until the end of his tenure at Assur. During Peter Miglus' excavations in 2000 and 2001, this room served the team as a dining hall, with a life-sized cardboard cutout of Saddam Hussein installed by SBAH looking on.⁴⁰

In preparation for Miglus' work at Assur, the Deutsche Orient-Gesellschaft funded the renovation of the north wing of the excavation house in 2000.⁴¹ In that part, the roof and walls were repaired and repainted, and new windows and doors as well as water pipes were installed. In the wing's northwestern corner, a bathroom was set up on the first floor and a kitchen on the ground floor. Moreover, all rooms were equipped with new furniture, including beds, cupboards, tables and chairs. These measures were carried out

under Miglus' supervision by Wathek Hindo (Baghdad), who at the time also refurbished the excavation house at

⁴⁰ As observed by Karen Radner, who was part of the excavation team in 2001.

⁴¹ Miglus 2000, 14.

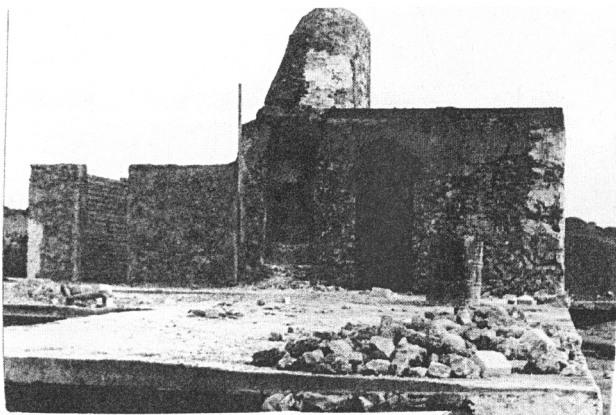


Fig. B4.5: View from the courtyard onto the house's northeastern corner in 1978, showing the only surviving portion of the first storey. Photo by Mr Muthhir for SBAH Sherqat; reproduced from Jarjis 2020, 73.



Fig. B4.8: Looking west from the roof across the garden in the courtyard of the excavation house in April 1989. Photo by Jörg Fassbinder.



Fig. B4.6: View from the river bank onto the house's northeastern corner in 1978, where the construction of the balcony is in progress. Photo by Mr Muthhir for SBAH Sherqat; reproduced from Jarjis 2020, 75.



Fig. B4.9: Looking towards the eastern entrance through the covered path leading through the courtyard in April 1989. Photo by Jörg Fassbinder.



Fig. B4.7: Manfred Stephani reading on the balcony overlooking the bank of the Tigris in April 1989. Photo by Jörg Fassbinder.

Kish for the Japanese team from Kokushikan University led by Ken Matsumoto.⁴²

B5. The Andrae House today

During the most recent restoration work undertaken in 2022-23, we generally did not introduce any further structural changes to the ground plan of the building (**Figs. B5.1-3**), with two exceptions. On the ground floor, we closed off the entrance door that led into the large room of the south wing, which had been created only after Andrae's tenure at Assur (**Fig. B5.4**; see **§B3**). Access to the house is now exclusively provided through

⁴² Peter Miglus, pers. comm. (email of 13 December 2023).

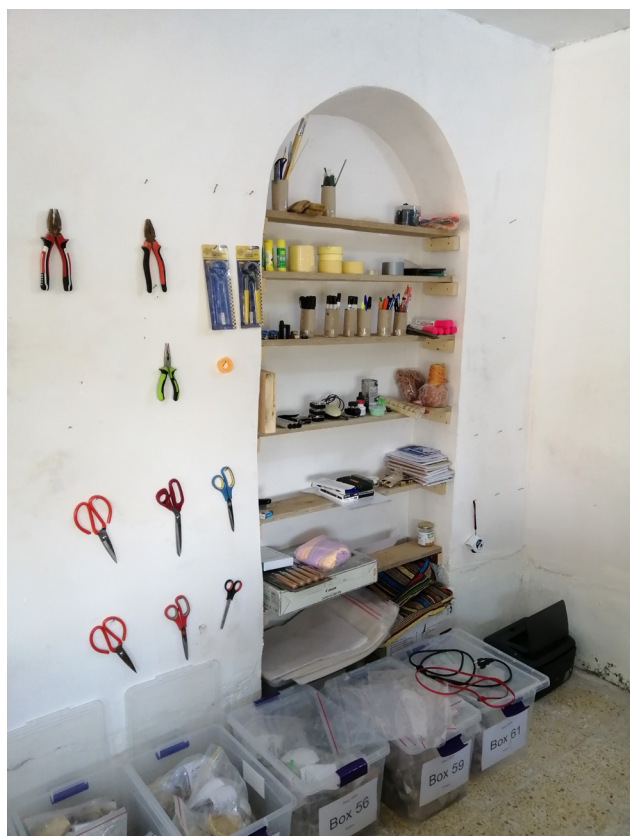


Fig. B4.10: A door-shaped niche in the western wall of the pottery lab (Room 8 in **Fig. B5.1**), used as a shelf space in 2023. Photo by Jana Richter.

the two courtyard gates in the east and the west, which are closed and locked at night, thereby sealing off the entire building (**Fig. B5.5**). Furthermore, in the first storey's northwestern corner, we turned a formerly doorless storage area into an additional small bedroom (Room 10a in **Fig. B5.2**).

In its present incarnation, the ground floor of the Andrae House offers space to accommodate find processing in the pottery and small finds lab in the northern part of the east wing, in the Great Hall of the west wing and in the outdoor areas of the courtyard and along the Tigris bank (**Figs. B5.6-7**). In the northwestern corner, on either side of the new ground-floor bathroom facilities, there is a restoration lab with its window facing west, for better light (room no. 12 in **Fig. B5.1**), and a workshop for wood and metalworking, with a window to the north (room no. 6 in **Fig. B5.1**). The remainder of the rooms on the north wing's ground floor provides storage and house either newly-built metal shelves bearing closed plastic boxes with pottery or the specialised drilling equipment for coring (room no. 10 in **Fig. B5.1**).

The room next to the staircase, with windows towards the courtyard, is occupied by the male Kurdish members



Fig. B4.11: The southern end of the Great Hall, before and after restoration 2023. Photographs by Akam Omar Ahmed Al-Qaradaghi.

of the team (room no. 9 in **Fig. B5.1**). The metal lattice door outside this room and the staircase can be locked to seal off this part of the north wing and thus also its first floor. The upper storey houses the non-Iraqi team members' bedrooms, a further bathroom and two office rooms, with a staircase providing access to the roof.

Returning to the ground floor, human and animal bones are stored in the northeastern ground floor room, accessible through the pottery and small finds lab in the east wing. All archaeological finds and samples from the excavation are delivered to the east gate by the Tigris, where also the door to the lab is located. The pottery is washed and dried outside the house along the river bank, and the flotation machine is set up there too as water is brought up from the Tigris with an electric pump.

The excavation tools are stored in the large room in the south wing, near the western entrance to the house; during the field season, most of this equipment stays on site in two tents and under the supervision of a guard who sleeps there. The rest of the south wing, including

its two-storey southeastern corner with an internally accessible, private section of the roof, is occupied by the rooms and bathroom facilities reserved for SBAH staff and guards, some of whom permanently reside in the house during the campaign. The southern part of the east wing houses the kitchen and the dining hall that serve the entire team. The water for the sanitary facilities and the kitchen is brought in from Sherqat's water purifying plant by truck and stored in two tanks set up on the northwestern and southeastern corners of the excavation house's roof.

In a working environment that relies heavily on computers and uses river water that is drawn with an electric pump from the Tigris, supplying the necessary electrical power turned out to be challenging, and sometimes damaging for the equipment. During the first excavation season in spring 2023, we had to rely on a combination of electricity provided by the government (for only four hours per day, not always at regular times), electricity provided by the nearest community diesel generator to which we were linked by an overland cable across a distance of about two kilometres (supplying power for another four hours per day), and electricity produced by our own, far less powerful diesel generator that could only be operated for a maximum of two hours at a time. This not only often proved insufficient for our needs but the transitions between these power supplies were difficult to manage, too.

During the spring campaign, following advice from SBAH, the excavation house was further secured by re-

storing the existing but badly dilapidated fenced enclosure with its own gate and guardian's house (visible in the background of **Fig. B5.7**). Cars can now only approach the excavation house through that gate, which lies northwest of the building. Additional pedestrian access is provided through a lockable door in the southern perimeter of the fence; this is the quickest way on foot or by bicycle (of which we have two in use) to the excavation area in the New Town.

In this new situation where SBAH considered the house and its contents reasonably safe also when no one is in residence, the decision was taken to install solar panels and a photovoltaic system that would provide the necessary power to run the house reliably (**Fig. B5.8**). Subsequently, Karen Radner secured funding from the Bavarian State Ministry for Science and Art, represented by Minister of State Markus Blume, and the Austrian Embassy in Baghdad, represented by its chargé d'affaires ad interim, Dr Andrea Nasi. The system was installed by a specialist company based in Sulaymaniyah in August 2023 and successfully put to the test when part of the team returned in November 2023 for a pottery study season. In the meantime, the main beneficiary of the stable supply of solar power has been the garden that Karen Radner and Jörg Fassbinder had planted in the spring of 2023, as the water pump originally installed to serve the flotation machine's tank now serves to deliver water to the citrus, pomegranate, apple and fig trees that have joined the surviving date palm and its newly planted companion (**Fig. B5.9**).

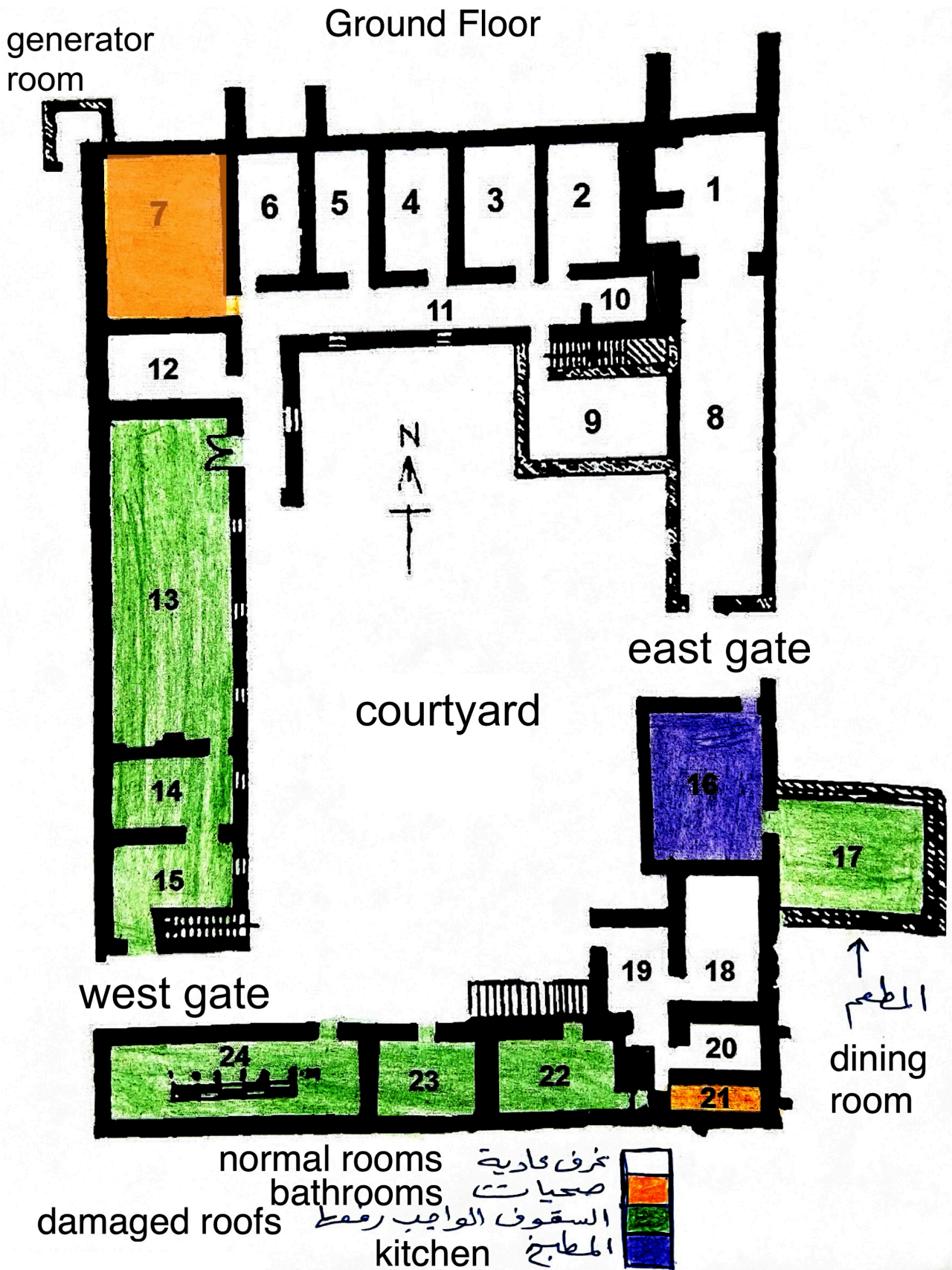


Fig. B5.1: Ground plan of the excavation house as of 2023: ground floor. Provided by SBAH Sherqat, annotated by Salim Abdullah Ali, with English labels prepared by Andrea Squitieri.

North wing: first floor

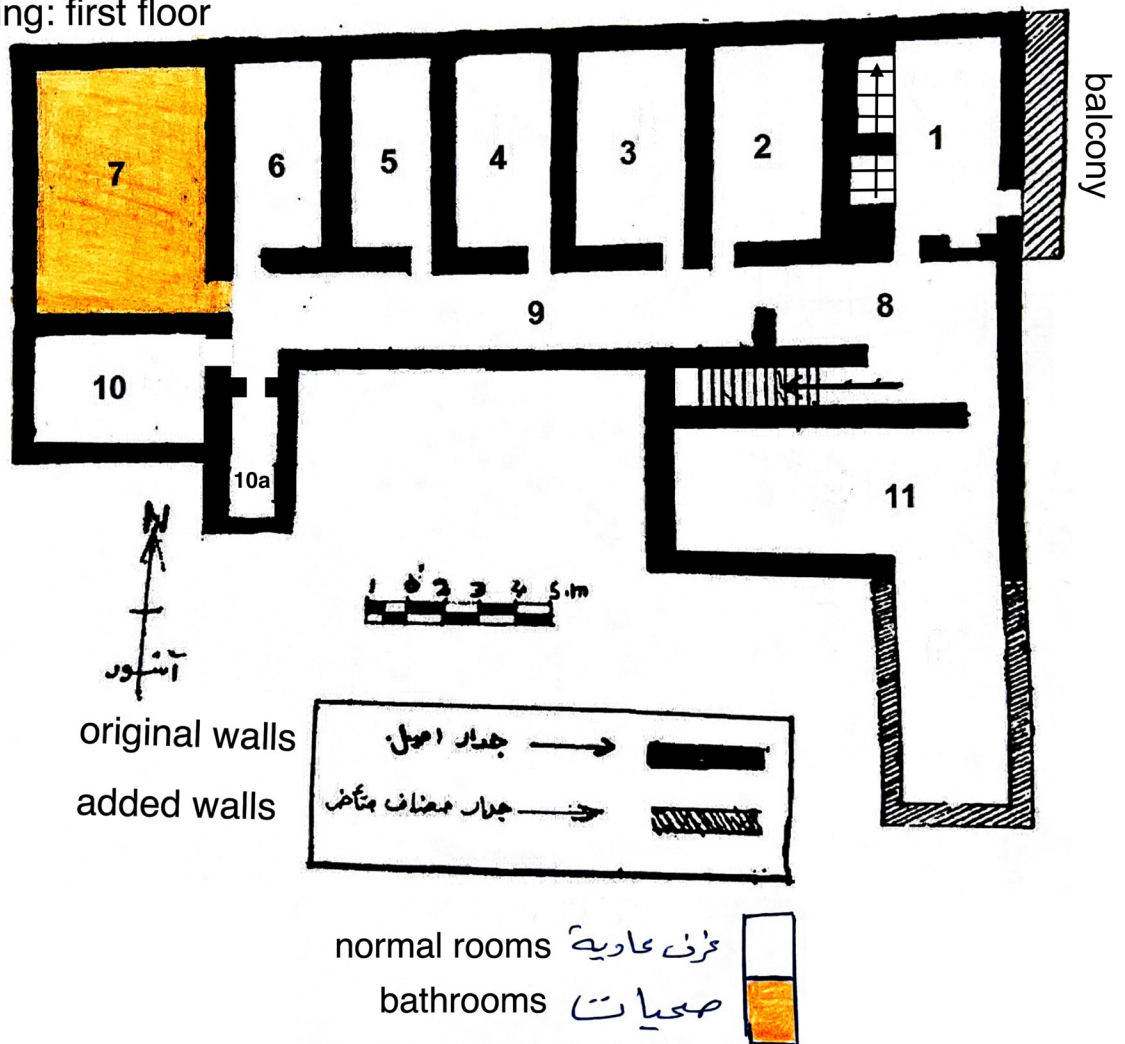


Fig. B5.2: Ground plan of the excavation house as of 2023: first floor of the north wing. Provided by SBAH Sherqat, annotated by Salim Abdullah Ali, with English labels prepared by Andrea Squitieri.

South wing: first floor

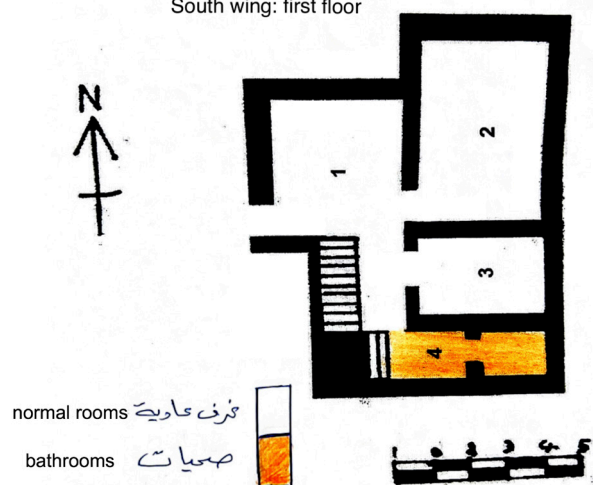


Fig. B5.3: Ground plan of the excavation house as of 2023: first floor of the south wing. Provided by SBAH Sherqat, annotated by Salim Abdullah Ali, with English labels prepared by Andrea Squitieri.



Fig. B5.4: View of the south wing of the excavation house, with the closed-up door visible in the centre of the façade. Photo by Andrea Squitieri.



Fig. B5.5 View of the west gate as seen from the courtyard, with the two plaques installed by SBAH Sherqat in commemoration of Walter Andrae's work at Assur and of the restoration of the excavation house in 2023 visible on the left-hand side between the doors leading into the excavation tool storage and the guard's room. Photo by Andrea Squitieri.



Fig. B5.6: A view from the balcony of "Andrae's office" towards the bank of the Tigris, showing the areas used as a sherd yard for pottery drying and sorting as well as taking collection photographs. Photo by Karen Radner.



Fig. B5.7: The flotation machine and the pottery washing platform, provided with water pumped up from the Tigris; the water tank is out of view towards the west. Beyond the fence demarcating the area of the excavation house, note the ziggurat and the remains of the Aššur temple where families are having holiday picnics on the occasion of the spring equinox (Nowruz) on 21 March 2023. Photo by Karen Radner.



Fig. B5.8: The solar panels installed on the roof of the south wing, with a view of the two-storey part of the building housing the SBAH staff. Photo by Andrea Squitieri.



Fig. B5.9: View over the garden in the excavation house's courtyard in early November 2023. Photo by Andrea Squitieri.

C. Mapping, geophysics and sediment coring in Assur, 2023

C1. Mapping Assur

Jens Rohde & Andrea Squitieri

A team led by Jens Rohde and Andrea Squitieri, with the participation of Cajetan Geiger, Jan Heiler and Jean-Jacques Herr, undertook a mapping survey across the New Town of Assur from 9-13 February 2023, with the following goals:

- to measure and create two fixed points with very high precision to be used as benchmarks for the entire site of Assur, for present and future use;
- to measure and create fixed points across the New Town, based on these benchmarks, for present and future use;
- to place temporary markers across the New Town, to use for the drone mapping undertaken at the time; and
- to establish the grids used for the magnetometer prospection (§C2) and the excavation (§D).

Since no official benchmarks were available in the vicinity of Assur, we created them by measuring two points with a high level of precision. The decision was made to place these points on the roof of Andrae’s house in the locations shown in **Fig. C1.1** by drilling a metal bar into the roof. The two points were named AS_house_01 and AS_house_02. We used a Leica GS18 T GNSS RTK as a rover and a Leica Viva GS10 as a base; they were connected to each other via a radio connection. The first step was to place the base on AS_house_01 and the rover on AS_house_02, maintaining this setting for 12 hours while both the base and rover measured. The base was set to measure on an “unknown point”. After the first round of measurements, we kept the rover’s final measurement. We then repeated the same setting with the base and rover reversed (the base now on AS_house_02 and the rover on AS_house_01), but this time we set the base over a known point (the rover’s last measurement). We maintained this setting for another 12 hours. Once again we kept the rover measurement of AS_house_01. Finally, we moved the base on AS_house_01 using the rover’s final measurement as a base point, and with this base, we re-measured AS_house_02 with the rover. With this method, we obtained two base measurements of AS_

house_01 and two rover measurements of AS_house_02 over an arc of 24 hours. The coordinates obtained, using the system WGS 84/UTM zone 38N, are:

Benchmark	Latitude (X)	Longitude (Y)	Altitude (Z)
AS_house_01	342427.701	3925227.226	168.133
AS_house_02	342446.273	3925205.443	168.042

Our second task was to create fixed points in the southern part of the New Town, around the target area for the excavation, as shown in **Fig. C1.1**. The fixed points were labelled ASo1 to ASo4. Subsequently, we measured them with the DGPS rover after placing the base on the benchmark AS_house_01. Measurements were taken for thirty minutes on each point. The coordinates obtained are:

Fixed point	Longitude (X)	Latitude (Y)	Altitude (Z)
ASo1	342673.865	3924371.741	162.333
ASo2	342689.938	3924221.942	161.230
ASo3	342523.933	3924335.873	156.022
ASo4	342532.598	3924466.467	158.930

These fixed points were used to create the grid for the magnetic survey and the excavation grid (§C2, §D1.1).

With the help of the local police guards, we were able to identify five of the points that had been placed by Manfred Stephani (cf. **Fig. B4.7**) in 1989 across Assur.⁴³ The Hrouda team had placed more such points, but most of these are no longer visible on the ground. We measured the identified points and named them AS23_HROUDA_ number (using the numbers indicated on the points themselves).

Fixed point	Longitude (X)	Latitude (Y)	Altitude (Z)
AS23_HROUDA_14	342002.53	3925383.42	178.638
AS23_HROUDA_15	342277.84	3925224.96	185.457
AS23_HROUDA_20	342447.22	3925250.09	161.713
AS23_HROUDA_27	341645.19	3925280.57	175.816
AS23_HROUDA_28	341946.61	3924966.21	185.306

⁴³ Stephani 1991.

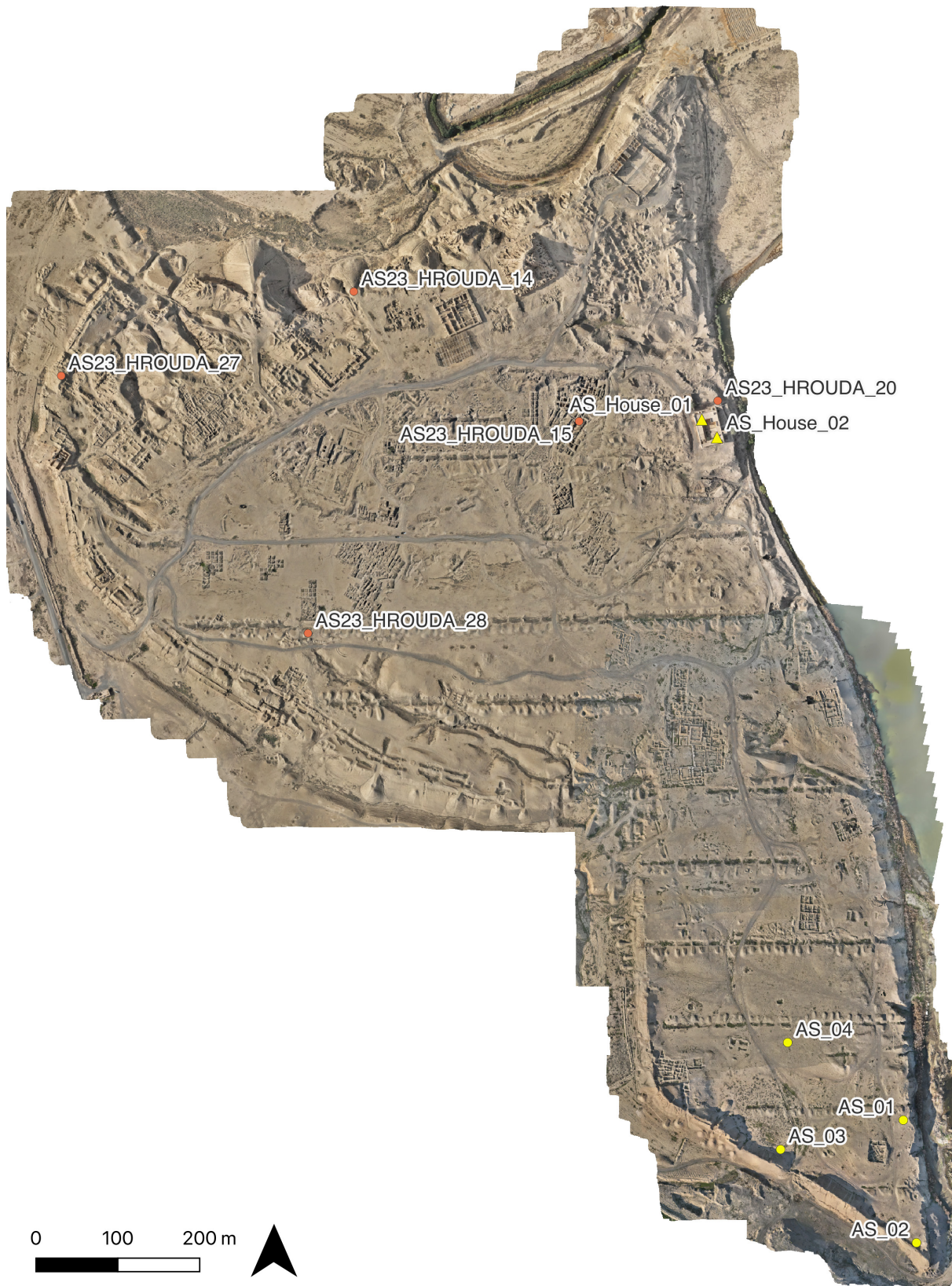


Fig. C1.1: Combined orthophoto of Assur showing the fixed points (yellow dots) and the benchmarks (yellow triangles) established in the 2023 campaign. The fixed points placed by the Hrouda team in 1989/90 are indicated as orange dots. Main Town orthophoto created by Jan Heiler, courtesy of Peter Miglus (Heidelberg University). New Town orthophoto created by Jens Rohde. Annotated by Andrea Squitieri.

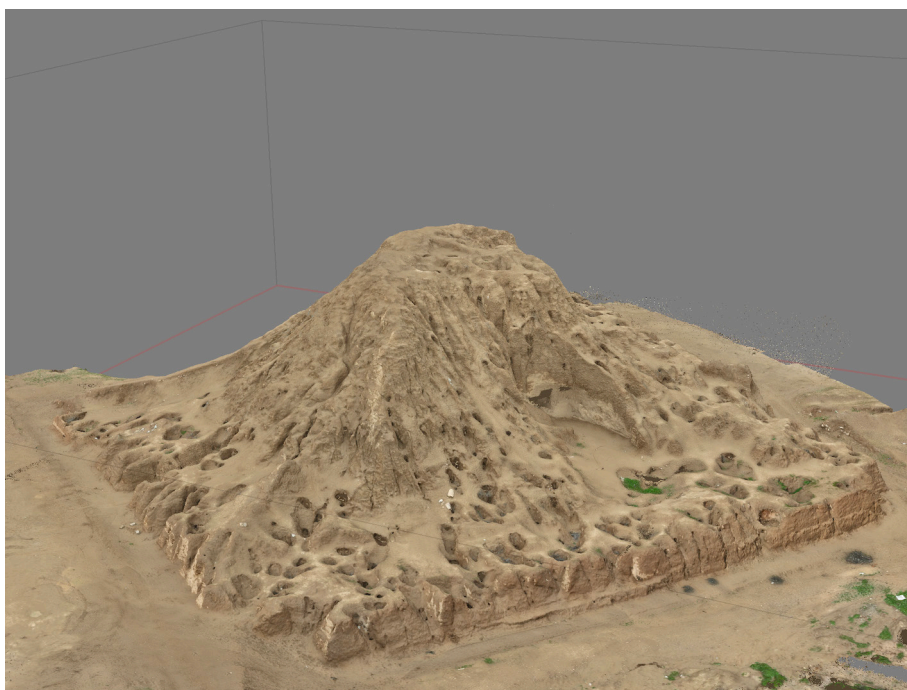


Fig. C1.2: Screenshot of the 3D model of the ziggurat of Assur created by Jens Rohde.

After taking these measurements, we mapped the New Town by drone photography. For that purpose, we placed temporary markers on the ground and measured them using the dGPS. Subsequently, we made three drone flights, flying at a height of less than 40 m over the surface. The drone employed is a DJI Mavic 3 Pro drone owned by LMU Munich's History Department. The drone photos were then processed using the software package Agisoft Metashape to create orthophotos, Digital Elevation Models (DEM) and 3D models of the target area.

At a later stage, a 3D model of the ziggurat was created at the request of the Sherqat SBAH office (**Fig. C1.2**).

C2. Geophysical prospecting in Assur, 2023⁴⁴

C2.1 Magnetometer prospecting at Assur, 2023

Jörg Fassbinder, Jean-Jacques Herr, Marco Wolf & Lena Ruider

In recent years, magnetometer prospecting, which was for the first time applied in 1956 in England by Martin Aitken and John Belshé,⁴⁵ has developed into a very powerful tool to map large archaeological sites in detail be-

fore or even instead of excavation.⁴⁶ This has been the result of both the technical and scientific development of archaeological geophysics, as well as the wide acceptance of the method among archaeologists.⁴⁷ The resumption of fieldwork at Assur by a team headed by Karen Radner (LMU Munich) and F. Janoscha Kreppner (University of Münster) offered the chance to apply once again geophysical methods at Assur.

The ancient city of Assur plays a crucial role in the field of archaeological geophysics in Iraq as it offers the possibility of large-scale magnetometer prospecting. The very first archaeo-geophysical measurements in Iraq were carried out already in the 1960s. From 1969 to 1972, Guiseppa Ratti and his colleagues Roberto Pra-

to and Giorgio Mortinotti measured both magnetic and resistivity profiles on selected areas in Seleucia, situated in central Iraq not far from Baghdad, in order to detect ancient canals, kilns and fireplaces on the site. The team conducted four prospecting campaigns in Seleucia, with some additional work also undertaken in Hatra in northern Iraq, for a total duration of 7 months. For their magnetic measurements, they applied a proton magnetometer (Elsco type 592/N) with a sensitivity of 1 nanotesla and a measurement frequency of 6 seconds per point.⁴⁸ Although they claim to have performed geophysical mapping, the published works present solely magnetic profile measurements instead of contour maps.⁴⁹ Besides magnetic measurements, the same team also conducted electric resistivity measurements in Hatra, but due to the dry conditions during the summer, these were not successful.

It was Barthel Hrouda, then professor of Near Eastern Archaeology at LMU Munich, who undertook pioneering efforts to introduce and apply geophysical methods in the Middle East when he invited Helmut Becker to perform archaeomagnetic dating on samples from Isin in southern

⁴⁶ Fassbinder 2023.

⁴⁷ Stone 2023.

⁴⁸ Ralph 1964.

⁴⁹ Ratti 1971; Lanza/Manzini/Ratti 1972. For the still severely restricted image processing and display of data of that time see Scollar/Krückeberg 1966.

⁴⁴ This chapter was language-edited by Karen Radner.

⁴⁵ Belshé 1957; Aitken 1958; 1961.

Iraq in 1976.⁵⁰ Because of the Iran-Iraq War (1978-1988), it took another 13 years before Hrouda was able to organise a first magnetometer prospection. Meanwhile, the method for a “large scale” magnetometer survey had been developed and automated by Becker and Jörg Fassbinder at the Bayerisches Landesamt für Denkmalpflege (BLfD) in Munich. In 1989, this method was applied for the first time to an archaeological site in Iraq, namely Assur.

None of the archaeological work undertaken at Assur since 1989 involved or applied geophysical measurements. The resumption of fieldwork in 2023 offered Jörg Fassbinder the chance to return to Assur to continue the large-scale magnetometer survey on the site as well as introduce additional geophysical methods to the site.

C2.1.1 The data of the 1989 magnetometer survey at Assur

The first magnetometer survey in Assur was conducted in April 1989 with a caesium magnetometer Scintrex/Varian CS-V101 in a so-called “variometer” configuration.⁵¹ One survey probe was carried ca. 30 cm above the ground while the second magnetometer probe served as a basis for the removal and corrections of diurnal variations and other secondary variable disturbances coming from technical installations located near the survey area. In a measuring grid of 20 × 20 m with a profile spacing of 50 cm, we obtained 1600 measured values (Fig. C2.1). The frequency of magnetic data collection with the new caesium magnetometer Scintrex/Varian CS-V101 was 10 times



Fig. C2.1: Magnetometer prospecting in Assur in April 1989, with Jörg Fassbinder operating the handheld caesium magnetometer (Varian 101) in the so-called “variometer” configuration. Photo by Manfred Stephani.

⁵⁰ These samples remain untouched and are kept in the geophysics storage of LMU Munich’s Department of Earth and Environmental Sciences.

⁵¹ Becker 1991.

per second with a sensitivity of 0.1 Nanotesla. We used our newly developed semi-automatic data storage system on a handheld Epson HX-20 computer with a mini-tape recorder, then commonly used by dictation machines. In less than three weeks, we were able to survey an area of 2 hectares in the main part of the city of Assur, with a spatial resolution of 50 × 50 cm.

Once back in the Munich laboratory, we transmitted the data to an IBM DEC computer for further processing and visualisation of the data as a magnetogram image. Hardcopies from the magnetogram were produced by taking photographs of the computer screen.

The data was archived at the Bayerisches Landesamt für Denkmalpflege on an IBM DEC computer and magnetic tapes readable by the Epson HX-20 handheld computer. In 1996-97, in the course of routine maintenance for all data produced by the geophysical team led by Helmut Becker and Jörg Fassbinder, these old recordings were transferred to a PC running on Microsoft Windows NT and transformed into files readable by PCs with DOS and Windows operating systems. This also included the material for Assur. In 2015, the original data from 1989 was recovered by applying old programs, reprocessing and displaying them by using up-to-date visualisation programs (i.e., Geoscan, Geoplot 4 and Golden Software Surfer) in order to present these measurements as high-resolution magnetogram images.

In 2023, the 1989 data set was merged with the new data of 2023, without further processing. The magnetic anomalies can now be displayed and visualised using the same dynamics (Fig. C2.2).

C2.1.2 Resuming magnetometer prospecting at Assur in 2023

The city of Assur is situated on the western bank of the Tigris. The city lies on a slight elevation ca. 10 m above the average water level above the river. Fortification walls enclose the city, which are still preserved to a height of c. 10 m in many parts. Inside lies an area covering ca. 0.65 square kilometres, extending ca. 1500 m in the north-south direction and between 500 and 700 m in the east-west direction.

Walter Andrae investigated this large area by digging a series of parallel excavation trenches across the entire city in east-west direction. These and other, more recent excavation trenches and the big heaps of excavated soil create an uneven and irregular surface. On the one hand, this situation impedes the creation of a complete magnetogram. On the other hand, conducting multi-channel magnetometry with a wheeled device is utterly impossible, and

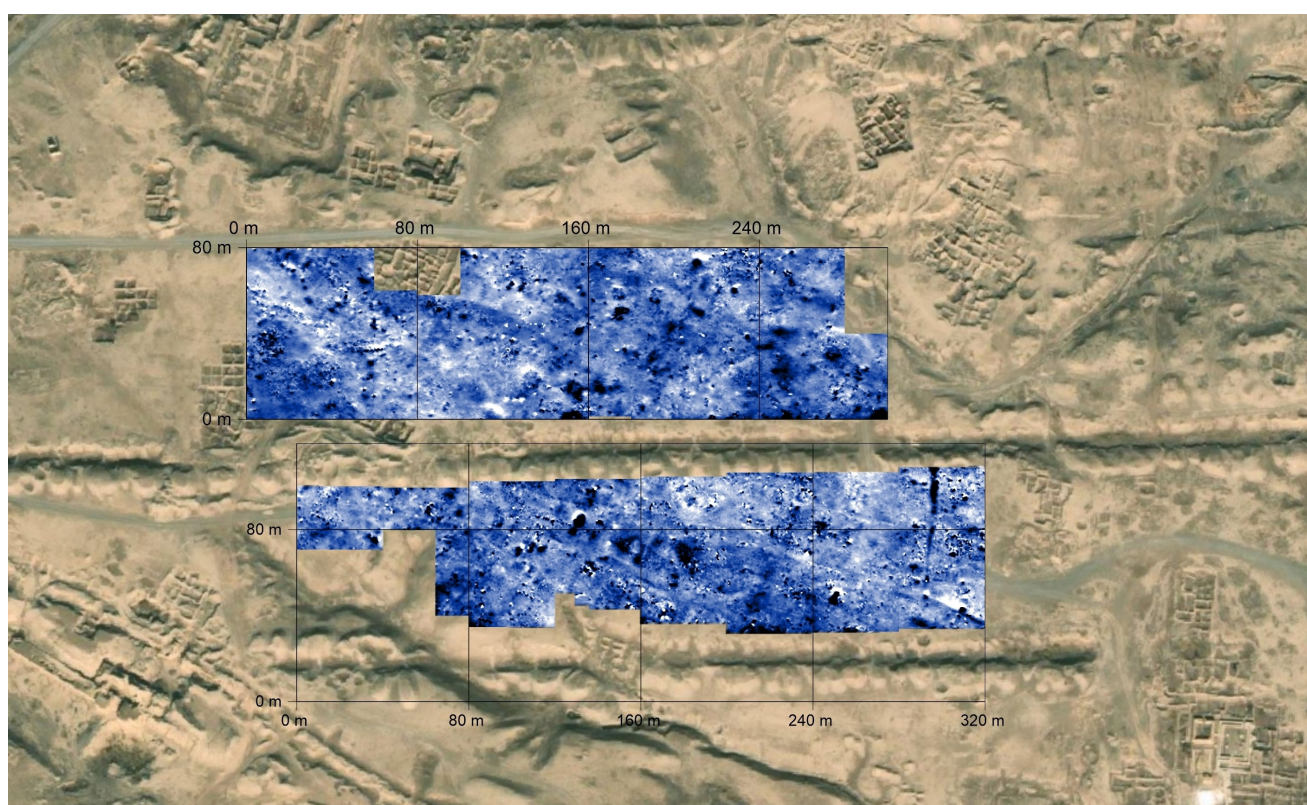


Fig. C2.2: Magnetometer measurements of the survey areas Ass23b and Ass89a taken in the “Mittlere Unterstadt” of Assur (Fassbinder/Becker/Wolf/Herr). In 1989, the caesium Scintrex/Varian CS-101 magnetometer was applied in a single sensor variometer configuration, with a sensitivity of ± 0.10 nanotesla, using a sampling density of 50×50 cm; dynamics ± 30 nanotesla in 256 grey scales. In 2023, the caesium total field magnetometer Geometrics G-858-special was applied in duo-sensor configuration, with a sensitivity ± 10 picotesla, using a sampling density of 25×50 cm; dynamics in 256 grey scales; 40 m grid; total Earth’s magnetic field at Assur (02/2023): 46.180 ± 30 nanotesla.

the same applies to geophysical drone prospecting.⁵² The only option is therefore to use the handheld magnetometer and to produce a mosaic of magnetograms across the entire city wherever the terrain permits it.

The new geophysical survey in Assur aims to obtain an archaeological overview of the organisation and design of the city and to support the renewed excavations in the New Town. From a variety of potential survey methods, we chose the magnetometer prospecting method. Magnetometry is a “passive” method that measures the variation in the ambient Earth’s magnetic field. “Active” methods, namely radar and resistivity prospecting, are suitable for detecting stone buildings, but the application of these methods is time-consuming and requires suitable ground conditions, both topographically and geochemically. The delimiting boundary conditions at Assur are twofold. Firstly, we are dealing with sandy clay soils, which can dampen the penetration of the radar waves. Secondly, the rough and uneven topography of the site

renders a high-resolution radar survey impossible. Resistivity prospecting, on the other hand, is not only the most time-consuming prospecting method but its results might also be limited by the poor conductivity of the almost entirely dry, sandy topsoil layers at Assur. These theoretical assumptions, however, should be tested on selected areas in the future.

Therefore, at this stage of the project, magnetometer prospecting remains the most suitable method for a large-scale and high-resolution prospecting. The already-mentioned poor terrain conditions at Assur, however, pose a great challenge. Parts of the area are partly inaccessible due to the presence of deep trenches left by previous excavations, and other parts are covered by heaps of excavated soil and/or stones to a height of up to 3-4 m. These conditions require magnetometer equipment and a special configuration that tolerates tilting the instrument and does not require keeping precisely the same distance to the ground.

In order to reach the highest possible sensitivity combined with a maximum speed of prospecting and merge the new data with the 1989 measurements, we adapted

⁵² Stele *et al.* 2023.



Fig. C2.3: Magnetometer prospecting in Assur in February 2023, with Jean-Jacques Herr operating the handheld duo-sensor caesium magnetometer. Photo by Jörg Fassbinder.

and modified our caesium total field magnetometer (Geometrics G-858). We applied both sensors not as vertical gradiometers but in the so-called “duo-sensor” configuration. In this configuration, we mount the probes parallel to each other on a wooden frame and carry them in zigzag mode c. 30 +/- 10 cm above the ground (**Fig. C2.3**). The profiles of our 40 × 40 m grid were oriented east-west to minimise technical disturbance and interactions of the magnetometer probes with the electronic parts and the batteries of the device. The great advantages of this configuration have been described in greater detail in many previous publications.⁵³ In short, in comparison to fluxgate or other gradiometer measurements, the resulting data of the “duo-sensor” configuration provide us with higher magnetic intensity, hence more information on the buried features and more so on deeper parts of the archaeological layers and structures.⁵⁴ Compared to other methods, the interpretation of magnetic data is very complex and often does not provide clear results.

Therefore, in order to interpret the results obtained from Assur, we applied a combined interpretation using:

1. the intensity of the magnetic anomaly (based on magnetic properties);
2. the “magnetic shape” of the feature (based on archaeological science);
3. the direction and intensity of the remanent magnetisation of the feature;
4. the induced magnetisation of building materials (based on in situ measured volume magnetic susceptibility);
5. the morphological analyses of the topography of the site (based on ground observations and assessment of the orthophotos and the DEMs provided by the drone).

Points 1, 3, and 4 are based on the theoretical background of applied geophysics and rock magnetism. Supplementary susceptibility measurements allow us, for example, to assign positive and negative anomalies to the same archaeological structure (**Fig. C2.4**). In situ magnetic susceptibility measurements carried out on the site include measurements on rocks used for buildings, on topsoil and as well on baked bricks we found in the survey area (**Fig. C2.5**).

The intensity of the magnetic anomalies in Assur has a similar range to those of other archaeological sites in Iraq, including the Dinka Settlement Complex in the Kurdish Region of Iraq, Khorsabad (ancient Dur-Sharrukin) in northern Iraq, and Uruk, Fara, and Isin in southern Iraq. Interestingly, this seems to be independent of the very different geological conditions present in the different parts of the country. The alluvial sediment of the Tigris characterises the sites located in northern Iraq, while in the south, the Euphrates sediments dominate.⁵⁵

C2.1.3 First results of the 2023 magnetometer prospecting in the New Town of Assur

The total Earth’s magnetic field in Assur in February 2023 ranged around $46,177.5 \pm 17.1$ nanotesla. The magnetogram images generally are dominated by rather strong magnetic anomalies in the range of +/- 25-30 nanotesla.

The first impression of the magnetogram of the entire area, processed as total field measurement without filter, reveals large differences in the magnetic intensity of the topsoil. Dark areas of high magnetic background indicate high activity, which is due to the use of fire and the contamination with magnetic minerals in the topsoil. Areas with lighter colours were found in the southwestern part of the New Town, but partly also between some city quarters and in the northwestern part of our survey area.

It has emerged that Assur’s uneven topography plays a major role in the shape of the anomalies and that it is reflected disproportionately in our results. The old trenches excavated by Walter Andrae, which have left deep linear depressions across the site, show up as negative anomalies, while the small earth mounds left by subsequent archaeological excavations generate high magnetic anomalies and can easily lead to misinterpretation. Consequently, apart from a few exceptions, these anomalies cannot be assessed and interpreted without a precise consideration of the topography. Caution is also advised when interpreting fireplaces. Ideally, this type of feature can only be

⁵³ Fassbinder/Ašandulesei 2016; Fassbinder 2023.

⁵⁴ Linford *et al.* 2007; Mathé/Lévêque/Druez 2019; Hahn *et al.* 2022.

⁵⁵ Hahn *et al.* 2022.

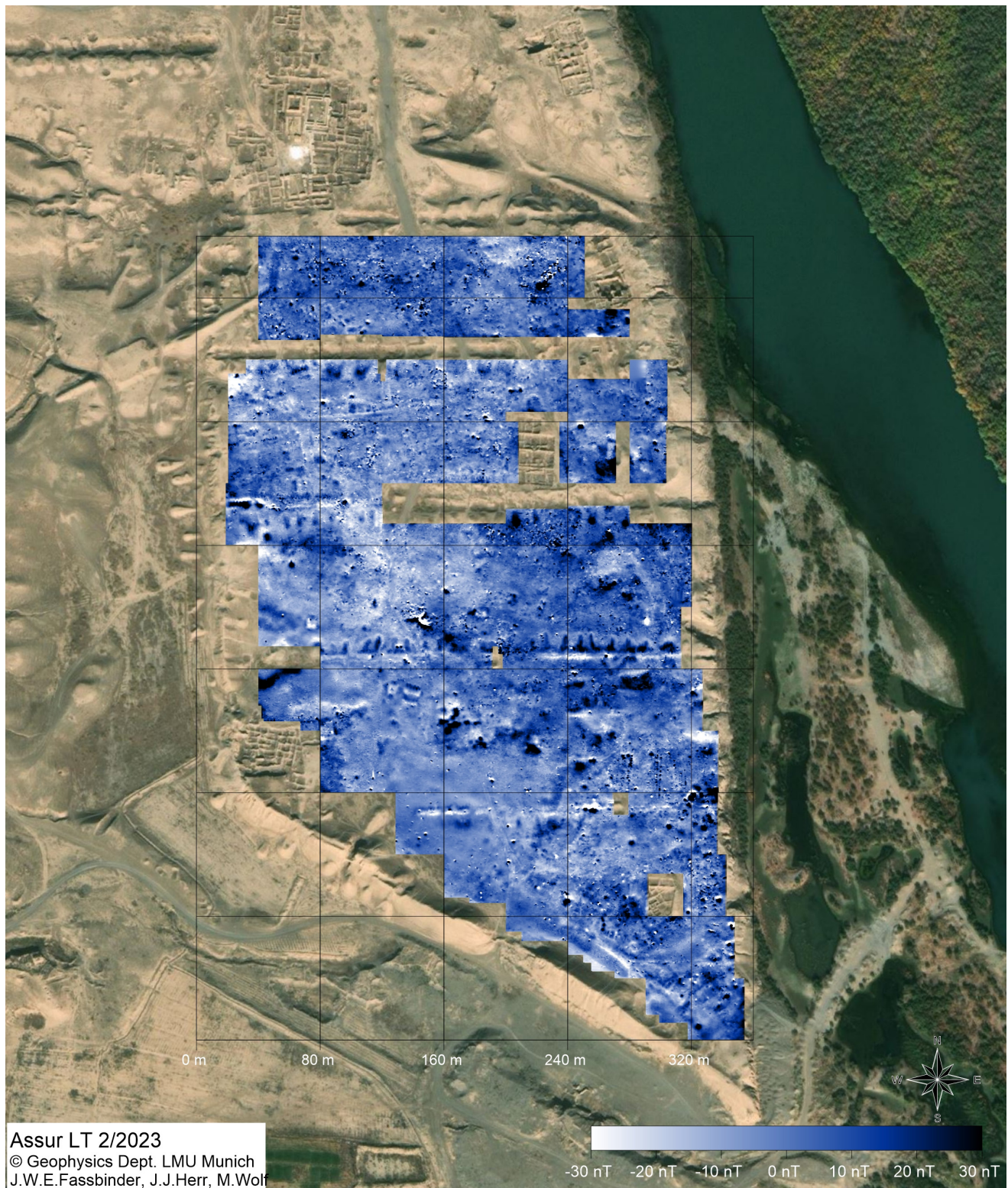


Fig. C2.4: Magnetometer measurement of the survey area Ass23a (520 × 320 m) in the New Town of Assur. Caesium total field magnetometer Geometrics G 858-special in duo-sensor configuration, with a sensitivity of ± 10 picotesla, using a sampling density of 25×50 cm, interpolated to 25×25 cm. Total Earth's magnetic field at Assur 02/2023: $46,177.5 \pm 17.1$ nanotesla, standard deviation.



Fig. C2.5: Magnetic volume susceptibility measurements taken *in situ* in Assur with a handheld Kappa-meter SM30 (Zh-Instruments). Clockwise from top left: Gypsum rocks (diamagnetic, with “negative” kappa value), limestone, baked bricks and topsoil.

distinguished by the metal scrap that occurs in modern barbecue fires but never inside ancient kilns. Furthermore, magnetic anomalies of sundried mudbrick walls can be both positive and negative and in the worst case, traces fade out without contrast into the adjacent soil.⁵⁶

While we had to exclude a wide band of 25 m because of disturbances due to the presence of rubble and litter, especially tin cans and other modern deposits, the interpretation of the new magnetogram of the New Town of Assur indicates the possible presence of c. 180 buildings and more than 101 pyrotechnological installations (kilns) and yielded clear evidence for the magnetic traces of a lightning strike in the centre of our survey area (**Fig. C2.4**). We identified c. 41,000 m² of built-up area within the 150,000 m² of measured area (**Fig. C2.6**).

However, we must stress that Walter Andrae’s excavations in the area of the Parthian Palace demonstrated that the “Parthian” occupation levels can reach a depth of 4 metres, and low-lying occupation levels assigned to that period were identified in the New Town in Andrae’s search trenches 11I to 14I.⁵⁷ As magnetometer prospecting reaches depths of 1–2 m below the surface most if not all structures identified in the magnetogram should belong to this later occupation of the New Town.

In the following, we present our preliminary interpretations. We have limited ourselves to marking the ground maps and orientation of building complexes, while kilns can be easily identified by their high magnetic intensity

and remanent magnetisation. At this time, we chose to refrain from going into further detail as we intend to interpret the data once all accessible areas have been surveyed and the various geophysical measurements completed.

C2.1.3.1 The urban layout of the New Town of Assur

As already observed by Walter Andrae and Heinrich Lenzen, some composite walls built up with gypsum fragments and baked brick fragments are visible directly at the surface of the site; this helped them to reconstruct the urban layout and the road network of the northern part of the New Town, to the south of the so-called Parthian Palace.⁵⁸ The new magnetometer results confirm the presence of certain linear structures that Andrae and Lenzen had identified as streets.⁵⁹ The magnetogram shows the street to the south of the Parthian Palace that they designated as “Ost-West Strasse 11X,” with a width of 3.1 m,⁶⁰ and also the “Ost-West Strasse 12V 13I,” with a width of 3.1 m;⁶¹ in the western part of the New Town, a 4–5 m large northern section of the “Nord-Süd Strasse I” is visible; and to the east, we identified remains of that same street.

Based on the local road networks, the New Town can be divided into two areas of similar size. The northern

⁵⁶ Fassbinder 2017.

⁵⁷ Miglus 1996, plans 155b–156c.

⁵⁸ Andrae/Lenzen 1933, 55.

⁵⁹ Andrae/Lenzen 1933, pl. 2.

⁶⁰ Andrae/Lenzen 1933, 56.

⁶¹ Andrae/Lenzen 1933, 56.

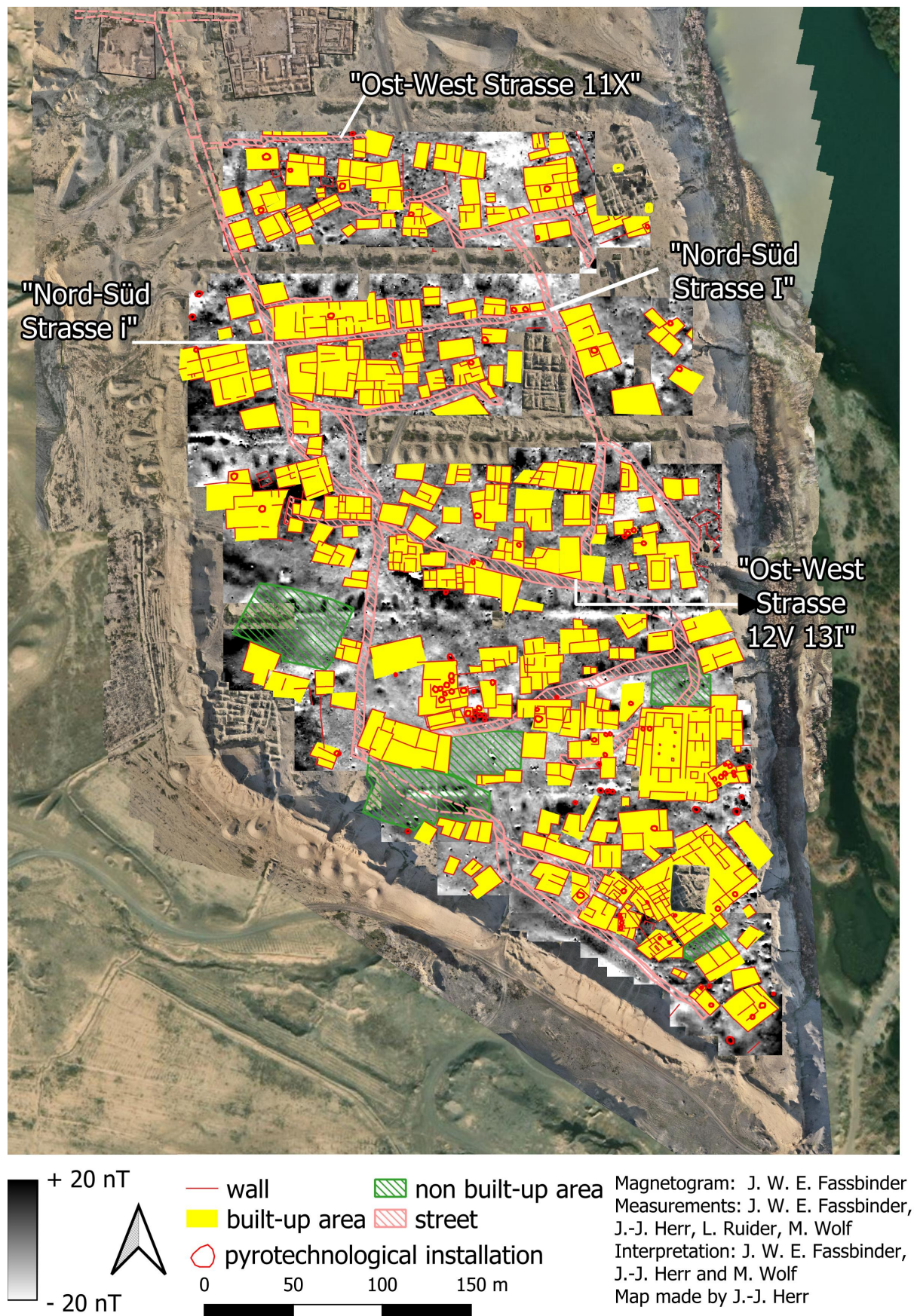


Fig. C2.6: Preliminary interpretation of the magnetic anomalies observed in the New Town of Assur.

half consists of an area of circa 7.2 ha that is structured by two parallel streets running north-south, with three perpendicular east-west-oriented streets. This northern part of the New Town can be divided into five districts (**Fig. C2.7**). Three districts are located at the centre and present as a densely built-up area, accessible from the east and the west by two north-south-oriented streets. A fourth district, occupied by relatively large buildings, is located along the western city wall. A fifth district is situated next to the Tigris, east of Andrae and Lenzen's "Nord-Süd Strasse I"; the presence of several modern disturbances allows the identification of only a few buildings in the magnetogram.

The southern half of the New Town takes up an area of 6.4 ha, reaching from "Ost-West Strasse 12V 131" to the city wall. It is delimited in the east by hills that slope down westwards to a depression where water accumulates during the rainy season. In February 2023, bushes and grass sprouted here, which we had to remove during our survey to take the magnetometer measurements. In the New Town's southern half, the main streets follow the city wall to the south and a street that is oriented from northeast to southwest runs throughout the settled area.

This southern part of the New Town can be divided into four districts (**Fig. C2.8**). South of the "Ost-West Strasse 12V 131" lies the first district, an area of triangular shape that is marked in the southwest, downhill, by a complex with at least 19 pyrotechnological installations. This might indicate an area specialised in firing activities such as pottery kilns or metallurgy. The second district lies in the eastern part of the New Town's southern half and is occupied by a 2,782 m² large building complex. Its layout is comparable to that of the Parthian Palace, although this structure is twice the size. It seems that this building had a significant impact on the New Town's layout because the two north-south streets converge towards it. A third district with a large built-up area of 2,643 m² lies on an elevation in the southwest, and this is where the excavations of the State Board of Antiquities and Heritage (SBAH) of 2002 and the new work of 2023 (Trench NT1 2023: **§D2**) took place; the walls identified there are perhaps associated with different levels of occupation and/or a compact settled area. Finally, a fourth district lies on the elevation situated within the southwestern corner of the city wall, south of an area that seems not to have been developed. About a third of this area was excavated by SBAH in 1979-80, exposing a substantial building from the Neo-Assyrian period; the stone-footed walls of several rooms are still visible in the old trenches. The open area to its north is situated next to a badly preserved section of the wall; in the future, we want to test the hypothesis of whether a gateway led through the wall in this location.

C2.1.3.2 Some glimpses into the architecture of the New Town

Most of the built-up areas observed in the various districts take up between 100 and 250 m². For comparison, "Haus Y" and "Haus X", which Andrae excavated and dated to the Late Parthian period ("spätparthisch"), occupy areas of 380 m² and 345 m², respectively, and the largest house of that period ("Grosses Wohnhaus westlich des Palastes in h10"⁶²) an impressive 991 m². Still, the Parthian Palace, which is an older construction ("altparthisch"), is much larger and takes up an area of 4,656 m².⁶³ Based on the fact that many of the excavated Parthian-period houses have an impressive size we assume that at least some of the built-up areas represented in yellow in the annotated magnetogram (**Figs. C2.6-8**) are single buildings. In one case, it is possible to discern a rectangular building complex with a large rectangular space in the centre and rows of rooms on its eastern, western and southern sides (**Figs. C2.9a-b**). This layout is similar to that of the aforementioned "Grosses Wohnhaus", which has a central courtyard opening northwards to the adjoining street. The courtyard gives access to the eastern, western and southern wings of rooms.

As we already stressed above (**§C2.1.3.1**), the large building complex of 2,782 m² (**Figs. C2.10a-c**) identified in the second district of the southern half of the New Town, next to the Tigris, shares several features of its layout with the Parthian Palace. This tripartite complex lies south of an open area and at the southeastern end of the "Ost-West Strasse 12V 131". Its thick walls are 1.8 m wide and seem to be built with stones and fragments of baked bricks, parts of which are still visible on the site surface. The building's westernmost part features a rectangular area measuring 23 m in north-south orientation and 16 m in east-west orientation. Both at its northern and southern sides, this central area seems to open towards a square room, which would parallel the north and south iwans of the Parthian Palace. The rectangular area's longer sides are lined by what may be column bases, placed at a distance of about 3 m from the walls. West of this large central area, we identified several small rectangular rooms. To its east, at the centre of the complex, there are four rectangular suites with several rooms. To the northeast, a series of rooms seems to be organised around a square space, which might parallel the peristyle of the Parthian Palace. Due to the great structural similarities, we tentatively consider this complex a "Secondary Parthian Palace".

⁶² Andrae/Lenzen 1933, pls. 7-8.

⁶³ Andrae/Lenzen 1933, pl. 1.



+ 20 nT
 - 20 nT
 — Approximate limit of district
 — wall
 ■ built-up area
 ○ pyrotechnological installation
 ▨ non built-up area
 ▨ street
 0 50 100 150 m
 Magnetogram: J. W. E. Fassbinder
 Measurements: J. W. E. Fassbinder, J.-J. Herr, L. Ruider, M. Wolf
 Interpretation: J. W. E. Fassbinder, J.-J. Herr and M. Wolf
 Map made by J.-J. Herr

Fig. C2.7: The districts of the New Town's northern half.

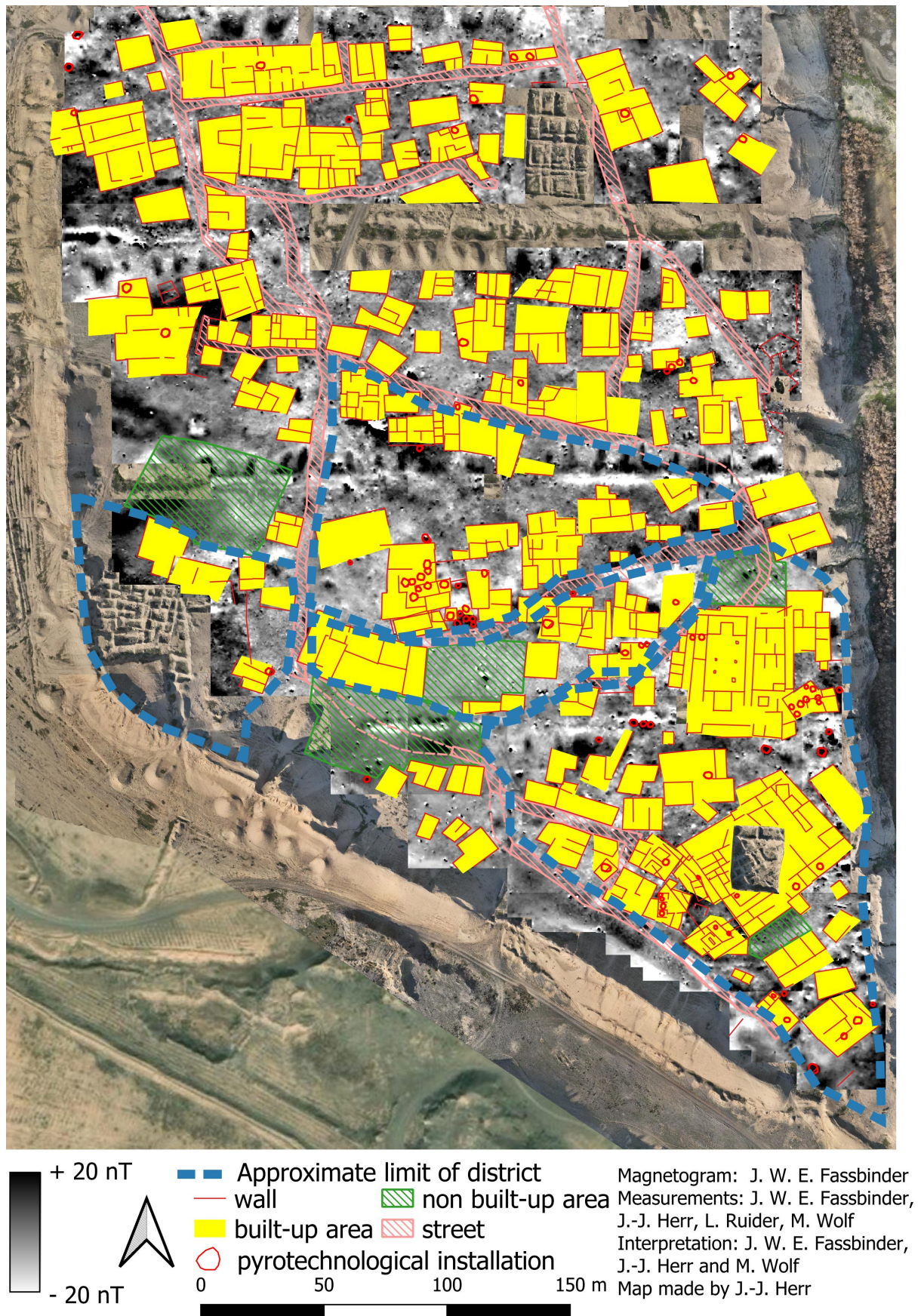


Fig. C2.8: The districts of the New Town's southern half.

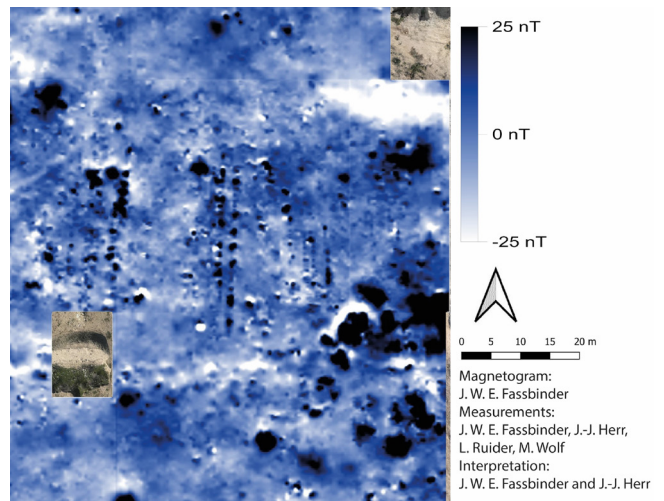
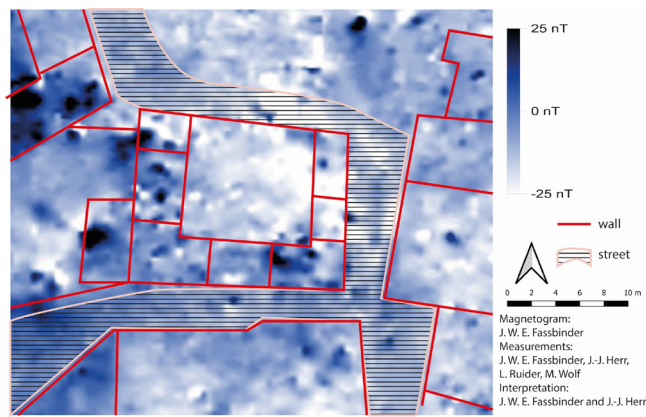
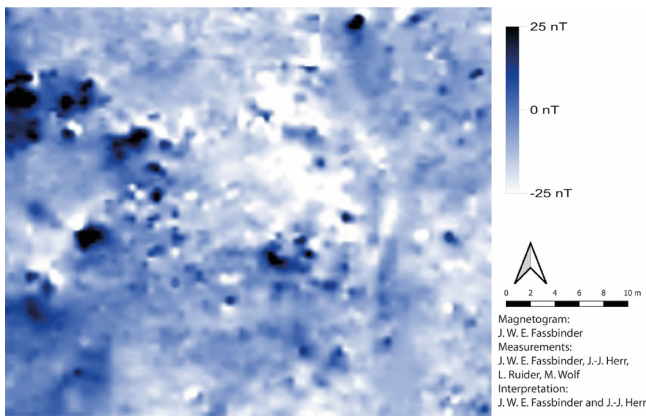


Fig. C2.9: A building with three wings of rooms around a central courtyard: a) magnetogram; b) interpretation.

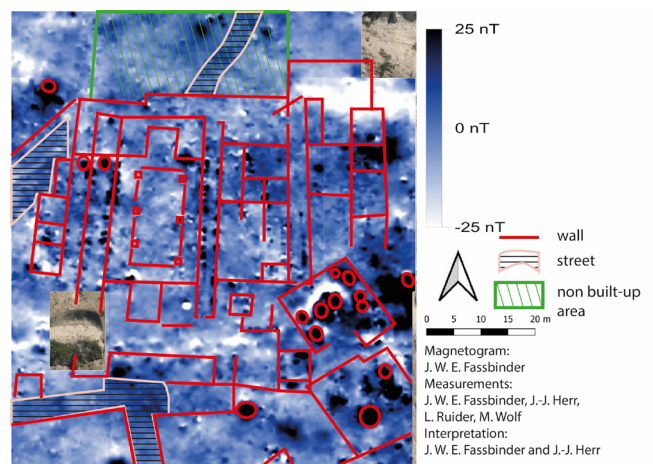
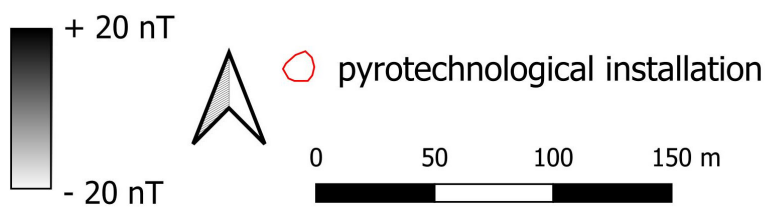
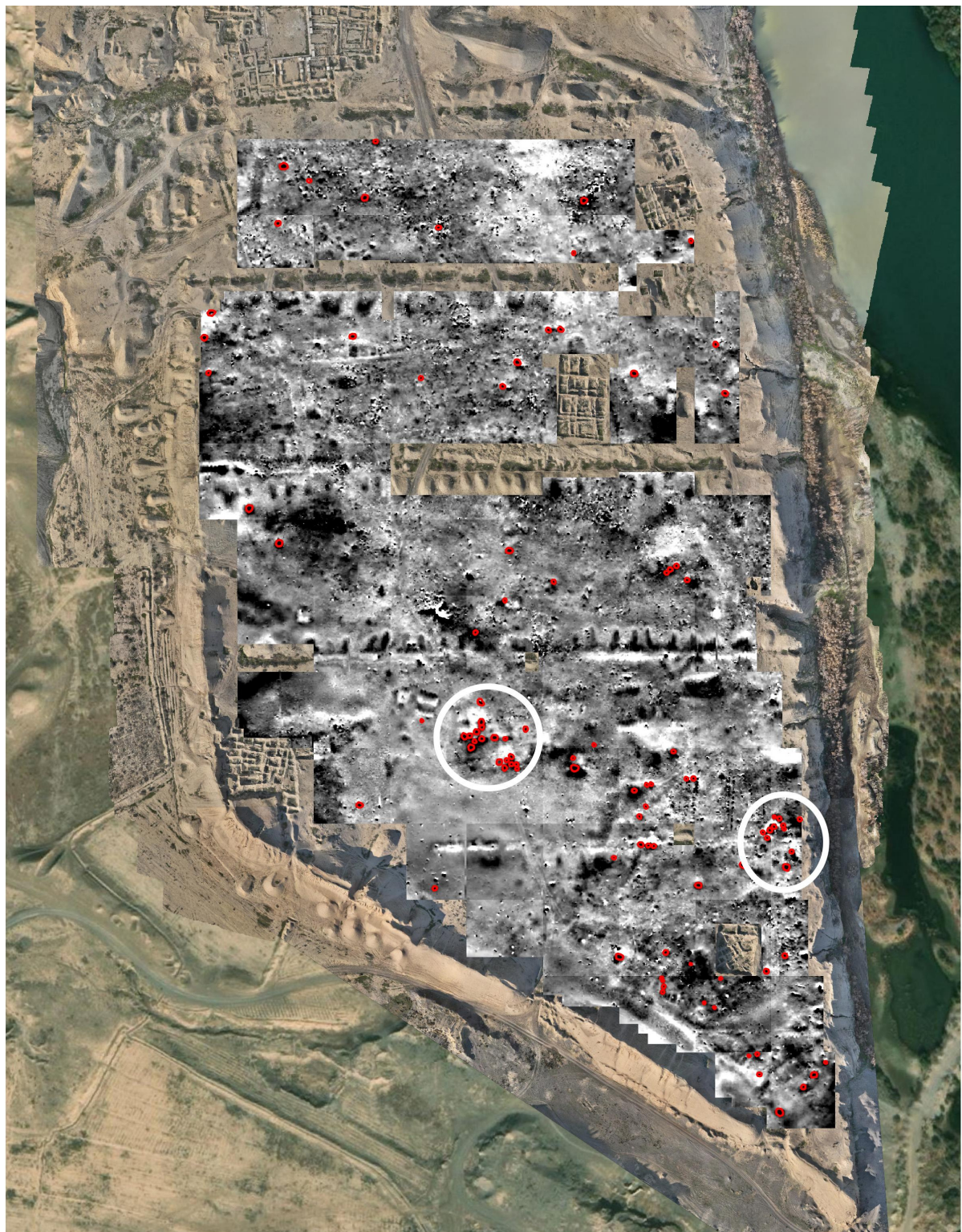


Fig. C2.10: Large residence building, comparable to the so-called “Parthian Palace”: a) orthophoto; b) magnetogram; c) interpretation.



Magnetogram: J. W. E. Fassbinder
 Measurements: J. W. E. Fassbinder, J.-J. Herr, L. Ruider, M. Wolf
 Interpretation: J. W. E. Fassbinder, J.-J. Herr and M. Wolf
 Map made by J.-J. Herr

Fig. C2.11: Pyrotechnological installations in red, battery kilns in white.

C2.1.3.3 Thoughts on the pyrotechnological installation

The analysis of the magnetogram revealed 101 pyrotechnological installations that are evenly distributed across the New Town of Assur (Fig. C2.11). The majority of the pyrotechnological installations have been identified within a built-up area or a building complex; only rarely are they situated in an open area. The installations are either in the centre of a building unit, most likely inside a courtyard, or in a location at the edge of a building unit. During the SBAH excavations of 2002 in what we have described as the third district in the southern half of the New Town (§C2.1.3.1), two two-chambered pottery kilns, with a vaulted firing box and preserved grate (Figs. C2.12 and



Fig. C2.12: Remains of a two-chamber pottery kiln with preserved grate. Photo by Jean-Jacques Herr.

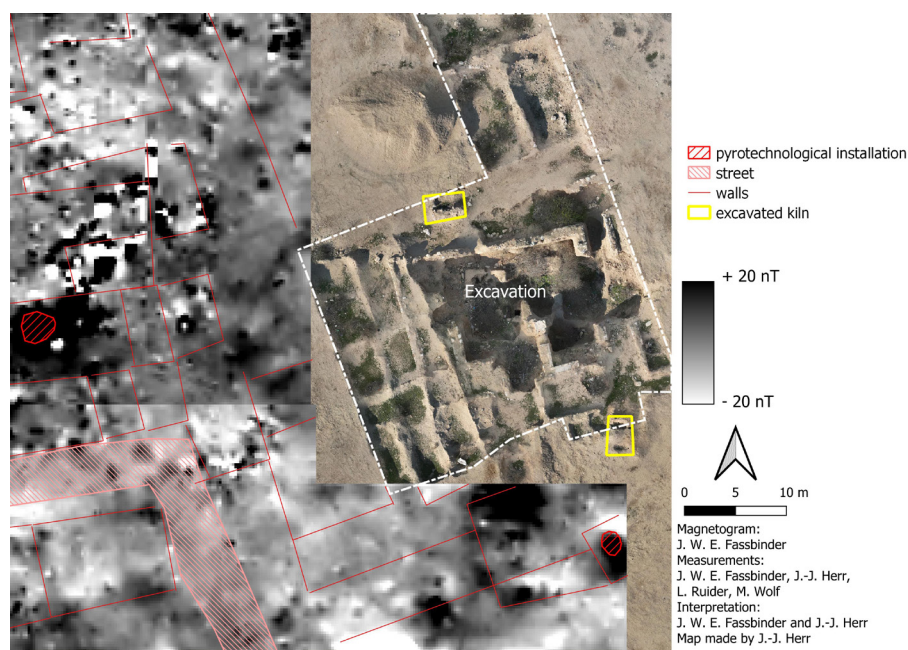


Fig. C2.13: Excavated kilns (in yellow) next to the SBAH excavation, possibly of Parthian date.

C2.13) illustrate how at least some of these pyrotechnical installations looked like.

In addition, there are two clear clusterings of pyrotechnical installations: the first to the west of our “Secondary Parthian Palace” (§C2.1.3.1), and the second to the east of it. This distribution suggests a battery-like kiln structure and might hint at an industrial workshop economy of production, either for pottery production or for metallurgy.

C2.1.4 Conclusions

Compared to other sites worldwide, the range of magnetic anomalies measured in Iraq, by now in more than 20 archaeological sites, is quite high. At Assur, too, archaeological features show up in the range of ± 30 nanotesla.

For the interpretation of the data, the total field caesium magnetometer has the marked advantage that it not only allows us to discern zones and areas of high activity but that the direction of remanent magnetisation also enables us to differentiate between old and new structures. The orientation of areas with higher magnetisation and linear anomalies that are aligned in parallel or orthogonal directions allow us to distinguish different building complexes and districts within the larger settlement. Another important aspect of a total field caesium magnetometer survey is the possibility of locating and providing clear evidence of “empty spaces”, i.e. areas that show no or almost no traces of buildings or accumulation of magnetic iron oxides.

However, unlike the magnetic measurements in the Dinka Settlement Complex in the Peshdar Plain in the Kurdish Autonomous Region of Iraq or in Uruk in southern Iraq, the results of the measurements from Assur are rather diffuse and complicated to interpret. Moreover, modern iron-containing waste is frequently left by visitors to this UNESCO-listed World Heritage site, and this heavily contaminates the area. The previous measurements taken in April 1989, which had yielded comparatively poor interpretation results, had made it clear in advance that the interpretation of the magnetic measurements would greatly benefit from the application of additional geophysical methods such as soil and mineral

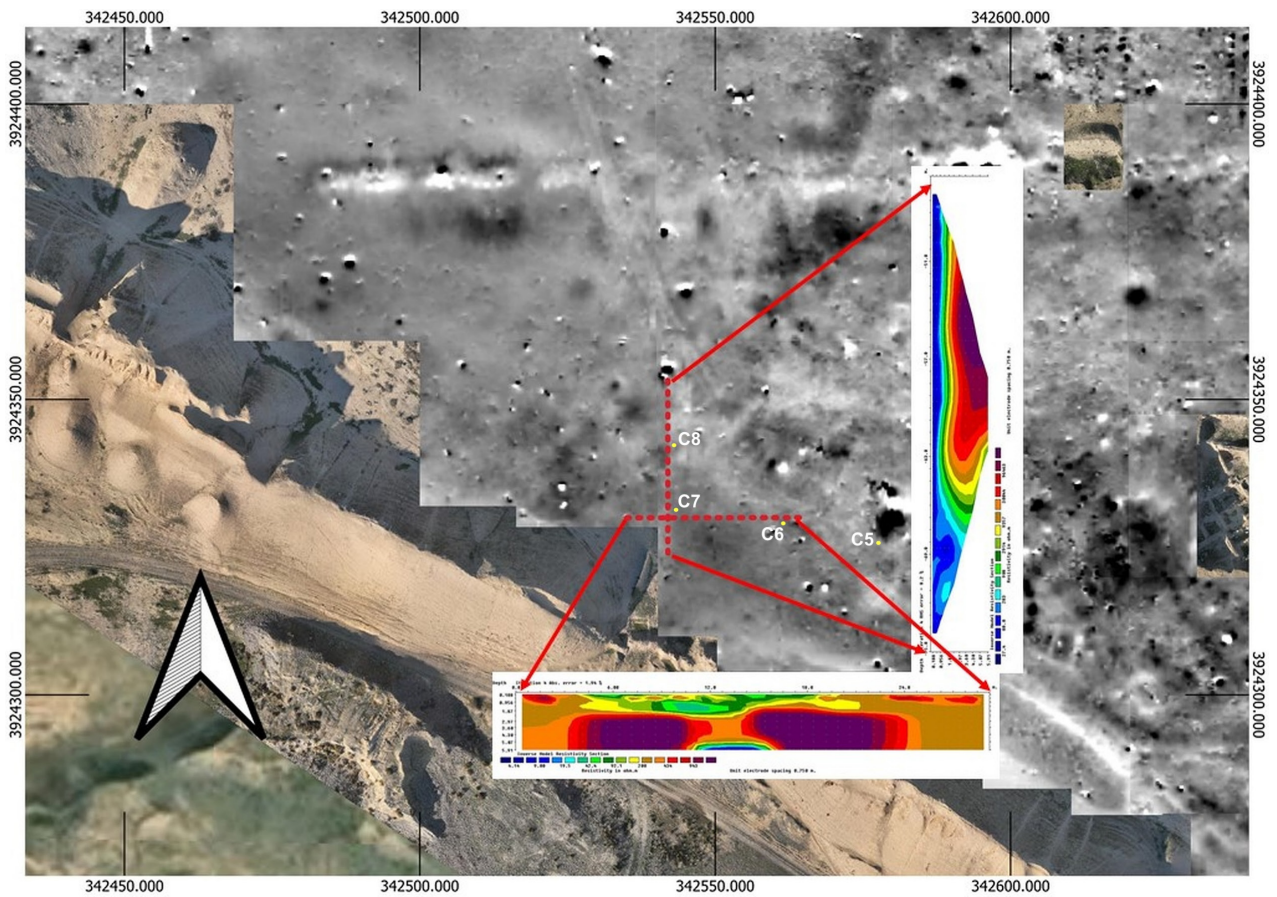


Fig. C2.14: New Town of Assur, ERT Profiles 2 and 3 (dipole-dipole): 30 m profiles cross sections and their location in relation to the magnetogram. Probe separation 0.75 m. Measured in dipole-dipole constellation. Note also the location of the cores C5-C8 (see §C3). Created by Jörg Fassbinder.

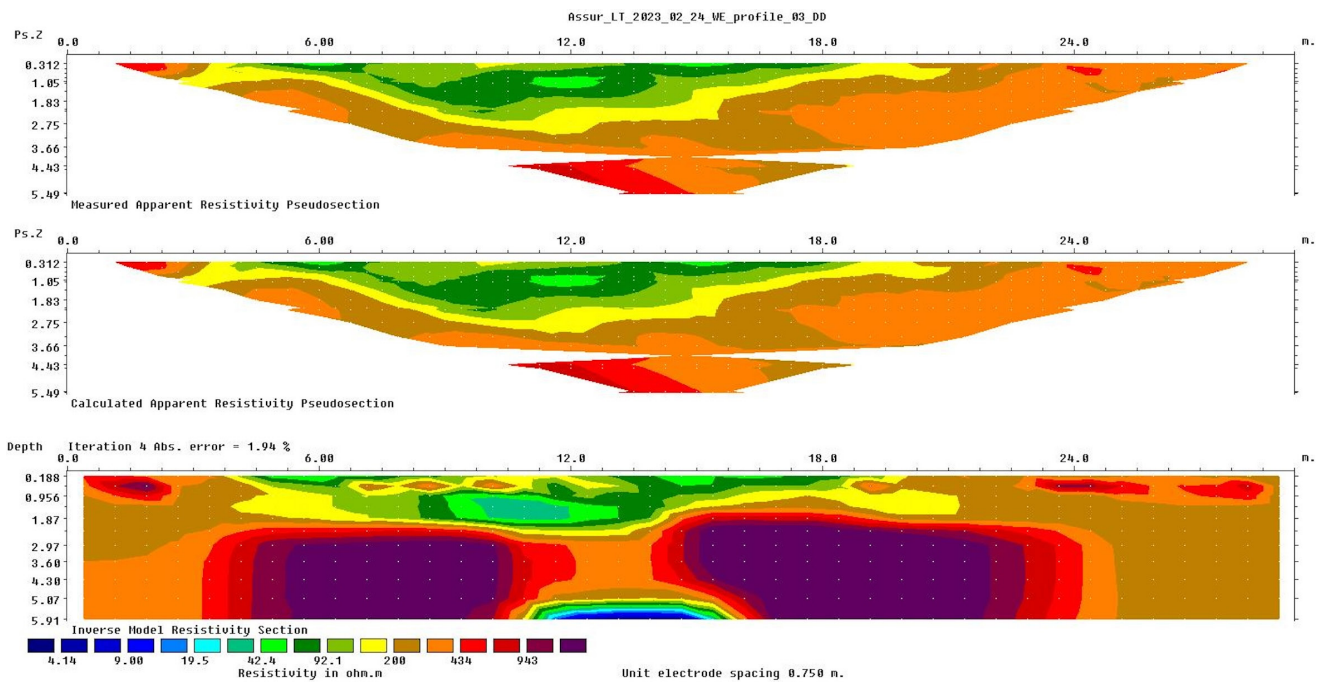


Fig. C2.15: New Town of Assur, ERT Profile 3 (dipole-dipole): 30 m profile across a building. Probe separation 0.75 m. Measured in dipole-dipole constellation. Created by Jörg Fassbinder.

magnetic analysis (§C4) and electrical resistivity tomography (ERT; §C2.2).

Beyond that, as the previous sections have demonstrated, the comprehensive interpretation of the data requires input not only from geophysicists but also from specialists with a comprehensive knowledge of relevant architectural layouts and ground plans. The mixed team working together in Assur in 2023 was ideally suited to tackle the difficulties presented by the site.

C2.2 Electrical Resistivity Tomography (ERT) prospecting in the New Town of Assur, 2023

Jörg Fassbinder & Marco Wolf

The first-ever electrical resistivity tomography (ERT) prospecting undertaken at Assur in February 2023 was a proof-of-concept campaign, designed to test the site's suitability for the method. We applied the ERT equipment model 4Point light 10W, manufactured by E. Lippmann.⁶⁴ The resulting measurements of ERT profiles allow us to distinguish different soil layers beneath the surface and to estimate the depths of these layers. We selected a probe spacing of 75 cm, which allows a penetration depth of up to 5 m. Judging from the excavated areas in the New Town, this depth should allow us to reach the undisturbed virgin sediments and enable us to distinguish between different layers of occupation, at the very minimum represented by the earlier Assyrian and the later Parthian-period settlement identified by Andrae's work and later excavations.

In this first test campaign, we measured two profiles with a length of 30 m (40 × 75 cm) each: the first from west to east and the second perpendicular from north to south across a possible road in the lowest-lying area of the New Town of Assur (Fig. C2.14). Already now, these ERT profiles can be combined with the magnetogram created for this area (§C2.2) as well as the results of the coring undertaken in that same area. In the future, we plan to correlate the ERT measurements in Assur with the results of the geoarchaeological sediment analysis of the cores (§C3) and the mineral-magnetic analyses of selected samples taken from these cores (§C4). Integrating such data, and of course, also the results of the ongoing excavations, will improve our understanding of the areas under investigation.

This first trial run has been successful, and we intend to continue ERT prospecting in the New Town of Assur

in the upcoming field season of spring 2024. Once more data has been collected, further data processing will be performed in LMU Munich's geophysics laboratory to create more sophisticated 2D models. For now, as an example, the measured data of ERT Profile 3 is plotted in the two images on the top while the bottom image shows the inverse model of the same profile featuring the different resistance values (Fig. C2.15).

C3. Geoarchaeological coring in the New Town of Assur, 2023

Mark Altaweel

This work represents the very first geoarchaeological coring ever undertaken at Assur. Using the percussion coring system (Cobra TT) owned by LMU Munich's History Department, eight sediment cores were taken in the southern part of the New Town of Assur between 13 and 25 February 2023, after a car had been procured that was able to transport the very heavy equipment. The field team was led by Mark Altaweel, with the participation of Andrea Squitieri, Amer Mohammed Yasim, Omar Laith Allawi, and Ahmed Khidr Ahmed (known as Arabi).

The primary purpose of extracting sediment cores was to gain further data for the settlement history of the New Town area by identifying occupation levels in various areas. Most of our activity was focused on areas near or within the areas of the new excavation. The nearby excavations of the SBAH undertaken in 2002 had revealed Neo-Assyrian and later activity, but that work has never been completed nor has it been published; as the trench was never backfilled, the remains excavated there are still visible (Fig. C3.1). The coring was meant to enhance the results of the excavations in spring 2023, which demonstrated the existence of several levels of occupation as well as various burial levels within a trench of 120 m² in the southern part of the New Town (§D).

The second goal of the coring work was to investigate the presence and location of an ancient, north-south oriented street that likely connects to a city gate located in the southern stretches of the fortification walls encircling the city. Evidence for the existence of this street was observed in the results of the magnetometer prospecting (§C2), and coring was used to validate those results.

The third goal was to procure sediment samples for mineral magnetic analysis in order to support the evaluation of the results of the magnetometer survey (§C4).

The results of this initial round of coring, which we intend to continue in spring 2024, are detailed below.

⁶⁴ For a comprehensive description of the instrument and its application see Parsi *et al.* 2023.



Fig. C3.1: Locations of the 2023 cores (yellow dots) in relation to the NT1 2023 trench (white line). Created by Andrea Squitieri.

C3.1 The scope of the 2023 work

Our investigation represents the first time a corer was used in Assur to extract sediment cores. It continued previous work in the Shahrizor⁶⁵ and Peshdar Plain,⁶⁶ both in the Kurdish Autonomous Region of Iraq, that had provided ample experience in the use of a core sampler (“window sampling”, for analysis in the field and possible sampling of specific contexts for later lab analysis) and clear plastic tubes (for taking out the entire core, which is then analysed in a lab).

For this first assessment of the suitability of coring, we did not take core samples in clear tubes, also because it was not clear at the time whether these could be exported. Instead, we applied window sampling using the tube sampler, primarily to recover sediments for field analysis. The arid environment and the resultant hardness of the sediments make the effort of coring in Assur in February comparable to extracting cores in early autumn in the locations in Iraqi Kurdistan. The hard, rocky and clay-silt sediments observed at Assur are mainly a mix of anthropogenic remains with some natural windblown deposits. This complicated coring as the numerous pebbles, rocks, ceramics, bricks, and other debris greatly increased the probability of obstructions, which then can prevent the corer from reaching the desired depths.

Therefore, the preliminary results of the magnetometer prospection (§C2) were used to guide where core samples were to be taken, enabling us to select locations that would prove the easiest to penetrate. In some places, we were able to reach a depth of 5 m. **Fig. C3.1** shows the locations of the eight cores taken in 2023, labelled C1 to C8, which were then assessed in the field (**Figs. C3.2-C3.3**). In addition, we took sediment samples from the cores in intervals of 50 cm (as far as possible) in order to study their magnetic susceptibility; these samples were labelled CO1 to CO33 (**Table C3.1**; for the results of their analysis, see §C4).

The first set of cores was extracted in a mounded area close to the site of the 2002 SBAH excavations (§D3) in the New Town, which helped to guide the analysis of the recovered sediment samples from our core borings. This is an area of demonstrated Neo-Assyrian occupation, with the presence of later graves and buildings conventionally described as “Parthian”.⁶⁷

The second set of cores was taken in a flat area where no apparent architecture is present on the surface. This,

combined with the general emptiness of this area, suggests the presence of an ancient street, most likely of Assyrian date, that may have also been used during later periods. The evidence from satellite imagery indicates the presence of a major north-south road that led from Assur to northern Babylonia.⁶⁸ As there is a modern village just south of the New Town, this ancient road cannot be observed outside of Assur’s fortifications. This lends additional importance to investigating our street, as it likely leads to the same city gate to which the overland road may have once connected.

C3.2 The cores and their description

Figs. C3.2 and **C3.3** present the core sections, showing the types of sediments and anthropogenic finds observed. In the following, the cores are described in full. **Table C3.1** offers a concordance between the sediment samples and the cores from which they were taken.

Core C1

Located near the apex of one of the mounded areas within the New Town, this core reached a level of around 450 cm below the surface. The first 0-80 cm demonstrated remains of silty-sandy sediment, light brown in colour, reflecting windblown sediment and the likely abandonment of this area. Some pebbles, but no clear intact architectural remains, are evident. Starting 80 cm below the surface, the silty sediments become more compact with clear charcoal and small pottery fragments evident; small white gypsum stones are also evident. Mud brick is also evident in the compact sediments. A potential floor is reached at about 120-130 cm, where more pebbles were encountered with compact sediment. The sediment sample CO31 was taken at 150 cm. From around 140-150 cm, the core boring is silty and compact, with whitish gypsum inclusions. Some scattered pebbles, pottery flakes, and ash are evident. The sediment sample CO32 was taken at 250 cm below the surface. The types of sediments encountered in the previous level continue. By around 275 cm below the surface, a group of larger pottery fragments mixed with larger pebbles, and possibly another floor level, were encountered. A rim fragment was collected at 260 cm. Below this level, the sediments are loose with a mix of pottery, flakes, ash, pebbles, and white gypsum inclusions. Pottery fragments are evident at 300 cm, but no floor level is visible. Below 300-350 cm, the sediments are loose and begin to appear more natural and archaeological remains

65 Marsh/Altaweel 2020.

66 Altaweel/Eckmeier 2019.

67 Miglus 1996.

68 Altaweel 2008, pl. 17: fig. 47.

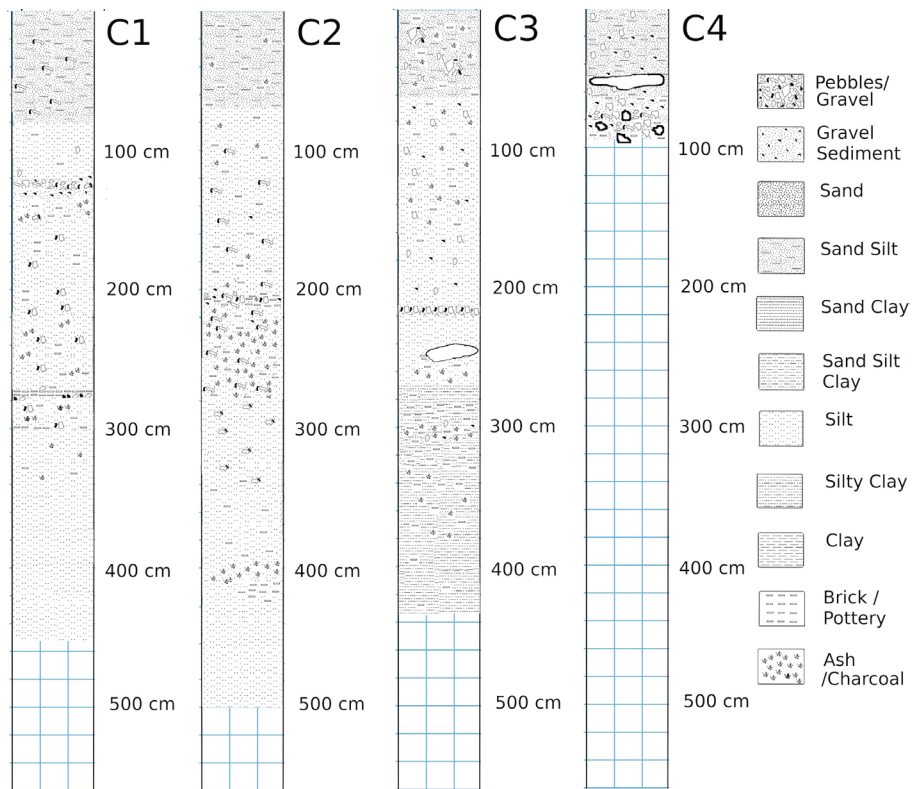


Fig. C3.2: Schematic drawing of cores C1 to C4. Created by Mark Altaweel.

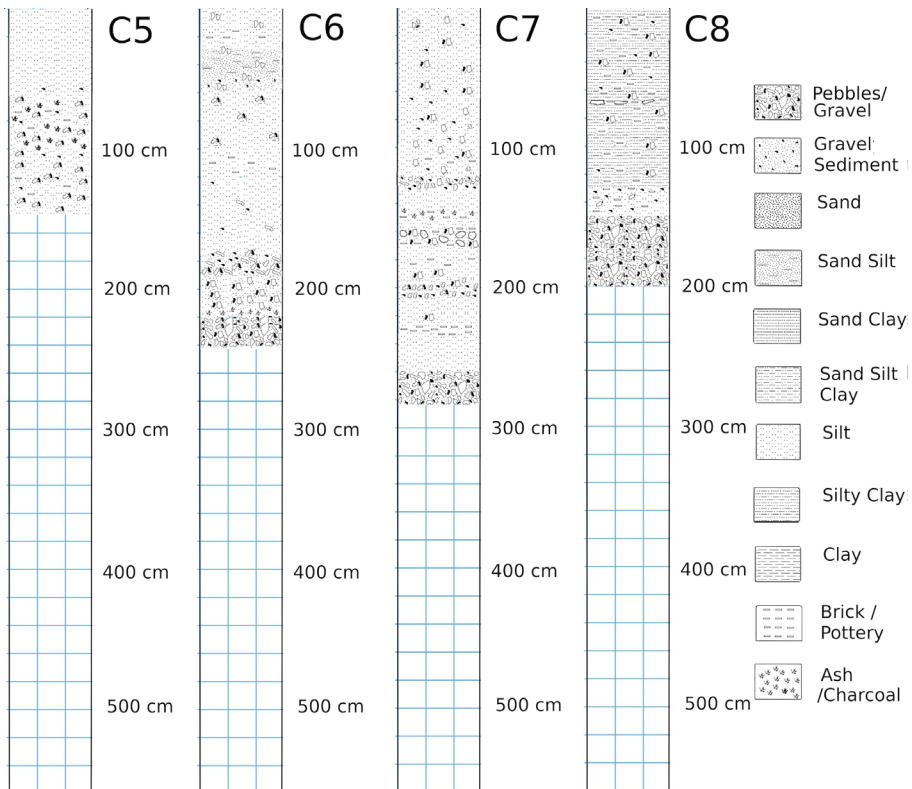


Fig. C3.3: Schematic drawing of cores C5 to C8. Created by Mark Altaweel.

Sample no.	Core	Depth from surface	Absolute elevation
CO01	C7	100 cm	155.03 m
CO02	C7	150 cm	154.53 m
CO03	C7	200 cm	154.03 m
CO04	C7	250 cm	153.53 m
CO05	C8	50 cm	155.35 m
CO06	C8	100 cm	154.85 m
CO07	C8	150 cm	154.35 m
CO08	C6	50 cm	155.66 m
CO09	C6	110 cm	155.06 m
CO10	C6	160 cm	154.56 m
CO11	C6	230 cm	153.83 m
CO12	C5	70 cm	155.89 m
CO13	C5	120 cm	155.39 m
CO14	C5	50 cm	156.09 m
CO15	C2	50 cm	162.32 m
CO16	C2	150 cm	161.32 m
CO17	C2	200 cm	160.82 m
CO18	C2	270 cm	160.12 m
CO19	C2	330 cm	159.52 m
CO20	C2	390 cm	158.92 m
CO21	C2	430 cm	158.52 m
CO22	C2	490 cm	157.92 m
CO23	C3	50 cm	160.99 m
CO24	C3	110 cm	160.39 m
CO25	C3	160 cm	159.89 m
CO26	C3	225 cm	159.24 m
CO27	C3	270 cm	158.79 m
CO28	C3	320 cm	158.29 m
CO29	C3	370 cm	157.79 m
CO30	C3	420 cm	157.29 m
CO31	C1	150 cm	161.41 m
CO32	C1	250 cm	160.41 m
CO33	C6	360 cm	159.31 m

Table C3.1: List of the sediment samples taken from the cores for mineral magnetic analysis. Created by Andrea Squitieri.

markedly diminish. At 360 cm, the sediment sample CO33 was taken.

Core C2

This 5 m deep core boring was taken close to C1 and near the top of the mound. Sediments are a light brown silt-sandy mix with some pebbles and pottery fragments in the first 0-70 cm below the surface. The sediment remains appear windblown. The sediment sample CO15 was taken at 50 cm. From 70-120 cm, the sediments appear compact and silty with some ash, pottery, and white calcite evident. Below 120 cm, the sediments appear looser and more reddish. Larger pebbles and pottery fragments with white inclusions are evident. Mixed, broken mud-brick is also seen. At 150 cm, the sediment sample CO16 was

taken. From 195-245 cm, ash, some mud brick fragments, pottery fragments, small pebbles, and white inclusions are evident in the silty remains. Sediment samples were taken at 200 cm (CO17) and 270 cm (CO18). At 205-210 cm, a possible floor level was encountered where a concentration of rocks and pottery is seen. Below this level, between 210-235 cm, there's an ashy layer, which appears dark in colour. From 240-295 cm, pottery and stone fragments are seen, with ash continuing down to 280 cm. It appears that a thick, ashy layer encompasses the level between 210-280 cm, likely demonstrating a major fire. A lot of stones are mixed with mud brick, silty material, and mud brick fragments. From 300-410 cm, two sediment samples were taken at 330 cm (CO19) and 390 cm (CO20). From 300-350 cm, very loose silty sediment was encountered, with pebbles. At 340 cm, some pottery fragments are evident. From 350-400 cm, there are mud brick fragments, white inclusions, and pottery fragments down to 400 cm. From 410-460 cm, loose silty soil with white inclusions is evident. Large pottery sherds were encountered at around 410-420 cm; the core may have penetrated a complete vessel. Above the pottery, there is an ashy layer. Below the pottery, the sediments are fairly loose, with natural calcium carbonate inclusions encountered. No archaeological materials are evident below 430 cm. Sediment samples were taken at 430 cm (CO21) and 490 cm (CO22).

Core C3

Core sample C3 was placed on the same mound but on a downward slope and reached a depth of about 4.35 m. In the first 0-65 cm below the surface, windblown sediments similar to those seen in the first two core samples were encountered. A sediment sample was taken at 50 cm (CO23). Sediments included pebbles, ash, and pottery fragments, with white calcareous inclusions. From 65-120 cm, sediments are silty and loose, with pebbles and some pottery fragments. There is also ash with white inclusions. The layer from 120-175 cm is also similar, although potential mud brick remains were encountered. Two sediment samples were taken at 110 cm (CO24) and 160 cm (CO25). From 175-210 cm, loose silty sediment with pebbles and stone, including calcium nodules, were encountered. Around 210-220 cm, a concentration of pebbles is found, which could represent an ancient floor. At around 250 cm, a very large stone is visible, which also seems to be associated with mud brick. A sediment sample was taken at 225 cm (CO26). From 255-300 cm, silty sediment with greyish and brown colour was encountered. Possible mud brick is seen at 260-270 cm. Ash and charcoal are visible at around 260 cm. From 260 cm, the sediment becomes more reddish, changing from the greyish colour above. From 260-335 cm, the reddish sediment continues.

The sediments also become harder and somewhat clay-like. There is a possible mud brick layer between 280 and 330 cm. In fact, at this level, the coring may have pierced through a wall or a layer of thick mud bricks. Charcoal is mixed in at around 300 cm. There are also pebbles and chunks of large fragments of charcoal at this level, perhaps reflecting the same fire event evidenced in C2, along with some baked brick fragments reaching towards 335 cm. Two sediment samples were taken at 270 cm (CO27) and 320 cm (CO28). The next level reached between 335-435 cm, with two sediment samples taken at 370 cm (CO29) and 420 cm (CO30). From 335-385 cm, the greyish-red sediments are silty-clayey mixed with mud brick and ash. The bottom half of this segment may have only reached a depth of 400 cm, given the angle of the slope. From 385-435 cm, the silty-clay material is compact and also reddish but fades into more grey. Here, it is more grey than the level from 335-385 cm. Tiny fragments of pottery are mixed with mud brick materials. Virgin soil may have not been reached by the C3 core sample.

Core C4

This core boring was positioned near the base of the excavated mound and, because of the rocks and debris it encountered, only reached a depth of about 92 cm. The sediments from 0-66 cm below the surface are compact, with pebbles and stones. At a depth of 50 cm, the corer encountered a large gypsum stone that was bored through only with great difficulty. Some baked bricks are also evident in the sediment. Between 66-92 cm deep, we noticed large stones mixed in the debris and more baked brick fragments. We believe the remains of a wall or some significant stone presence, likely stone and brick debris from construction, is evident at this level. In other words, this could be wall debris from a collapsed building encountered starting at around 50 cm below the surface and continuing to 92 cm below the surface. This thick debris prevented any further penetration by the coring instrument.

Core C5

This core boring was positioned in the flat area closer to the possible location of a southern gate of Assur. Given the resistance it encountered from many stones, the core only reached a depth of 145 cm. Sediment samples were taken at 50 cm (CO14), 70 cm (CO12), and 120 cm (CO13). From 0-60 cm, the sediments are silty, powdery, and devoid of archaeological remains; pebbles are evident at 60-100 cm as well as some ceramics. Below 100 cm, the sediments are ashy and blackish in colour. There is a mix of stones and calcium nodules, and the texture of the sediment is soft and powdery. The corer was unable to bore any further and it is difficult to assess whether a

clear street, or possibly even bedrock, was encountered at the base of the core borehole.

Core C6

The next core reached a depth of around 240 cm before we again encountered stones that were too dense to penetrate. Sediment samples were taken at 50 cm (CO08), 110 cm (CO09), 160 cm (CO10), and 230 cm (CO11). The sediments between 0-30 cm are silty and compact with some pottery fragments around 20 cm. The sediments are somewhat sandy below 30 cm. From 0-58 cm, pebbles are found throughout. From 58-105 cm, silty powdery sediment, with pebbles and material that appears to have been washed or water-transported, is found. Some pottery or brick fragments are found at 110 cm. From around 120 cm, the sediment is more compact, with calcite nodules, and in places, it is powdery and mixed with pebbles. It looks like an alluvial deposit formed by erosion. There is no clear evidence for occupation, with many pebbles encountered around 180 cm below the surface. From 190-244 cm, there are mostly loose sediments with pebbles, with ashes in the bottom part. The pebbly layer starting at 220 cm could be the bedrock.

Core C7

This core was also taken in the flat area closer to the city walls of Assur, where it extended 280 cm deep. We specifically attempted to place it along what we believed to be an ancient street, using as our guide the results of the geophysical survey undertaken in this area just before we started coring (§C2). As before, the corer encountered rocks which were challenging to penetrate and it was difficult to go as deep as we wished. Sediment samples were taken at 100 cm (CO01), 150 cm (CO02), 200 cm (CO03), and 250 cm (CO04). From 0-50 cm, the sediments are loose, silty, greyish-brownish, with small pebbles. From 50-120 cm, loose sediment with pebbles is evident. Some pottery appears around 110 cm. Between 120-130 cm there are many compact pebbles. Possibly a paved street that ran towards the southern gate existed at this level. Around 150 cm there are some mud brick remains and ash found in the sediments. Between 160-170 cm, larger rocks and some pottery were found. From 170-230 cm, the sediment is very compact and silty. Around 180 cm some small pottery fragments appear. There are many pebbles around 200-210 cm which may also represent another level for a possible paved road or street. Around 230 cm there is again pottery or baked bricks. From 260 cm we find small river-moulded pebbles that are likely the result of natural accumulation as they are distinctive from the pebbles that lie above them. They appear to form a thick layer which likely continues to a very deep level.

Core C8

The last core boring, which reached approximately 200 cm in depth, was also placed in the flat area where we believe a possible street/road was located. Three sediment samples were taken at 50 cm (CO05), 100 cm (CO06), and 150 cm (CO07) below the surface. From 0-70 cm, we observed silty-clayey wet sediment that contained pottery and pebbles. Three large brick fragments are visible at about 70 cm. From 70-130 cm, the sediment is dark and clayey-silty with pebbles and pottery fragments, largely resembling what was observed above in the same core. Approximately 130 cm deep, the sediments change from brown to grey, with dry sediments encountered. Below 130 cm, the sediment is loose, dry, and grey with pebbles mixed with pottery and bricks. From 150-200 cm, the borer mainly encountered stones and this likely represents bedrock material, similar to C7. In fact, in an attempt to confirm that this was bedrock, the corer hit the stone and was temporarily stuck. Given the density of the rock encountered, an interpretation of this level as bedrock seems supported.

C3.4 Discussion and preliminary results

The cores C1-C4 demonstrate the presence of at least two main occupation layers and a likely burial level, with two likely floors found in core C1 (120-130 cm and 275 cm). The observed occupation levels extend to a depth of about 3-3.5 m below the surface, below which more natural sediment is encountered. Evidence of anthropogenic debris below the lowest floor may be from the construction of the building and/or evidence of a burial layer. The core C2 demonstrates an even deeper level of occupation, reaching a depth of 4.2 m where it encountered a likely complete ceramic jar. Only one floor was seen in this core (at 2.1 m). However, a significant fire event is evident below this floor, which may signify the destruction of an earlier building. This burned layer could be the Neo-Assyrian destruction since, once the slope in the mound is accounted for, the level roughly matches that of the house excavated by an Iraqi team. However, this cannot be determined without additional proof for the date of this level. Just below 4 m in C2, a potential grave with fill above it is evident. We think this to be a grave because the ceramic in our core sample appears to have been from a complete jar, and such large or well-preserved jars are typically preserved in burial contexts. Additionally, C3 may show continuity with what C2 demonstrated, with the floor around the same level as C2 and ash and debris fill below also suggesting potential destruction or a fire. The remains from C4 encountered less than 1 m from the surface likely

indicate either a wall or building debris, as the location of this core was near the base of the small mound. This area may be near the outer walls of the structure.

Regarding the cores taken near the possible street or flat areas near the southern gate, the results from core borings and sampling demonstrate potential pavement, in any case, evidence for the use of stone in connection with the street. The clearest evidence for this comes from core C7, which found one possible street just over 1 m below the surface, and a second possible street around 2 m below the surface. In fact, between these two levels, large stones and pottery found around 1.6 m deep might also suggest yet another street level. These two or three potential pavement levels suggest that, if indeed a street is located here, it has several phases across time. On the other hand, the cores C5, C6, and C8 did not show clear evidence for a potential street. Cores C6-C8 appear to have reached the bedrock approximately 2-3 m below the surface in this part of Assur. With each of our core samples, we attempted to core deeper than the levels in which stones were encountered to certify we hit bedrock and not other types of stones. In some ways, if what is found in core C7 is evidence of a paved street, then this might be similar to the processional street connecting the Tabira Gate and the sacred areas of Assur. This could suggest that this street may have been intended as one of the main traffic arteries leading south of the city. "Hollow ways", or remnants of ancient roads, emerge south of Assur and connect to central Mesopotamia. While generally speaking, these hollow ways cannot be easily tied to a specific city gate, given their clarity and degree of preservation on remote sensing imagery, some of these could potentially lead into the southern gate that connected to the street we associate with core C7.⁶⁹

In conclusion, these first results already give us some further insights into Assur's New Town area. On the one hand, they confirm in broad strokes the existence of two major occupation phases, separated by evidence of destruction that is marked in some places by thick layers of ashes; these correspond to the "Assyrian" and "Parthian" phases of the city's history, to use the basic classifications first employed by Walter Andrae. It is necessary to point out that the 2023 excavations have already produced a more detailed stratigraphy which, in concert with the 14C dates (§D1.3), produces a much more nuanced picture of the occupation of one area within the New Town. Overall, most, if not all of the small mounds that today characterise Assur's New Town area are likely to be buildings occupied in Assyrian times, with instances of later reuse.

69 Altaweel 2008.

On the other hand, the coring work documents the presence of a street with as many as three phases. Future work will need to verify the extent of this street and its various building phases as well as its connection to the gate. Crucially, the evidence of core C7 suggests that the street may have been paved, and further work is needed in other parts of the street in order to verify this and to assess whether the street was paved in its entirety or only partially.

C4. Soil and sediment magnetism in Assur, 2023

Andreas Stele, Sandra Hahn, İnci Nurgül Özdoğru & Jörg Fassbinder

Enrichment of magnetic minerals in the topsoil and archaeological sediments not only plays a crucial role but indeed forms the essential basis for any successful magnetometer prospecting. Magnetometry (§C2) is a potential method. This means that magnetic field anomalies can overlap and add up; their intensity does not change linearly with distance and therefore rarely allows a simple and clear interpretation. In the New Town of Assur, we have to deal with a large number of overlapping settlement layers from the Late Bronze Age to (at least) the Parthian period, all of which appear in the measurement image at the same time. In addition to the processes of enrichment and new formation of magnetic minerals, thermo-remanent magnetisation also plays a major role in the reliable geophysical interpretation of magnetometer data.

In Assur, we had the opportunity to examine, for the first time, a series of sediment samples that had been made available through geoarchaeological drilling undertaken in February 2023 under the direction of Mark Altaweel in the southern part of the New Town (§C3). The mineral magnetic analyses that we performed at LMU Munich are conservative, i.e. the samples are not destroyed or consumed after the examinations and are available for further analyses. After the measurements in the LMU Munich laboratories had been completed parts of the sample materials were sent to Eileen Eckmeier (University of Kiel) for further sediment analyses, and the remainder was returned to Iraq in late October 2023.

The results of the mineral magnetic analyses we present here allow us to provide a wide and comprehensive physical interpretation of the magnetometer prospecting results, the value of which for further prospecting cannot be overestimated.

C4.1 Approach and methodological background

At the laboratory of the Bayerisches Landesamt für Denkmalpflege (BLfD) in Munich, the colours of the 33 samples (Table C3.1) were determined, using the revised Munsell Standard Soil Color Charts (SSCC), and magnetic susceptibility parameters were measured, using a Bartington MS2B dual frequency sensor (MS2B). Hysteresis, back-field curves and thermomagnetic measurements of selected samples were carried out at LMU Munich's geophysics laboratory.

In the dry state, mainly humic substances and iron compounds determine the colour of the substrates, like sediments and soils. With the visual colour determination, we record the following parameters: colour depth and intensity (hue), colour saturation (chroma) and colour brightness or dark level/grey value (value). Using these parameters and taking into account the grain size of the substrates, we can make statements about the humus content (hc) and colour-determined, pedogenic iron minerals in samples.⁷⁰

Using magnetic susceptibility as a proxy of the magnetic contrast, findings and soils, as well as anthropogenically influenced sediment layers, can be distinguished. Enrichment processes and volume/mass contents of geogenic, pedogenic, sedimentary, and anthropogenic ferromagnetic iron compounds control such contrasts.⁷¹ Moreover, they ultimately determine whether archaeological structures appear as anomalies in the magnetic survey data or not. We used the MS2B instrument to measure the low-frequency volume magnetic susceptibility (κ_{lf}) at 470 Hz, and the high-frequency volume magnetic susceptibility at 4700 Hz. From these two κ parameters, the frequency-dependent (κ_{fd}) magnetic susceptibility was calculated. By taking into account the mass and the density of the samples, the mass-specific magnetic susceptibility (χ) was determined.⁷² Summarised and simplified, χ reflects the mass of all magnetic particles, κ_{lf} reflects the volume normalised magnetic contrast, and κ_{fd} allows conclusions to be drawn about the relative proportion of ultrafine magnetic particles, the so-called superparamagnets (SP), in the respective sample.

For a better understanding of the magnetomineralogy and the magnetic susceptibility contributors in the samples, we carried out rock-magnetic measurements with a one-component Lakeshore Vibrating Sample Magneto-

70 Scheinost/Schwertmann 1999; Ad-hoc-AG Boden 2005; Blume *et al.* 2010.

71 Fassbinder 1994; Dearing 1999.

72 Dearing *et al.* 1996.

meter (VSM) and a Mag-Instruments Variable Field Translation Balance (VFTB). Hysteresis loops, continuous in-field measurement of the magnetisation as a function of an external magnetic field which is cycled from zero to the maximum positive field of 500 mT up to the maximum negative value of -500 mT and back to 500 mT, backfield demagnetisation curves, a zero-field measurement of the magnetisation as a function of an external field up to 500 mT, applied in the opposite direction as the initial saturation field, and isothermal remanent magnetisation (IRM) acquisition curves, a zero-field measurement of the magnetisation after demagnetisation as a function of an external field from zero to 500 mT, were performed for four selected samples. The hysteresis loops were corrected for the paramagnetic contribution by the slope above 350 mT. The standard hysteresis parameters, saturation magnetisation M_s , remanent saturation magnetisation M_{rs} , coercivity B_c , remanent coercivity B_{cr} and saturation isothermal remanent magnetisation IRMs, were calculated from these measurements. Thermomagnetic curves (M/T curves), a continuous measurement of the saturation magnetisation (in a field of 300 mT) while heating in the air from room temperature to 700° C and back to room temperatures with a heating rate of 40° C/min, were obtained for the same set of samples. Heating in the air promotes oxidation processes, yet reducing conditions cannot be avoided in parts of the sample in the VFTB sample holder, as organic material in the soil samples releases CO and CO₂ gases from their decomposition at elevated temperatures.⁷³ The behaviour of the heating and cooling branch of the M/T curves and their derivatives (dM/dT) can help to determine the magnetominerology directly by the observed Curie temperatures,⁷⁴ or indirectly by the observed changes in the magnetisation due to secondary formed minerals by oxidation or reduction of the initial mineralogy.⁷⁵

C4.2 Results and discussion

Substrate magnetism results should always take into account the environmental conditions. In our case, in addition to the specific (geo)archaeological setting, the lithology and associated parent rock materials of the sediments, palaeosols and recent soils are relevant. Lithologically, the cores are located at the transition between the polygenetic sediments of the Tigris floodplain in the east and

the clastic rocks of the Injana Formation (Late Miocene) in the west.⁷⁶ According to the FAO/UNESCO Soil Map of the World and due to the vicinity of the Tigris streambed, fluvisols are mapped as the standard soil type.⁷⁷ However, the findings from the coring (§C3) indicate that the sediments and soils analysed were all subject to mainly terrestrial conditions (see, for example, the carbonate nodules, which were also observed in deep sediment layers).

The measured values of κ_{if} are relatively high for Miocene sediments and soils formed on such parent material.⁷⁸ With regard to the magnetic survey data, however, the highest magnetic contrast can be observed in core C5 (for which, see §C3.2). The southern positive part of a high-intensity magnetic anomaly (+/- 100 nT) was drilled here. The sample CO12 from this core shows the highest κ_{if} value and marks the interfering body, the so-called mass anomaly, for the high-intensity anomaly in the magnetogram (Fig. C2.4). Ash and charcoal are documented for this mass anomaly layer. We can assume that there was a high-temperature effect on the findings/sediments at a depth of 70 cm and that the intense anomaly could indicate remnants of an oven or something similar. Slightly lower magnetic contrasts can be observed for the buried layers of the presumed ancient road in cores C6 and C7 (for which, see §C3.2). The archaeological layers/findings suggest that the high κ_{if} samples CO01, CO03 and CO09 act as mass anomalies and create the magnetic anomaly in the survey data associated with the ancient roads.

Samples from anthropogenically influenced substrates thus show higher κ_{if} . The tendency to decrease with depth is less pronounced with this parameter than with κ_{fd} (Fig. C4.1 and note the weak negative correlation of κ_{fd} /depth in Table C4.1). Chroma and the associated humic content, on the other hand, tend to increase with depth, which is typical in floodplains and river margins of dry regions. Natural and anthropogenic signals, therefore, overlap. The question arises whether the magnetic susceptibility parameters can serve as proxies for anthropogenic influence on soils and sediments in Assur.

Since χ is a frequently used parameter of magnetic susceptibility, it can be compared with the specific literature data. In addition, there are characteristic values developed for this parameter, like the pedogenic enhancement ratio (χ_{max}/χ_{min}), in which the maximum values (χ_{max}), usually determined in the topsoils, are compared with the parent

73 Jordanova/Jordanova 2016.

74 Fabian/Shcherbakov/McEnroe 2013.

75 E.g. Hanesch/Stanjek/Petersen 2006.

76 Sissakian/Al-Ansari/Knutsson 2014; Sissakian *et al.* 2016.

77 FAO/UNESCO Soil Map of the World (2023): <https://www.fao.org/soils-portal/data-hub/soil-maps-and-databases/faounesco-soil-map-of-the-world/en/> (last accessed 17 January 2024).

78 Compare e.g. Gilder/Chen/Şen 2001.

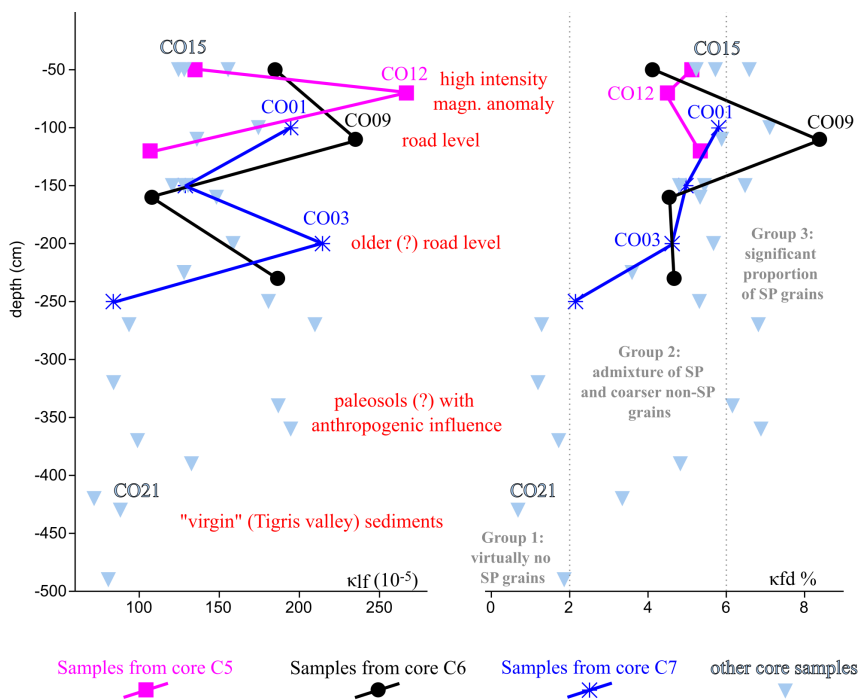


Fig. C4.1: Magnetic susceptibility parameters κ_{f} (x-axis on the left) and κ_{fd} (x-axis on the right) versus depth (y-axis) of the core samples in the area of the southern city of Assur. Samples from drilling cores within magnetic survey anomalies are highlighted, and the samples discussed in the text are labelled. A brief interpretation of the respective levels is shown in red in the centre. The categorisation of the groups and classification of the κ_{fd} values (on the right) is based on Dearing 1999 and Dearing *et al.* 1996. Created by Andreas Stele.

n = 33	χ	κ_{f}	κ_{fd}	depth	mass	humic content	Hue 10 YR chroma	Hue 10 YR value
χ								
κ_{f}	0.98							
κ_{fd}	0.70	0.64						
depth	-0.39	-0.38	-0.54					
mass	-0.22	-0.04	-0.45	0.18				
humic content	-0.30	-0.29	-0.25	0.29	0.22			
chroma	-0.55	-0.49	-0.55	0.56	0.48	0.69		
value	0.06	0.07	0.06	-0.21	-0.07	-0.91	-0.48	

Table C4.1: Linear correlation (r) matrix of selected parameters of the core samples in the area of the southern city of Assur. Significant positive correlation coefficients are marked in green, and weak positive correlations in blue. Significant negative correlations are marked in red, and weak negative correlation coefficients in orange. Created by Andreas Stele.

rock material values (χ_{min}).⁷⁹ Although, in this case, we are dealing not only with recent soils and paleosols but also with sediments, the ratio fits here because all suscepti-

bility parameters tend to decrease with depth (Fig. C4.1 and Table C4.1).

The comparison of our χ results with the values from the soil and sediment magnetism literature on similar lithology⁸⁰ shows that all samples have high χ , suggesting high mass fractions of magnetic particles. Due to the relatively wide range of χ values, the pedogenic enhancement is correspondingly high: 3.6, a value that would be typical for fertile chernozems on loess but definitely not for fluvisols. This already indicates that the genesis and the enhancement of magnetic particles are only a little dependent on natural, pedological processes but mainly on anthropogenic influence.

The κ_{fd} parameter provides the best evidence for this claim: on the one hand, the parameter decreases with depth; on the other hand, the values themselves and their comparison with values/classifications from the literature provide indications of the possible anthropogenic origin of the superparamagnets. It is known from experiments that clays used for the production of pottery or bricks develop significant superparamagnetic contents of $\geq 6\%$ when baked at 400°C and higher temperatures.⁸¹ Using the categorisation of κ_{fd} values,⁸² the Assur core samples can be divided into three groups: group 1 with virtually no SP grains; group 2 with an admixture of SP and coarser non-SP grains; group 3 with a significant proportion of SP grains.

For comparison and further confirmation of the hypothesis of anthropogenic SP, we took a fresh sediment sample from the banks of the Tigris, below the excavation house. This control sample showed the following susceptibility parameter values: $\chi = 0.8 \cdot 10^{-6} \text{ m}^3 \text{ kg}^{-1}$; $\kappa_{f} = 909 \cdot 10^{-6}$; $\kappa_{fd} = 1\%$. Therefore, it can be assigned to group 1, representing "virgin" sediments and can be re-

79 Jordanova 2016.

80 E.g. Maxbauer 2020.

81 Kostadinova-Avramova/Kovacheva 2013.

82 Dearing 1999; Dearing *et al.* 1996.

Sample	Group	κ_{fd} (%)	κ_{fr} (10^{-6})	χ ($10^{-6} \text{ m}^3 \text{ kg}^{-1}$)	M_s ($*10^{-5} \text{ Am}^2$)	M_{rs} ($*10^{-6} \text{ Am}^2$)	B_c (mT)	B_{cr} (mT)	IRMs (μAm^2)
CO01	2	5.81	1946	1.32	2.45	4.28	10.02	29.48	4.14
CO09	3	8.38	2350	1.63	2.32	4.4	9.71	27.45	4.28
CO15	2	5.23	1281	0.91	1.64	2.71	9.36	27.95	2.66
CO21	1	0.68	882	0.60	1.52	1.96	7.59	19.82	1.69

Table C4.2: Susceptibility and hysteresis parameters of representative samples from the respective groups in **Fig. C4.1**, which were subjected to VFTB and VSM measurements. Created by Andreas Stele and Sandra Hahn.

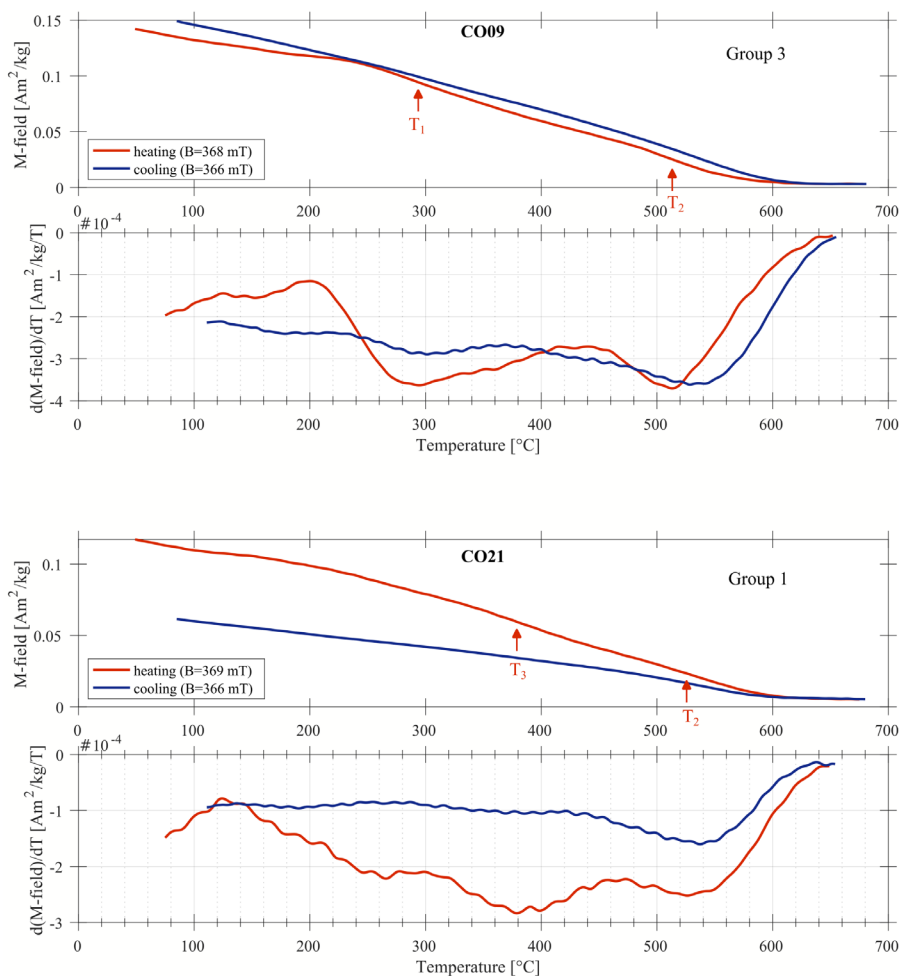


Fig. C4.2: Original thermomagnetic curves (M/T curves) (top in each case) and their derivatives (bottom in each case) for the representative samples (see **Fig. C4.1** to see which samples belong to which core). The Curie temperatures ($T_{1...}$) determined in each case and discussed in the text are shown using red arrows. Created by Sandra Hahn.

garded as the counterpart to group 3 with anthropogenic enrichment of SP due to the pottery and brick fragments in the samples with κ_{fd} of $\geq 6\%$ (**Fig. C4.1**, right). However, this poses the question of which magnetominerals are responsible for these different susceptibility parameters and whether further rock magnetic investigations can support our hypothesis of anthropogenic enrichment of SP. We conducted further magnetic analyses on at least one sample from each group to answer this question.

All representative samples show similar hysteresis parameters, despite partly different susceptibility parameters or belonging to different κ_{fd} groups (**Table C4.2**). Only sample CO09 stands out with slightly higher M_{rs} and IRMs values, but these are probably due to the higher SP content (see also high κ_{fd} values).

Regarding the M/T curves, in the original heating curves of all samples, a “hump and a bump” pattern can be observed (see also the representative sample CO21 in **Fig. C4.2**): the magnetisation rises slightly from $\sim 100^\circ \text{C}$ and falls again slightly at $\sim 380^\circ \text{C}$ where it marks the first thermomagnetic phase transition (hump $\Rightarrow T_3$). After a bump between 400 and 500°C , a further slight hump (T_2) can be traced between 500 and 550°C . This pattern indicated the presence of maghemite, an oxidation product of magnetite.⁸³ Maghemite is unstable between 300 and 400°C (see T_3) and transforms into haematite in the first thermomagnetic phase during heating. The second thermomagnetic phase (T_2) is due to the non-oxidised/non-maghemitised magnetite in the samples. The magnetite phase remains largely intact after heating, while maghemite transforms almost completely, as shown by the cooling curves of the samples in **Fig. C4.2**. Maghemite was thus formed during the weathering of magnetite under atmospheric conditions and can be interpreted as a pedogenic magnetic phase in the soils and palaeosols

of Assur, while magnetite probably forms the original sedimentary phase.

The M/T curves of the samples CO01, CO15 and CO21 are very similar; only CO09 shows again slight thermomagnetic differences between 120 and 400°C (**Fig. C4.2**). It can be assumed that this also has to do with the higher

⁸³ Bilardello 2020; Maxbauer 2020.

proportion of the SP grains in the sample CO09. This is because T₁ is apparently not produced by maghemite but by a magnetic phase that is superimposed on the maghemite phase. The source and type of this phase are not clearly definable; it can be either pedogenic (SP maghemite?) or anthropogenic (SP titanomagnetite or titanomaghemite?). It is, in any case, not sedimentary. The available data and observations, especially sample CO09, indicate that the SP fraction could produce this phase in the southern part of the city of Assur and, therefore, be of anthropogenic origin. Similar thermomagnetic phases were observed, e.g., in pottery fragments or anthropogenic sediment layers.⁸⁴

C4.3 Conclusions

In 2023, soil colour and geophysical in situ analyses were undertaken on 33 soil and sediment samples from the southern part of the New Town of Assur.

These analyses allowed the detection of magnetic interfering bodies in the sediment profiles responsible for anomalies in the magnetograms of Assur (§C2). It has been found that in the areas of cores C6 and C7 (for

which, see §C3.2), former road layers produce magnetic anomalies in the survey data. In contrast, the high-intensity magnetic anomaly in the area of core C5 (for which, see §C3.2) is produced by highly heated anthropogenic substrates.

Regarding magnetomineralogy, magnetite was found as the original sedimentary phase and maghemite as their pedogenic oxidation product. In addition to the maghemitisation of magnetite, there is further enrichment of the soils and sediments with superparamagnetic grains of an undetermined magnetomineral. This enrichment seems to be anthropogenic.

When geoarchaeological surveys and analyses are conducted in the future, parameters of magnetic susceptibility and the determination of soil colours can be additionally used to distinguish natural and anthropogenic substrates in Assur. Especially the frequency dependence of the magnetic susceptibility (κ_{fd}) with values higher than 6% can be used as a meaningful parameter for anthropogenic influence on soils and sediments on the given lithological unit. This is important as far as such analyses do not require complex instruments; they can be carried out relatively quickly and on-site.

	χ ($10^{-6} \text{ m}^3 \text{ kg}^{-1}$)	κ_{if} (10^{-6})	κ_{fd} (%)	Hue 10 YR	Hue 10 YR	humic content (%)
				chroma	value	
N	33	33	33	33	33	33
Min	0.50	718.00	0.68	1.00	5.00	0.75
Max	1.82	2668.00	8.38	4.00	7.00	3.00
Sum	33.39	47983.00	156.13	77.00	210.00	41.50
Mean	1.01	1454.03	4.73	2.33	6.36	1.26
Std. error	0.06	84.17	0.32	0.15	0.11	0.11
Variance	0.12	233790.20	3.48	0.79	0.43	0.40
Stand. dev	0.34	483.52	1.87	0.89	0.65	0.63
Median	0.93	1326.00	5.12	2.00	6.00	1.25
25 prcntil	0.83	1073.50	3.85	2.00	6.00	0.75
75 prcntil	1.29	1856.00	5.84	3.00	7.00	1.50

Table C4.3: Supplemental statistics. Created by Andreas Stele.

84 See e.g. Sample 2 in Stele *et al.* 2019.

D. Excavating in the New Town of Assur in 2023

D1. The 2023 work plan and its implementation

Karen Radner & Andrea Squitieri

According to the permit issued in April 2022, our excavations take place in the New Town of Assur (**Fig. D1.1**). In 2002, the SBAH conducted a series of excavations in this part of Assur, in four separate trenches; the results of this work have not been published. The largest of these trenches was designated as “New Town 4” and situated on a low mound in the southeastern part of the New Town, close to the river and the southernmost part of the fortification walls (**Fig. D1.2**). This work brought to light a substantial Assyrian building. As the SBAH trench was never backfilled, many of the structures that were then

exposed are still preserved although rain and wind have caused much erosion (**Fig. D3.1**).

The preliminary results of the magnetometer prospection conducted just before the start of the 2023 excavation (**§C2**) suggested the presence of building structures directly west of those exposed by the Iraqi team. We decided to concentrate on only this one area, excavating a trench named NT1 2023 (for New Town, trench 1, year 2023). After we celebrated Walter Andrae’s birthday on 18 February 2023, unveiling a plaque honouring his achievements in Assur and dedicating the new work to his memory, the excavation started on 19 February 2023. The field team was led by F. Janoscha Kreppner, supervised by Jens Rohde and consisted of Jan Heiler, Veronica Hinterhuber, Tarik Willis and Marco Wolf.



Fig. D1.1: View of the Assur New Town from the south. In the foreground: the NT1 2023 trench and the 2002 SBAH trench. Photo by Jens Rohde, taken with a DJI Mavic 3 Pro drone.



Fig. D1.2: Orthophoto of the Assur New Town with the NT1 2023 trench in red and the 2002 SBAH trench in white. Created by Jens Rohde, annotated by Andrea Squitieri.

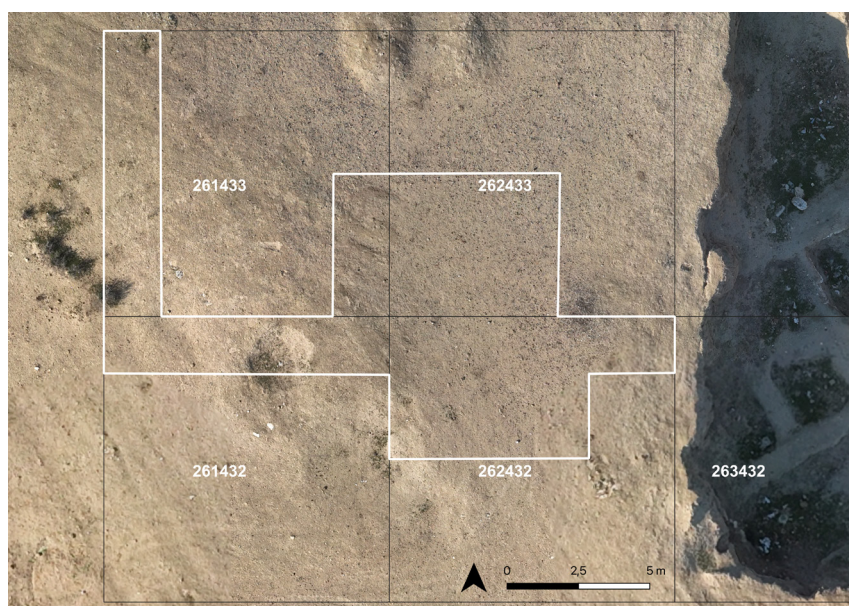


Fig. D1.3: The NT1 2023 trench and the excavation grid. Created by Andrea Squitieri.

The initial work programme was to expose a T-shaped trench, with a 20 m long, 2 m wide arm running from east to west (starting from the western section of the Iraqi trench), and another arm, perpendicular to the first, also 2 m wide and 20 m long, extending north to south. Already in the first week of excavations, the original work plan had to be drastically modified. At that time, the remains of a substantial chamber tomb came to light, just below the surface. It was this substantial burial place, rather than a further part of the Assyrian building unearthed by SBAH in 2002, that had been observed in the preliminary magnetometer results. Because a key objective of the new excavations is to gather data that goes beyond the evidence recovered by Andrae and subsequent excavators at Assur, the discovery of the tomb was not a disappointment as it was quickly apparent that it would yield a significant amount of human remains, suitable both for radiocarbon dating and DNA analysis – neither of which had ever been conducted with material from Assur. It was therefore decided to fully expose the tomb, and this necessitated enlarging the east-west part of the trench. All our subsequent work focused on this area and, upon the chamber tomb's removal on 8 March 2023, the structures underneath. On 23 March 2023, we met another of our key objectives when we reached the virgin soil.

Because of these developments, the southern section of the north-south part of the planned T-trench was not excavated, and only the upper levels of the northern section were unearthed. These modifications resulted in a roughly L-shaped trench covering an area of 120 m² (Fig. D1.3), and the results of its excavation are discussed in §D2.

At the beginning of the excavations, a baulk of 2 metres was left in place between the new trench and the SBAH trench. In the course of the campaign, it became necessary to secure and clean the western profile of the SBAH trench. The substantial wall Locus:262432:075 (§D2.7.1) was found to provide sufficient protection for the new excavation, and it was decided to use the opportunity to excavate the corners of two adjoining rooms, the better parts of which had been exposed by SBAH in 2002. Our goal was to reach the rooms' floors and to obtain materials suitable to produce radiocarbon dates, and in this, we were successful (for the results see §D1.3). This work is presented in §D3.

D1.1 A new digital documentation system for Assur

Our digital documentation system builds upon the experiences gained with the Peshdar Plain Project (PPP) since 2015.⁸⁵ Christoph Forster (www.datalino.de), who had created the documentation infrastructure for PPP, was now commissioned to design the new Assur Excavation Database as a server-based MySQL database, accessible remotely by all members of the team via a user-friendly web interface. Originally in English only, parts of this interface have since been translated into Arabic to allow the local colleagues of SBAH Sherqat to use it in the future.

In the database, all archaeological contexts are documented within a 10 × 10 m square grid using the locus-collection system, in which the locus (pl. loci) is defined as a stratigraphic unit. The grid is aligned northwards within the WGS 84/UTM 38N coordinate system (EPSG: 32638). Each square is assigned a six-digit number, with the first three digits corresponding to the Easting coordinates of the southwestern square corner, and the last three to the Northing coordinates of the same corner. E.g., the southwestern corner of Square 261432 has the UTM coordinates 342610 E, 3924320 N. In 2023, the excavation took place in the squares 261432, 261433, 262432, 262433 and 263432 (Fig. D1.3).

In the excavation, each locus is named after the square number followed by a progressive number (e.g. Locus: 261432:001 is Locus 1 in Square 261432). Whenever a locus

⁸⁵ Kreppner/Forster/Squitieri 2016.

extends across multiple squares, it is either assigned to the square where it occupies the greatest area, or to the square in which it is first identified. Individual finds, samples (§D1.2) and collections of fragmentary material (usually pottery sherds and bones) retrieved from a locus are identified by the prefix AS, which stands for Assur, and receive an additional progressive number after the locus number (e.g., AS 261432:001:001 is Collection 1 in Locus 1 of Square 261432).

The field team members measured the locus outlines and the findspots of samples and small finds using a Leica dGPS (base model GS10; rover model GS18) owned by LMU Munich's History Department. Measurements on floors were carried out following a specific protocol, described below (see §D1.2.1). At the end of each excavation day, Jens Rohde took drone photos using a DJI Mavic 3 Pro to keep track of the excavation progress. On the same day, he processed the drone photos in the software package Agisoft Metashape and thus created the necessary orthophotos as well as 3D models and digital elevation models (DEM).

D1.2 A sampling strategy for Assur: objectives and methods in 2023

The sampling strategy introduced in 2023 has three main objectives that concern absolute dating, bioarchaeology and DNA analysis.

For the first objective, we seek to obtain samples suitable for radiocarbon and therefore absolute dating. For floors and other architectural contexts, we sample both seeds and charcoal (§D1.2.1), and for burials, we select appropriate teeth (§D1.2.2). The goal is to enable the establishment of a more detailed chronological sequence for the city's occupational history. A special focus is given to the period after the fall of the Assyrian Empire and the capture of Assur in 614 BC, to develop a more nuanced understanding of what is traditionally lumped together as the "Parthian" occupation of Assur.

For our second objective, we seek to collect a broad range of bioarchaeological samples that will serve us and others as evidence for the reconstruction of the relationship of Assur's inhabitants with their environment throughout time, with a particular focus on changes and continuities. To this aim, we used the following approaches in 2023. On the one hand, sediment samples assumed to contain phytoliths, all pieces of charcoal and all animal bones were routinely collected during the excavation and registered in the database in order to ensure that all necessary contextual information was recorded. On the other hand, once a floor was securely identified in the excavation, sediment samples were collected and transported

to the excavation house where they underwent flotation, with the primary goal to collect seeds and other palaeobotanical remains. Such datasets have not previously been systematically collected at Assur.

Finally, our third objective is to obtain, for the first time in Assur, material suitable for human DNA analysis, an approach that has become very prominent in recent years.⁸⁶ Gathering data from Mesopotamia is a priority, as very little material is currently available for this part of the ancient world. Building on experiences from PPP since 2015, we primarily identify molars as samples for export as they are suitable both for radiocarbon dating and for DNA extraction, and also offer possibilities for calculus analysis as well as stable isotope and trace elements analysis, among other things. Such analyses feed back into the second objective for our sampling strategy. Moreover, we have a broader interest in collecting as much information as possible on the deceased from burials at Assur, as the human remains unearthed during Andrae's excavations were never systematically collected and are therefore no longer available for analysis,⁸⁷ seriously hampering our understanding of the funerary culture at this site through the ages. In May 2023, the molars were submitted for DNA extraction and analysis to the Max-Planck-Institut für evolutionäre Anthropologie in Leipzig, and afterwards for radiocarbon dating to the Curt-Engelhorn-Zentrum Archäometrie (CEZA) of the Reiss-Engelhorn-Museen in Mannheim (for results see §D1.3).

D1.2.1 Sampling floors

A standardised protocol has been used in the PPP's exploration of the Dinka Settlement Complex since 2015, and this was also applied in the 2023 excavations at Assur when exposing the floors of Building A (§D2.6.2-3). For tightened spatial control, these floors were gridded with a 1 × 1 m grid, with the grid vertices and each square's centroid measured using the dGPS. Subsequently, the deposit overlying the floor was excavated square by square. Each square was assigned specific numbers for "collections" of pottery and animal bones and "samples" for phytoliths, charcoal, and flotation. Each collection is linked to the dGPS-measured square centroid. Phytolith samples were taken by collecting small amounts of soil in randomised spots ("blind sampling") of each floor square. Charcoal was collected once identified and measurements were taken on the spot with the dGPS. For flotation, 100% of

⁸⁶ Orlando *et al.* 2021.

⁸⁷ Hauser 2012.

the soil layer covering the floor, typically about 3-4 cm, was collected from each floor square in the field.

Gridding was not necessary for the much smaller surfaces of the floors of “Room 5” and “Room 6”, which were exposed in the baulk of the former Iraqi trench with the goal of gaining dates for the structures excavated in 2002. The procedure used there is discussed in §D3.

Once the flotation samples were delivered to the excavation house, responsibility for the further steps of sampling was transferred from the field team to Karen Radner, Jana Richter and Andrea Squitieri who constituted the flotation team. The flotation machine now set up at Assur (Fig. D1.4) is the one PPP had employed in the Peshdar Plain since 2015 when it was constructed in Sulaymaniyah using the same design and the same workshop as the machines employed for flotation at the Bestansur exca-



Fig. D1.4: The flotation machine in use at Assur. Photo by Karen Radner.

vations led by Roger and Wendy Matthews (University of Reading) and at the excavations of Gurga Chiya and Tepe Marani directed by Robert Carter and David Wengrow (University College London).⁸⁸

The purpose of flotation is to separate light fractions, principally containing seeds, from heavy fractions (micro-artifacts, micro-pottery fragments, and tiny bones, as well as any gravel in the soil). To this end, we use fine-weave bags with mesh sizes of < 1 mm to collect the light fraction, whereas the heavy fraction is caught in the flotation machine using a net with a mesh size of 1 mm and afterwards collected in sieves for drying. After the light fractions have dried in the flotation bags and the heavy fractions in the sieves, the two sets are bagged and labelled separately, with the amount in litres indicated on the labels and in the excavation database.

In contrast to the Peshdar Plain where supplying the flotation machine with the necessary water and electricity is unproblematic, the conditions encountered in Assur

in the spring of 2023 were challenging. The machine was installed in front of the excavation house but there is no functioning well and all water needed for the running of the excavation house is delivered by truck. It was therefore necessary to install a pump that would bring up the water required for flotation from the Tigris. Because the river was in flood at the time we set up the machine, the water could not be used directly for flotation because it was too muddy. It was first collected in a separate tank so that the mud would sink to the bottom. The clean water was then pumped into the flotation system. Already procuring and purifying the water required a substantial amount of electricity. In addition, the flotation machine itself had to be run, with its own pump that ensures the continuous flow of the water between the three tanks. The infrastructure available to us at the time could not easily provide the power supply needed. Running the flotation machine therefore required careful scheduling and balancing with the other needs in the excavation house, including the kitchen. Unlike in the Peshdar Plain, it was not possible to run the machine continuously for a whole day.⁸⁹

We use both seeds and charcoal for radiocarbon dating of architectural contexts. While all charcoal is used for wood analysis (§H2) some pieces are sampled for radiocarbon analysis; if possible we try to select part of a large piece and keep the rest for wood analysis. Although the dates derived from short-lived seeds are generally thought to be much more precise for dating archaeological contexts (but see §D1.3), charcoal has the logistical advantage of being available for radiocarbon analysis as soon as the samples have been exported from Iraq. In contrast, the tiny seeds can only be radiocarbon-dated after a palaeobotany specialist has isolated them from the light fraction sample and identified them (§H3).

D1.2.2 Sampling human burials

Our protocol for the excavation of human burials entails the creation of separate loci for each deposit within the grave: the skeletons and the surrounding soil are therefore treated as separate loci. Before removing any bones, the skeleton is described in the field and documented with photos and 3D models.

In 2023, we unearthed burial contexts from three different chronological horizons and were able to collect the corresponding human remains. Furthermore, we collect-

88 Greenfield 2016.

89 This vexing issue has now been resolved as a photovoltaic system was installed in August 2023. For details see §B5.

ed sediment samples for parasitology analysis from the head, the pelvis and the area below the feet from the undisturbed burial contexts of Grave 3 and Grave 4. From there, we were also able to collect further sediment samples from the torso for phytolith analysis, as well as textile fragments from Grave 3 (currently analysed by a team headed by Dr Annette Paetzgen Schieck of the Deutsches Textilmuseum in Krefeld) and leather fragments from Grave 4 (currently analysed by a team headed by Prof. Dr Joris Peter at LMU Munich's Institut für Paläoanatomie). The textile and leather fragments were consolidated on the spot by Andrea Squitieri using a solution of 5% Polyvinyl Butyral 30 mixed with ethanol.⁹⁰ Subsequently, each fragment was encased in aluminium foil for safekeeping and transportation.

After recording and sampling, the human bones from all burial contexts were collected, curated, and stored for further anthropological studies. The remains unearthed in 2023 will be analysed on-site in the spring of 2024 by Dr Rafał Fetner (University of Warsaw). As discussed above, selected molars from all burial contexts have already been exported and submitted for DNA and radiocarbon analysis. Unfortunately, the collagen levels of the teeth from Graves 3 and 4 proved too low to allow radiocarbon dating. The other molars yielded clear results (see §D1.3).

D1.3 First radiocarbon dates from the 2023 excavations

On 8 May 2023, after export permission for six months had been secured from all relevant authorities, all samples were exported from Baghdad to Munich by Jana Richter and subsequently handed over to various specialists and labs. The leftovers were transported back to Iraq by Jana Richter and Andrea Squitieri on 22 October and formally returned to SBAH in Baghdad on 23 October 2023.

The following samples were submitted for radiocarbon analysis:

1. Eight human teeth, selected from all three burial contexts uncovered in 2023 – the chamber tomb (Grave 1; §D2.3), the two sarcophagus burials (Grave 3 and Grave 4; §D2.5) and the Neo-Assyrian burial (Grave 5; §D2.8), were dispatched for DNA extraction to the Max-Planck-Institut für evolutionäre Anthropologie in Leipzig on 10 May 2023. Due to the state of preservation, only five of these molars (3× chamber tomb, 2× Grave 5) were deemed suitable for radiocarbon dating. Those

were sent from Leipzig to the Curt-Engelhorn-Zentrum Archäometrie (CEZA) of the Reiss-Engelhorn-Museen in Mannheim, where they arrived on 22 May 2023. Radiocarbon dates for four teeth were received on 14 September 2023, whereas the collagen levels in one molar from the chamber tomb (lab number MAMS 63062) were found to be too low to allow for analysis. Note that one of the four successful samples, another molar from the chamber tomb (lab number MAMS 63060), had a low collagen level (0.4%) but the carbon-to-nitrogen ratio (3.3) was deemed acceptable to go forward with the analysis.

2. From 34 available samples, five pieces of charcoal were selected for radiocarbon dating based on stratigraphic relevance: from the NT1 2003 trench, one sample each from the floor of Room 2 in Building A (§D2.6.2) and from the level just above the virgin soil in test sounding (§D2.10), and from the sondage next to the 2002 SBAH trench, one sample each from either of the two floors of “Room 6” (§D3.1) and the floor exposed in “Room 5” (§D3.2). Chunks of these charcoals were dispatched to CEZA on 15 May 2023 while all that remained of these samples was handed over with the other material to Katleen Deckers (University of Tübingen) for wood analysis on 14 June 2023. Radiocarbon results for all five charcoal samples were received on 14 September 2023.
3. The light fraction of the above-floor soil samples collected through flotation were handed over to Claudia Sarkady for palaeobotanical analysis on 26 May 2023 and received back on 6 October 2023. Eight carbonised seeds were selected for radiocarbon dating based on stratigraphic relevance: from the NT1 2023 trench, one seed from Room 1 (§D2.6.1), three seeds from Room 2 (from what we understand to be different parts of the same floor, cut by the chamber tomb: §D2.6.2) and one seed from Room 3 (§D2.6.3) in Building A; and from the sondage near the Iraqi excavation, one seed each from either of the two floors of “Room 6” (§D3.1) and another seed from the material above the floor in “Room 5” (§D3.2). We received the results of the radiocarbon analysis on 3 January 2024.

Currently, we have 17 radiocarbon dates from teeth, charcoal and carbonised seeds at our disposal, presented in **Table D1.1**. For convenience, we use the signature AsRC (for **Assur RadioCarbon**) to refer to these and all future radiocarbon dates from our excavations. The table is organised according to material and laboratory numbers.

The table combines the AsRC numbers, the excavation sample numbers and the CEZA lab IDs with information about the samples' materials and find contexts as well as

⁹⁰ According to instructions provided by the conservation specialist Carmen Gütschow (Berlin).

AsRC no.	LAB ID	Excavation sample no.	Material	Context	Relative stratigraphy	14C Age (BP)	68.3 %	95.4 %	C Coll. %	Eastings (UTM38N)	Northings (UTM38N)	Elevation (m asl)
AsRC 1	MAMS 63060	AS 262432:021:004:001	Human tooth	On the floor of the chamber tomb's Subdivision 3	NT1 2023 Phase 8	1818 ± 42	cal AD 167-325	cal AD 122-345*	0.4	342625.28	3924329.27	161.21
AsRC 2	MAMS 63061	AS 262433:021:005:001	Human tooth	On the floor of the chamber tomb's Subdivision 5	NT1 2023 Phase 8	1891 ± 19	cal AD 124-203	cal AD 83-215	2.6	342621.12	3924330.89	161.21
AsRC 3	MAMS 63063	AS 262432:070:002:001	Human tooth	Upper fill of Grave 5	NT1 2023 Phase 3	2489 ± 19	cal BC 756-548	cal BC 770-542	4.8	342625.08	3924328.62	160.2
AsRC 4	MAMS 63064	AS 262432:070:002:002	Human tooth	Upper fill of Grave 5	NT1 2023 Phase 3	2507 ± 19	cal BC 768-570	cal BC 775-545	4.6	342625.08	3924328.62	160.2
AsRC 5	MAMS 63165	AS 262432:079:003	Charcoal	Fill of pit cutting the virgin soil	NT1 2023 Phase 1	3214 ± 15	cal BC 1503-1451	cal BC 1506-1440	61	342625.39	3924328.58	158.88
AsRC 6	MAMS 63166	AS 261432:011:033	Charcoal	On floor of Building A Room 2	NT1 2023 Phase 5	2109 ± 14	cal BC 158-60	cal BC 173-53	67	342617.71	3924329.72	162.08
AsRC 7	MAMS 63167	AS 263432:002:003	Charcoal	On the upper floor of Room 6	/	2466 ± 14	cal BC 749-540	cal BC 755-482	60	342630.22	3924327.49	161.15
AsRC 8	MAMS 63168	AS 263432:006:003	Charcoal	On the lower floor of Room 6	/	2458 ± 15	cal BC 747-517	cal BC 751-422	65	342630	3924327.5	160.96
AsRC 9	MAMS 63169	AS 262432:066:012	Charcoal	On the floor of Room 5	/	3082 ± 22	cal BC 1405-1301	cal BC 1416-1278	5.3	342629.79	3924329.61	160.07
AsRC 10	MAMS 65645	AS 261432:011:001	Seed	On floor of Building A Room 2	NT1 2023 Phase 5	2521 ± 16	cal BC 774-590	cal BC 778-551	66	342619.38	3924329.53	162.04
AsRC 11	MAMS 65646	AS 261433:005:002	Seed	On floor of Building A Room 1	NT1 2023 Phase 5	2132 ± 15	cal BC 196-108	cal BC 341-57	65	342610.66	3924337.54	161.71
AsRC 12	MAMS 65647	AS 261433:020:002	Seed	On floor of Building A Room 2	NT1 2023 Phase 5	2113 ± 15	cal BC 166-61	cal BC 176-52	62	342618.52	3924331.51	162.04
AsRC 13	MAMS 65648	AS 263432:002:001	Seed	On the upper floor of Room 6	/	2467 ± 16	cal BC 749-541	cal BC 756-481	59	342630.21	3924327.86	161.11
AsRC 14	MAMS 65649	AS 262432:058:007	Seed	On floor of Building A Room 3	NT1 2023 Phase 5	2415 ± 15	cal BC 513-414	cal BC 658-407	64	342624.45	3924325.5	162.05
AsRC 15	MAMS 65650	AS 262433:066:002	Seed	From the deposit above the floor of Room 5	/	2500 ± 15	cal BC 759-568	cal BC 771-545	64	342630.41	3924329.65	160.13
AsRC 16	MAMS 65651	AS 262433:068:002	Seed	On floor of Building A Room 2	NT1 2023 Phase 5	2764 ± 15	cal BC 927-844	cal BC 975-835	62	342624.64	3924333.97	162.22
AsRC 17	MAMS 65652	AS 263432:006:002	Seed	On the lower floor of Room 6	/	2433 ± 15	cal BC 716-422	cal BC 734-412	58	342630.26	3924327.42	160.97

* The date range is not reliable because of the low level of collagen.

Table D1.1: Summary table of the radiocarbon dates available from the NT1 2023 trench and the sondage linked to the 2002 SBAH trench. Compiled by Andrea Squitieri.

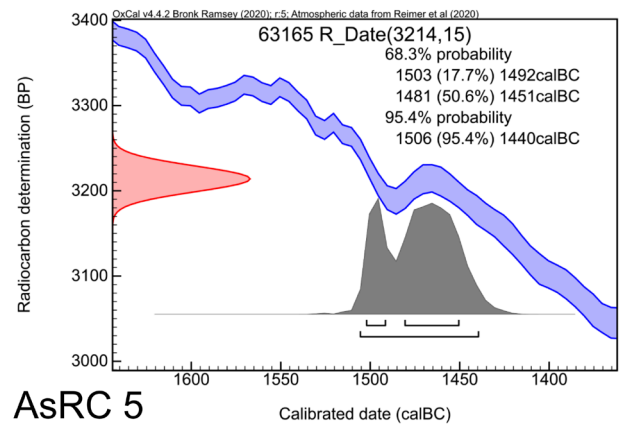
their place in the relative stratigraphy (where available). This is followed by the uncalibrated dates (^{14}C BP) and the calibrated results with 68.3% and 95.4% probability as well as the carbon and collagen levels within the sample. This is concluded by the samples' coordinates and their elevation in metres above sea level.

From NT1 2023, the oldest available date (AsRC 5 = Fig. D1.5) comes from a charcoal from directly above the virgin soil and gives a radiocarbon date range of around 1500 BC.

Two teeth from the disturbed Grave 5, whose 7th century BC date is suggested by a fibula of Pedde's type C8⁹¹ among its burial goods (§F8: no. 236), produced radiocarbon dates that, as expected, fall firmly into the Hallstatt Plateau⁹² (AsRC 3 = Fig. D1.6; AsRC 4 = Fig. D1.7).

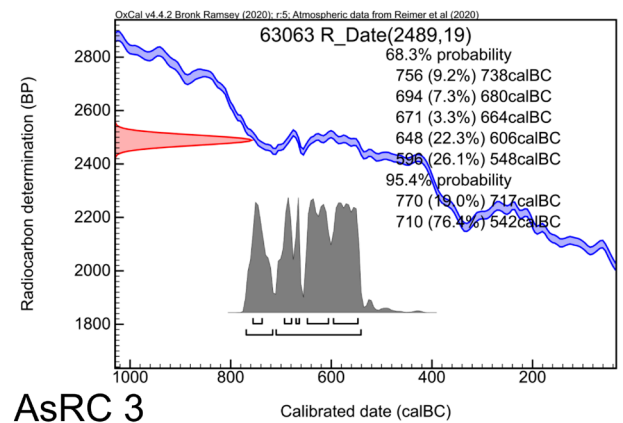
A piece of charcoal and a carbonised seed from the floor of Room 2 of Building A, down from which the sarcophagus burial (Grave 3) was dug, yielded radiocarbon dating ranges from the mid-second to the mid-first century BC (AsRC 6 = Fig. D1.8; AsRC 12 = Fig. D1.9); the inscription incised on Grave 3's sarcophagus is an alphabetic dating formula for the eleventh month of the year 153 of the Seleucid Era, that is July/August of 158 BC (§G2). This can also easily be reconciled with the radiocarbon dating range of another carbonised seed from Building A that stems from the floor of Room 1 (341-57 calBC; AsRC 11 = Fig. D1.10).

However, three other carbonised seeds from the floors of Room 2 and Room 3 of Building A yielded radiocarbon date ranges that are substantially earlier, namely 975-835 calBC (AsRC 16 = Fig. D1.11), 778-551 calBC (AsRC 10 = Fig. D1.12) and 658-407 calBC (AsRC 14 = Fig. D1.13). Two of these seeds were collected from grid squares directly adjoining the much younger underground chamber tomb (Fig. D1.14; cf. §D2.3). The presence of older plant materials in this area may be connected to the construction of that building, which was set into a pit that cut through several earlier occupation layers. The third seed (AsRC 14), however, cannot easily be connected to this construction pit. It is noteworthy that its dating range falls squarely outside of the Neo-Assyrian period, and it is therefore certainly evidence from a later occupation phase. There are of course multiple scenarios that could help account for the presence of older seeds in the floor deposits of Building A, such as the reuse of cultural debris as construction material for a newly made floor. In any case, these findings have serious repercussions for the evaluation of these palaeobotanical remains, as these



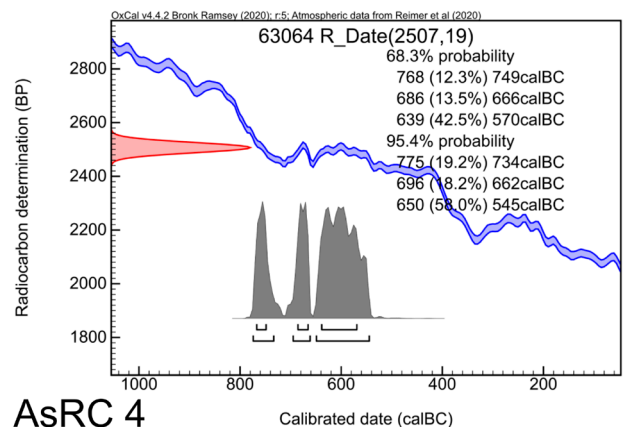
AsRC 5

Fig. D1.5: Calibrated radiocarbon determination for charcoal sample AsRC 5 (MAMS 63165) from the pit cutting the virgin soil. Prepared by Andrea Squitieri.



AsRC 3

Fig. D1.6: Calibrated radiocarbon determination for tooth sample AsRC 3 (MAMS 63063) from the upper fill of Grave 5. Easting and northing coordinates are approximate. Prepared by Andrea Squitieri.



AsRC 4

Fig. D1.7: Calibrated radiocarbon determination for tooth sample AsRC 4 (MAMS 63064) from the upper fill of Grave 5. Prepared by Andrea Squitieri.

91 Pedde 2000, 245-250, pl. 55-56: nos. 739-769: "Fibel mit länglichen, kreuzschraffierten Blocksegmenten".

92 On the problem of the Hallstatt Plateau for the radiocarbon calibration curve, see e.g. van der Plicht 2004.

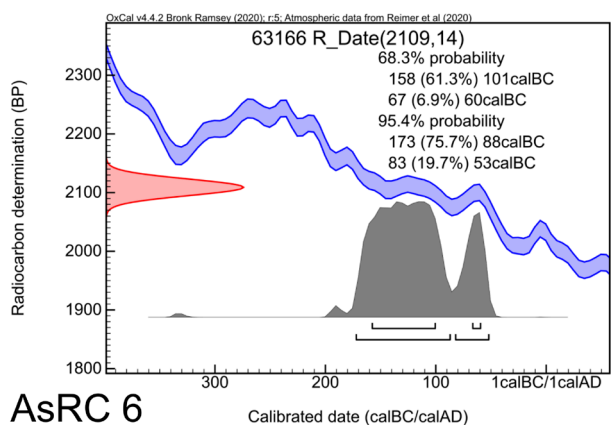


Fig. D1.8: Calibrated radiocarbon determination for charcoal sample AsRC 6 (MAMS 63166) from the floor of Room 2 of Building A. Prepared by Andrea Squitieri.

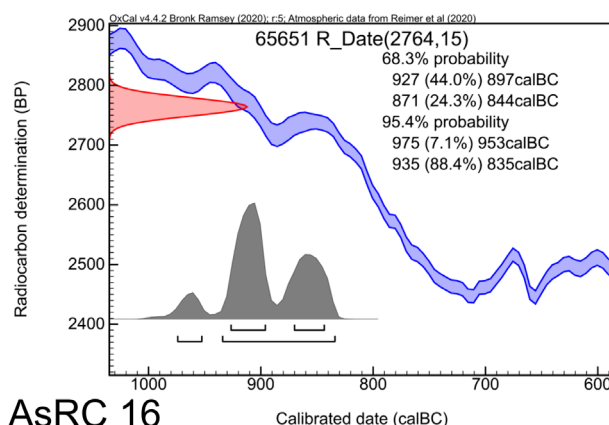


Fig. D1.11: Calibrated radiocarbon determination for the seed sample AsRC 16 (MAMS 65651) from the floor of Room 2 of Building A. Prepared by Andrea Squitieri.

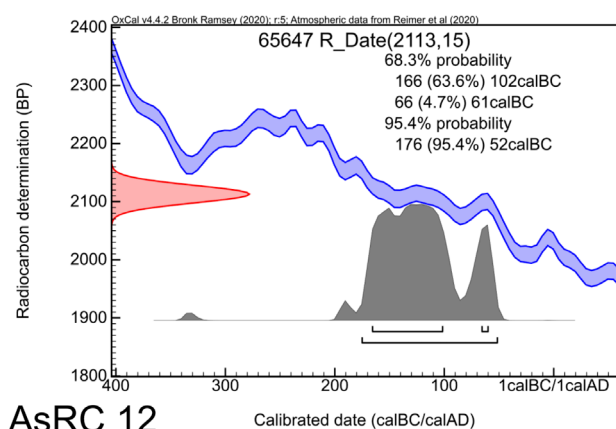


Fig. D1.9: Calibrated radiocarbon determination for the seed sample AsRC 12 (MAMS 65647) from the floor of Room 2 of Building A. Prepared by Andrea Squitieri.

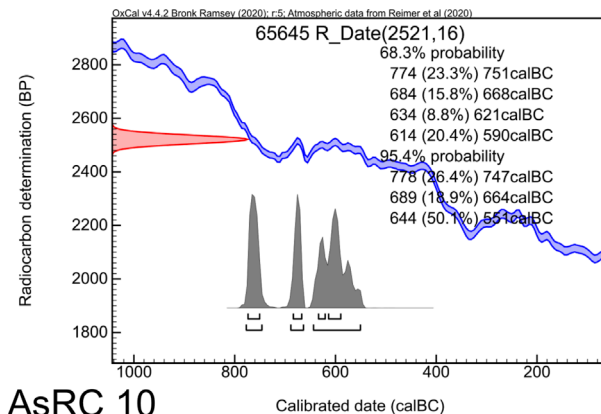


Fig. D1.12: Calibrated radiocarbon determination for the seed sample AsRC 10 (MAMS 65645) from the floor of Room 2 of Building A. Prepared by Andrea Squitieri.

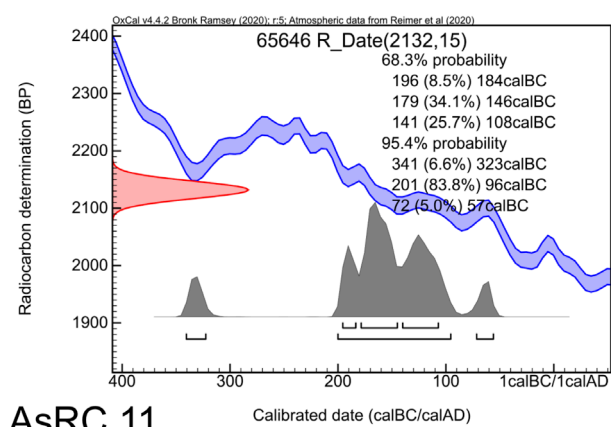


Fig. D1.10: Calibrated radiocarbon determination for the seed sample AsRC 11 (MAMS 65646) from the floor of Room 1 of Building A. Prepared by Andrea Squitieri.

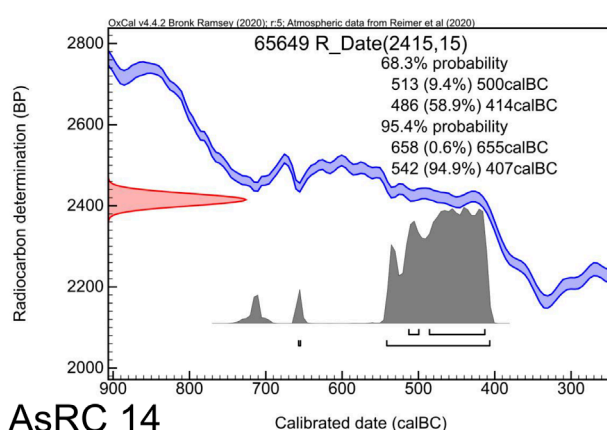


Fig. D1.13: Calibrated radiocarbon determination for the seed sample AsRC 14 (MAMS 65649) from the floor of Room 3 of Building A. Prepared by Andrea Squitieri.

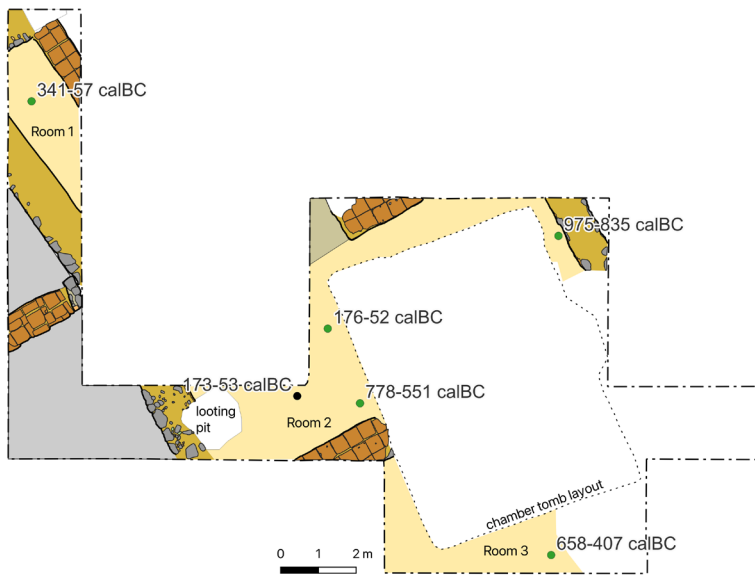


Fig. D1.14: Floor plan of Building A, indicating the sample locations. Black dots represent the find spot of charcoal; green dots represent the centre of the flotation sampling grid from which the carbonised seeds derive. All dating ranges are 95.4 % probability. Drawn by Jan Heiler, annotated by Andrea Squitieri.

cannot all be interpreted as representing a contemporary assemblage of the second century BC (§H3.13).

We are on safe grounds again when it comes to the two molars from two separate individuals deposited in the chamber tomb (AsRC 1 = Fig. D1.15; AsRC 2 = Fig. D1.16). These were radiocarbon dated to the first centuries AD, matching the Parthian date already assumed, based on the building's architecture (§D2.3) and the associated pottery (§E.1.2).

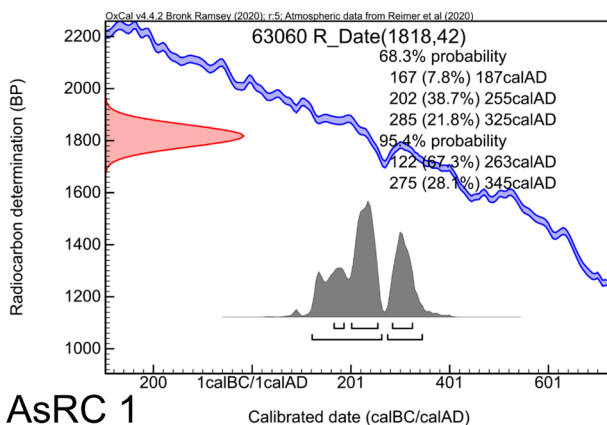


Fig. D1.15: Calibrated radiocarbon determination for tooth sample AsRC 1 (MAMS 63060) from the floor of the chamber tomb's Subdivision 3. Note that according to the lab report, the result has a low level of reliability due to the low amount of collagen. Easting and northing coordinates are approximate. Prepared by Andrea Squitieri.

In the sondage next to the SBAH trench of 2002 (Fig. D1.17), the oldest date is from a piece of charcoal found directly above the floor of "Room 5"; this floor lies roughly on the level of the floors exposed by the Iraqi excavations. The charcoal's radiocarbon dating range from the late 15th to the early 13th century BC falls into the Late Bronze Age (AsRC 9 = Fig. D1.18). This charcoal sample is therefore considerably older than the 7th century BC dating assumed for the building by the Iraqi archaeologists at the time of excavation (personal communication, Salim Abdullah Ali who led the work in this trench in 2002; see §D3.2). However, to complicate matters, a carbonised seed from the 20 cm layer above the floor produced a radiocarbon date range of 771-545 calBC (AsRC 15 = Fig. D1.19) and therefore matches such a dating well, as it falls flatly into the Hallstatt Plateau. We intend to enlarge the sondage in "Room 5" in 2024 to further clarify the situation.

A 7th century dating is likely for the four radiocarbon date ranges from the two floor levels exposed in "Room 6", all of which fall into the Hallstatt Plateau: the charcoal sample from the upper floor (AsRC 7 = Fig. D1.20); another charcoal sample from the lower floor (AsRC 8 = Fig. D1.21), a carbonised seed from the upper floor (AsRC 13 = Fig. D1.22); and another seed from the lower floor (AsRC 17 = Fig. D1.23). Dating these floors to the 7th century BC is further strengthened by the fact that fragments of a dimpled goblet made of the characteristic Assyrian Palace Ware (Vessel 00-06-J01; §E1.8) were found directly on the lower floor. We need to emphasise that the two floor levels of "Room 6" lie at a considerably

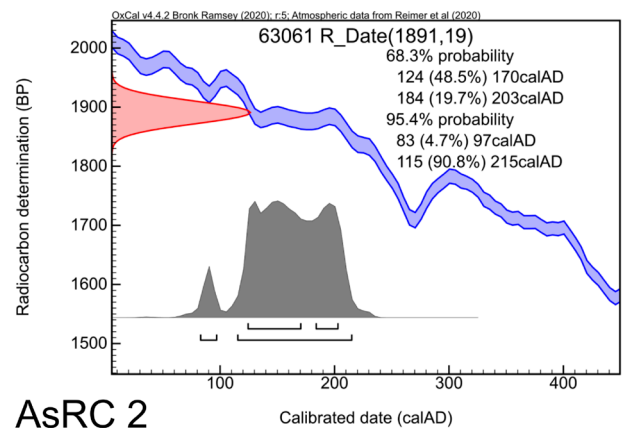


Fig. D1.16: Calibrated radiocarbon determination for tooth sample AsRC 2 (MAMS 63061) from the floor of the chamber tomb's Subdivision 5. Easting and northing coordinates are approximate. Prepared by Andrea Squitieri.

higher elevation than those reached by the Iraqi excavations (§D3.1), which are situated around a metre below.



Fig. D1.17: Orthophoto of the sondage, showing “Room 5” and “Room 6” at the end of their excavation. Black dots represent the find spot of charcoal; green dots represent the centre of the flotation sampling grid from which the carbonised seeds derive. All dating ranges are 95.4% probability. Orthophoto by Jens Rohde, annotated by Andrea Squitieri.

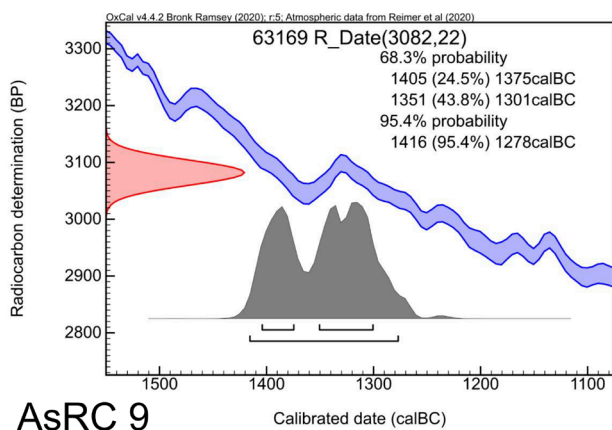
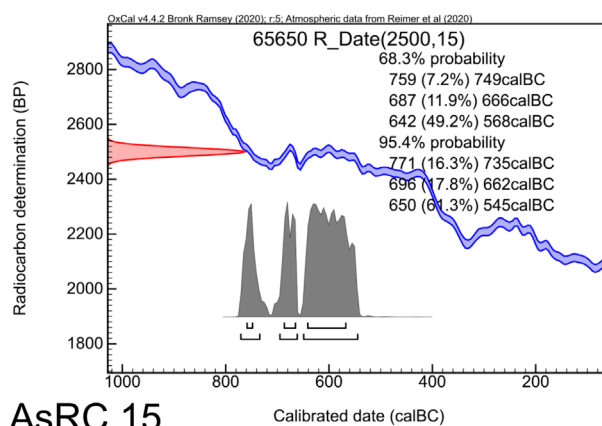
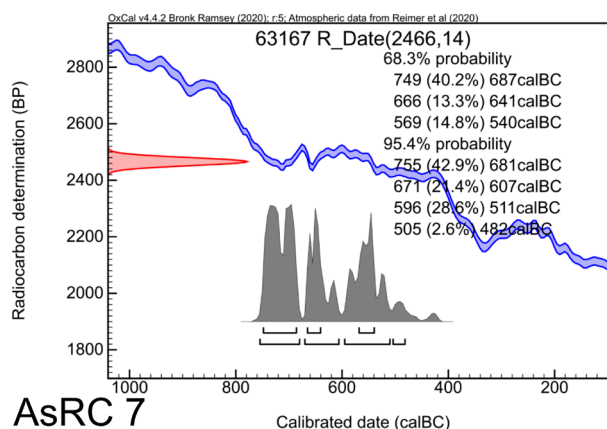


Fig. D1.18: Calibrated radiocarbon determination for the charcoal sample AsRC 9 (MAMS 63169) from the floor of “Room 5”. Prepared by Andrea Squitieri.



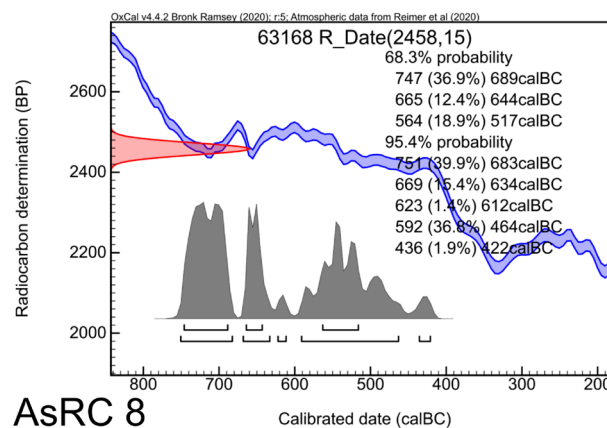
AsRC 15

Fig. D1.19: Calibrated radiocarbon determination for the seed sample AsRC 15 (MAMS 65650) from the floor of “Room 5”. Prepared by Andrea Squitieri.



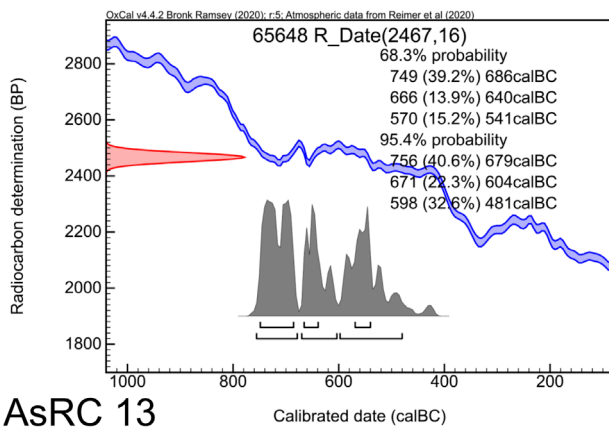
AsRC 7

Fig. D1.20: Calibrated radiocarbon determination for the charcoal sample AsRC 7 (MAMS 63167) from the upper floor of “Room 6”. Prepared by Andrea Squitieri.



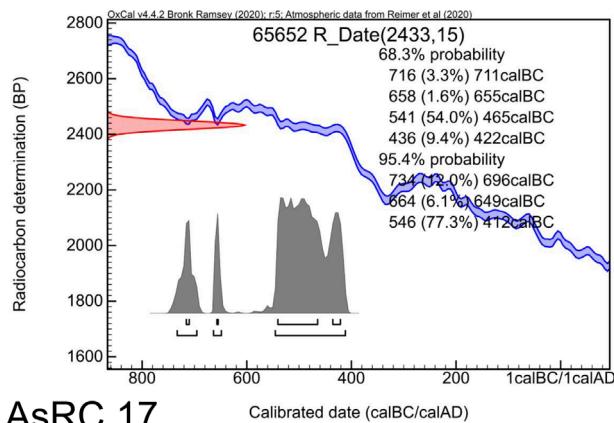
AsRC 8

Fig. D1.21: Calibrated radiocarbon determination for the charcoal sample AsRC 8 (MAMS 63168) from the lower floor of “Room 6”. Easting and northing coordinates are approximate. Prepared by Andrea Squitieri.



AsRC 13

Fig. D1.22: Calibrated radiocarbon determination for the seed sample AsRC 13 (MAMS 65648) from the upper floor of “Room 6”. Prepared by Andrea Squitieri.



AsRC 17

Fig. D1.23: Calibrated radiocarbon determination for the seed sample AsRC 17 (MAMS 65652) from the lower floor of “Room 6”. Prepared by Andrea Squitieri.

D2. Excavating trench NT1 2023 in the New Town of Assur⁹³

F. Janoscha Kreppner, Jens Rohde & Andrea Squitieri

D2.1 The relative stratigraphy

The relative stratigraphy established as a result of the 2023 excavations in the trench NT1 2023 comprises 9 local stratigraphic phases between the topsoil and the virgin soil. Each phase has been named with a progressive number following the prefix NT1 2023. In the table below, the 9 stratigraphic phases between the topsoil and the virgin

soil are listed along with the main features associated with them and the corresponding absolute dates, if available.

Stratigraphic phase	Main features	Absolute dates (95.4% probability for ¹⁴ C; see §D1.3)
Topsoil	Soft brown soil; §D2.2	-
NT1 2023 Phase 9	Looting pit and looted Grave 2; §D2.2	-
NT1 2023 Phase 8	Chamber tomb (= Grave 1); §D2.3	83-215 calAD
NT1 2023 Phase 7	Architecture; §D2.4	-
NT1 2023 Phase 6	Grave 3 and Grave 4; §D2.5	159/158 BC (from alphabetic inscription; §G2)
NT1 2023 Phase 5	Architecture (Building A); §D2.6	173-53 calBC 176-52 calBC 341-57 calBC*
NT1 2023 Phase 4	Architecture (Building B); §D2.7	-
NT1 2023 Phase 3	Grave 5; §D2.8	770-542 calBC 775-545 calBC
NT1 2023 Phase 2	Architecture; §D2.9	-
NT1 2023 Phase 1	Deep sounding; §D2.10	1506-1440 calBC
Virgin soil	Hard reddish soil; §D2.10	-

* For the older dates see the discussion in §D1.3.

The loci associated with each of the 9 stratigraphic phases, plus topsoil and virgin soil are summarised in **Table D2.1**, which is organised as follows:

- The rows are ordered chronologically, spanning from the oldest (bottom) to the most recent (top) phases.
- The columns refer to spaces, such as rooms.
- Roughly contemporary deposits and installations can be read in the table horizontally.
- The cells of the table contain a brief description of each locus.
- The background colours of the cells indicate the interpretation and duration of the deposits. The most relevant are: the yellow colour indicating occupation and use of floors and installations; the brown colour indicating post-occupation periods (non-use/erosion processes); and the grey colour indicating graves.

Each occupation phase is divided into four sub-phases:

- First Construction sub-phase (construction of walls and their foundations);
- Construction sub-phase (construction of floors and installations);

⁹³ This chapter was language-edited by Karen Radner.

- Occupation sub-phase (use of floors and installations); and
- End of the Occupation sub-phase (destruction and/or abandonment of floors and installations)

D2.2 The trench surface, the topsoil and NT1 2023 Phase 9

At the start of the excavations, the trench surface was found covered with pebbles, pottery sherds, modern glass and metal fragments. In the topsoil,⁹⁴ characterised by a soft brown soil, we found two seemingly isolated long human bones (Locus:262432:005) and a pit (cut: Locus:262432:008, fill: Locus:262432:009), both in the north-eastern part of Square 262432. Nine finds were collected from the trench surface and the topsoil (§F, nos. 1-9). The only item of any chronological significance is a fragment of a rotary quern (AS 262432:012:004) that belongs to a type of grinding tool that spread across the Near East between the second and third century AD and the industrialisation era.⁹⁵

A looting pit identified in the northern part of Square 261432 was assigned to NT1 2023 Phase 9. The pit cut (Locus:261432:012) was already visible on the site surface (Fig. D2.1). It had an oval shape measuring about 200 × 150 cm and cut into the structures of the NT1 2023 Phase 5 (Figs. D2.20, D2.21). The pit was excavated to a depth of c. 130 cm. The upper fill (Locus:261432:013) yielded a broken grinding stone (AS 261432:013:003) and another stone tool, possibly a pestle (AS 261432:013:004; see §F, nos. 23-24). This fill was situated above a stone accumulation (Locus:261432:016), in which we found two fragmentary



Fig. D2.1: The looting pit Locus:261432:012, which destroyed Grave 2. Photo by Tarik Willis.

baked bricks (AS 261432:016:004 and 261432:016:005), and a broken grinding stone (AS 261432:016:003; see §F, nos. 20-22). Below the stones, we excavated Locus:261432:015, which yielded scattered human bones, pottery sherds, and 79 small finds, of which 76 were beads (§F, nos. 10-16). This is interpreted as the remains of a burial that had been disturbed by looting and was named Grave 2.

D2.3 NT1 2023 Phase 8: the chamber tomb (= Grave 1)

The chamber tomb, named Grave 1, has a rectangular layout with a northwest-southeast orientation and covers an area of about 6 × 8 m (Figs. D2.2, D2.3). Radiocarbon analysis of a molar from one of the skeletons found as part of the assemblage on the floor of the chamber tomb's Subdivision 5 (§D2.3.3.2) resulted in a dating range of 83-215 calAD (95.4% probability; see §D1.3) and therefore falls into the time when Assur was part of the kingdom of Hatra.⁹⁶

The tomb consists of a northern and a southern chamber, separated by a main corridor that runs roughly in an east-west direction. The main entrance to the tomb was located on the eastern side of the building. Both chambers were divided into four subdivisions, organised in two pairs on both sides of the northern corridor and the southern corridor (labelled S1 to S8 in Fig. D2.2).

The construction of the tomb (pit cut: Locus:262433:050) destroyed the architecture of older phases, from NT1 2023 Phase 7 down to NT1 2023 Phase 4. Towards the east, near the tomb entrance, we identified a small pit (cut: Locus:262433:079), measuring c. 250 × 100 cm, that ran into the eastern section of the excavation area. Although it was not excavated, we interpret this as the construction pit for the tomb entrance.

The walls of the chamber tomb were built in a single phase using unworked stones of varying size (30 cm to 1 m in diameter) that were set irregularly. The gaps between the stones were filled with smaller stones, baked brick fragments, pottery sherds, and broken stone tools. This building material was held together by a clay mortar, which was reddish-brown with white inclusions. The walls' faces were originally covered by one or two layers of white plaster (up to 2 cm thick). Inside the walls of the chamber tomb, we found the fragments of three baked bricks with cuneiform inscriptions of Adad-nerari I of Assyria (1305-1274 BC: AS 262433:049:002, AS 262433:049:003, and AS

94 The trench surface and the topsoil were divided between various loci, see Table D2.1.

95 Frankel 2019.

96 This radiocarbon dating range matches the dates provided by the Aramaic inscriptions found by Andrae, for which see Beyer 1998.

Building B Unroofed Area 4	
NT1 2023 Phase 4: POST-OCCUPATION	Locus:262432.031 soft greyish soil with few inclusions, potsherds, Locus:262432.032 soft greyish soil with few inclusions, potsherds, Locus:262432.034 soft greyish soil with few inclusions, potsherds, Locus:262433.029 dry soft, well sorted brown silty soil with few pebbles, Locus:262433.032 soft well sorted brown silty soil with few sherds and few pebbles
	Locus:262432.047 mud brick collapse, Locus:262433.051 greyish-brown hard soil, mixed with pebbles, stones, ceramic sherds and brick fragments, Locus:262432.051 dense greyish-beige soil, Locus:262432.057 dry soft, well sorted, brown silty soil with few sherds, some pebbles, few bones, Locus:262432.059 mud brick debris, Locus: 262433.065 mudbrick debris
NT1 2023 Phase 4: END OF OCCUPATION	
NT1 2023 Phase 4: OCCUPATION	Locus:262433.059 pit cut with fill Locus:262433.055, Locus:262432.062 pit cut with fill Locus:262432.063, Locus:262433.052 pit cut with fill Locus:262433.053, Locus:262433.061 pit cut with fill Locus:262433.062 reddish-brown, crumbly, yellowish-brown and brick fragments, Locus:262433.063 reddish-brown, crumbly, yellowish-brown and brick fragments, Locus:262433.064 mud brick installation with fill Locus:262433.071, white plaster installation with fill Locus:262433.070, Locus:262433.046 pit cut with brick lining Locus:262433.048 and fill Locus:262432.048
NT1 2023 Phase 4: CONSTRUCTION	Locus:262432.058 and Locus:262433.080 beaten mud floor, Locus:262432.061 and Locus:262432.073 substruction of floor: package of stones, broken bricks, sherds
NT1 2023 Phase 4: FIRST CONSTRUCTION	Locus:262433.054 wall, Locus:262433.077 construction pit cut with fill Locus:262433.073, Locus:262432.075 wall
NT1 2023 Phase 3: Grave 5: Locus:262432.069 pit cut with looted fill Locus:262432.070 (C14 sample) and Locus:262432.071	
NT1 2023 Phase 2: POST-OCCUPATION	Locus:262433.072 package with larger irregularly but clearly set stones, burnt brick fragments and mixed with a reddish grey mud material and lots of sherds, Locus:262432.067 moist dense but not very hard reddish-brown mud material, Locus:262432.074 dry hard, well sorted, reddish-brown silty soil with Locus:262432.088 brownish-red grey soil with ceramic sherds and little pieces of charcoal
NT1 2023 Phase 2: END OF OCCUPATION	
NT1 2023 Phase 2: OCCUPATION	Locus:262433.075 loose greenish-grey crumbly soil, Locus:262433.076 dense reddish-brown clay
NT1 2023 Phase 2: CONSTRUCTION	Locus:262433.071 row of stones, drain (?)
NT1 2023 Phase 2: FIRST CONSTRUCTION	Locus:262432.080, Locus:262433.061, Locus:262433.063 southern walls, Locus:262432.084 and Locus:262432.085 northern walls
NT1 2023 Phase 1 VIREIN	Locus:262432.076 soft greyish and well sorted mud material with larger and smaller stones, lots of sherds, Locus:262432.086 and Locus:262432.087 beaten mud floors (?), Locus:262432.078 pit cut with fill Locus:262432.079 (C14 sample)
Late Bronze Age	Locus:262432.077

Table D2.1 (continued): The relative stratigraphy of NT1 2023 trench. Prepared by F. Janoscha Kreppner.



Fig. D2.2: Plan of the chamber tomb. Drawn by Jan Heiler, annotated by Andrea Squitieri.



Fig. D2.3: Orthophoto of the chamber tomb. Created by Jens Rohde, annotated by Andrea Squitieri.

262433:003:003; see §G1) and a bronze fibula (AS 262433:003:002; see §F, no. 29).

Based on the observations of the wall structures (described in detail in §D2.3.3.1 and §D2.3.4.1), we assume that the northern chamber and the southern chamber were both covered by a pitched brick barrel vault (in German: *Ringschichtengewölbe*). This vaulting technique is already attested elsewhere at Assur in contemporary chamber tombs.⁹⁷

D2.3.1 The main entrance

The main entrance to the chamber tomb was located to the east (Figs. D2.2, D2.3, D2.4). On the outer side, the entrance was bordered by the wall Locus:262433:047 to the north and the wall Locus:262433:048 to the south. The first wall had a preserved length of c. 95 cm and a maximum width of c. 35 cm. Since the wall ran into the eastern border of our excavation trench, we could not docu-

⁹⁷ See especially Andrae 1933, 97: grave Ass. 13971.

ment its total length. Its preserved height was c. 30 cm above the level of the floor (Locus: 262433:044).

The wall Locus:262433:048 had a preserved length of c. 60 cm and a maximum width of c. 30 cm. This wall, too, ran into the eastern border of our excavation trench. It was preserved to a height of c. 25 cm above the floor.

The floor on the outer side of the entrance (Locus: 262433:044) covered an area of 100 × 60 cm. It was paved with two rows of bricks and flat stones covered with white plaster (**Fig. D2.4**). The first row was located right next to the threshold and consisted of two complete bricks measuring c. 30 × 30 × 7 cm and one half-sized brick of c. 16 × 30 × 8 cm. The second row consisted of two bricks and various flat stones that were placed to fill the gap between the bricks and the nearby wall (Locus:262433:047).

The entranceway was bordered to the north by a door jamb (Locus:262433:043), which measured c. 75 × 25 cm. Here, we could observe up to three courses of stones and mortar, preserved to a height of c. 60 cm above the entrance threshold (Locus:262433:010) and c. 70 cm above the level of the floor (Locus:262433:044) situated right outside the entrance, to the east. The face of the door jamb was covered with white plaster, preserved to a



Fig. D2.4: The main entrance to the chamber tomb. Photo by Marco Wolf, annotated by Andrea Squitieri.

height of c. 75 cm above the floor level and c. 30 cm above the threshold.

To the south, the entranceway was bordered by another door jamb (Locus:262432:046). Here, only one upright stone was preserved, which was 65 cm long and 40 cm wide. It protruded from the wall (Locus:262432:038) by about 20 cm. The face of that door jamb, too, was covered with white plaster.

The threshold (Locus:262433:010) separated the outside floor (Locus:262433:044) to the east from the floor of the main corridor (Locus:262433:037) to the west (**Fig. D2.4**). The threshold was constructed of brick fragments, pottery sherds, pebbles, and smaller stones bound together by a clay mortar of greyish-brown colour, and then covered with white plaster to create an even surface. It was 70 cm long, 60 cm wide and 12-14 cm higher than the surrounding floors.

In the northeast corner, next to the threshold and in front of wall Locus:262433:043, a door socket was found (Locus:262433:038: **Figs. D2.4-D2.5**). This was a flat, dark grey stone of roughly square shape, measuring c. 40 × 35 cm. The stone shows no other signs of being worked apart from a shallow depression of a diameter of c. 15 cm, with an uneven surface. This depression was located on the very spot where the door hinge was expected to be, and the stone can therefore be identified as a door socket. It was covered with white plaster, traces of which were found on its top and sides.

The upper deposits that accumulated in the main entrance were Locus:262433:017 and Locus:262433:007. The former consisted of dark brown soil containing brick fragments, plaster fragments and stones, while the latter was a reddish brown, crumbly soil. Two bronze fragments were collected from Locus:262433:017 (AS 262433:017:002 and AS 262433:017:003; see **§F, nos. 115-116**).

D2.3.2 The main corridor

The tomb's main corridor is about 90 cm wide and 4 m long (**Figs. D2.2-D2.3**) and divides the northern chamber from the southern chamber. Consequently, it was bordered by the internal walls of the northern and the southern chambers to the north and the south, respectively. To the west, it was bordered by a short wall (Locus:262432:040), which joined wall Locus:262432:037 to the south, and wall Locus:261433:019 to the north. This wall had a length of about 1 m, a width of about 70 cm (and thus wider than the other walls) and a preserved height of about 45 cm. A white plaster layer covered its face and was preserved to a height of c. 30 cm.

The floor of the main corridor was divided into two halves by a line of upright bricks (Locus:262432:045).



Fig. D2.5: The eastern floor of the main corridor, Locus: 262433:037. Photo by Marco Wolf.

Only one brick was preserved, but the imprint of the other bricks could be seen on the floor. This line of bricks separated the eastern floor (Locus:262433:037) from the western floor (Locus:262432:025). The eastern floor (**Fig. D2.5**) covered an area of about 250 × 90 cm, and the western floor had an area of c. 150 m × 90 cm. Both floors were 8-10 cm thick and constructed from a mix of pottery sherds, pebbles, and brick fragments, bound together with mortar and covered with white plaster. In front of the threshold (Locus:262433:010), the floor (Locus:262433:037) was paved with a row of two bricks (c. 30 × 30 × 8 cm) and one half-sized brick (14 × 30 × 8 cm).

The deposit on the eastern floor was called Locus:262433:026 and on the western floor Locus:262432:024. Both consisted of greyish soil mixed with large fragments of plaster which had fallen in from the surrounding walls. Whereas Locus:262432:024 yielded only a few bones, five finds were collected from Locus:262433:026: a small rectangular ceramic item with smooth sides, possibly used as a polisher (AS 262433:026:001), and four flat fragments of iron (AS 262433:026:003, AS 262433:026:004, AS 262433:026:005, and AS 262433:026:006; see **§F, nos. 47-48**).

The upper deposits that accumulated in the main corridor are summarised in the table below:

Locus:262433:015 contained an iron fragment (AS 262433:015:003) and a possible whetstone (AS 262433:015:004; see **§F, nos. 117-118**).

D2.3.3 The northern chamber

D2.3.3.1 The walls and the vault

Excluding the walls, the northern chamber occupies an area of about 10.5 m². The northwest wall (Locus:262433:003) is c. 5.5 m long, c. 60 cm wide and preserved to a height of c. 1.1 m above the floor (Locus:262433:040). On the highest preserved part of the wall, some stones (Locus:262433:046) were found which were slightly shifted inwards to form a cantilever element. On top of these stones, three bricks (Locus:262433:045), measuring about 30 × 30 × 8 cm each, leaned vertically against the eastern wall of the tomb (Locus:262433:004; **Fig. D2.6**). We interpret the cantilever element and the three bricks as the remains of the pitched barrel vault that once covered this chamber.

The northeastern wall (Locus:262433:004) of the northern chamber has a length of c. 3 m and a width of c. 70 cm and is preserved to a maximum height of c. 90 cm above the floor (Locus:262433:039). To the south, wall Locus:262433:004 is connected to a wall that accommodates the entrance to the northern chamber. The part of the wall that connects to wall Locus:262433:004 was named



Fig. D2.6: The cantilever element Locus:262433:046 on the NW wall of the chamber tomb. The white circle indicates the vertical bricks leaning against the eastern wall of the tomb. Photo by Marco Wolf.

Eastern part of the main corridor	Locus:262433:036	Soft, greyish-brown soil with some pebbles located near the entrance to the northern corridor
	Locus:262433:015	Reddish-brown, very crumbly soil, mixed with brick fragments and some pebbles
Western part of the main corridor	Locus:261432:010	Soft, greyish-brown soil with some pottery sherds, many pebbles, some brick fragments and a few stones

Locus:262433:018 whereas the part on the other side of the entrance was called Locus:262433:019. Wall Locus:262433:018 has a preserved length of c. 1.6 m, but because its western portion was destroyed, its reconstructed total length is c. 2 m. Its maximum width was c. 45 cm and it was preserved to a height of c. 70 cm above the floor (Locus:262433:037). Wall Locus:262433:019 is about 2 m long and 50 cm wide and preserved to a height of c. 90 cm above the floor (Locus:262433:031). To the southwest, the northern chamber was bordered by wall Locus:261433:019, which is c. 3.5 m long and c. 50 cm wide and preserved to a height of c. 80 cm above the floor (Locus:262433:031).

D2.3.3.2 Subdivisions 5 to 8 and the northern corridor

The northern chamber was divided into four subdivisions (S5 to S8 in Fig. D2.2), all with a similar structure, and arranged in pairs on both sides of the northern corridor. All these subdivisions are 2 m long and 1.2 m wide. They are delimited by rows of baked bricks (30 × 30 × 8 cm) that were set on their narrow edges in an upright position and covered with white plaster. A third of each brick, about 10 cm, was sunk into the floor, and this indicates that they were set before the floor was laid down. The

line of bricks bordering the northern corridor to the east was called Locus:262433:041, and the one to the west was Locus:262433:042. Between subdivisions 5 and 6, the line of bricks was named Locus:262433:033 and between subdivisions 7 and 8 Locus:262433:028; the middle part of the latter was not preserved.

Each subdivision was paved with baked bricks that were covered with a 2-3 cm thick, white plaster. This brick floor was laid down only along the edges. In the centre, the floor consisted of an 8-10 cm thick layer of white plaster mixed with pottery sherds and small stones. As they form one architectural unit, the brick and the plaster floor received one locus number in each subdivision. The floors of Subdivisions 5 and 6 (Locus:262433:031 and Locus:262433:027, respectively) were well preserved (Figs. D2.7a-b). In Subdivision 7, only the brick part of the floor (Locus:262433:040) was preserved, while the plaster layer in the middle had been badly damaged (Fig. D2.7c). In Subdivision 8, the whole floor (Locus:262433:039) was damaged and preserved only at the four room corners (Fig. D2.7d).

The northern corridor is c. 2.5 m long and c. 50 cm wide. Its floor (Locus:262433:030) was paved with complete and half-sized baked bricks, set in an alternating pattern, and covered with a white plaster layer, which contained pottery sherds, small brick fragments and pebbles (Fig. D2.8).

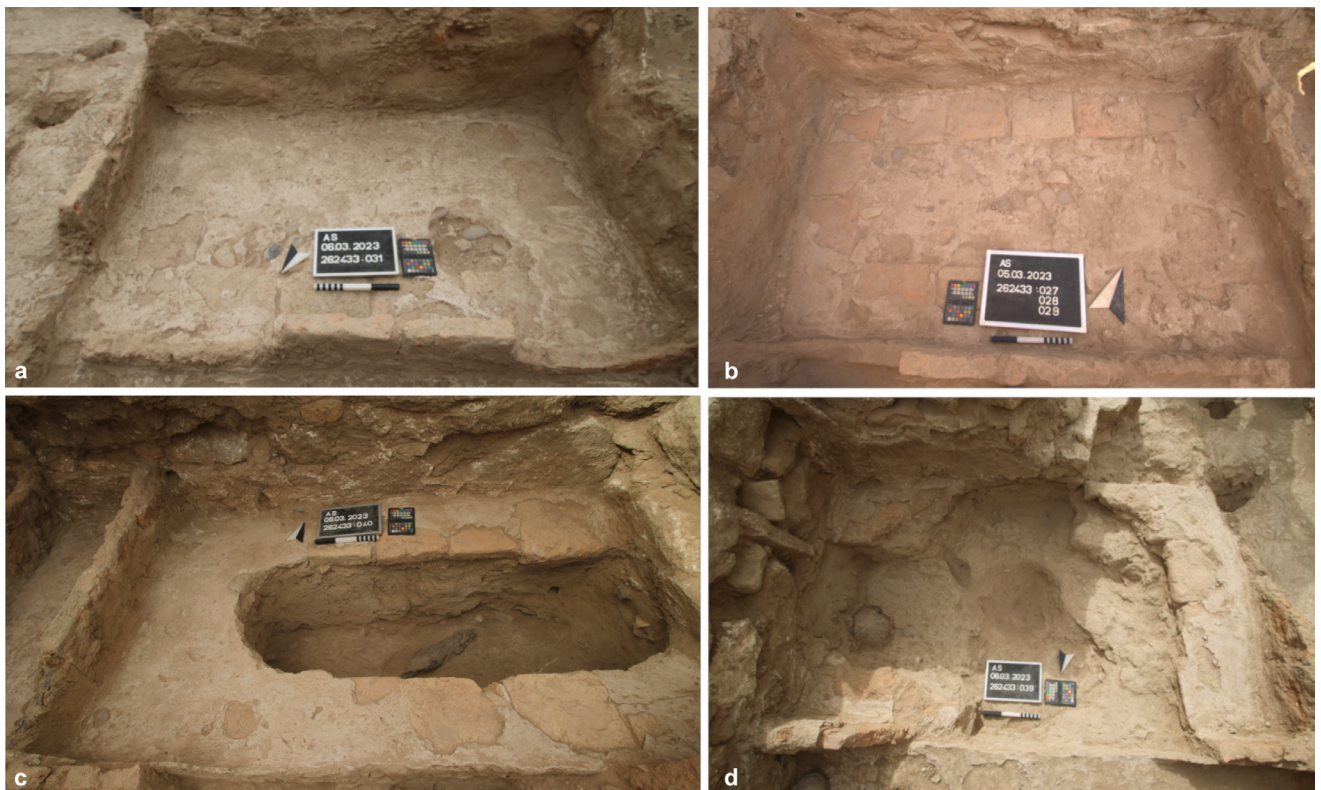


Fig. D2.7: The floors of the subdivisions of the northern chamber. a) Subdivision 5; b) Subdivision 6; c) Subdivision 7; d) Subdivision 8. Photos by Tarik Willis and Marco Wolf.



Fig. D2.8: The northern corridor of the northern chamber. Photo by Marco Wolf.

D2.3.3.3 The floor deposits

In the subdivisions and the northern corridor, the floor deposits consisted of soft, reddish-brown soil containing many pottery sherds, white plaster fragments, baked brick fragments and pebbles. They also contained human and animal bones, as well as small finds (**Fig. D2.9**).

In Subdivision 5, the floor deposit (Locus:262433:021) contained in its southern part a large concentration of disarticulated human and animal bones (**Fig. D2.10a**). The human bones belonged to at least two individuals, as two skulls were found. A molar taken from one of these (sample AS 262433:021:005:001) was radiocarbon dated to 83-215 calAD (95.4% probability; **§D1.3**). Near one of the skulls, a ceramic bowl was found broken in two fragments



Fig. D2.9: Orthophoto of the northern chamber with the indication of the subdivision numbers. Created by Jens Rohde, annotated by Andrea Squitieri.

(part of collection AS 262433:021:006). In the northwestern corner, a fully preserved, large ceramic vessel (registered as vessel G01-S05-V01) was found lying on one side directly on the floor. It is a four-handled jar with an ovoid body covered in a honeycomb decoration and based on parallels, it can be dated to the late Sasanian / Early Islamic period (**Fig. D2.10b**; see **§E1.2**). Because the chamber tomb was constructed at the beginning of the Common Era, this vessel must have been placed at this location centuries after the tomb's main period of use. The soil inside the vessel (Locus:262433:016) was dark brown and very loose; it was sampled for flotation (for the results, see **§H3.12**) and phytolith analysis.

In Subdivision 6, the floor deposit (Locus:262433:022) contained in the western part a large amount of disarticulated and poorly preserved human and animal bones.

In Subdivision 7, the floor deposit (Locus:262433:023) could be followed below the bricks located along the edges of the subdivision because the middle part of the floor had been damaged, as already mentioned (**Fig. D2.10c**). In this deposit, we found a large concentration of disarticulated human bones; based on the number of preserved skulls, they belong to at least four individuals. Among the bones, we found parts of a possible sarcophagus lid (part of collection AS 262433:023:001) and 14 finds, which are listed in the table below and discussed in **§F, nos. 31-44**.

AS number	Short object description
AS 262433:023:006	Glass shard
AS 262433:023:007	Glass shard
AS 262433:023:008	Curved bronze fragment
AS 262433:023:009	Head of bronze pin
AS 262433:023:010	Fragment of glass bowl
AS 262433:023:011	Glass rim fragment
AS 262433:023:012	Small ceramic ball
AS 262433:023:013	Stone biconical item, possibly a weight
AS 262433:023:014	Glass handle
AS 262433:023:015	Neck of a glass bottle
AS 262433:023:016	Bronze shaft with curved tip
AS 262433:023:017	Bronze fragment
AS 262433:023:018	Small bronze sheet fragments
AS 262433:023:019	Cylindrical bead made of carnelian



Fig. D2.10: The floor deposits in a) Subdivisions 5 (right) and 6 (left); b) Subdivision 5 with the decorated four-handled vessel G01-S05-V01 on the floor; c) Subdivision 7; d) Subdivision 8.

The floor deposit (Locus:262433:024) in Subdivision 8 could also be traced below the bricks located at the subdivision's edges (Fig. D2.10d). In addition to a few human and animal bones, this deposit yielded a broken lower grinding stone made of basalt (AS 262433:024:003; see §F, no. 45).

In the northern corridor, the floor deposit (Locus: 262433:025) yielded a few human and animal bones and one glass shard (AS 262433:025:003; see §F, no. 46).

D2.3.3.4 The upper deposits

Above the floor deposits in the northern chamber's subdivisions, we excavated several other deposits which had accumulated over time, some of which contained the collapse of the tomb's structures. The table below summarises the main characteristics of these deposits, arranged from the bottom up, with indications of their location within the tomb.

Location	Locus	Short locus description
Northern corridor	Locus:262433:034	Cut and fill respectively of a small pit
	Locus:262433:035	
Western half of the northern chamber	Locus:262433:014	Reddish-brown crumbly soil mixed with small fragments of plaster, bricks and pebbles
	Locus:261433:018	
	Locus:262433:011 Locus:261433:016	Wall collapses made of large stones (15 - 45 cm diameter) mixed with a yellowish-brown soil
	Locus:261433:015	Soft, greyish-brown soil with some pottery sherds, pebbles, white plaster fragments, some brick fragments
Eastern half of the northern chamber	Locus:262433:020	Collapse consisting mostly of large stones and bricks
	Locus:262433:013	Reddish-brown, crumbly soil mixed with pottery sherds, brick fragments and white plaster fragments

Location	Locus	Short locus description
Northern chamber	Locus:262433:012 Locus:262433:006	Wall collapse made of brick and stone fragments embedded in a reddish-brown, very crumbly soil mixed with pottery sherds
	Locus:262433:005	Wall collapse made of brick and stone fragments embedded in a greyish compact soil mixed with pottery sherds

The table below lists the small finds retrieved from these deposits (see §F, nos. 107-120).

AS number	Short object description
AS 261433:018:003	Fragment of a lower grinding stone made of basalt
AS 261433:018:004	Fragment of a possible stone tool
AS 261433:015:002	Fragment of a bronze pin with curved tip
AS 261433:015:003	Glass shard covered with iridescent patina
AS 262433:020:002	Fragment of a lower grinding stone made of basalt
AS 262433:020:003	Fragment of bronze
AS 262433:013:002	Fragment of plaster with several small holes carved in it
AS 262433:012:003	Fragment of a lower grinding stone made of basalt
AS 262433:005:002	Fragment of a lower grinding stone made of basalt
AS 262433:005:003	Fragment of a bronze nail or pin



Fig. D2.11: Orthophoto of the southern chamber with indication of subdivision numbers. Created by Jens Rohde, annotated by Andrea Squitieri.

D2.3.4 The southern chamber

D2.3.4.1 The walls and the vault

The southern chamber was constructed symmetrically to the northern chamber (Figs. D2.2, D2.3) and its walls were built using the same technique. Unlike in the northern chamber, we did not find evidence of the presence of a vaulted roof because of the level of preservation of the walls. However, we can safely assume that the southern chamber too had a vaulted roof.

In the southeast, the southern chamber was bordered by a wall (Locus:262432:039), which is c. 6 m long and about 50 cm wide and preserved to a maximum height of c. 40 cm; the western part of this wall was preserved only to a height of c. 10 cm.

The chamber's southwestern wall (Locus:262432:037) was about 3.2 m long and about 50 cm wide. It was preserved to a height of about 1 m in its northern part and only c. 25 cm in the southern part.

The internal wall (Locus:262432:035) of the southern chamber borders the main corridor to the southwest. It has a length of about 2.1 m and a preserved height of c. 80 cm. The plaster covering its wall face was preserved only in the lowest part.

The other internal wall (Locus:262432:036) of the southern chamber borders the main corridor to the southeast. It has a length of about 2 m and a preserved height of c. 30 cm. Only the lower part of the wall was preserved, except for at its western end where two large stones lay on top of each other, with the bigger one measuring c. 40 × 25 × 8 cm. At the western end of the wall, a plaster layer of a thickness of 1-3 cm was preserved to a height of c. 40 cm, higher than the preserved level of the stones.

The eastern wall (Locus:262432:038) of the southern chamber was about 3 m long and preserved to a height of about 45 cm.

D2.3.4.2 Subdivisions 1 to 4 and the southern corridor

The southern chamber was divided into four subdivisions (S₁ to S₄ in Fig. D2.2 and Fig. D2.11), all with a similar structure, and arranged in pairs on both sides of the southern corridor. They were constructed in the same way as their counterparts in the northern chamber. Each covers a surface area of

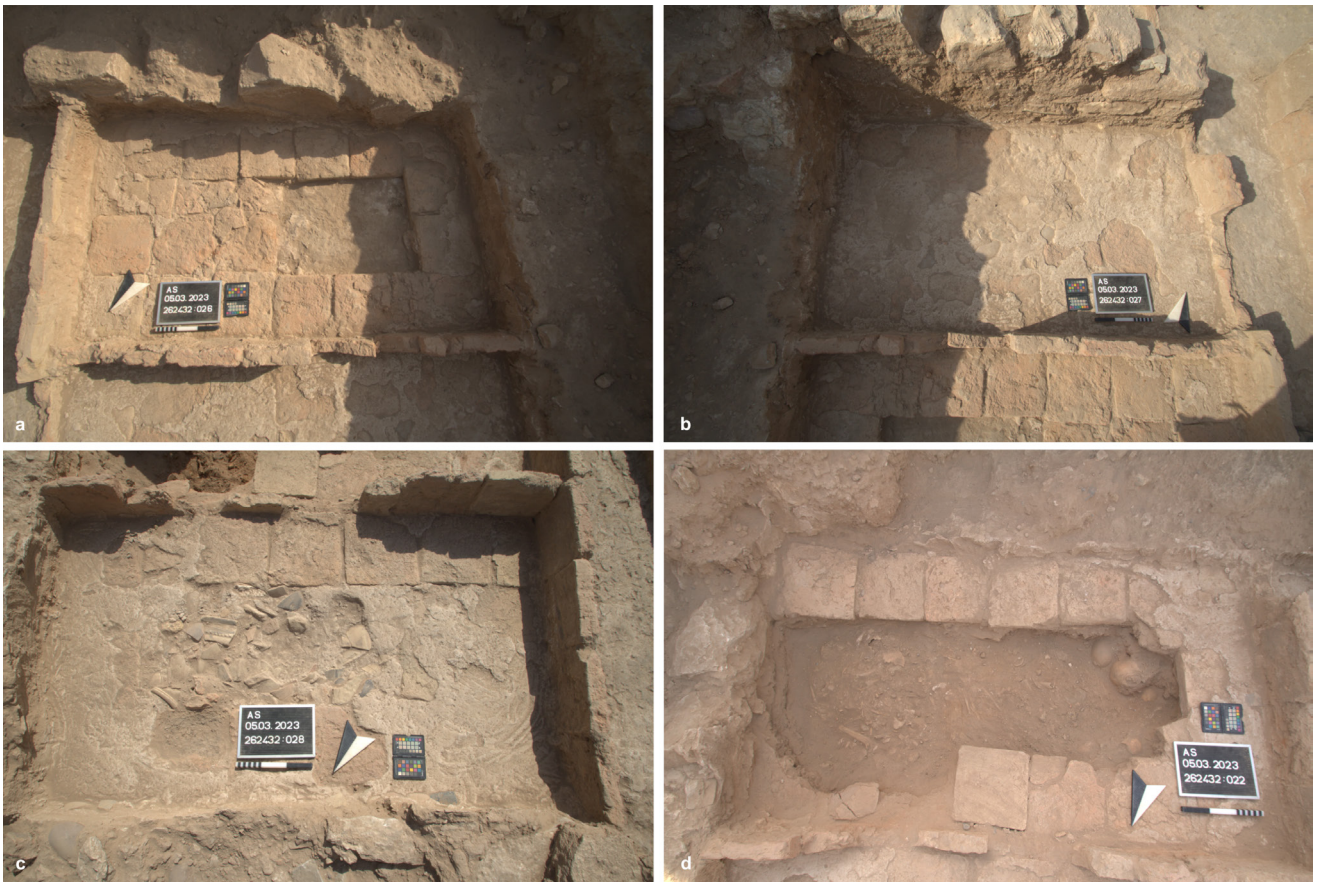


Fig. D2.12: The floors of the Subdivisions in the southern chamber. a) Subdivision 1; b) Subdivision 2; c) Subdivision 3; d) Subdivision 4. Photos by Jan Heiler and Veronica Hinterhuber.

about 2 m² and was bounded by plastered baked bricks set in an upright position. The two lines of bricks flanking the southern corridor are Locus:262432:041 to the west and Locus:262432:042 to the east. Subdivisions 1 and 2 are divided by the brick line Locus:262432:043, and Subdivisions 3 and 4 by the brick line Locus:262432:044.

As in the northern chamber, the subdivisions were paved along the edges with baked bricks covered with white plaster, while the middle part of the spaces was taken up by a thick white plaster layer, mixed with stones and pottery sherds. The floors were called Locus:262432:026 in Subdivision 1, Locus:262432:027 in Subdivision 2, Locus:262432:028 in Subdivision 3 and Locus:262432:029 in Subdivision 4 (**Fig. D2.12a-d**). In Subdivision 4, the floor was badly damaged, as no plaster layer was identified in the centre and the bricks were only preserved along the northeastern edge.

The southern corridor was paved similarly to its northern counterpart, with baked bricks and half-sized baked bricks set in an alternating pattern and covered by a white plaster (floor: Locus:262432:030).

D2.3.4.3 The floor deposits

The floor deposit (Locus:262432:019) of Subdivision 1 (**Fig. D2.13a**) yielded a large number of disarticulated human bones mixed with animal bones, along with a bronze fragment (AS 262432:019:003), a bronze needle (AS 262432:019:004) and a glass shard (AS 262432:019:005; see **§F, nos. 49-51**).

In Subdivision 2, the floor deposit Locus:262432:020 contained a high number of disarticulated human and animal bones. It yielded also a composite item made of iron and bone (AS 262432:020:004), a pointed stone item that is possibly a stylus (AS 262432:020:005), a glass shard (AS 262432:020:006) and a perforated rounded pottery sherd (AS 262432:020:007; see **§F, nos. 52-55**). Along the northern edge of the subdivision, a partially preserved sarcophagus was found (**Fig. D2.13b**), of a type that had previously been excavated at Assur.⁹⁸ It had a flat base, upright walls, two straight long sides and one preserved short curved side (registered as G01-S02-V01, from the

⁹⁸ Andrae 1933, pl. 45.



Fig. D2.13: The floor deposits. a) Subdivision 1; b) Subdivision 2 with the sarcophagus G01-S02-V01; c) Subdivision 3; d) Subdivision 4. Photos by Jan Heiler and Veronica Hinterhuber.

collection AS 262432:020:001; see **§F, no. 56**); some of its fragments were found scattered on the floors of both subdivisions 1 and 2, as well as in the southern corridor. The fill of the sarcophagus did not contain any finds.

The floor deposit (Locus:262432:021) of Subdivision 3 (**Fig. D2.13c**) contained disarticulated human and animal bones scattered across the unit, with two clusters located along the eastern side. These were registered as collections AS 262432:021:004 in the north and AS 262432:021:005 in the south. Each cluster consisted of a skull and many long bones. Four small finds were collected on this floor: a spherical carnelian bead (AS 262432:021:003), a fragment of another carnelian bead (AS 262432:021:006), an undecorated tridacna shell (AS 262432:021:007) and a rim fragment of a basalt vessel (AS 262432:021:008; see **§F, nos. 57-60**).

In Subdivision 4, the floor deposit (Locus:262432:022) was traced below the bricks located along the edges of the subdivision (**Fig. D2.13d**). This deposit yielded the largest amount of human bones from anywhere within the chamber tomb. Although the bones were disarticulated, it was possible to observe two clusters. In the first, five skulls had been grouped below a layer of bones. The second cluster is along the western edge of the subdivision and consists of 10 skulls that seem to have been arranged one next to the other. This deposit yielded 56 objects, including beads in various materials, shells, metal earrings and other personal ornaments (see **§F, nos. 61-106**).

Lastly, the floor deposit (Locus:262432:023) in the southern corridor contained only a few human bones.

D2.3.4.4 The upper deposits

Above the floor deposits in the southern chamber, several deposits accumulated over time, some of which contained the collapse of the chamber tomb's wall and ceiling structures. The table below summarises the main characteristics of these fills, arranged from the bottom up, with an indication of their locations.

Location	Locus	Short locus description
Northern half of the southern chamber	Locus:262432:007	Reddish-brown soil mixed with stones of varying sizes (2 to 20 cm in diameter), several fragments of baked bricks and white plaster fragments
	Locus:262432:004	
	Locus:262432:006	
Southern half of the southern chamber	Locus:262432:013 Locus:262432:018	

The table below shows the small finds collected from these fills (see **§F, nos. 121-131**).

AS number	Short object description
AS 262432:007:005	Bronze shaft of a needle or a pin
AS 262432:004:003	Grinding stone fragment
AS 262432:004:006	Worked basalt fragment
AS 262432:004:007	Grinding stone fragment
AS 262432:004:008	Stone tool fragment
AS 262432:006:002	Bronze earring fragment
AS 262432:013:003	Bronze fragment
AS 262432:013:008	Perforated bronze sheet
AS 262432:013:004	Glass shard
AS 262432:013:006	Pottery slag
AS 262432:013:010	Grinding stone fragment

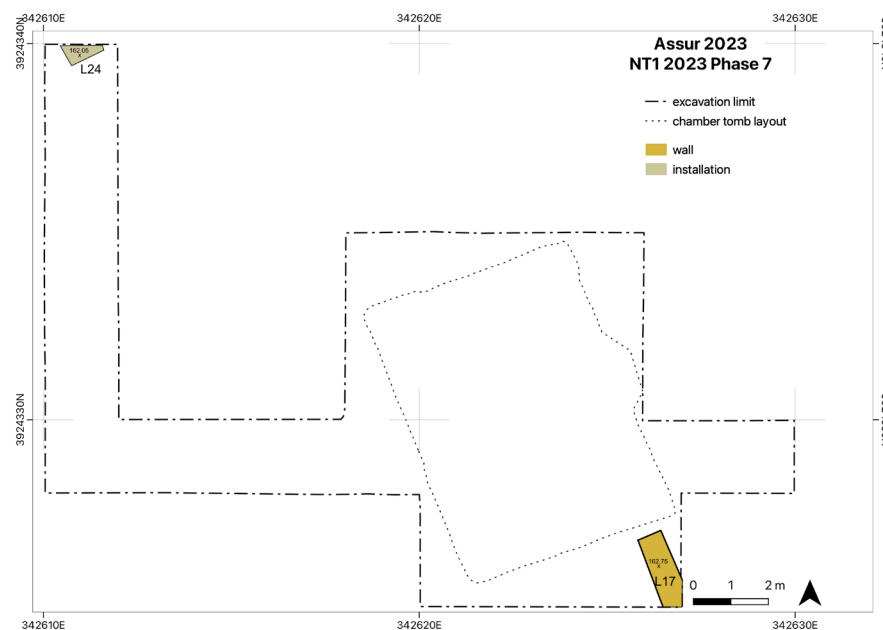


Fig. D2.14: Plan of NT1 2023 Phase 7. Drawn by Jan Heiler, annotated by Andrea Squitieri.

D2.4 NT1 2023 Phase 7

NT1 2023 Phase 7 is stratigraphically located immediately below the chamber tomb and its remains are very meagre (**Fig. D2.14**). They comprise a wall (Locus:262432:017) located on the southeastern edge of the excavation area and a partially excavated stone installation (Locus:261433:024) located on the northwestern edge of the excavation area.

The wall (Locus:262432:017) was already visible on the site surface and exposed over a length of c. 1.8 m. It is about 40 cm wide and preserved to a height of c. 35 cm. To the north, it was cut by the chamber tomb. Only

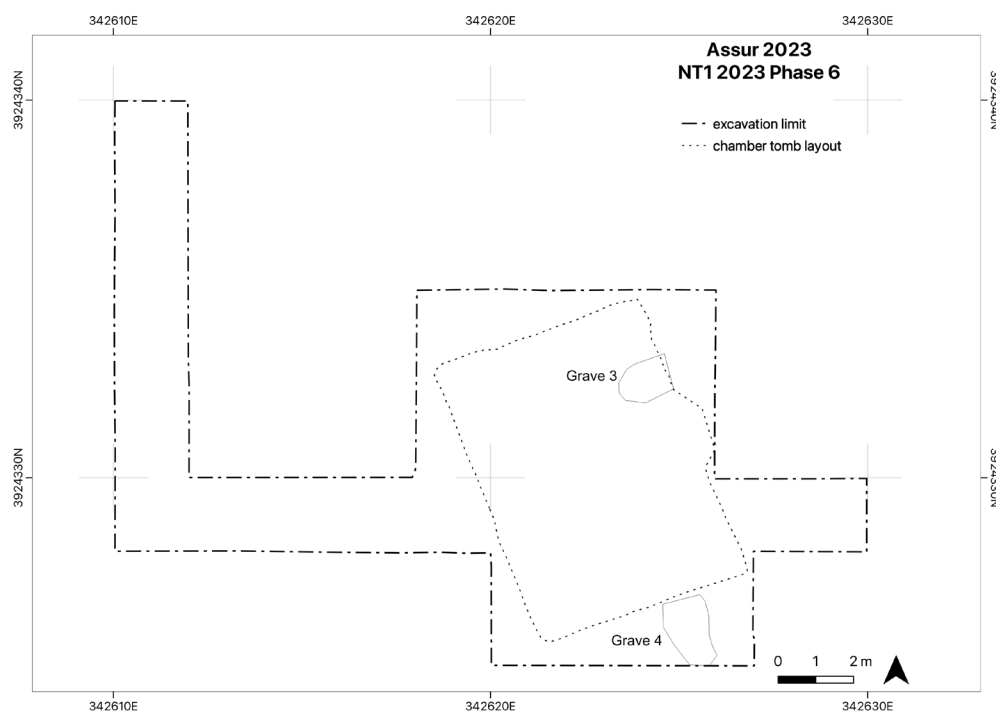


Fig. D2.15: Plan of NT1 2023 Phase 6: Graves 3 and 4. Drawn by Jan Heiler, annotated by Andrea Squitieri.

the stones forming the wall base were found. To the east of the wall, a fill (Locus:262432:016) was excavated that consisted of greyish soil with mudbrick debris, pottery sherds and bones.

The installation (Locus:261433:024) was assigned to this phase because it cut the structures of NT1 2023 Phase 5. It consisted of two rows of roundish stones that formed a corner. The original size and shape of this installation remain unclear as it continues beyond the excavation limit. To the southeast of the installation, a deposit of loose soft greyish soil with some pebbles and pottery sherds (Locus:261433:012) was unearthed.

D2.5 NT1 2023 Phase 6: Graves 3 and 4

NT1 2023 Phase 6 (Fig. D2.15) consists of Grave 3 and Grave 4. These are two inhumation burials that each contained an ovoid-elliptic sarcophagus (in German: *Stülpwannensarkophag*) of a type previously attested in Assur.⁹⁹ Both these graves cut the architecture of NT1 2023 Phase 5 (Building A), which indicates that they are of a younger date than this phase.

An absolute date for Grave 3 is provided by the alphabetic inscription engraved on its sarcophagus, which gives

a date in the 11th month of the year 153 of the Seleucid Era, corresponding to July/August of 158 BC (see §G2). The sarcophagus of Grave 4 was not inscribed, but its stratigraphic position and the similarity to the sarcophagus of Grave 3 suggest that it too dates to the mid-second century BC. Regrettably, the molars taken from the two burials to undergo radiocarbon analysis did not have high enough collagen levels to permit this (§D1.3).

D2.5.1 Grave 3

Grave 3 was located in the northeastern part of the excavation area. Its cut (Locus:262433:057 and Locus:262433:066) had an oval shape measuring about 1.6 × 1 m. The upper part of the grave was damaged by the later construction of the chamber tomb. However, the sarcophagus (AS 262433:058:004) was found intact with all its inventory at the bottom of the grave fill (Fig. D2.16). It is described in §F, no. 142 and its inscription is discussed in §G2. The grave fill was made up of two parts. The upper part (Locus:262433:056) reached a depth of c. 1.2 m from the top of the grave cut and consisted of a compacted light-grey soil, mixed with pottery sherds, stones and pebbles. A small glass fragment was found in this fill (AS 262433:056:003). The lower part (excavated as Locus:262433:058 and Locus:262433:067) was c. 30 cm thick and consisted of a mix of a compact soil with reddish-grey colour and a loose

⁹⁹ Andrae 1933, pl. 44; Haller 1954, 50–51; Hauser 2021, 158.



Fig. D2.16: The inscribed sarcophagus of Grave 3. Photo by Marco Wolf.

soil of yellowish-brown colour, with pottery sherds and pebbles.

Underneath the sarcophagus, the skeleton (Locus:262433:060) had been laid down, apparently directly on the soil (**Fig. D2.17**). The bones were poorly preserved and found embedded in dark-brown, very loose soil. The upper part of the body was better preserved than the lower part, with parts of the ribs, the spinal cord and both hands still distinguishable. The other parts of the skeleton were highly fragmented and the feet were completely lost.

Nonetheless, we could still identify position and orientation. The skeleton was laid down in a crouched position and the skull, poorly preserved as it was, was most likely facing southeast; radiocarbon analysis of one of the better-preserved molars was not successful (§D1.3). The hands were positioned in front of the body. The right arm on the right side was in an angled position in front of the chest, and the left arm stretched out in front of it, with the left hand just above the knees.

To the front of the deceased's left arm, at the height of the chest, an amphora with a green glaze (AS 262433:060:001, also registered as vessel G03-Vo2, see §E1.3) was found



Fig. D2.17: The skeleton of Grave 3. Photo by Marco Wolf, annotated by Andrea Squitieri.

in an upright position; a soil sample from the inside of the amphora was taken for phytolith analysis (sample: AS 262433:060:017). Around the left hand's ring finger, a corroded iron ring was found (AS 262433:060:003), while a piece of glass (AS 262433:060:008) was found lying in between the bones of the right hand. Among the remains of the hip bone, there were three beads (AS 262433:060:005, AS 262433:060:006 and AS 262433:060:007) whereas a dome-shaped bead (AS 262433:060:010) was found underneath the skull. After removing the skeleton, we found another bead (AS 262433:060:016).

Small fragments of textiles (AS 262433:060:009) were found on top of the middle part of the skeleton; these were exported and are currently undergoing analysis by a team headed by Dr Annette Paetz gen. Schieck at the Deutsches Textilmuseum in Krefeld. We also collected samples for parasitology and phytolith analysis. On top of the skeleton, fragments of plaster with a porous surface (AS 262433:060:011) were found. We assume that these fell from the inside of the sarcophagus, whose texture they match.

After the sarcophagus was removed, its rim was found to have covered a completely preserved green glazed bowl (AS 262433:058:006; also registered as vessel G03-Vo1; see

§E1.3). We assume that this bowl too was a part of the grave inventory but accidentally ended up underneath the sarcophagus' rim when it was placed over the burial.

The grave finds, listed in the table below, are further described in §F, nos. 132-144.

AS number	Short object description	Spatial relation to the skeleton
AS 262433:060:001 (also vessel Go3-Vo2)	Green glazed amphora (see §E1.3)	In front of the left arm
AS 262433:058:006 (also vessel Go3-Vo1)	Green glazed bowl (see §E1.3)	Under the sarcophagus' rim
AS 262433:060:003	Iron ring	Around the left hand's ring finger
AS 262433:060:005	Glass/frit spherical bead	Among the hip bones
AS 262433:060:006	Glass/frit spherical bead	Among the hip bones
AS 262433:060:007	Glass/frit spherical bead	Among the hip bones
AS 262433:060:008	Small glass fragment	Among the right hand's bones
AS 262433:060:009	Textile fragments	On top of the middle part of the skeleton
AS 262433:060:010	Dome shaped bead	Underneath the skull
AS 262433:060:016	Cylindrical white bead	Underneath the skeleton

D2.5.2 Grave 4

Grave 4 was located in the southern part of the excavation area (Fig. D2.15). The grave pit (cut: Locus:262432:052) had an oval shape measuring c. 2 × 1 m and was about 1.5 m deep (Fig. D2.18). It cut the structures of the NT1 2023 Phase 5 and was only minimally damaged by the construction of the later chamber tomb.

The grave's upper layer (Locus:262432:053) was about 80 cm thick and consisted of a greyish, very dense soil with pottery sherds, stones and bones. A small bronze fragment was found in this fill (AS 262432:053:003, see §F, no. 153). The grave's lower layer (Locus:262432:054) was about 60 cm thick and composed of very friable reddish soil, mixed with pottery sherds and small stones. It yielded a stone bead in the shape of a convex cone disc (AS 262432:054:003, see §F, no. 150). The sarcophagus (AS 262432:054:004) was found at the bottom of this fill (Fig. D2.18). Although of a slightly different size, its shape is similar to the sarcophagus of Grave 3 (see §F, no. 152).



Fig. D2.18: The sarcophagus of Grave 4. Photo by Veronica Hinterhuber.

There is no inscription incised on it, however. Remains of bitumen were sticking to the outside, which indicates that it had been originally coated in that substance at least partially – very likely because there is an ancient hairline crack running through the fabric that had been identified once the piece had been fired.

Underneath the sarcophagus, the skeleton (Locus: 262432:055) was found in a very bad state of preservation (Fig. D2.19). Nevertheless, the deceased's position and orientation were still discernible. The skeleton was placed in a crouched position, lying on its left side, with the head towards south and facing west. The deceased's arms were positioned in front of the body and both angled in front of the chest, with the right arm set above the left. The position of the legs showed a similar posture, crouched with the right leg being positioned above the left.

The best-preserved bones of the deceased were those in the lower and middle parts of the body, and the remains of the feet could be collected. Identifiable were the long bones from the femur, tibia and fibula, parts of the pelvis and the sternum as well as some of the vertebrae



Fig. D2.19: The skeleton of Grave 4. Photo by Veronica Hinterhuber.

and ribs, although most of these bones were fractured. The worst preserved part of the skeleton was its skull, although parts of the upper jaw were still intact, with some teeth still in place; radiocarbon analysis performed on the best-preserved molar was nevertheless unsuccessful (§D1.3).

Some pottery sherds were found near the skeleton (collection: AS 262432:055:004) along with a small unworked snail shell (AS 262432:055:009) and two bronze fragments (AS 262432:055:011 and AS 262432:055:012). All these finds are discussed in §F, nos. 145-153. A small piece of white plaster was also found which had probably fallen from the inner surface of the sarcophagus (AS 262432:055:013), as in the case of Grave 3 (§D2.5.1). Small fragments of leather (collection AS 262432:055:003) were found around the feet, which currently undergoing DNA analysis by a team headed by Prof. Dr Joris Peters at LMU Munich's Institut für Paläoanatomie; the first results indicate that

the leather comes from the skin of a ruminant.¹⁰⁰ We also collected samples for parasitology and phytolith analysis.

D2.6 NT1 2023 Phase 5: Building A

NT1 2023 Phase 5 was identified closely below the topsoil (Fig. D2.21). The remains assigned to this phase consist of three rooms, which were part of what we called "Building A". Room 1 was located to the northwest, Room 2 to the west and Room 3 to the southwest. The building's complete extent remains unclear because part of it continues outside the 2023 excavation area. Moreover, its eastern part was heavily damaged by the later construction of the underground chamber tomb (§D2.3).

The radiocarbon analysis of a piece of charcoal from the floor deposit of Room 2 yielded a dating range of 173-53 calBC and that of a carbonised seed from the same context 176-52 calBC, while another carbonised seed, this time from Room 1, produced a dating range of 341-57 calBC (all 95.4% probability; see §D1.3). The date in the alphabetic inscription of Grave 3, which cuts the floor of Room 2, provides a *terminus ante quem* of July/August 158 BC (§G2). Building A was certainly in use during the Hellenistic period.

This otherwise clearcut situation is complicated by the substantially earlier dating ranges of three more carbonised seeds from the floors of Room 2 and Room 3, namely 975-835 calBC, 778-551 calBC and 658-407 calBC (all 95.4% probability; see §D1.3). At least the first two of these seeds must derive from contexts that predate the construction of Building A, which is certainly not a Neo-Assyrian-period building. Whether this also applies to the third seed is open for discussion as its radiocarbon dating range postdates the Neo-Assyrian period. How the presence of these older materials can be explained is a question that we hope to clarify in the future (for now, see §D1.3).

D2.6.1 Room 1

Room 1 is situated in the northwestern part of Building A (Figs. D2.20-D2.21). Only an area of 5 m² was exposed as this room continues under the eastern and western sections of our excavation area. It is a narrow elongated space bounded by the wall Locus:261433:008 to the northwest, the wall Locus:261433:009 to the northeast and the wall Locus:261433:010 to the southwest. Although the

¹⁰⁰ Joris Peters, pers. comm., October 2023.



Fig. D2.20: Plan of NT1 2023 Phase 5. Drawn by Jan Heiler, annotated by Andrea Squitieri.



Fig. D2.21: Orthophoto of NT1 2023 Phase 5. Locus numbers in red indicate floors. Created by Jens Rohde, annotated by Andrea Squitieri.

state of preservation of the walls is relatively poor, it was possible to gather information about their building technique. The walls were erected on a base made of stones of varying sizes. The gaps between the stones were filled with a greyish-brown mortar mixed with pottery sherds and pebbles. The same type of mortar was also used to bind together the mudbricks. The bricks' surface measured 38 × 38 cm but their height could not be established. Also, due to erosion, they were not always fully preserved. In some instances, it was possible to observe that the wall faces had been covered by a reddish-brown plaster, with pebbles and white inclusions.

The northwestern wall (Locus: 261433:008) of Room 1 continued under the northern and western sections beyond the excavation trench. This wall was exposed over a length of c. 85 cm and survived to a maximum height of about 30 cm above the floor level (Locus:261433:006). Only the bottom of the wall was preserved. The relation between this wall and the northeastern wall (Locus:261433:009) is not clear, as both were cut by a stone installation (Locus:261433:024) located in the northeastern corner of the trench, exactly where a hypothetical wall corner would have been placed. This installation dates to the younger NT1 2023 Phase 7 (§D2.4).

The northeastern wall (Locus: 261433:009) was excavated over a length of c. 2.3 m. It is about 70 cm wide and preserved to the height of c. 40 cm above the floor level. The southwestern wall (Locus: 261433:010), located roughly in the middle of our trench, continues under the western and eastern sections of our excavation trench. This wall was already partially visible on the surface before we started the excavation. The wall was exposed to a length of c. 3.2 m and 1.1 m wide, with a preserved height of about 10-20 cm above the floor level. We were able to observe a row of stones along the southwestern bottom edge of the wall, together with traces of plaster, but no mudbrick structures could be identified.

The floor (Locus:261433:006) of Room 1 was a beaten earth surface of a greyish colour, with many pottery sherds and small pebbles embedded in its matrix. In the northwestern part, it was badly preserved due to the presence of an animal burrow. The floor was covered by a thin deposit (Locus:261433:005), made of a light brown and soft soil, with many pottery sherds and pebbles. It yielded two stone tools in the shape of discs with smooth surfaces, possibly used as polishers (AS 261433:005:005 and AS 261433:005:009), an unworked shell (AS 261433:005:006), and a pottery slag (AS 261433:005:008; see §F, nos. 154-157). In the southwestern part of the floor, a concentration of loose ashes mixed with many pebbles was observed (Locus:261433:007), which suggests that the end of Room 1's occupation was caused by fire.

Above the floor deposit of Room 1, there were two more deposits (Locus:261433:004 and Locus:261433:003). The former consists of light brown soil, containing pottery sherds, pebbles, stones, mudbrick debris and one conical shell bead (AS 261433:004:003, §F, no. 158). Locus: 261433:003 contained collapsed mudbricks.

To the south of Room 1, we identified a wall (Locus: 261433:011) that extends to the southwest of wall Locus: 261433:010. At the corner of these two walls, three large stones were identified (Locus:261433:025). Wall Locus: 261433:011 was exposed over a length of about 2 m and about 90 cm wide. It showed a poor state of preservation, being heavily eroded along the slope. This wall was most likely part of Building A, but could not be assigned to a specific room because we did not identify any floor abutting it.

D2.6.2 Room 2

Room 2 is situated to the east of Room 1 and the north of Room 3. Its layout is not clear because the construction of the chamber tomb destroyed the eastern part of this room. Moreover, due to the excavation limits, we were not able to find any of the room's corners. Therefore, we can only estimate that the room had originally a surface of 48 m², of which 15 m² have been investigated in 2023.

Room 2 is delimited by the wall Locus:261432:008 to the west, the wall Locus:261432:009 to the south, the wall Locus:262433:078 to the east and the wall Locus:261433:022 to the north (Fig. D2.21). All walls were built in a similar technique as those of Room 1.

The best-preserved wall is the southern wall (Locus: 261432:009), which is oriented from northeast to southwest. It was excavated over a length of c. 2 m and about 1 m wide, corresponding to two bricks and a half-sized brick that are set side by side. The wall is shared with Room 3 and abutted on both sides by the floors of Room 2 and Room 3, respectively. This means that the wall was preserved to its original width. It survived to a height of 30-35 cm above the most recent floor level, but because a 2 cm thick plaster was applied to the wall faces, it was not possible to see the mudbrick courses.

The western wall (Locus:261432:008) has a preserved width of about 1.2 m and an exposed length of about 2.2 m. Only the wall's stone base survives. To the northeast, the wall could be followed for only about 60 cm from the northern edge of the trench, while the rest was cut by a looting pit (Locus:261432:012, belonging to NT1 2023 Phase 9; see §D2.2). In the preserved part of the wall, it was possible to observe that the wall was covered by a 2-5 cm thick plaster.

The northern wall (Locus:261433:022) was exposed over a length of c. 2 m and about 1 m wide, corresponding again to the dimensions of two bricks and a half-sized brick set side by side. The wall was preserved to a height of 33-47 cm above the floor (Locus:261433:023). To the west, it was bordered by a doorway (installation: Locus:261433:026) and to the east by the limit of the excavation trench. At the bottom of this wall, it was possible to see one course of stones in the south and the west. The western stones were 31-42 cm long, while the remaining stones were 15-20 cm in size. The wall face was covered by a 2 cm thick plaster, which made it impossible to see the mudbrick courses.

Finally, the eastern wall (Locus:262433:078) was exposed over a length of c. 2.2 m and about 85 cm wide. It was preserved at a height of c. 35 cm above the floor level.

In those portions of Room 2 that had not been destroyed by the construction of the later chamber tomb, we defined three levels of floors, one on top of the other. This floor sequence was visible in the section of the modern looting pit (Locus:261432:012) that disturbed the western part of the room, cutting the wall Locus:261432:008 (Figs. D2.20-D2.21).

Only the uppermost floor was fully exposed. This floor extended around the northern part of the chamber tomb and was identified across three squares. In each square, it was labelled separately (Locus:261432:014, Locus:261433:023, and Locus:262433:069). The floor consisted of a beaten earth surface with a greyish colour and some pottery sherds, pebbles and stones embedded in it.

The floor deposit (named Locus:261432:011, Locus:261433:020 and Locus:262433:068 in the respective squares) consisted of a soft, greyish-brown soil with abundant pottery sherds, pebbles, mudbrick debris, a few bones and charcoal. A charcoal piece (sample AS 261432:011:033) was collected from this deposit and produced a radiocarbon dating range of 173-53 calBC (95.4% probability; see §D1.3), closely matching the date offered by the inscription on the sarcophagus of Grave 3 (§D2.5.2) whose grave pit was cut down from that floor level.

Six finds were collected from Room 2's floor and listed in the table below (see §F, nos. 159-165). The most significant is a small stamp seal made of lapis lazuli (AS 261432:011:028), which was found to the west of wall Locus:261432:009 (see §F6.1).

AS number	Short object description
AS 261432:011:028	Stamp seal made of lapis lazuli (§F6.1)
AS 261432:011:034	Iron fragment
AS 261433:020:026	Bronze fragment
AS 261433:020:028	Bronze fragment

AS number	Short object description
AS 261433:020:030	Stilt (kiln support)
AS 262433:068:004	Fragment of a lower grinding stone made of basalt

The upper deposit of Room 2 (called Locus:261432:007, Locus:261433:017, Locus:261433:021 and Locus:262433:065 in the respective squares) consisted of mudbrick debris embedded in soft greyish soil and yielded a high quantity of pottery sherds, pebbles, and a few ashes. This deposit was in turn covered by a grey-light brown deposit (Locus:262433:008 and Locus:262433:009). The finds collected from these fills are listed in the table below (§F, nos. 166-170).

AS number	Short object description
AS 261432:007:003	Clay fragment with roof impression
AS 261432:007:004	Flat pointed tool made of bone
AS 261433:017:004	Bronze fragment
AS 262433:065:003	Ceramic slag
AS 262433:065:004	Bronze fragment

D2.6.3 Room 3

Room 3 was located in the southern part of Building A (Fig. D2.20). It was not possible to determine its complete extent as it was cut in the north by the construction of the chamber tomb (of NT1 2023 Phase 8; see §D2.3), and in the east by both Grave 4 (of NT1 2023 Phase 6; see §D2.5.2) and the wall Locus:262432:017 (of NT1 2023 Phase 7; see §D2.4).

To the north, Room 3 was bounded by the wall Locus:261432:009, shared with Room 2. To the east and the south, it continued beyond the limits of the excavation area. The floor (Locus:262432:060) of Room 3 consisted of a beaten earth surface of greyish-beige colour, with a few pottery sherds and small pebbles embedded in it. To the northwest, the floor abutted the easternmost excavated point of the wall (Locus:261432:009).

The floor deposit (Locus:262432:058) was a soft soil of brownish-reddish colour, with some white spots. Some bones and a few small pottery sherds were found in this deposit, along with a clay loom weight (AS 262432:058:032), a disc made of lead (AS 262432:058:034) and an iron slag (AS 262432:058:044; see §F, nos. 171-173).

Above this deposit, we excavated the upper fill of the room as Locus:262432:051. This consisted of a greyish, very loose soil, with some ashy spots, that yielded a few sherds and bones. Three bronze fragments were found in this fill, among which was a possible nail (AS 262432:051:003-005; see §F, nos. 174-175).

D2.7 NT1 2023 Phase 4: Building B

D2.7.1 The walls

NT1 2023 Phase 4 is stratigraphically located between NT1 2023 Phase 3 (to which Grave 5 belongs, which produced two radiocarbon dating ranges of 770-542 calBC and of 775-545 calBC, both with 95.4% probability; see §D1.3) and between NT1 2023 Phase 5 (to which Building A belongs, whose youngest radiocarbon dating ranges are 173-53 calBC, 176-52 calBC, and 341-57 calBC (all 95.4% probability; see §D1.3). It comprises two walls that have been assigned to what we dubbed “Building B”. These walls are Locus:262433:054 to the north and Locus:262433:075 to the southeast. Both walls delimited an open area called “Unroofed Area 4” (Figs. D2.22-D2.23).

The foundation of the northern wall (Locus:262433:054) was built into a construction pit (Locus:262433:077), filled with stones, baked brick fragments and soil (fill: Locus:262433:073; Figs. D2.24-D2.25). The wall was exposed over a length of c. 5.8 m. It is about 1.3 m wide and preserved to a height of about 50 cm, including its foundation. The surviving three courses of mudbricks have a format of 38 × 38 × 12 cm or a half-sized format of 38 × 19 × 12 cm. The bricks were held together by a mortar consisting of crumbly brown clay with white inclusions and traces of chaff. The southern face of the wall was covered with a plaster layer, 3 to 6 cm thick, made of clay of a brownish-red colour, with white inclusions.

The southeastern wall (Locus:262432:075) was exposed over a length of c. 2 m. When first observed, it had a width of c. 75 cm, but it became broader towards the bottom where it reached a width of 1.4 m at the lowest excavated level. The wall was preserved to a height of about 1.3 m on the western side and about 2 m on the eastern side.

D2.7.2 Unroofed Area 4

D2.7.2.1 The floor and its substructure

What we call “Unroofed Area 4” is a squarish space measuring about 6.6 × 6.7 m (Figs. D2.22-D2.23). The substructure of its floor (registered as Locus:262432:061 and Locus:262432:073) was only partly excavated. It consisted of irregularly arranged stones mixed with small pebbles and burnt brick fragments, embedded in a reddish-grey soil matrix. A large quantity of pottery sherds was collected from it, along with the small finds listed in the table below (see also §F, nos. 176-189).

AS number	Short object description
AS 262432:061:003 AS262432:061:006 AS 262432:061:012 AS 262432:061:008	Four bronze fragments
AS 262432:061:014	Iron fragment
AS 262432:061:004	Fragments of a glassy material
AS 262432:061:005	Unworked shell
AS 262432:061:007 AS 262432:061:013 AS 262432:061:010 AS 262432:061:009	Four stone tools
AS 262432:061:011	Head of a male figurine
AS 262432:073:002	Basalt mortar fragment
AS 262432:073:004	Grinding stone fragment

The floor of “Unroofed Area 4” (Locus:262433:080 and Locus:262432:068) consisted of a beaten earth surface, with a thickness of 5 to 7 cm, with pebbles, stones, bone fragments and pottery sherds embedded in it (Fig. D2.23). In some spots, concentrations of white inclusions were visible. The floor’s surface was not excavated completely because it continues beyond the western and southern limits of the excavation area.

D2.7.2.2 The occupation levels

Multiple pits and installations were identified on the floor of “Unroofed Area 4” (Fig. D2.22). These features are divided into two two groups of installations, which were separated by three superimposed fills. They are described below in stratigraphic order, starting with the features belonging to the lowest occupation level.

Located towards the south, the pit cut (Locus:262432:048) had in its excavated part a semi-circular shape, measuring c. 1 m in the north-south direction and c. 2 m in the west-east direction. Towards the bottom, the pit narrowed so that in the lowest excavated part it measured about 45 cm from north to south and c. 1.8 m from east to west. The pit was lined with at least four courses of upright mudbricks (Locus:262432:090; Fig. D2.26). The fill of the pit (Locus:262432:049) was excavated to a depth of about 1 m and consisted of reddish-brown, loose soil, with abundant white inclusions, some ash and charcoal. It yielded pottery sherds, bones, and five small finds: an iron and a bronze fragment (AS 262432:049:003 and AS 262432:049:004), two clay loom weights (AS 262432:049:006 and AS 262432:049:007) and the torso of a male figurine (AS 262432:049:005) (see §F, nos. 190-194).

To the northeast, an installation (Locus:262433:071) was found that abutted the northern wall (Locus:262433:054).

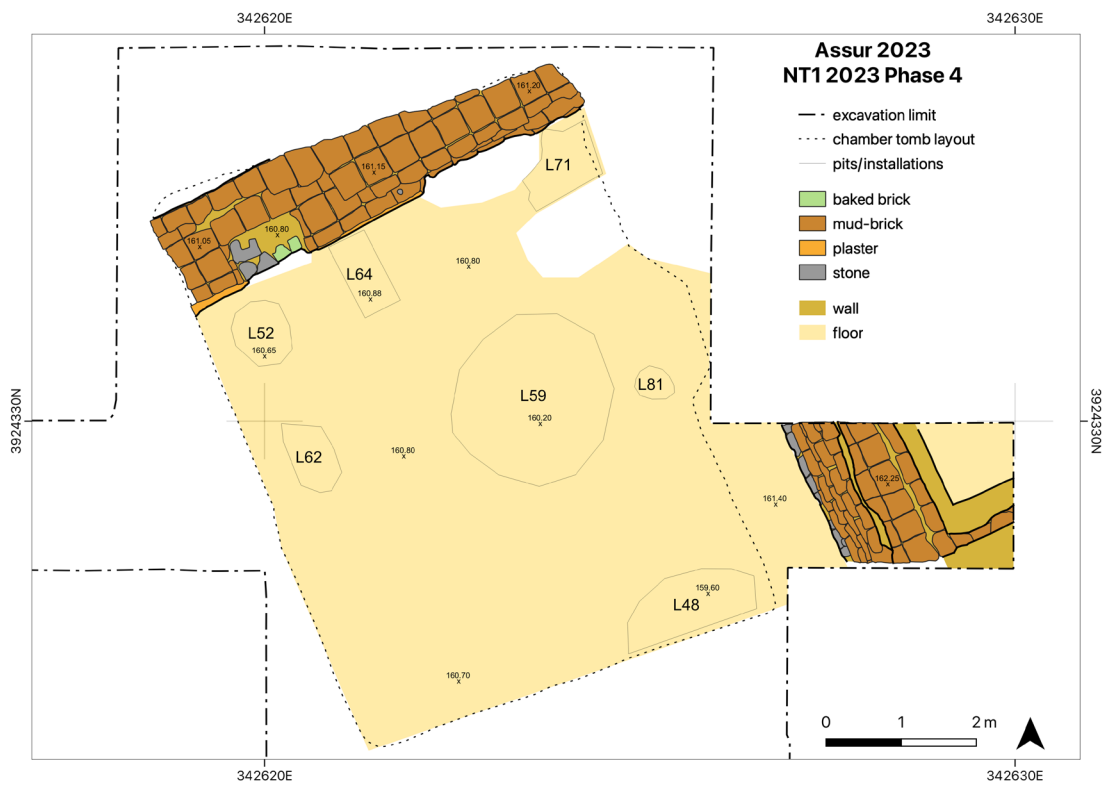


Fig. D2.22: Plan of NT1 2023 Phase 4. Drawn by Jan Heiler, annotated by Andrea Squitieri.



Fig. D2.23: Orthophoto of NT1 2023 Phase 4. Locus numbers in red indicate floors. Created by Jens Rohde, annotated by Andrea Squitieri.



Fig. D2.24: Wall Locus:262433:054 belonging to Building B. Photo by Marco Wolf.



Fig. D2.25: Wall Locus:262433:054 belonging to Building B. Note in the foreground the installation Locus:262433:074 belonging to the older NT1 2023 Phase 2. Photo by Marco Wolf.

It was only partially excavated since it continued beyond the eastern section of our excavation area. The installation consisted of two layers of white plaster, each only a few millimetres thick. These layers were spread over a surface of at least 95×80 cm, thus forming the outline of a basin. On top of the plaster, we documented a 1-2 cm thin layer of light brown soil that could be a third layer of the installation. The fill covering the installation (Locus:262433:070) consisted of compact brown soil mixed with white inclusions that contained charcoals, small fragments of bricks, pebbles and pottery sherds as well as a bronze fragment (AS 262433:070:003; see §F, no. 195).

To the west of the installation (Locus:262433:071), we found another installation (Locus:262433:064), made of one row of five mudbricks set on top of the floor (Locus: 262433:080).

To the southwest of that second installation (Locus: 262433:064), we identified a pit cut (Locus:262432:062), which had an oval shape of about 100×65 cm. Its fill (Locus:262432:063) consisted of a loose greyish soil that contained pottery, some bones, three bronze fragments (AS 262432:063:005, 007 and 008) and three unworked shells (AS 262432:063:003, 004 and 006; see §F, nos. 196-201).

The aforementioned pits and installations were all covered by the deposits Locus:262433:063, Locus:262432:050, Locus:262432:064 and Locus:262433:062. These consisted of a compact greyish-brown soil yielding pebbles, pottery



Fig. D2.26: The semicircular pit Locus:262432:048 with its brick lining. The walls in the background belong to the older NT1 2023 Phase 2. Photo by Jens Rohde.

sherds, bones, and several small finds, listed in the table below (see also §F, nos. 202-209):

AS number	Short object description
AS 262433:063:003	Stilt (kiln support)
AS 262433:063:004	Unworked shell
AS 262433:063:005	Basalt whetstone
AS 262433:063:006	Stone vessel rim
AS 262432:050:006	Stone biconical bead
AS 262433:063:007 AS 262432:050:004 AS 262432:050:005 AS 262432:050:009	Iron fragments
AS 262432:050:003 AS 262432:050:007 AS 262432:050:008 AS 262432:050:010 AS 262432:064:003	Bronze fragments
AS 262433:062:003	Bronze pin with curved tip

Above these deposits, we identified three further pits. The first pit cut (Locus:262433:081) had an oval shape with a length of c. 50 cm and a width of c. 40 cm. It was not excavated.

The second pit cut (Locus:262433:059) had a rounded shape of about 2.3 m in diameter. Its fill (Locus:262433:055) was excavated to a depth of 90 cm and consisted of reddish-brown soil with some pottery sherds, mudbrick fragments, bones and pebbles. This fill also yielded a broken whetstone made of basalt (AS 262433:055:003), two bronze fragments (AS 262433:055:004 and 006), a baked brick that had possibly been used as a door socket (AS 262433:055:007) and two clay loom weights (AS 262433:055:005 and 008; see §F, nos. 210-215). At the bottom of the pit, we reached the walls of NT1 2023 Phase 2 (§D2.9).

The third pit cut (Locus:262433:052) had a circular shape with a diameter of about 80 cm. Its fill (Locus:262433:053) consisted of a darkish-brown loose soil that contained some pottery sherds, pebbles, stones and a clay loom weight (AS 262433:053:002; see §F, no. 216).

D2.7.2.3 The upper deposits

Several deposits accumulated after the abandonment of “Unroofed Area 4.” Only those to the west of the south-eastern wall (Locus:262432:075) had not been cut by the construction of the later chamber tomb (§D2.3).

To the west of the wall, we identified three fills consisting of mudbrick debris. From the bottom up, these fills are Locus:262432:065, Locus:262432:059, and Locus:262432:057. Only Locus:262432:059 yielded some small

finds, which are listed in the table below (see §F, nos. 217-221).

AS number	Short object description
AS 262432:059:005; AS 262432:059:006; AS 262432:059:009	Three bronze fragments
AS 262432:059:008	Iron fragment
AS 262432:059:002	Lead perforated object
AS 262432:059:004	Glass shard
AS 262432:059:007	Fragment of a grinding stone

The deposits cut by the chamber tomb consisted of mudbrick debris, mixed with pebbles and baked brick fragments. From the bottom up, these are Locus:262433:061, Locus:262433:051, and Locus:262432:047.

The finds collected from these deposits are listed in the table below and discussed in §F, nos. 217-230, 233-234). The most notable object is a complete beaker with a nipple base (AS 262432:047:002, discussed in §E1).

AS number	Short object description
AS 262433:051:002	Basalt whetstone
AS 262433:051:004	Bronze fragment
AS 262433:051:005	Perforated pottery sherd
AS 262433:051:006	Bronze ring with overlapping ends
AS 262433:051:007	Stilt fragment (kiln support)
AS 262433:051:009	Pointed bone tool
AS 262433:051:011	Reworked baked brick
AS 262433:051:012	Glass shard
AS 262433:051:013	Flint flake
AS 262432:047:005	Bronze fragment
AS 262432:047:002	Beaker with nipple base (§E1)

Additional fills were identified higher up in the stratigraphic sequence, directly underneath each of the chamber tomb’s subdivisions. These are Locus:262433:029, Locus:262433:032, Locus:262432:031, Locus:262432:032, Locus:262432:033, and Locus:262432:034. Of these, Locus:262432:032 yielded a rim fragment of a basalt vessel (AS 262432:032:002) and a bronze fragment (AS 262432:032:003), while Locus:262433:032 yielded a clay chunk bearing a bronze imprint (AS 262433:032:002; see §F, nos. 231-232, 235).

D2.8 NT1 2023 Phase 3: Grave 5

NT1 2023 Phase 3 comprises a pit grave (Grave 5; Fig. D2.27). Its grave cut (Locus:262432:069) was detected below the substructure of the floor of “Unroofed Area 4.”

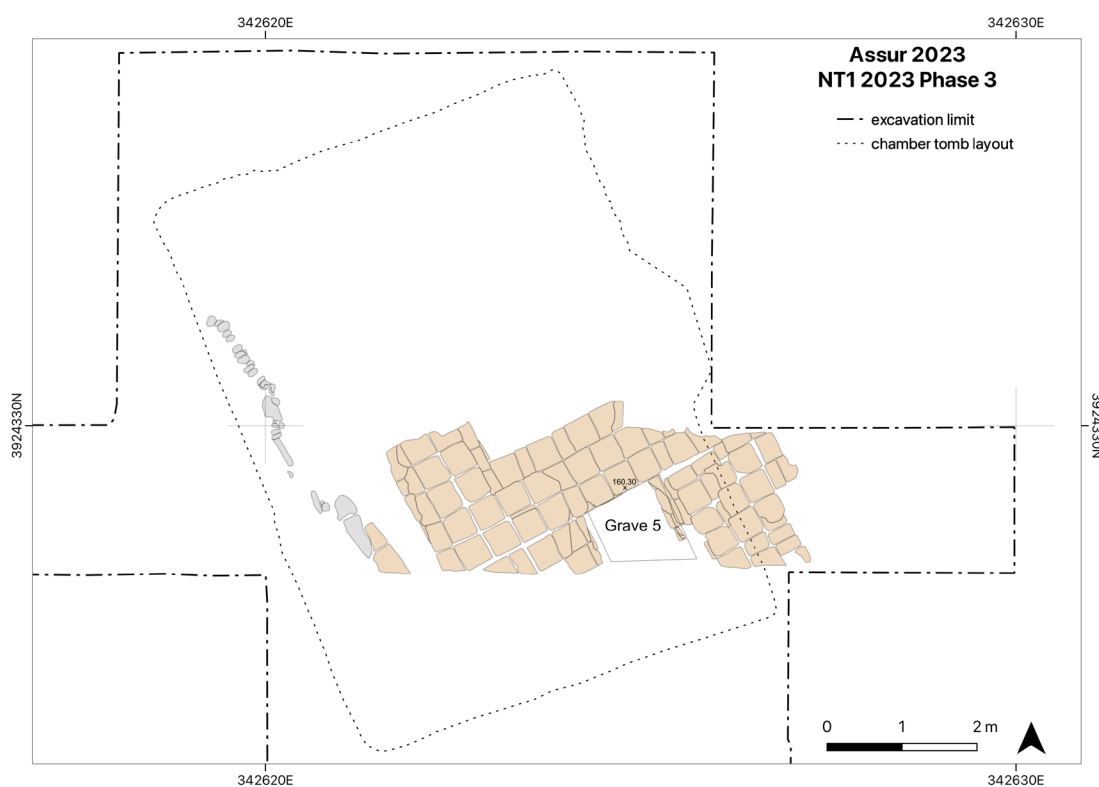


Fig. D2.27: Plan of NT1 2023 Phase 3: Grave 5. The older NT1 2023 Phase 2 is shown with transparency. Drawn by Jan Heiler, annotated by Andrea Squitieri.



Fig. D2.28: The upper fill of Grave 5. Photo by Jens Rohde.



Fig. D2.29: The lower fill of Grave 5. Photo by Jens Rohde.

As this belongs to NT1 2023 Phase 4 (§D2.7), the grave is older than that. Moreover, the grave cut went through the architecture of NT1 2023 Phase 2 (§D2.9), making it younger than the latter.

In the grave's upper fill (Locus:262432:070), disarticulated and very badly preserved human bones were found (collection AS 262432:070:002; **Fig. D2.28**). Two of the molars (samples AS 262432:070:002:001 and AS 262432:070:002:002) were radiocarbon dated to 770-542 calBC and 775-545 calBC (both 95.4% probability; see §D1.3). Two fragmentary vessels were collected (collec-

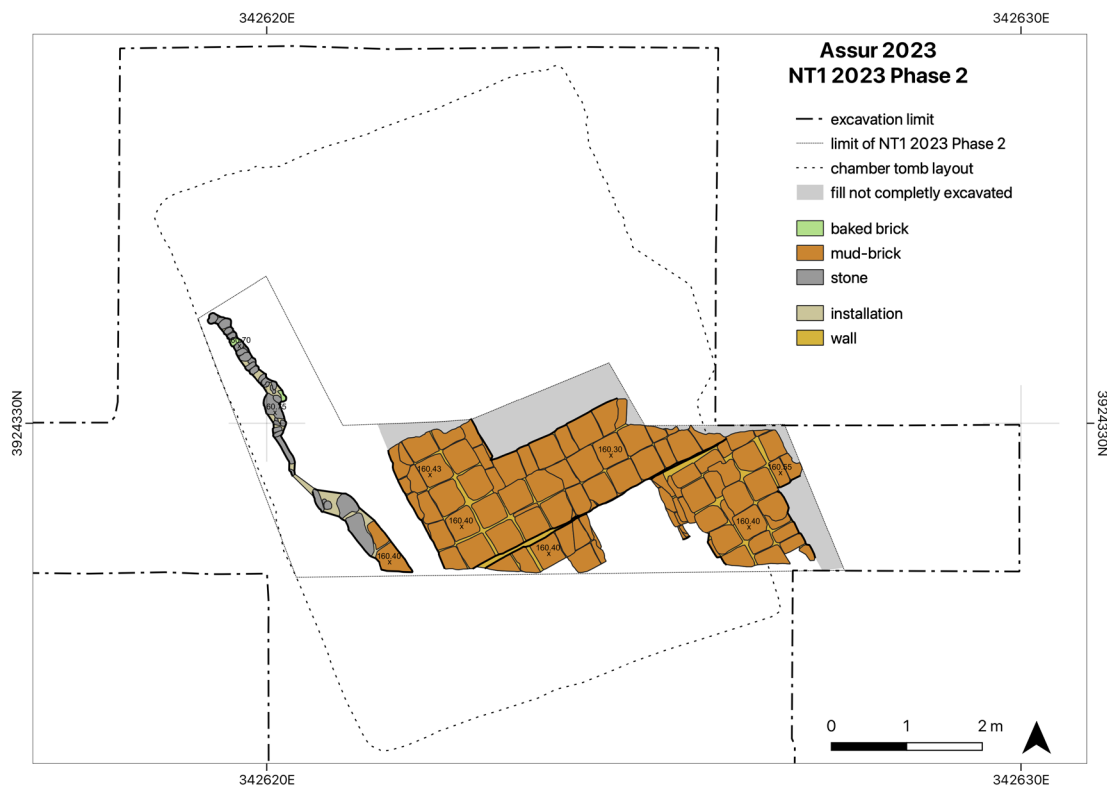


Fig. D2.30: Plan of NT1 2023 Phase 2. Drawn by Jan Heiler, annotated by Andrea Squitieri.

tion AS 262432:070:003 and 004), along with a complete ovoid glazed miniature vessel (AS 262432:070:005; see §E1), which can be securely dated to the late Neo-Assyrian period.¹⁰¹

The grave's lower fill (Locus:262432:071; Fig. D2.29) included a bronze fibula (AS 262432:071:003; see §F, no. 236) of a type that has been dated to the 7th and early 6th century BC.¹⁰²

Since the floor of the "Unroofed Area 4" of Building B (NT 1 2023 Phase 4; §D2.7.2), and in particular its substructure, covered Grave 5 without interruption and thus sealed it, no functional connection could be established to this or any other floor from which the grave had been dug. It is for this reason that we assigned it its own stratigraphic phase = NT 1 2023 Phase 3.



Fig. D2.31: Orthophoto of NT1 2023 Phase 2. Created by Jens Rohde, annotated by Andrea Squitieri.

D2.9 NT1 2023 Phase 2

NT1 2023 Phase 2 (Figs. D2.30, D2.31) comprised six mudbrick walls, three of which joined together to form a

T-shape. While these walls were not completely excavated, their structure could be observed in the sections of a test sounding which was opened below Grave 5 to reach the virgin soil (§D2.10).

Wall Locus:262432:084 was excavated over a length of about 3.5 m. It was constructed of three rows of mudbricks with a total width of about 1 m. In the northern section of the test sounding, it was possible to see that

¹⁰¹ Hausleiter 2010, pl. 9: Ass. 2482a.

¹⁰² Type C8, see Pedde 200: 245-250, pl. 55-56: nos. 739-769: "Fibel mit länglichen, kreuzschraffierten Blocksegmenten".

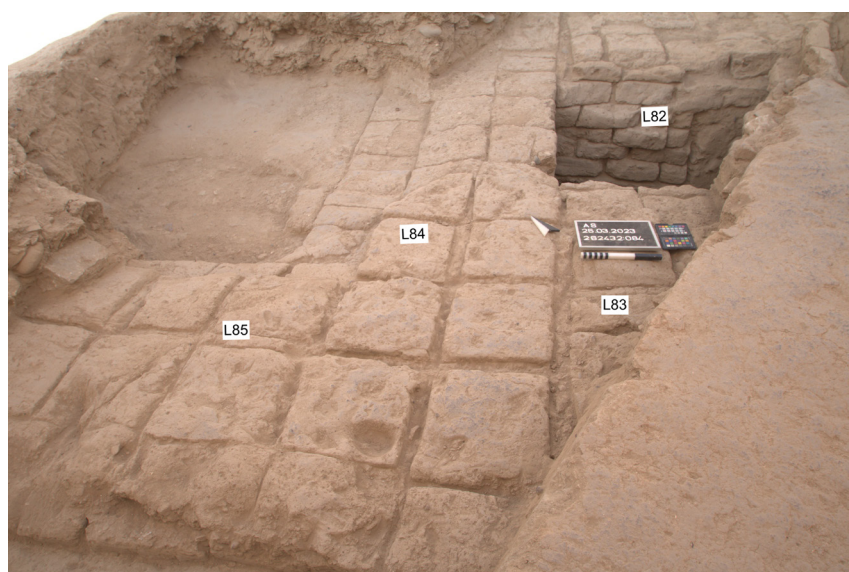


Fig. D2.32: The walls of the NT1 2023 Phase 2. Photo by Jens Rohde, annotated by Andrea Squitieri.



Fig. D2.33: The walls of NT1 2023 Phase 2 around the test sounding. Photo by Jens Rohde, annotated by Andrea Squitieri.

the wall was made of six courses of bricks, each c. 13 cm high (Figs. D2.32, D2.33). To the west, wall Locus:262432:085 was bound to this wall, forming a corner.

Wall Locus:262432:085 was excavated over a length of c. 1.5 m. It had a preserved width of around 1 m and was made of at least two courses of mud-bricks.

Situated to the east, wall Locus:262432:082 was preserved to a length of around 55 cm and a width of around 90 cm. It was bound to walls Locus:262432:080 to the east and Locus:262432:081 to the south. To the west, the wall was cut by the younger Grave 5 (§D2.8). In the section of the test sounding opened below that grave, it was possible to see that the wall was constructed of two bricks and a half-sized bricks set side by side and preserved up to five courses high (Figs. D2.32-D2.33). The maximum preserved height of the wall was around 60 cm.

Wall Locus:262432:083 was possibly the continuation of wall Locus:262432:082 on the western side of Grave 5. It was preserved over a length of around 55 cm. Two and a half rows of mudbrick were visible, with a preserved width of around 90 cm. In the western section of the test sounding, it was possible to see that the wall consisted of five courses of bricks, reaching a total height of c. 60 cm.

Wall Locus:262432:080 was located to the northeast and had the same orientation as wall Locus:262432:082. It was preserved for a length of around 1 m, with two and a half rows of mudbricks visible, for a total width of around 90 cm. The wall was bound to wall Locus:262432:082 to the west and wall Locus:262432:081 to the south, and it abutted wall Locus:262432:084 to the north. It is important to note that, to the east, this wall ran below wall Locus:262432:075, which belongs to NT1 2023 Phase 4 (Fig. D2.34), thus indicating that it was older than the latter.

Finally, wall Locus:262432:081, located to the southeast, was preserved over a length of around 1 m. With three rows of bricks, its total width was around 1 m. This wall was bound to wall Locus:262432:080 to the northeast and wall Locus:262432:082 to the northwest. In the corner created by the walls Locus:262432:080, Locus:262432:081 and Locus:262432:082, a fill (Locus:262432:088) was identified, but not excavated. To the east, this fill ran below the already-mentioned wall Locus:262432:075 that belongs to NT12023 Phase 4.

Importantly, Wall Locus:262432:084 of the two bonding northern walls Locus:262432:084 and Locus:262432:085 is founded deeper than the wall segments Locus:262432:083 and Locus:262432:082, which were set against it from the south and bonding with Locus:262432:080 and Lo-

cus:262432:081. This indicates that the northern wall complex already existed before the southern wall complex was added.



Fig. D2.34: Wall Locus:262432:080 going below wall Locus:262432:075 of the younger NT1 2023 Phase 4. Photo by Jens Rohde, annotated by Andrea Squitieri.



Fig. D2.35: The installation Locus:262433:074. Photo by Marco Wolf.



Fig. D2.36: The installation Locus:262433:074, detail of the northern part. Photo by Marco Wolf.

All the walls of NT1 2023 Phase 2 as well as the fill (Locus:262432:088) were covered by the deposits Locus:262432:074 and Locus:262432:067. Both were made of hard, reddish-brown soil containing pottery sherds, pebbles, bones and mudbrick debris. Two stone bowl fragments were retrieved from these fills (AS 262432:074:004 and 262432:074:005) as well as two bronze fragments (AS 262432:074:003 and AS 262432:067:003; see §F, nos. 239-242).

In the western part of the excavated area, we identified an installation (Locus:262433:074; **Figs. D2.30-D2.31**). There was no physical connection between this installation and the walls described above. However, because the installation went underneath the NT1 2023 Phase 4 wall Locus:262433:054, it was assigned to NT1 2023 Phase 2. The installation was oriented in a roughly north-south direction and was exposed over a length of c. 4 m (**Figs. D2.35-D2.36**). It consisted of at least two courses of stones, stacked on top of each other, reaching a total height of 21-25 cm. To the southeast, some mudbricks set

next to stones were very likely part of the installation. Towards the north, a row of vertically set baked bricks was found, running in parallel to the stones of the installation and going below the NT1 2023 Phase 4 wall Locus:262433:054. We propose to interpret this installation as a drain.

To the east of the drain, and running parallel to it, we identified a fill (Locus:262433:076), which consisted of dense reddish-brown soil, with white inclusions, charcoal and cobbles. This fill yielded two fragmentary bronzes (AS 262433:076:003 and 004) and an iron fragment (AS 262433:076:005).

To the west of the drain, and partially covering it, we excavated another fill (Locus:262433:075). It consisted of loose greenish-grey crumbly soil, with a large concentration of pebbles and pottery sherds. This fill yielded the fragments of a small Egyptian blue bead (AS 262433:075:002) and a rounded bronze fragment (AS 262433:075:003).

Covering these two fills, fill Locus:262433:072 consists of reddish-grey soil, with stones, burnt brick fragments and many pottery sherds. This fill yielded a worked round pebble (AS 262433:072:003) and a shell fragment (AS 262433:072:004). All finds from the

fills connected to the drain are described in §F, nos. 243-249.

D2.10 NT1 2023 Phase 1 and the virgin soil

The remains of NT1 2023 Phase 1 were identified in a 1 × 1.2 m test sounding excavated underneath Grave 5, and the virgin soil was reached at the bottom of this sounding (Figs. D2.37-D2.38). The sounding fill (Locus:262432:076) was made of a soft greyish soil, containing stones, a high amount

of pottery sherds (collection AS 262432:076:001) and bones. Two beads made from shell (AS 262432: 076:004 and 006), a fragmentary carnelian bead (AS 262432:076:005) and a bronze fragment, possibly belonging to a nail or a needle shaft (AS 262432: 076:007), were collected from this fill (see §F, nos. 252-255).

In the sections of the test sounding, we identified two floors, each marked by a line of pottery sherds. Floor Locus: 262432:087 (Fig. D2.38) was identified in the eastern section and ran below wall Locus:262432:082 (of NT1 2023 Phase 2; §D2.9). Floor Locus:262432: 086 was identified in

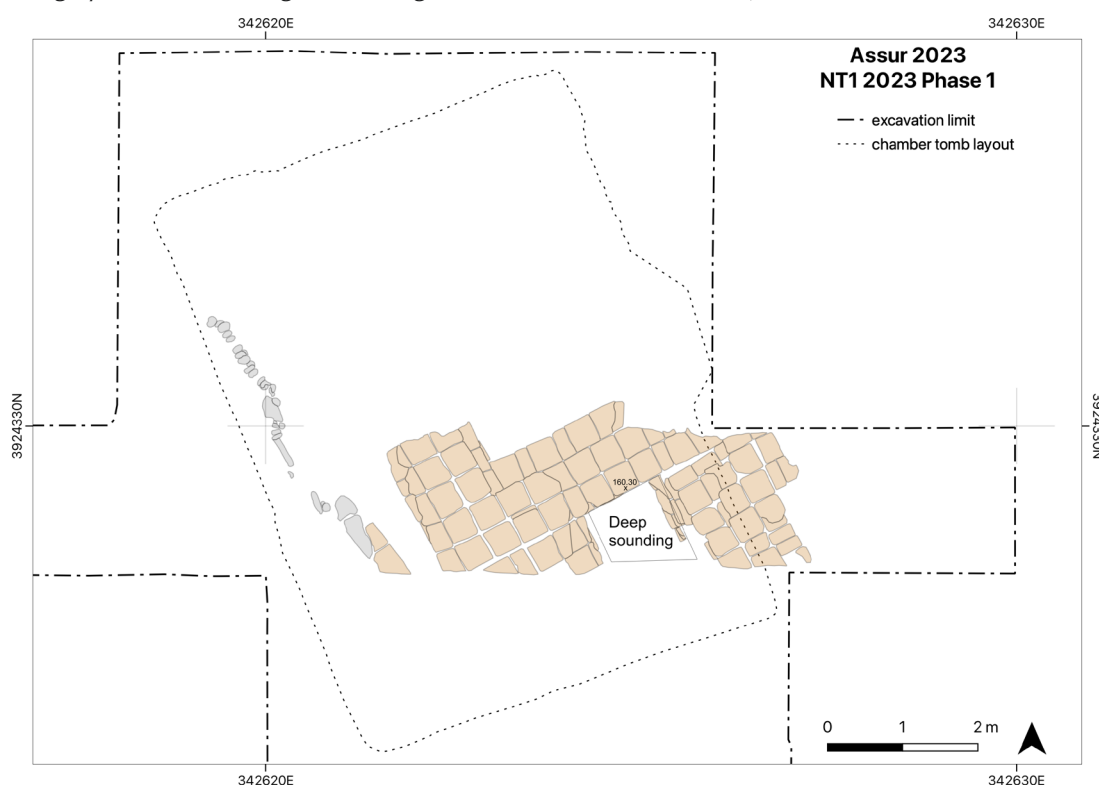


Fig. D2.37: Plan of NT1 2023 Phase 1. The younger NT1 2023 Phase 2 is shown with transparency. Drawn by Jan Heiler, annotated by Andrea Squitieri.



Fig. D2.38: The floor Locus:262432:087 as visible in the section of the test sounding. Photo by Jens Rohde, annotated by Andrea Squitieri.



Fig. D2.39: The floor Locus:262432:086 as visible in the section of the test sounding. Photo by Jens Rohde, annotated by Andrea Squitieri.

the western section (**Fig. D2.39**), almost at the same elevation as the floor in the eastern section (Locus:262432:087). It ran below wall Locus:262432:083 (of NT1 2023 Phase 2; **§D2.9**). A flint flake was collected from directly above this floor (AS 262432:086:001; see **§F, no. 250**).

When we reached the virgin soil, we noticed the presence of a pit cutting it. This pit (cut: Locus:262432:078 and fill: Locus:262432:079; **Fig. D2.40**) was located in the southeastern corner of the sounding and measured about 40 × 25 cm. Its fill was 20–30 cm thick and made of a very soft greyish soil, with ashy spots, that contained a few sherds and animal bones. The fill yielded only one small find, a small sphere made of a whitish stone covered by patina (AS 262432:079:002; see **§F, no. 251**). A piece of charcoal (sample AS 262432:079:003) from this fill was radiocarbon dated to 1506–1440 calBC (95.4% probability; see **§D1.3**).

The virgin soil (Locus:262432:077) was reached at an elevation of 159.08 m above sea level, which is about 4 m below the modern site surface (**Fig. D2.40**). The soil had a reddish colour, with some white spots, and was of a very hard consistency.

D3. Excavating a sondage linked to the 2002 SBAH trench

Karen Radner, Andrea Squitieri & Jens Rohde

The 2023 excavation trench is situated immediately to the west of an area excavated by the State Board of Antiquities and Heritage in 2002, then designated as “New Town 4”. There, the Iraqi team had uncovered residential architecture that was assigned to the Neo-Assyrian period underneath what was interpreted as Parthian architecture and tombs. While the results of this work have never been published, parts of the field documentation have kindly been shown to us by SBAH Sherqat, courtesy of Salim Abdallah who had acted as the trench supervisor in 2002.

The 2 m wide baulk left between our new trench and the SBAH trench was meant to provide structural protection for our ongoing excavation work. After the heavy rainfalls in mid-March, cleaning work was undertaken on the western profile of the Iraqi trench. This showed that the corners of two adjoining rooms east of the wall Lo-

cus:262432:075 (**§D2.7.1**) could be uncovered with relative ease. The bulk of these rooms had been excavated in 2002. Salim Abdullah Ali thought that all parts of the Assyrian building exposed in 2002 date to the same time, assumed to be the 7th century BC. As cleaning the section revealed



Fig. D2.40: The virgin soil (Locus:262432:077) and the pit cutting it (Locus:262432:079). Photo by Jens Rohde, annotated by Andrea Squitieri.



Fig. D3.1: Orthophoto created in February 2023 of the SBAH trench excavated in 2002. The yellow line indicates the sondage excavated in 2023 and described in **§D3**. Created by Jens Rohde, annotated by Andrea Squitieri.



Fig. D3.2: Orthophoto of Room 5 and Room 6. Created by Jens Rohde, annotated by Andrea Squitieri.



Fig. D3.3: The lower floor Locus:263432:007 of Room 6 and wall Locus:262432:089. Photo by Jens Rohde.



Fig. D3.4: The upper floor Locus:263432:003 of Room 6. Photo by Jens Rohde.

two floor levels in what we called “Room 6”, this provided a welcome opportunity to put this assumption to the test, especially as both were situated at an altitude higher than the present surface of the Iraqi trench and therefore the floors originally exposed.

At that time, the ongoing work in NT1 2023 had already demonstrated that the local stratigraphy was more complex than the binary division in “Parthian” and “Assyrian” that had been used for the Iraqi excavation. It was therefore decided to quickly excavate both rooms down to floor level in order to gain samples, chiefly for radiocarbon dating and secondarily also for bioarchaeological analysis. Differently from the usual protocol (§D1.2), the floors were not gridded for sampling due to the limited area of their exposure.

Fig. D3.1 indicates the extent of the excavations subsequently undertaken on 21 and 22 March 2023. The two rooms are separated from each other by a wall running in an east-west direction (Locus:262432:089; see §D2.7.1), with Room 5 in the north and Room 6 in the south (**Fig. D3.2**). Because the rooms are divided from the rest of our excavations by wall Locus:262432:075 they cannot be connected stratigraphically to the remains of Building B (§D2.7) and also not to each other.

D3.1 “Room 6”

Room 6 is delimited to the west by wall Locus:262432:075 and to the north by wall Locus:262432:089, and an area of about 1.4 m² in the room’s western part was exposed on 22 March 2023.

Two floor levels had been identified when cleaning the western section of the Iraqi trench, separated only by a thin layer of soil. The lower floor (Locus:263432:007) lies c. 160.94 m above sea level and is a beaten earth surface (**Fig. D3.3**). This was covered by the deposit Locus:263432:006, which consisted of reddish brown soil and was sampled for flotation according to the usual procedure (§D1.2). A charcoal from this deposit produced a radiocarbon date of 751-422 calBC. This matches the radiocarbon results of 734-412 calBC for a randomly selected carbonised barley seed (*Hordeum vulgare*) from the flotation sample (both 95.4% probability; see §D1.3). The deposit contained fragments of a Palace Ware goblet with dimple decoration (registered as vessel 00-06-J01, see §E1).

On top of the deposit Locus:263432:006 was another deposit of light brown soil named Locus:263432:005, and above this, there was another beaten earth floor level (Locus:263432:003), situated c. 161.17 m above sea level (**Fig. D3.4**). The floor was covered by Locus:263432:002, a deposit of dark grey loose soil that was sampled for flota-

tion according to the usual procedure. A charcoal from this context yielded a radiocarbon dating range of 755-482 calBC, while a randomly chosen carbonised *Hordeum vulgare* seed produced a dating of 756-481 calBC (both 95.4% probability; see §D1.3).

The deposit Locus:263432:00 was in turn covered by Locus:263432:001, consisting of about 20 cm of light brown silty soil with chunks of mud fragments, perhaps once parts of a roof construction.

The relative stratigraphy of Room 6 is shown in **Table D3.1**. It is worth emphasising yet again that the two floors lie at a considerably higher altitude than the part of the room excavated in 2002 by SBAH.

Room 6	
Post occupation	Locus:263432:001 mud brick debris
End of Occupation	Locus:262432:002 (two C14 samples) soft silty soil, with plaster pieces from the walls, bones (predominantly human), potsherds
Construction	Phase 2: Locus:263432:003 beaten mud floor
End of Occupation	Locus:263432:005 beige brown silty soil Locus:263432:006 (two C14 samples) reddish brown silty moderately sorted moist loose soil
Construction	Phase 1: Locus:263432:007 beaten mud floor
First construction	Locus:262432:089 wall

Table D3.1: Stratigraphic table of Room 6, in the sondage linked to the 2002 SBAH trench. Prepared by F. Janoscha Kreppner.



Fig. D3.5: Walls Locus:262432:075 and Locus:262432:089 bordering Room 5. Photo by Photo by Tarik Willis.

D3.2 "Room 5"

The procedures for the excavation and sampling in this part of the sondage do not match our usual protocols, and therefore no relative stratigraphy can be offered. The goal was to reach the relative altitude of the floors that the Iraqi excavations had exposed; according to Salim Abdullah Ali who had led the work in 2002, these were the first floor levels encountered.

The corner of Room 5 that was excavated on 21 March 2023 is a small area of about 1.5 m², situated in Squares 262432 and 263432. It is delimited to the west by wall Locus:262432:075 and to the south by wall Locus:262432:089. This wall was observed over a length of c. 2 m and is about 1 m wide at the bottom and about 70 cm at the top (**Fig. D3.5**). On the wall face, there was a plaster layer of about 2 cm in thickness, made of brownish-red clay with pebbles and white inclusions. Because of that plaster, it was not possible to see the individual mudbricks.

A narrow trench was excavated whose eastern edge ran parallel to wall Locus:262432:075 at a distance of 175 cm



Fig. D3.6: The floor Locus:262432:072 of Room 5. Photo by Tarik Willis.

and whose northern edge ran parallel to wall Locus:262432:089 at a distance of 115 cm. The sondage followed the wall plaster down to a floor (Locus:262432:072). This floor consists of a greyish-brown beaten earth surface with some sherds, pebbles and stones embedded in it (**Fig. D3.6**). A piece of charcoal, which was taken directly from the floor, was radiocarbon dated to 1416-1278 calBC (95.4% probability; see **§D1.3**).

The floor level lies at c. 160.05 m above sea level and therefore substantially below the floors identified in “Room 6”. Unlike these floors, it had not been exposed by cleaning but by digging down from the site surface. Although the floor Locus:262432:072 is today situated at a slightly lower altitude than the part of the room excavated in 2002 by SBAH this could be due to the accumulation of material eroded due to rainfall and wind since the area’s first exposure.

Once the floor Locus:262432:072 had been identified in the southwestern corner of the sondage, a 20 cm thick layer of soil on top of the floor was excavated as a unit for sampling (Locus:262432:066), described as consisting of soft brownish soil. The soil taken was divided into two equal parts. Three teams with three workers each led by Andrea Squitieri, Kamal Rasheed Raheem and Salim Abdullah Ali sieved half of the soil using 5 mm sieves, yielding some pottery sherds (none of them chronologically diagnostic: collections AS 262432:066:003 and AS 262432:066:004), bones and further charcoal. The other half of the material was processed in the flotation machine to collect material for palaeobotanical analysis. A randomly selected grain

seed (*triticum sp.*) from Locus:262432:066 was submitted for radiocarbon analysis, producing a dating range of 771-545 calBC (95.4% probability; see **§D1.3**) and thus divided by centuries from the date of the charcoal identified on the floor.

All the soil above Locus:262432:066 was excavated as one excavation unit of a thickness of about 90 cm (across two squares: Locus:262432:056 and Locus:263432:004); it is important to stress that this unit does not represent a locus as otherwise used in the rest of the excavation. It consisted of soft brownish soil with mudbrick debris and, in the upper parts, with a thick concentration of ashes and some spots of reddish soil. The finds are of mixed date, but all substantially later than the material from Locus:262432:066. A complete white glazed miniature amphora (from Locus:262432:056) can be dated to the mid-second to mid-third century AD (AS 263432:004:002 = **§E1.7**) whereas some of the metal items are of likely modern origin (AS 262432:056:006 = **§F, no. 263**; AS 262432:056:007 = **§F, no. 264**; AS 262432:056:009 = **§F, no. 266**; AS 262432:056:010 = **§F, no. 267**).

The layer covering this unit (Locus:262432:056 and Locus:263432:004) and the two walls (Locus:262432:075 and Locus:262432:089) was described as a greyish-brown soil (Locus:262432:010). In it, a terracotta figurine fragment was found, in the shape of a horse’s head and neck (AS 262432:010:006; see **§F, no. 280**).

In 2024, we plan to follow up this initial work with more detailed excavations in “Room 5”, targeting the area immediately north of the 2023 sondage.

E. Pottery from Assur, 2023

E1. From Late Bronze Age to the early Islamic period: the pottery repertoire of the 2023 excavations of Assur

F. Janoscha Kreppner, Jana Richter & Andrea Squitieri

During the field campaign in February and March 2023, pottery was processed by Ellen Coster, F. Janoscha Kreppner, Jana Richter, Susanne Weber, Hero Salih Ahmed (seconded from Sulaymaniyah Directorate of Antiquities and Heritage), as well as Amr Mohammad Jasim, Sakhar Mohammad Ajaj and Omar Laith Allawi from SBAH Sherqat; Britta Irgang supported their work between 6-18 March 2023.

During the study season from 22 October to 5 November 2023, the pottery team was headed by Jana Richter and Andrea Squitieri and consisted of Ellen Coster, Susanne Weber, Amr Mohammad Jasim, Sakhar Mohammad Ajaj and Omar Laith Allawi.

F. Janoscha Kreppner and Ellen Coster selected 45 ceramic samples from the different stratigraphic contexts for petrography and XRF analysis. The pieces were temporarily exported to Germany where Silvia Amicone undertook petrographic analysis at the Competence Center Archaeometry – Baden Wuerttemberg (University of Tübingen) while at LMU Munich, Michaela Schauer oversaw XRF analysis (§E2).

E1.1 Workflow

The pottery workflow as employed in 2023 comprised a series of ten distinct steps to ensure the systematic documentation of all excavated pottery sherds that then underpins all further analysis:

1. Washing. Once the excavated pottery sherds reach the excavation house, the sherd collections are washed and scrubbed by hand in a purpose-built water basin that we constructed in February 2023 just outside the house on the river bank, utilising water pumped up from the Tigris (Fig. B5.7). Weather permitting, the collections are then sun-dried in the nearby pottery yard (German *Scherbengarten*) alongside the eastern wing of the excavation house. In the rainy days of March 2023, the collections had to be moved indoors to the Great Hall for drying.
2. Sorting. Once dry, the sherds are sorted into diagnostic and non-diagnostic categories. In this first season, the diagnostic sherds were further classified based on shapes (e.g., rim, base, handle, decorated body sherds) and also fabrics, to collect samples for the first round of material analyses (petrography and XRF analyses, see §E2).
3. Collection photo. A photo of all diagnostic and non-diagnostic sherds belonging to the same collection, arranged by shape and fabric, is taken in an open-air setting (Fig. B5.6).
4. Labelling. All diagnostic sherds are then labelled on their inner surfaces, using ink applied on a layer of glue. The label incorporates information regarding the square, locus, collection, and individual number of each sherd. In this first season, we registered all this information in full (e.g. AS 262432:061:001:001) but we intend to encode this in a simplified manner in the future to save time and also ink, which is not available locally.
5. Single sherd photo. Each diagnostic sherd is photographed on its own in the indoor photo studio, capturing three images: the inner surface, the outer surface, and the profile.
6. Photo upload. The photos of the sherd collections and the individual sherds are bulk-uploaded onto the project database (§D1.1).
7. Coding. Each diagnostic sherd is described according to a fixed protocol, and a numeric code is assigned to represent its shape. This information is entered into the database. In addition, technological observations are documented in aid of identifying samples suitable for material analyses.
8. Drawing. As long as its state of preservation and shape allows for it, each diagnostic sherd is drawn with a Laser Aided Profiler (LAP) manufactured by the Slovakian company Držik s.r.o. (www.laseraidedprofiler.com; Fig. E1.1). The LAP's two laser modules capture the profile and orientation of the sherd, generating as output SVG files that can be further modified as necessary. This method has two major advantages compared to manual drawing. Firstly, drawing each sherd requires only 3-4 minutes. Secondly, the LAP software generates a drawing database, from which the open-source software package CeraMatch (<https://github.com/demjanp/CeraMatch>) can generate hierarchical clusters of ceramic shapes based on shape similarity identified by

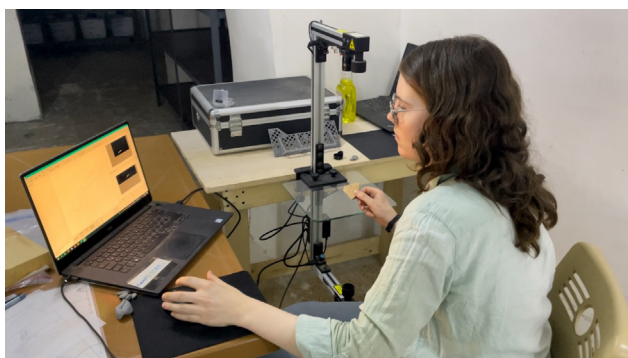


Fig. E1.1: Ellen Coster operating the Laser Aided Profiler (LAP) in the Assur pottery lab in October 2023. Photo by Andrea Squitieri.

the calculation of four metrics, namely diameter, axis, Dice, and rim Dice.¹⁰³

9. 3D modelling. Complete vessels are captured in 3D using the Agisoft Metashape software package. From these 3D models, two-dimensional drawings can be generated as needed using the open-source software framework GigaMesh (<https://gigamesh.eu>), exported as SVG files.
10. Storage. In the final step, the sherds are stored in dedicated areas of the excavation house, packaging diagnostic and non-diagnostic sherds separately in numbered boxes, thus ensuring the organisation, preservation and accessibility of each pottery collection.

E1.2 Pottery from the Parthian chamber tomb (= Grave 1)

Based on radiocarbon dating, the chamber tomb (= Grave 1) can be assigned to the Parthian period (see §D1.3). Most of the pottery remains found on the floors of the tomb consist of fragmented sherds. Only one vessel was unearthened in a complete state of preservation (G01-S05-V01), while two could be restored from fragments (G01-S05-V02 and G01-S09-V02). These three pieces are described below.

Among the sherds collected from the tomb, we were able to identify some shapes that are typical of the Hellenistic/Parthian tradition in northern Mesopotamia, namely simple bowls, fish plates, hole-mouth jars, and craters with offset rims.¹⁰⁴ Moreover, it was possible to

identify sherds belonging to carinated bowls of the local Iron Age tradition, which continued to be attested during the Parthian period. Because a study of the complete pottery inventory of the chamber tomb is the subject of an MA thesis currently being written by Ellen Coster under the supervision of F. Janoscha Kreppner at Münster University, this material is not fully discussed here as it will be published in due course.

In general, the level of fragmentation of the pottery found in the tomb was very high. Only a few joins were made, and the sherds concerned were encountered scattered throughout the tomb so that fragments of the same vessel were in some cases identified at opposite corners of the building. This points to a period of gradual abandonment and looting after the tomb ceased to serve as a burial place. We assume that it was looters or squatters who brought the water jar G01-S05-V01 (see below) into the tomb; that vessel therefore provides a rough date – the Late Sasanian/Early Islamic period – for when the tomb was damaged.

Pottery collections & vessels from floor deposits	Context
AS 262432:019:001	Subdivision 2
AS 262432:020:001	
AS 262432:021:001	Subdivision 3
AS 262432:022:001	Subdivision 4
AS 262432:022:009	
AS 262432:023:001	Southern corridor
AS 262432:024:001	Main corridor
AS 262432:026:001	Subdivision 1
AS 262433:021:001	Subdivision 5
AS 262433:021:006	
AS 262433:022:001	Subdivision 6
AS 262433:023:001	Subdivision 7
AS 262433:024:001	Subdivision 8
AS 262433:025:001	Northern corridor
Vessel G01-S05-V01	Subdivision 5
Vessel G01-S05-V02	Subdivision 5

Reg. number: Vessel G01-S05-V01 (also AS 262433:021:007; **Figs. E1.2a-b**)

Dimensions: max. body D. 55 cm; H. 60 cm; neck D. 23 cm; rim D. 26 cm.

Description: Large vessel with ovoid body, rounded base, straight neck about 8 cm high, and everted rim. Four loop handles connect the shoulders to the neck. The rim surface is decorated with three grooves. The neck and the start of the shoulders are decorated with wavy lines separated by two bands of lines forming small squares. The body is decorated with honeycomb decoration patterns

¹⁰³ Demjàn/Pavúk/Roosevelt 2002, 8: “Dice similarity is a metric based on calculating Dice’s coefficient, where the similarity of two samples is expressed as double their area of overlap, divided by the total area of both samples.”

¹⁰⁴ Hauser 1996, figs. 4a, 4m, 5f, 8.



Fig. E1.2: Water jar G01-S05-V01 = AS 262433:021:007 from the chamber tomb: (a) photo by Ellen Coster; (b) drawing generated by Marco Wolf from the 3D model made in Agisoft Metashape, using the software package GigaMesh.

alternated with vertical lines which cross the vessel's height. At the bottom, the decorative motifs are not preserved.

Comparisons: The vessel was found completely preserved on the floor of Subdivision 5. It was clearly deposited in the tomb at a much later date when it no longer served as a burial place. Vessels similar in shape and decoration have been found at several sites in north and central Iraq,¹⁰⁵ and are dated to the Late Sasanian/ Early Islamic period.¹⁰⁶ Fragments of sherds with comparable wavy lines and honeycomb decoration were reported for Assur's caravanserai.¹⁰⁷



Fig. E1.3: Amphora G01-S09-V02, as reconstructed by Akam Omar Ahmed Al-Qaradaghi from several fragments collected in the chamber tomb: (a) photo by Marco Wolf; (b) drawing generated by Marco Wolf from the 3D model made in Agisoft Metashape, using the software package GigaMesh.

¹⁰⁵ Simpson 1996, 100; Nováček *et al.* 2016.

¹⁰⁶ We are grateful to Dr Mustafa Ahmad (German Archaeological Institute, Berlin) for comparisons and references.

¹⁰⁷ Andrae/Lenzen 1933, pl. 56a-n.

Reg. number: Vessel G01-S09-V02 (**Fig. E1.3**)

Dimensions: body D. 27 cm; base D. 9 cm; H. 33 cm.

Description: The vessel was reconstructed from several fragments found in Subdivisions 1 and 2, and in the south-

ern corridor. It is an amphora with two vertical handles, 15 cm long, consisting of two coils applied together. Next to the handle, two small cones are applied. The rim has a line incised on top, and four under it. About 2 cm under the rim, two knobs are applied, about 2 cm in diameter each. The neck is straight, 11 cm long, with a band incised in the middle of it. The body is bulbous, with a 0.6 cm thick band at the point where the neck and body meet. The lower body of the vessel part is irregularly made so that it does not stand straight. It might be possible that, before the firing process, the vessel was deformed.

Comparisons: A very similar amphora was found during the excavations of the Freie Universität of Berlin, and assigned to Phase II (c. 117 – 198 AD).¹⁰⁸ Two additional similar amphorae were found by Andrae.¹⁰⁹

Reg. number: Vessel G01-S05-V02

Dimensions: D. 12.5 cm; H. 4.7 cm

Description: Small everted bowl with a flat base and vertical rim, reconstructed from joins found in Subdivisions 5 and 10.

E1.3 Pottery from Grave 3

Grave 3 is an inhumation burial deposited underneath an ovoid-elliptic sarcophagus (in German: *Stülpwannen-sarkophag*) with an alphabetic inscription that provides the date July/August 158 BC (§D2.5.1 and §G2). Inside the sarcophagus (for which see §F5 no. 142) and near the skeleton, two complete vessels were found, unlike in the near contemporary Grave 4 which contained no such material.

Reg. number: Vessel G03-V01 (also AS 262433:058:006; **Fig. E1.4**)

Dimensions: H. 4.5 cm; D. 11 cm; base D. 6 cm

Description: Everted bowl with a rounded rim and a disc base. It is covered by a greenish glaze that is not completely preserved.

Reg. number: Vessel G03-V02 (also AS 262433:060:001; **Figs. E1.5a-b**)

Dimensions: H. 20.5 cm; max. body D. 14.5 cm; base D. 7.5 cm

Description: The amphora has a flat everted rim, a narrow conical neck, an ovoid body with two vertical handles and a low disk base. On the shoulders, it has a linear



Fig. E1.4: Bowl G03-V01 = AS 262433:058:006 from Grave 3. Photo by Ellen Coster.



Fig. E1.5: Amphora G03-V02 = AS 262433:060:001 from Grave 3: (a) photo by Ellen Coster; (b) drawing generated by Marco Wolf from the 3D model made in Agisoft Metashape, using the software package GigaMesh.

decoration. The vessel is covered by a glaze whose colour ranges from green to brown.

E1.4 Pottery from Building A

As far as we can say at present, Building A consists of three rooms, Rooms 1, 2 and 3, which were only partially exposed in 2023 (§D2.6). The youngest radiocarbon dates available from charcoal and seeds from the floors of Rooms 1 and 2 indicate a dating to the mid-second to the mid-first century BC (§D1.3). The table below lists the pottery collections from the floor of each room. No complete vessels were found, and so far, none could be restored from the sherds.

¹⁰⁸ Hauser 1996, fig. 6a.

¹⁰⁹ Andrae/Lenzen 1933, pls. 46h, 46k.

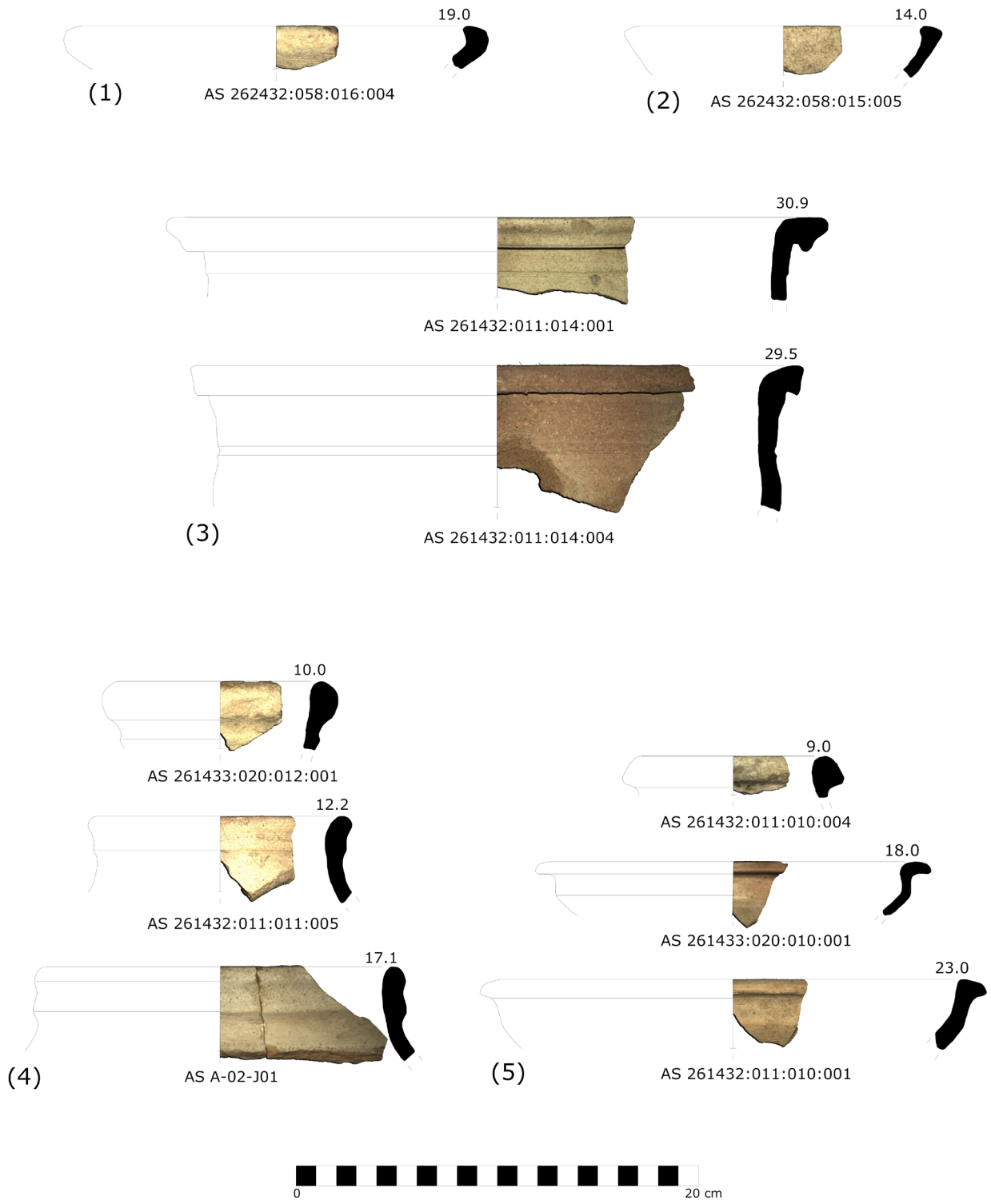


Fig. E1.6: Morphological pottery types from Building A. LAP drawings by Ellen Coster, prepared by Marco Wolf.

Pottery collections from floor deposits	Location
AS 261433:005:001	Room 1
AS 261432:011:010 to 018 AS 261433:020:009 to 016 AS 262433:068:001	Room 2
AS 262432:058:009 to 016	Room 3

The typologically significant pottery sherds collected from the floors of Building A (see below, **Fig. E1.6**) mostly belong to the Hellenistic tradition. Represented are bowls with incurved rims (**Fig. E1.6: 1**),¹¹⁰ bowls with internally thickened rims (**Fig. E1.6: 2**),¹¹¹ craters with offset rims (**Fig. E1.6: 3**),¹¹² jars with rolled-over rims,¹¹³ and jars with thickened rims (**Fig. E1.6: 4**).¹¹⁴ In addition, there are many sherds of carinated bowls that stand firmly in the local Iron Age tradition, which seems to have continued until the second century BC at Assur (**Fig. E1.6: 5**).

E1.5 Pottery from Building B

The pottery from Building B comes from the pits and installations that belong to the occupation phase of Outdoor Area 4 (**§D2.7.2**), for which no radiocarbon dates are currently available. Nevertheless, this building covers and therefore certainly postdates Grave 5, which was radiocarbon dated to 770-542 calBC (95.4 % probability; **§D1.3**). Based on the evidence of the pottery discussed here, the use of Outdoor Area 4 floor can be assigned with confidence to the late Neo-Assyrian period. As its floor covered Grave 5, a date to the early 8th century or even earlier BC for the use of the floor can be excluded.

The following pottery collections belong to the occupation level of Outdoor Area 4: AS 262432:050:001, AS 262432:061:001, AS 262432:068:001, AS 262433:062:001, and AS 262433:063:001.

The typologically diagnostic pottery sherds from these collections belong to the Iron Age tradition (see below, **Fig. E1.7**). Simple bowls are attested, with different types of rims, including a type of brim rim which is typical of the Iron Age and is commonly found in Assur and other Neo-Assyrian period sites (**Fig. E1.7: 1-2**).¹¹⁵ Also present in the assemblage are carinated bowls of different types,

which constitute another staple of the Neo-Assyrian period tradition (**Fig. E1.7: 3**). Based on Stefano Anastasio's classification scheme,¹¹⁶ we can preliminarily identify the following:

- carinated bowls of the Middle Assyrian tradition, which continued into the Iron Age;
- carinated bowls with undercut rims;
- carinated bowls with flaring rims;
- carinated bowls with straight and slanting rims; and
- carinated bowls with sharp-cut lips.

This is the entire range of carinated bowl types of the Iron Age in Assyria. All these types are already known from previous excavations in Assur.¹¹⁷ They continue to be attested in northern Mesopotamia after the collapse of the Assyrian Empire, as evidenced by the pottery repertoire of the "Red House" in Dur-Katlimmu (Tell Sheikh Hamad), situated across the Djezira on the Khabur river.¹¹⁸

Some sherds from Building B belong to large open vessels whose rim diameter can reach over 30 cm (**Fig. E1.7: 4**); such pieces are often called craters, after the Greek pottery nomenclature. In our assemblage, these vessels can have different types of rims, and all these types are attested in sites dating to the Neo-Assyrian period or the post-Assyrian period.¹¹⁹ Only one rim sherd is markedly different, as its fabric was tempered with minerals (**Fig. E1.7: 5**). Several rim sherds belong to closed shapes and can be assigned to bottles or jars of types that are also but not exclusively attested in the Iron Age tradition (**Fig. E1.7: 6-7**).¹²⁰

Whereas this section is concerned with pottery coming from the occupation phase of Outdoor Area 4, a complete vessel found in the collapse above the floor level is worth mentioning:

Reg. number: Vessel B-04-Vo1 (also AS 262432:047:002; **Fig. E1.8**)

Dimensions: max. D. 8 cm; H. 9 cm.

Description: Almost complete beaker with a straight body that ends in a straight rim. It has a nipple base, with a diameter of 1.4 cm. The outside surface is greenish and reddish. On the inside, cracks are visible surrounded by black colour.

¹¹⁰ For comparisons, see Gavagnin/Iamoni/Palermo 2016, fig. 20.1-6; Macginnis *et al.* 2020, fig. 19k.

¹¹¹ For comparisons, see Hauser 1996, fig. 5b.

¹¹² For comparisons, see Gavagnin/Iamoni/Palermo 2016, fig. 22.11.

¹¹³ For comparisons, see Gavagnin/Iamoni/Palermo 2016, fig. 22.1-4.

¹¹⁴ For a comparison, see Hauser 1996, fig. 5g.

¹¹⁵ Anastasio 2010, 34; Hausleiter 2010, pl. 55.

¹¹⁶ Anastasio 2010, 36-41.

¹¹⁷ Hausleiter 2010.

¹¹⁸ Kreppner 2006.

¹¹⁹ Anastasio 2010, pl. 18-19.

¹²⁰ Anastasio 2010, pl. 29.

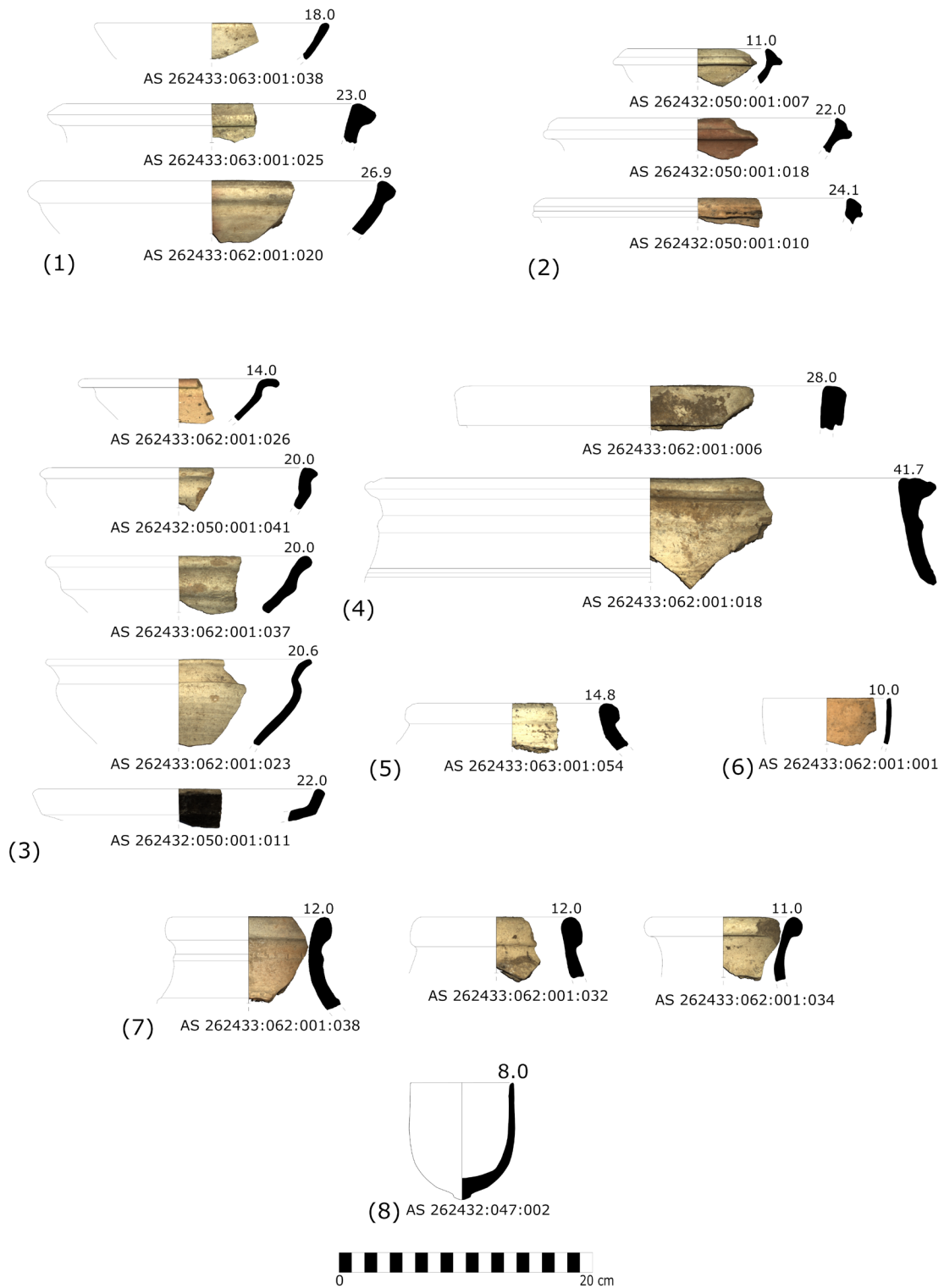


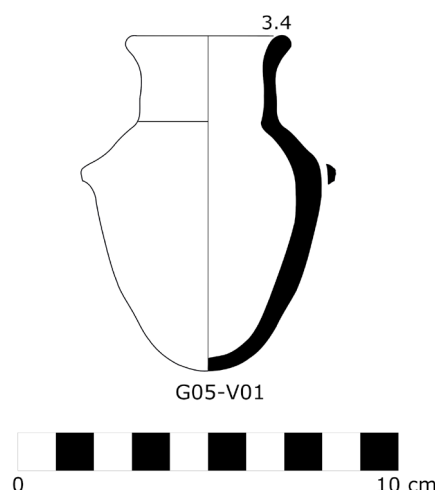
Fig. E1.7: Morphological pottery types from Building B. LAP drawings by Ellen Coster, prepared by Marco Wolf.



Fig. E1.8: Beaker B-04-V01 = AS 262432:047:002 from the collapse above Building B. Photo by Ellen Coster.



Fig. E1.9: Miniature jar G05-V01 = AS 262432:070:005 from Grave 5: (a) photo by Ellen Coster; (b) drawing generated by Marco Wolf from the 3D model made in Agisoft Metashape, using the software package Giga-Mesh.



Comparisons: This vessel type is commonly found in Assur and other Neo-Assyrian sites, and in Tell Sheikh Hamad also in the post-Assyrian context.¹²¹

E1.6 Pottery from Grave 5

Grave 5 was a disturbed inhumation grave located just beneath the floor of Outdoor Area 4 (§D2.8). Two teeth from the burial could be radiocarbon-dated and produced dating ranges of 770-542 calBC (95.4% probability) and 775-545 calBC (95.4% probability; §D1.3). The grave had an upper and a lower fill.

The only complete vessel found in this grave comes from the upper fill, and can be dated to the late Neo-Assyrian period:

Reg. number: Vessel G05-V01 (= AS 262432:070:005; **Fig. E1.9a-b**)

Dimensions: rim D. 4 cm; neck D. 3 cm; body max. D. 5.4 cm; H. 8.7 cm.

Description: Miniature jar with a rounded base, an ovoid body, two small perforated handles attached at the shoulder level, and a cylindrical neck ending with a slightly everted rim. The neck and the rim are covered by a reddish glaze. About 0.7 cm below the neck, a band formed of reddish-glazed triangles runs around the jar's body. Below this, one greenish band is present followed by a

reddish band, below which a greenish glaze starts again and covers the base.

Comparisons: Parallels suggest a late Neo-Assyrian date for this jar.¹²²

In addition to this vessel, the grave's upper fill yielded sherd fragments of the rim of a large closed vessel (registered as collection AS 262432:070:003). A few centimetres underneath the thickened rim, there is a ridge decoration. The rim's maximum diameter is about 40 cm. From the same pottery collection, several fragments belonging to a second vessel were identified whose base measures 7 cm in diameter.

The grave's upper fill also yielded some additional fragmentary sherds that were registered separately as the pottery collection AS 262432:070:001. Among these pieces were a nipple base and rims of several carinated bowls, representing the Iron Age chronological horizon.

The disturbed grave's lower fill yielded an unexpectedly high quantity of sherds (collection AS 262432:071:001) compared to the upper fill. About 130 diagnostic sherds were identified in this collection and these represent not only Iron Age shapes but also typical Late Bronze Age shapes. This mix of Late Bronze Age and Iron Age pottery sherds is likely the result of whatever activity caused the burial to be disturbed in the first place.

¹²¹ Anastasio 2010, 171, nos. 6-8; Kreppner 2006, pl. 91.1; Hausleiter 2010, pls. 12w, 27l, 50a.

¹²² Hausleiter 2010, pl. 9: Ass 2482a.

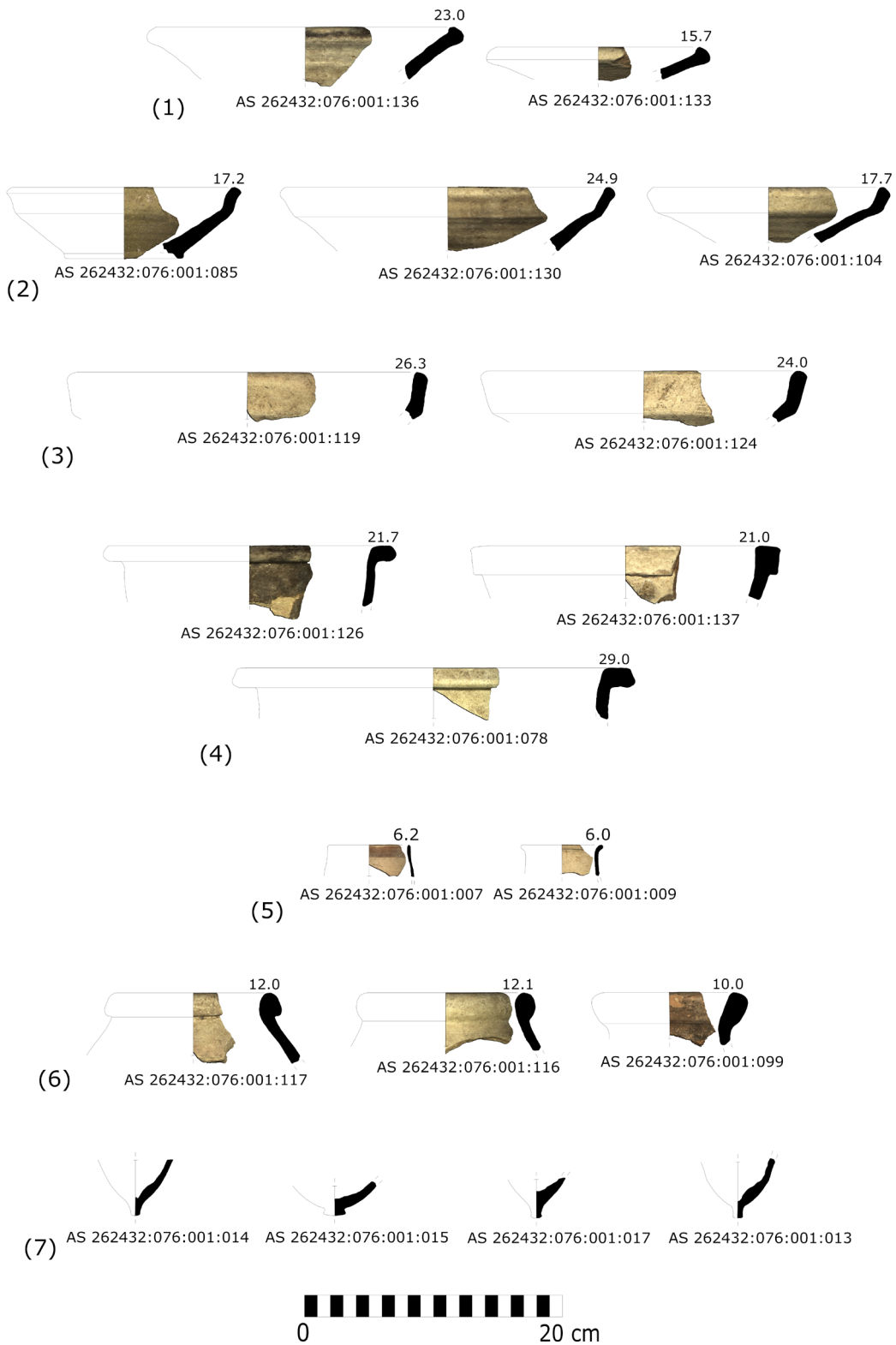


Fig. E1.10: Morphological pottery types from the deep sounding below Grave 5. LAP drawings by Ellen Coster, prepared by Marco Wolf.

E1.7 Pottery from the deep sounding below Grave 5

The deep sounding was opened below Grave 5, with the explicit objective of reaching the virgin soil (§D2.10). The fill of the sounding yielded many pottery sherds (collection AS 262432:076:001), among which 191 were identified as diagnostic.

Typologically, the sherds belong to the Late Bronze Age chronological horizon, with many clearly belonging to the Middle Assyrian tradition (see below, Fig. E1.10). We were able to identify fragments representing the entire range of the Middle Assyrian pottery repertoire from the 13th to the early 11th century BC as described by Peter Pfälzner for northern Mesopotamia in the Late Bronze Age:¹²³

- bowls with a conical body (German *konische Schale*) (Fig. E1.10: 1);
- carinated bowls (German *Knickwandschale*) with a slight carination (Fig. E1.10: 2);
- carinated bowls with a strong carination (Fig. E1.10: 3);
- deep bowls (German *Schüssel*) (Fig. E1.10: 4);
- beakers (German *Becher*) (Fig. E1.10: 5);
- bottles (German *Flasche*) (Fig. E1.10: 6);
- large vessels (German *Großgefäß*); and
- bases (German *Gefäßfuß*) of the following types: nipple, angular button, disc, and knob base (Fig. E1.10: 7).

At the bottom of this fill, where the virgin soil was reached, a pit was identified cutting into the virgin soil. From there, a piece of charcoal (AS 262432:079:003) was collected and radiocarbon dated to 1506-1440 calBC (95.4% probability; see §D1.3). This dating range provides a *terminus post quem* for the pottery repertoire collected from the fill of the sounding above.

E1.8 Pottery from the sondage linked to the 2002 SBAH trench

The corners of two rooms named “Room 5” and “Room 6” were excavated in a sondage opened in the baulk dividing our NT1 2023 trench and the 2002 SBAH trench (§D3). Both rooms were only partially investigated, as they are situated within the building that had been excavated by the Iraqi team.

“Room 5”

The floor of “Room 5” yielded a charcoal sample that was radiocarbon dated to 1416-1278 calBC whereas the radio-

carbon date derived from a carbonised seed was 771-545 calBC (95.4% probability; see §D1.3). The floor deposit yielded only a few pottery sherds, none of which could be identified as chronologically significant.

However, in the upper layer of the room’s fill (Locus: 262432:004), a complete miniature amphora was found that can be dated to the Parthian period. That the upper fills of this room accumulated over a longer time is confirmed also by the small finds retrieved from the room’s fills, several of which are of late date (§F12.1).

AS number: Vessel 00-05-V01 (= AS 263432:004:002; Fig. E1.11a-b)

Dimensions: H. 9.5 cm

Description: White glazed miniature amphora. The vessel has a low foot with concave sides and a flat base, and a slightly ovoid body with two handles starting from the shoulders and ending at the neck. The latter is cylindrical and ends with a flat everted rim. The glaze is shiny, white-greenish, chipped off in the lower part. Parts of the rim are broken off.

Comparisons: A similar amphora, but 22.8 cm tall and with a white-blue glaze, was found at Assur by the team of the Free University of Berlin headed by Reinhard Dittmann in 1988. This was assigned to “Phase II” and dated to the mid-second century AD to the mid-third century AD.¹²⁴

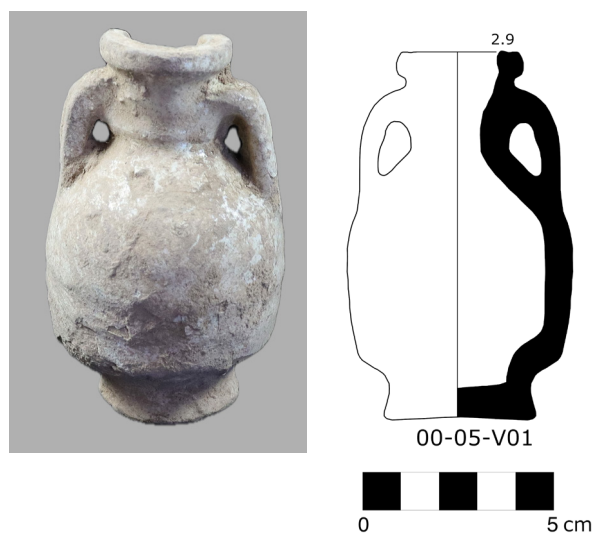


Fig. E1.11: Miniature amphora 00-05-V01 = AS 263432:004:002 from the upper layers of “Room 5”: (a) photo by Ellen Coster; (b) drawing generated by Marco Wolf from the 3D model made in Agisoft Metashape, using the software package GigaMesh.

¹²³ Pfälzner 1995, 59-70.

¹²⁴ Hauser 1996, fig. 6d.

“Room 6”

In “Room 6”, two subsequent floor levels were exposed at an elevation substantially higher than that of the floor of “Room 5” (for details, see §D3). Each was dated by the radiocarbon analysis of pieces of charcoal found above the floors to 751-422 calBC and 755-482 calBC, respectively, while two carbonised seeds from the lower floor produced the date ranges 756-481 calBC and 734-412 calBC (all 95.4% probability).

Several pottery fragments found on the lower-lying floor could be joined to reconstruct an almost complete vessel. This goblet is made of the so-called Assyrian Palace Ware, which matches the date provided by the radiocarbon analysis well.

AS number: Vessel 00-06-J01 (Fig. E1.12)

Dimensions: max. body D. 13 cm; base D. 2 cm; H. 13 cm

Description: Almost complete vessel, reconstructed from several joins, with a small button base, a tapered body, and a high neck (4 cm) ending with a slightly everted rim. The neck is marked in the middle by a ridge and the body shows a series of dimples as decoration. The photo shows a preliminary reconstructed state, and the vessel is currently undergoing final restoration by Akam Omar Ahmed Al-Qaradaghi.

Comparisons: This is a typical Palace Ware goblet, characteristic of the Neo-Assyrian period.¹²⁵

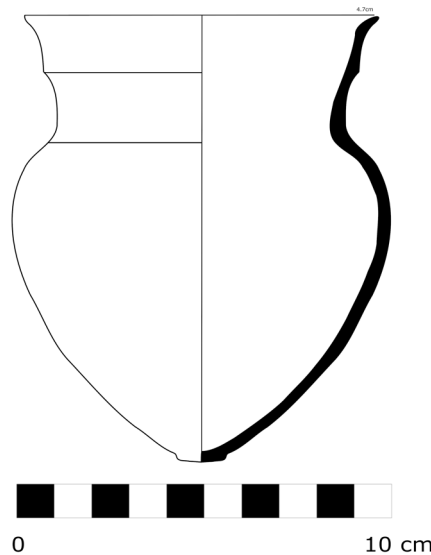


Fig. E1.12: Palace ware goblet 00-06-J01, as reconstructed by Akam Omar Ahmed Al-Qaradaghi from several fragments found on the lower floor of “Room 6”: (a) photo by Marco Wolf; (b) drawing generated by Marco Wolf from the 3D model made in Agisoft Metashape, using the software package GigaMesh.

E2. First steps towards a fabric classification for Assur: portable X-ray fluorescence (p-XRF) and petrographic analysis of Assur pottery, 2023

Michaela Schauer & Silvia Amicone

The study of pottery paste recipes and their distribution over time and space allows us to trace technological traditions connected to the selection and procurement of raw materials. In this chapter, we present the results of the portable X-ray fluorescence (p-XRF) and petrographic analysis carried out on 61 pottery fragments unearthed during the archaeological excavations undertaken at the New Town of Assur in 2023. These are part of 63 samples selected by F. Janoscha Kreppner and Ellen Coster in order to represent the main pottery fabrics as they had been preliminarily identified during the first field season through macroscopic observation with the naked eye, from the different chronological and stratigraphic contexts. Consequently, the fabrics discussed in this chapter cover materials from the Middle Assyrian, the Neo-Assyrian, the Hellenistic and the Parthian periods. Once exported to Germany, the samples were analysed by using an integrated approach that includes both portable X-ray fluorescence and ceramic petrography. Two samples had to be removed from the study for methodological reasons (as explained below, §E2.1), resulting in a dataset of 61 samples.

E2.1 Methodology and dataset

The dataset of 61 samples consists of pottery fragments assigned to four periods (Table E2.1). 14 samples (23%) were recovered from the floor of the chamber tomb and therefore assigned to the Parthian period (§D2.3). 11 samples (18%) were found in Building A, on the floors of Rooms 1 (7 samples), 2 (3 samples) and 3 (1 sample) and therefore classified as Hellenistic (§D2.6). 16 samples (26%) come from the floor of Unroofed Area 4 of Building B, and this pottery can be assigned to the Neo-Assyrian period (§D2.7). 20 samples (33%) come from the deep sounding and are typologically

¹²⁵ Anastasio 2010, pl. 28.1-2.

Period and context	Sample size (N)
Middle Assyrian	20
Deep sounding	20
Neo-Assyrian	16
Unroofed area 4 (floor)	16
Hellenistic	11
Building A Room 1 floor 1	7
Building A Room 1 floor 2	3
Building A Room 1 floor 3	1
Parthian	14
chamber tomb (floor)	14
Total	61

Table E2.1: List of the pottery samples selected from Assur in 2023 (n=61), with information on periods and stratigraphic contexts.

classifiable as Middle Assyrian (§D2.10). This dataset was analysed by p-XRF and petrography.

Portable X-ray fluorescence (p-XRF) is a method of determining the bulk chemistry on an elemental basis of a wide variety of materials including pottery, metals, stones or soils.¹²⁶ To identify the chemical composition, p-XRF uses the characteristic X-rays emitted by the atoms in the sample when exposed to the primary X-rays produced by the instrument.¹²⁷ A detector collects the information, while manufacturer-specific software identifies and quantifies it.¹²⁸ p-XRF is widely used in archaeometry as a quick, time and cost-effective screening method to characterise the chemical composition of pottery to understand production methods, raw material use, exchange and distribution networks. Samples can be easily analysed in the field, museum or laboratory. As the instrument can travel to the site or sample location, the results can be

discussed directly with the researcher and incorporated into the decision-making process of a project to achieve the researcher's objectives.¹²⁹ In the case of this project, however, the analysis took place at LMU Munich after the samples had been exported from Iraq.

The data for the chemical case study of the 2023 pottery samples from Assur was collected with a Niton XL3t (serial no. 97390) owned by LMU Munich's Department für Kulturwissenschaften und Altertumskunde. Three measurements were taken per sample at different parts of a fresh break using the TestAllGeo mode with an 8 mm collimator and a measurement time of 300 seconds (60 seconds for main, low, and high, 120 seconds for light filter). Only fragments of a sensible size with at least a total of 2.8 cm of fresh break were included. Therefore, only 62 samples were analysed. Sampling and data collection were performed by Marco Wolf from 9 to 11 August 2023 (temperatures of 28-35° C; relative humidity of 35-42 %) while Michaela Schauer carried out data processing and interpretation.¹³⁰

The data given by the device after its internal data processing, i.e. the analytical data, forms the basis for this study.¹³¹ As a first step in data processing, all samples are routinely checked for too-high standard deviation (value \leq sd 2 σ) and variation coefficients (= varcoef; value \leq 20%). Samples are excluded when more than 20% of the elements used show too-high varcoefs. Chemical elements for which less than 20% of samples have too-high variation coefficients and which can be corrected by a coefficient correction are considered to be reliable: SiO₂, TiO₂, Al₂O₃, Fe₂O₃, MnO, CaO, K₂O, V, Ni, Zn, Rb, Sr, Y, Zr, Nb.

As a consequence, one pottery sample exported from Assur had to be excluded, resulting in a dataset of 61 samples in total. Following that, quantitative values were calculated using coefficient correction IV (= coefcor IV) which was created following the Munich Procedure.¹³² Data interpretation was based on the analysis of individual scatter plots of chemical elements for each sample (for a summary of the results see **Table E2.2**). The multivariate plots presented in **Figs. E2.1-2** and **Fig. E2.4** are meant to visualise the overall results concisely and comprehensively.

After performing the p-XRF analysis, the 2023 pottery samples from Assur were brought to Tübingen where

¹²⁶ Potts 2008; Liritzis/Zacharias 2011; Shackley 2012; Johnson 2014; Neff/Voorhies/Umaña 2014; Shugar/Mass 2014.

¹²⁷ Pollard *et al.* 2007; Shackley 2011; Meschede 2015; Tipler *et al.* 2019.

¹²⁸ Liritzis/Zacharias 2011. All p-XRF manufacturers have their quantification algorithms, and only some provide additional actual raw data as intensities (e.g. Speakman/Little/Creel 2011; Helfert 2013; Aimers/Farthing/Shugar 2014; Wilke/Rauch/Rauch 2016; Bezur/Lee/Loubster 2020; Eslami/Wicke/Rajabi 2020).

¹²⁹ Peacock 1970; Potts 2008; Frahm/Doonan 2013; Shugar/Mass 2014; Ferguson 2014.

¹³⁰ As detailed in Schauer 2023a; 2024.

¹³¹ This is due to the fact that the device has not been set up by the producer to export raw data.

¹³² On this, see Schauer 2023b; 2024.

Sample ID	Registration no.	Context	Period	Petrofabric	Chemical group	SiO2	TiO2	Al2O3	Fe2O3	MnO	CaO	K2O	V	Ni	Zn	Rb	Sr	Y	Zr	Nb
AS01	AS 262432.022.001.014	Chamber Tomb (floor)	Parthian	1A	Parthian pottery	49.6	0.6	17.0	6.2	0.2	14.5	1.3	119	348	429	34	730	32	125	13
AS02	AS 262432.022.009.050	Chamber Tomb (floor)	Parthian	1B	Parthian pottery	50.7	0.5	18.4	6.4	0.1	12.2	2.1	99	229	101	78	456	28	112	13
AS04	AS 262433.021.001.026	Chamber Tomb (floor)	Parthian	2A	Parthian pottery	52.1	0.6	18.2	5.8	0.1	12.1	2.3	115	234	327	82	620	27	122	14
AS05	AS 262433.023.001.034	Chamber Tomb (floor)	Parthian	2A	Parthian pottery	53.0	0.6	14.8	6.6	0.1	13.8	2.0	109	181	78	47	440	27	140	14
AS06	AS 262432.022.009.052	Chamber Tomb (floor)	Parthian	3A	Parthian pottery	52.3	0.6	16.2	7.4	0.2	13.1	2.1	114	221	92	43	392	29	132	16
AS07	AS 262432.022.009.053	Chamber Tomb (floor)	Parthian	2B	Parthian pottery: outlier 7	55.0	0.7	16.6	6.9	0.2	11.8	2.9	119	150	123	66	736	31	159	18
AS08	AS 262433.023.001.035	Chamber Tomb (floor)	Parthian	4A	Parthian pottery	51.6	0.6	16.0	6.3	0.1	14.2	1.6	100	202	93	43	404	29	121	15
AS09	AS 262433.023.001.036	Chamber Tomb (floor)	Parthian	3B	Parthian pottery: outlier 6	52.3	0.8	15.2	7.6	0.2	14.8	2.7	124	186	107	81	310	33	186	20
AS10	AS 262433.023.001.037	Chamber Tomb (floor)	Parthian	4A	Parthian pottery	51.4	0.6	15.3	6.1	0.1	15.2	1.5	92	187	85	54	328	28	129	15
AS11	AS 262433.023.001.038	Chamber Tomb (floor)	Parthian	4B	Parthian pottery	52.2	0.6	15.9	6.3	0.1	13.5	2.0	107	177	93	60	452	29	136	16
AS12	AS 262432.021.001.036	Chamber Tomb (floor)	Parthian	3A	Parthian pottery	53.2	0.7	12.9	7.1	0.1	14.2	2.5	104	186	95	46	499	27	132	14
AS13	AS 262432.022.009.054	Chamber Tomb (floor)	Parthian	4B	Parthian pottery	59.6	0.6	13.5	6.5	0.1	10.1	2.6	96	168	63	60	316	23	107	13
AS14	AS 262432.022.001.015	Chamber Tomb (floor)	Parthian	4B	Parthian pottery	53.7	0.6	13.8	5.8	0.1	13.5	2.2	106	155	65	47	465	24	116	12
AS15	AS 262433.023.001.039	Chamber Tomb (floor)	Parthian	4B	Parthian pottery	52.6	0.7	13.7	7.5	0.1	13.2	2.6	107	237	75	60	357	24	100	12
AS16	AS 262432.050.001.068	Unroofed Area 4 (floor)	Neo-Assyrian	1B	Neo-Assyrian pottery: cluster 2	55.8	0.7	15.7	5.8	0.1	10.2	3.6	110	154	107	65	666	28	127	13
AS17	AS 262433.063.001.056	Unroofed Area 4 (floor)	Neo-Assyrian	1B	Neo-Assyrian pottery: cluster 1	50.1	0.7	17.0	6.5	0.1	14.1	1.8	116	207	91	55	419	31	128	15
AS18	AS 262432.050.001.069	Unroofed Area 4 (floor)	Neo-Assyrian	2D	Neo-Assyrian pottery: cluster 2	50.2	0.6	18.1	5.9	0.1	12.2	2.5	134	245	83	83	754	29	154	16
AS19	AS 262432.050.001.070	Unroofed Area 4 (floor)	Neo-Assyrian	1B	Neo-Assyrian pottery: cluster 1	51.9	0.6	16.7	5.8	0.1	14.8	1.3	95	172	109	35	552	26	134	16
AS20	AS 262432.050.001.071	Unroofed Area 4 (floor)	Neo-Assyrian	1B	Neo-Assyrian pottery: cluster 2	54.0	0.7	17.2	6.5	0.1	10.1	2.6	100	207	79	71	429	29	131	14
AS21	AS 262432.050.001.072	Unroofed Area 4 (floor)	Neo-Assyrian	1B	Neo-Assyrian pottery: outlier 2	43.5	0.6	9.5	7.1	0.2	27.5	2.6	91	174	84	63	642	28	128	15
AS22	AS 262432.050.001.073	Unroofed Area 4 (floor)	Neo-Assyrian	2A	Neo-Assyrian pottery: outlier 2	52.0	0.6	13.6	6.6	0.1	17.6	2.2	87	160	66	56	547	26	127	14
AS23	AS 262432.050.001.074	Unroofed Area 4 (floor)	Neo-Assyrian	2A	Neo-Assyrian pottery: cluster 2	55.2	0.6	14.7	6.2	0.1	12.5	2.9	107	161	157	76	497	27	155	15
AS24	AS 262432.050.001.075	Unroofed Area 4 (floor)	Neo-Assyrian	2A	Neo-Assyrian pottery: cluster 1	50.4	0.5	16.0	6.1	0.1	15.4	1.7	100	208	73	44	525	25	123	14
AS25	AS 262432.050.001.076	Unroofed Area 4 (floor)	Neo-Assyrian	2C	Neo-Assyrian pottery: outlier 5	53.6	0.7	12.9	5.5	0.1	19.1	2.4	100	119	95	49	421	27	159	14
AS26	AS 262432.050.001.077	Unroofed Area 4 (floor)	Neo-Assyrian	2B	Neo-Assyrian pottery: cluster 1	54.7	0.6	17.2	7.0	0.1	7.9	3.0	103	248	121	83	426	26	136	15
AS31	AS 262432.050.001.081	Unroofed Area 4 (floor)	Neo-Assyrian	3A	Neo-Assyrian pottery: cluster 1	51.4	0.6	14.4	7.1	0.1	16.7	1.6	102	193	88	42	476	27	130	15
AS32	AS 261433.005.001.045	Building A Room 1 floor	Hellenistic	1A	Hellenistic floor 1 pottery	49.7	0.6	18.5	6.9	0.1	11.4	2.2	118	250	81	64	283	28	141	17
AS33	AS 261433.005.001.046	Building A Room 1 floor	Hellenistic	2A	Hellenistic floor 1 pottery	52.4	0.6	16.0	5.6	0.1	12.4	2.9	112	217	138	58	521	25	111	13
AS34	AS 261433.005.001.047	Building A Room 1 floor	Hellenistic	2A	Hellenistic floor 1 pottery	53.2	0.6	15.5	6.7	0.1	12.1	2.9	98	201	79	87	431	27	156	15
AS35	AS 261433.005.001.048	Building A Room 1 floor	Hellenistic	1B	Hellenistic floor 2 pottery	48.2	0.6	16.6	6.3	0.1	16.9	1.0	108	221	88	28	545	29	151	18
AS36	AS 261432.011.013.005	Building A Room 1 floor	Hellenistic	2A	Hellenistic floor 1 pottery	52.3	0.5	15.2	5.7	0.1	15.3	2.4	89	207	69	50	563	25	143	13
AS37	AS 261433.005.001.049	Building A Room 1 floor	Hellenistic	2A	Hellenistic floor 1 pottery	57.5	0.6	13.6	5.5	0.1	12.3	3.2	102	145	69	53	369	22	97	11
AS38	AS 261432.011.013.006	Building A Room 1 floor	Hellenistic	4A	Hellenistic floor 2 pottery	54.0	0.6	15.6	6.0	0.1	14.0	1.3	111	207	77	31	418	27	113	13
AS39	AS 261432.011.013.007	Building A Room 2 floor	Hellenistic	4A	Hellenistic floor 2 pottery	53.5	0.6	14.0	6.5	0.1	13.5	2.9	105	160	73	55	391	26	109	13
AS40	AS 261433.005.001.050	Building A Room 2 floor	Hellenistic	4A	Hellenistic floor 1 pottery	54.2	0.7	10.9	6.7	0.1	16.2	3.1	88	149	79	54	363	22	118	12
AS42	AS 261433.005.001.051	Building A Room 3 floor	Hellenistic	3A	Hellenistic floor 3 pottery	52.2	0.6	13.0	7.8	0.2	13.8	2.0	104	194	77	28	326	29	148	17
AS43	AS 262432.058.015.004	Building A Room 3 floor	Hellenistic	1B	Middle-Assyrian pottery: outlier 1	47.3	0.6	18.2	6.6	0.1	14.9	1.1	137	349	172	39	337	30	132	16
AS44	AS 262432.076.001.058	Sounding fill	Middle Assyrian	1A	Middle-Assyrian pottery	52.3	0.4	17.8	6.4	0.1	13.3	1.3	88	187	68	40	509	28	129	14
AS45	AS 262432.076.001.059	Sounding fill	Middle Assyrian	1A	Middle-Assyrian pottery	50.8	0.7	14.9	7.5	0.2	16.1	2.5	107	181	84	67	475	28	118	15
AS46	AS 262432.076.001.060	Sounding fill	Middle Assyrian	1B	Middle-Assyrian pottery	52.9	0.6	14.8	7.3	0.2	13.4	2.8	97	168	71	75	454	28	165	16
AS47	AS 262432.076.001.061	Sounding fill	Middle Assyrian	2A	Middle-Assyrian pottery	51.2	0.6	18.0	6.5	0.1	12.4	2.4	127	266	90	80	468	29	128	15
AS48	AS 262432.076.001.062	Sounding fill	Middle Assyrian	1B	Middle-Assyrian pottery	49.8	0.6	15.5	6.9	0.1	15.7	2.8	100	218	101	79	778	30	177	16
AS49	AS 262432.076.001.063	Sounding fill	Middle Assyrian	1B	Middle-Assyrian pottery	51.3	0.5	16.4	5.8	0.1	16.4	1.1	92	168	84	30	675	27	143	15
AS50	AS 262432.076.001.064	Sounding fill	Middle Assyrian	1B	Middle-Assyrian pottery	53.2	0.6	16.8	6.3	0.1	11.3	2.7	97	188	85	73	390	27	103	15
AS51	AS 262432.076.001.065	Sounding fill	Middle Assyrian	1B	Middle-Assyrian pottery	51.9	0.6	14.4	5.8	0.1	16.7	1.9	103	156	82	43	633	28	142	15
AS52	AS 262432.076.001.066	Sounding fill	Middle Assyrian	2A	Middle-Assyrian pottery	49.5	0.6	13.0	6.7	0.1	20.7	2.0	80	124	76	63	458	29	126	15
AS53	AS 262432.076.001.067	Sounding fill	Middle Assyrian	2A	Middle-Assyrian pottery	54.8	0.6	13.3	6.3	0.1	15.3	3.0	84	161	261	66	450	24	110	12
AS54	AS 262432.076.001.068	Sounding fill	Middle Assyrian	2B	Middle-Assyrian pottery	51.9	0.6	14.6	6.7	0.1	16.2	1.9	98	179	79	47	453	29	151	15
AS55	AS 262432.076.001.069	Sounding fill	Middle Assyrian	2A	Middle-Assyrian pottery	52.9	0.6	15.7	6.6	0.1	14.0	2.0	103	191	92	59	429	28	128	14
AS56	AS 262432.076.001.070	Sounding fill	Middle Assyrian	2A	Middle-Assyrian pottery	52.6	0.7	13.5	6.2	0.1	17.0	3.3	108	141	85	70	451	25	156	13
AS57	AS 262432.076.001.071	Sounding fill	Middle Assyrian	2C	Middle-Assyrian pottery	50.2	0.6	12.3	6.1	0.1	19.8	2.1	90	160	67	52	610	24	123	13
AS58	AS 262432.076.001.072	Sounding fill	Middle Assyrian	2A	Middle-Assyrian pottery	53.6	0.6	14.6	5.9	0.1	15.6	2.1	95	144	72	58	490	26	128	13
AS59	AS 262432.076.001.073	Sounding fill	Middle Assyrian	4A	Middle-Assyrian pottery	54.2	0.7	14.2	7.1	0.2	14.4	2.7	101	131	93	80	374	29	137	16
AS60	AS 262432.076.001.074	Sounding fill	Middle Assyrian	4B	Middle-Assyrian pottery	52.2	0.6	13.8	6.4	0.1	16.3	3.0	105	171	88	76	556	26	138	14
AS61	AS 262432.076.001.075	Sounding fill	Middle Assyrian	2B	Middle-Assyrian pottery	54.3	0.7	15.5	6.7	0.1	13.0	2.8	111	174	87	76	388	27	132	17
AS62	AS 262432.076.001.076	Sounding fill	Middle Assyrian	4B	Middle-Assyrian pottery	57.7	0.6	13.2	6.1	0.1	12.5	2.6	101	153	82	48	215	22	94	11

Table E2.2: Results of the chemical analysis, with the petrographic fabric groups indicated in the column "Petrofabric".

they underwent petrographic analysis at the Competence Center for Archaeometry Baden-Württemberg (CCA-BW) of Tübingen University. The petrography of archaeological ceramics entails the description, classification, and interpretation of ceramic pastes or fabrics, adopting techniques that are derived from those used in geology and soil micromorphology to describe rocks and soils. This method allows researchers to gain insights into different technological aspects (e.g., forming technique and tempering) and helps to define raw material sources employed in pottery manufacturing.¹³³

Once the exported pottery sherds reached Tübingen, thin section samples were prepared by Johannes Seidler. Firstly, a slice from the vertical cross-section of each sherd was cut. After having been consolidated with an epoxy resin, these sections were lapped with silica powder (600 grain size) and pasted over a glass slide. The samples were then ground to approximately 40 µm using a Buehler PetroThin thin-sectioning system. Finally, they were brought to c. 20–30 µm thickness, again using silica powder (600 to 900 grain size) and covered with a removable transparent varnish. The thin sections were then studied by Silvia Amicone under a polarising microscope (Leica DM2500 P) to identify the compositional and technological characteristics of the materials under investigation.

E2.2 Results of the p-XRF analysis

When analysing the chemical composition of the samples in the individual scatter plots, there is no clear distinction between samples assigned to the four different period groups (described in §E2.3). Also, the application of multivariate analyses, namely Principal Component Analysis (PCA), which highlights the similarities in the chemical composition of the samples,¹³⁴ and Discriminant Analysis (DA), which stresses the differences,¹³⁵ did not produce different results either (Fig. E2.1).¹³⁶

For PCA, according to the Camargo test statistic, three principal components (PCs) are significant, explaining 64% of the total variation, thereby exceeding the necessary benchmark of 60%. For illustrative purposes, PC1 (27%) and PC2 (19%) are used. For PC1, significance loadings are given for SiO₂, Fe₂O₃, MnO, V, Ni, Y, Zr and Nb, and for PC2, for TiO₂, Al₂O₃, Fe₂O₃, MnO, K₂O and Ni.¹³⁷

For DA, the first discriminant functions (DF), using chronological phases as grouping variable, account for 52% of the total variation with SiO₂, K₂O, Rb, TiO₂, Nb, CaO and Fe₂O₃, presenting with the highest loadings for the first DF. High loadings are also shown by Al₂O₃, SiO₂, CaO, Fe₂O₃, Y and K₂O for the second DF which accounts for 32% of the total variance. Using the jackknife method, the classification accuracy is 32% (Middle Assyrian = 60%, Neo-Assyrian = 13%, Hellenistic = 45%, Parthian = 0%). The significance according to Pillai's criterion and Wilks' Λ calculated by a multivariate analysis of variance (MANOVA) is low as the values of the F-statistic of both criteria are below the corresponding table value and $p \geq 0.05$.¹³⁸

From a chemical point of view, therefore, there is a clear continuity in evidence for the use of raw clay and tempering material from the Middle Assyrian to Parthian period.

When analysing the chemical composition of the samples for each period, more details can be identified. The results are visualised in Fig. E.2.2: The PCA relates to the same statistics as previously detailed. DA is based on the chemical groups of the whole dataset. The first DF accounts for 30% of the total variance, with SiO₂, TiO₂, V, Nb and Al₂O₃ displaying the highest loadings. The second DF explains a total of 24% of the variance. The most influential elements are Fe₂O₃, SiO₂, Al₂O₃, V and Y. Following the results of the jackknife method, the classification accuracy is 34% (Middle Assyrian = 42%, Neo-Assyrian: Cluster 1 = 33%, Neo-Assyrian: Cluster 2 = 50%, Hellenistic: floor of Room 1 = 29%, Parthian = 25%, all others = 0%). The significance according to Pillai's criterion and Wilks' Λ calculated by a MANOVA is high, as $p < 0.05$ and at least the values of the F-statistic of Wilks' Λ are below the corresponding table value.

Going into detail, for the 20 samples assigned to the Middle Assyrian period we can observe a great homogeneity of the chemical composition (Fig. E2.2). Only one outlier shows high concentrations of aluminium, vanadi-

¹³³ Quinn 2022 (with previous literature).

¹³⁴ Drennan 2010; Hair *et al.* 2014. Note that PCA requires a minimum of 150 samples for the results to be considered statistically significant. As our dataset is well below this threshold, the results are therefore to be used with caution.

¹³⁵ Tabachnick/Fidell 2013; Hair *et al.* 2014. Note that DA ideally requires a minimum of 20 samples per group, and it should be noted that three of our four period groups fall under this threshold. For the MANOVA, the required minimum number of samples of 40–50 and 10 objects per group is reached.

¹³⁶ All pottery samples and all reliable elements within them were used to calculate multivariate statistics based on log₁₀ transformed data: Santos *et al.* 2008; Golitko 2011.

¹³⁷ Pillay *et al.* 2000; Legendre/Legendre 2012; Hair *et al.* 2014; Denis 2015; Camargo 2022.

¹³⁸ Zar 2010; Legendre/Legendre 2012; Tabachnick/Fidell 2013; Hair *et al.* 2014; Denis 2015.

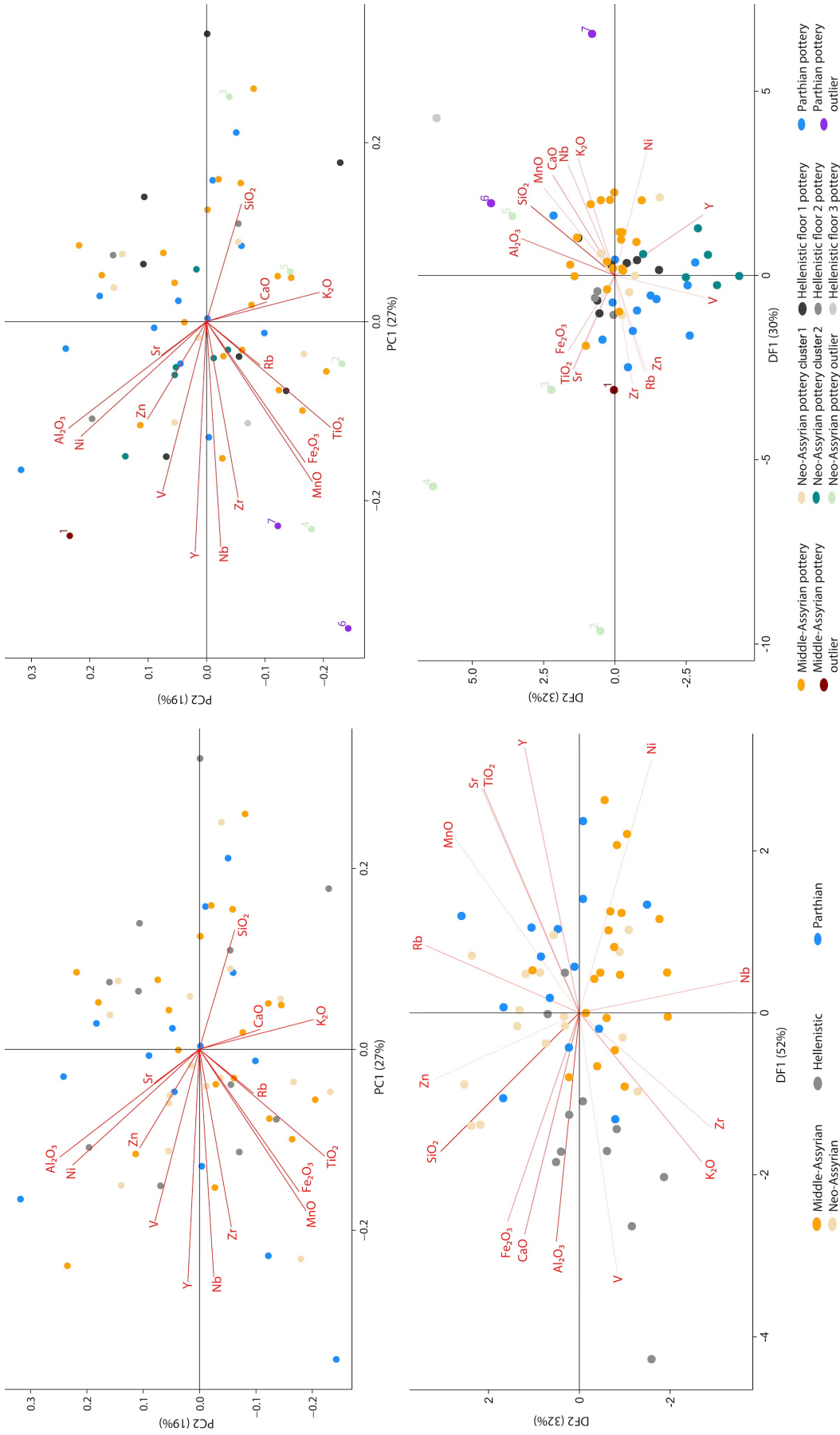


Fig. E2.2: Principal Component Analysis (top) and Discriminant Analysis (bottom) of pottery samples of Assur, with chemical pottery groups coded by colour (n=61). Chemical outliers are numbered. Prepared by Michaela Schauer.

Fig. E2.1: Principal Component Analysis (top) and Discriminant Analysis (bottom) of pottery samples of Assur, coded by colour (n=61). Prepared by Michaela Schauer.

um, yttrium, zinc, nickel and niob, but low silicon, potassium and rubidium values (Outlier 1 = sample AS44). Even if zinc cannot be used for this sample due to a too high variation coefficient,¹³⁹ it is likely that this sample has a different origin or is characterised by a special type of paste preparation or temper.

The 16 pottery samples assigned to the Neo-Assyrian group fall into the same range as those of the Middle Assyrian group regarding their overall chemical fingerprint. Yet they form two distinct clusters (**Fig. E2.2**): Cluster 1 consists of 6 samples (38%) showing lower potassium, silicon and rubidium but, for this data set, comparably higher calcium values. Cluster 2 consists of another 6 samples (38%) that are defined by high potassium, silicon and rubidium but relatively lower calcium and a tendency to high vanadium combined with medium yttrium values. Also, the elements potassium and rubidium are closely related and appear together in a number of minerals such as micas or feldspars. The differences between the two clusters may be due to the use of two different clay sources in the same region, or separate layers within the same clay source. The clusters, therefore, might hint at the production of different types of pottery with specific properties, or the presence of two pottery workshops/traditions at Assur in this period.

In addition to the two Neo-Assyrian clusters of six samples each, four distinct outliers were identified, amounting to 24% of the samples of that group:

Outlier 2 (= sample AS21) differs from both clusters in terms of its high calcium but low silicon and aluminium content; based on its potassium and rubidium concentrations, this sample falls in between both clusters, with vanadium, zinc and nickel values more closely resembling Cluster 2. It is plausible that a mixture of clays but also a special type of temper was used for the vessel from which this sample derives.

Outlier 3 (= sample AS28) is distinguished by low levels of aluminium, titanium, rubidium, zirconium, vanadium, yttrium, zinc and niobium, but a relatively high value of calcium, suggesting the use of a different clay source for the vessel from which this sample derives compared to the other pottery of the Neo-Assyrian group used in this study. However, this must be treated with caution as the variation coefficients for titanium, zircon and niob are too high.

Outlier 4 (= sample AS29) displays low strontium but high yttrium, zinc and niobium concentrations, and falls between Clusters 1 and 2 in terms of its potassium and

rubidium values. Following the petrographic analysis, the use of a specific temper (calcite) is most likely the reason for the chemical specifics.

Outlier 5 (= sample AS25) presents low iron and nickel, high zirconium and comparatively high silicon, titanium and calcium concentrations, which might be due to the use of the same clay source for Cluster 2 while applying a special preparation method.

Thus, the pottery production of the Neo-Assyrian period appears with a higher variability and two more or less distinct ways of using raw materials. Four samples show chemical signatures that indicate different production methods, either in terms of clay selection, clay mixing or tempering. Local production is very likely for at least the 12 samples (76%) in Clusters 1 and 2; however, the outliers are not too different either, so the use of other local materials is also plausible in these cases.

Comparing the results for the Middle Assyrian and the Neo-Assyrian, the chemical signatures of the related samples seem to suggest the use of similar clay sources. For the Middle Assyrian material, we may postulate that clays were more often mixed, whereas a more distinct selection process appears in evidence for the Neo-Assyrian material.

The chemical signatures of the 11 Hellenistic samples from Building A span generally the same range as the Middle Assyrian samples. No clear distinction can be made between the samples taken from the floors of Rooms 1 and 2 while the sample of the floor of Room 3 is chemically separated only due to its titanium and rubidium concentration (**Fig. E2.2**). The small number of samples does not allow for more interpretation.

The samples from the Parthian group show comparable chemical values to the earlier period groups. Only Outlier 6 (= sample AS09) shows relatively high concentrations of rubidium, zirconium, yttrium and niobium, which suggests the use of a different clay source. This might also apply to Outlier 7 (= sample AS07), which is characterised by high values of potassium, rubidium, strontium and niobium, but a low nickel value. Therefore, most of the pottery from this period (12 samples, that is 86%) was produced locally, with only the two outliers (14%) possibly of different origin.

In conclusion, it can be assumed from the chemical composition of the samples that the majority of the pottery analysed for this study was produced locally. The material from the different periods cannot be clearly separated, thereby demonstrating continuity in raw material use and production. However, seven outliers (12%) display a different chemical signature that may indicate the use of specific recipes and/or production techniques, or even non-local origins.

¹³⁹ This means that the variation coefficient is higher than 20% for the three measurements of this sample for the named chemical element.

E2.3 Results of the petrographic analysis

Five different fabrics were recognised according to compositional and textural characteristics, reflecting both provenance and technology (Table E2.3).

Fabric 1: Fine fabric (Fig. E2.3a-b)

This fabric is marked by inclusions between 0.05 and 0.1 mm average size. The main inclusions are quartz and feldspars (plagioclases), but also muscovite, amphibole and serpentinite are common; more rarely tiny fragments of metamorphic rocks, calcite and chert can be observed. The presence of elongated voids in some samples might suggest organic tempering, but they could also be derived from the combustion of naturally occurring organic materials present in the original clay used to produce this fabric. The fineness of this fabric suggests that the original raw material has been cleaned (probably through levigation).

Fabric 2: Medium-coarse fabric (Fig. E2.3e-h)

This fabric is marked by inclusions of 0.25 mm average size. The main inclusions are quartz and feldspars (plagioclases), but also muscovite, amphibole and serpentinite are common; more rarely tiny fragments of metamorphic rocks, calcite and chert can be observed. The presence of elongated voids in the same samples might suggest organic tempering. Still, it could also be derived from the combustion of naturally occurring organic materials present in the original clay used to produce this fabric. Within this fabric, minor compositional and textural characteristics enable the identification of subgroups:

- 2A: standard Fabric 2;
- 2B: serpentinite is more common;
- 2C: inclusions are more abundant;
- 2D: inclusions are very scarce.

Fabric 3: Chaff-tempered fabric (Fig. E2.3c-d)

This fabric is marked by inclusions of 0.1 mm average size. The main inclusions are quartz and feldspars (plagioclases), more rarely tiny fragments of metamorphic rocks and chert and tiny little fragments of serpentinite and amphiboles, were observed. Big, elongated voids filled with charred materials are surely evidence of tempering with organic materials (probably chaff). The finesse of this fabric suggests that the original raw materials have been cleaned (probably through levigation). However, one sample (Outlier 6 = sample AS09) also contains relatively big fragments of micritic calcite (1 mm average size) and it might represent the use of a slightly different clay source and uncleaned clay (Fabric 3B).

Fabric 4: Coarse fabric, mineral-tempered (Fig. E2.3i-k)

This fabric is marked by inclusions between 0.5 and 2 mm average size. The main inclusions are quartz and feldspars (plagioclases), but also muscovite, amphibole and serpentinite are common; more rarely tiny fragments of metamorphic rocks, calcite and chert can be observed. The presence of elongated voids in the same samples might suggest organic tempering. Still, it could also be derived from the combustion of naturally occurring organic materials present in the original clay used to produce this fabric. The strong bimodal distribution of the inclusions suggests mineral tempering.

Fabric 5: calcite-tempered fabric (Fig. E2.3l)

This fabric is dominated by the presence of sparitic calcite of 0.5 mm average size. There is also very fine quartz. The finesse of this fabric suggests that the original raw materials have been cleaned (probably through levigation) and tempered with sparitic calcite.

Fabric group	Name	Subgroup	Clay preparation technique	Coarseness
1	Fine fabric	A	Levigated clay?	Very fine (0.05 mm average size)
		B	Levigated clay?	Fine (0.1 mm average size)
2	Medium coarse fabric	A	Unprocessed?	Medium fine (0.25 mm average size)
		B	Unprocessed?	Medium fine with common serpentinite (0.25 mm average size)
		C	Unprocessed?	Medium fine with abundant inclusions (0.25 mm average size)
		D	Unprocessed?	Medium fine scarce inclusions (0.25 mm average size)
3	Chaff tempered fabric	A	Chaff tempering	Fine (0.1 mm average size)
		B	Chaff tempering	Coarse micritic calcite (1 mm calcite average size)
4	Mineral tempered fabric	A	Mineral tempering	Coarse calcareous (0.5 mm average size)
		B	Mineral tempering	Very coarse calcareous chaff tempering (1-2 mm average size)
5	Calcite tempered fabric		Calcite tempering	Coarse (0.5 mm average size)

Table E2.3: Fabric groups identified in the pottery samples selected from Assur in 2023: overview.

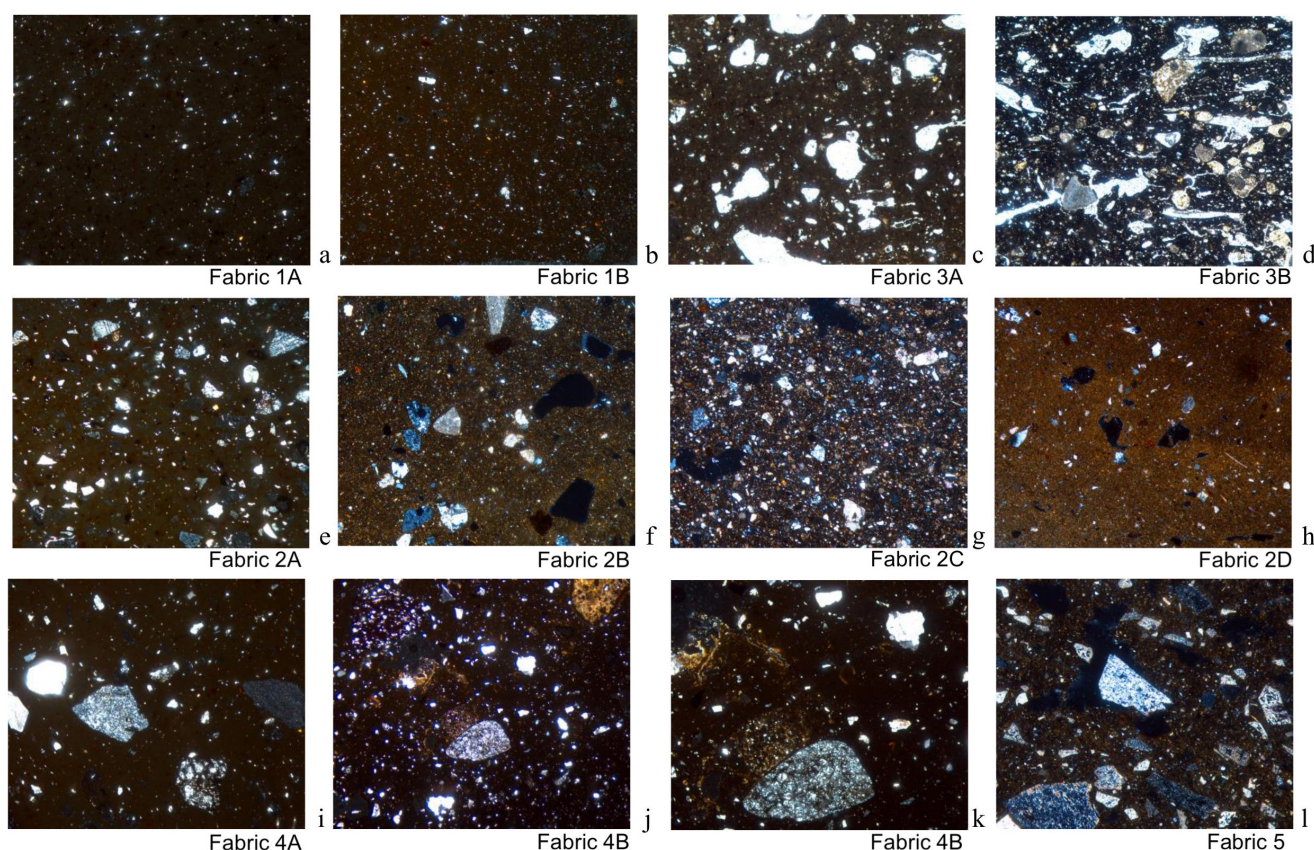


Fig. E2.3: Thin section micrographs of selected samples from Assur (field of view 3 mm unless noted otherwise): a) AS01: Fabric 1A; b) AS02: Fabric 1B; c) AS06: Fabric 3A; d) AS09: Fabric 3B; e) AS05: Fabric 2A; f) AS26: Fabric 2B; g) AS25: Fabric 2C; h) AS63: Fabric 2D; i) AS08: Fabric 4A; j) AS11: Fabric 4B (field of view 6 mm); k) AS11: Fabric 4B; l) AS29: Fabric 5. Prepared by Silvia Amicone.

E2.4 Discussion

In terms of chronology, fabric groups 1A, 1B, 2A and 3A were used in all periods of the sample set, with Fabric 3B being restricted to the Parthian period, although it is currently attested only in one sample. Even if Fabrics 2C, 2D and 5 seem more common in the Middle and Neo-Assyrian groups, there is too little data to state this with any certainty. Fabric 2B is more common in the Middle and Neo-Assyrian groups, while Fabrics 4A and 4B seem to appear more frequently in the Hellenistic and Parthian periods (**Table E2.4**).

The combination of p-XRF and petrographic results shows that finer fabrics, especially samples of Fabric 1B assigned to the Neo-Assyrian period, could be differentiated more precisely by p-XRF. Also, generally rare petrographic fabrics such as Fabric 3B (Outlier 6 = sample AS09), Fabric 2C (Outlier 5 = sample AS25) and Fabric 5 (Outlier 4 = sample AS29) correspond well with the results of the chemical analysis, which also identified specific chemical fingerprints for these samples. Chemical Outlier 1 (= sample AS44) shows no petrographic peculiarities,

but as the fabric is very fine, this is not to be expected. This is where geochemistry is most helpful in dealing with this type of fabric. For chemical Outlier 2 (= sample AS21), even though it belongs to Fabric 1A, this sample is conspicuous from a petrographic point of view. It is highly polished with almost no visible temper and no evidence of clay mixing. It is therefore very likely that this sample was made from a different clay source. On the other hand, ceramic petrography demonstrates that chemical Outlier 3 (= sample AS28) is highly contaminated by post-depositional calcite, and this might be the reason why it shows an unusual chemical composition. In the case of chemical Outlier 7 (= sample AS07), no petrographic distinctive features could be identified. Finally, it can be said that the chemical outliers of each period mainly represent petrographic fabrics that are rare in that particular period (**Table E2.4**).

When comparing the petrographic fabrics and sample chemistry, no clear clusters can be separated in the scatter or multivariate plots. The PCA displayed in **Fig. E2.4** relates to the same statistics as previously detailed. On the other hand, DA is based on the petrographic groups.

Chem. group / petro. group	1A	1B	2A	2B	2C	2D	3A	3B	4A	4B	5	Total
Middle Assyrian												
pottery	1	5	6	2	1	1			1	2		19
pottery outlier 1	1											
Neo-Assyrian												
pottery cluster 1		2	2				2					6
pottery cluster 2		2	1	2		1						6
pottery outlier 2		1										1
pottery outlier 3										1		1
pottery outlier 4											1	1
pottery outlier 5					1							1
Hellenistic												
floor 1 pottery	1		3				1		2			7
floor 2 pottery		1							2			3
floor 3 pottery		1										1
Parthian												
pottery	1	1	2				2		2	4		12
pottery outlier 6								1				1
pottery outlier 7					1							1
Total	4	13	14	5	1	3	5	1	7	7	1	61

Table E2.4: Comparison of the results of p-XRF and petrographic fabric analyses (n=61).

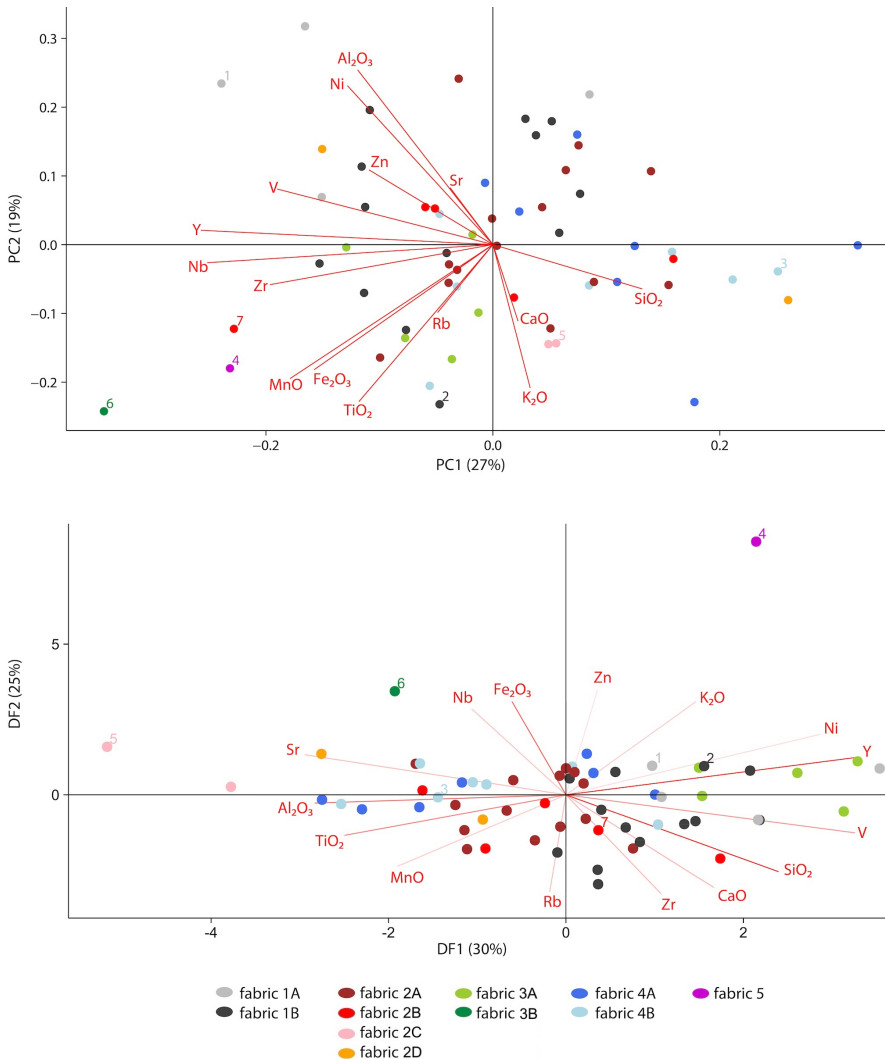


Fig. E2.4: Principal Component Analysis (top) and Discriminant Analysis (bottom) of pottery samples of Assur, with petrographical pottery groups coded by colour (n=61). Chemical outliers are numbered. Prepared by Michaela Schauer.

The first DF accounts for 28% of the total variance with SiO₂, Fe₂O₃, Y, Zr, TiO₂ and CaO, displaying the highest loadings. The second DF explains a total of 23% of the variance. The most influential elements are Y, SiO₂, Al₂O₃, TiO₂ and V. Following the results of the jackknife method, the classification accuracy is 34% (Fabric 1A = 25%, Fabric 1B = 38%, Fabric 2A = 50%, Fabric 2C = 100%, Fabric 3A = 80%, Fabric 4B = 14%, all other fabrics = 0%). The significance according to Pillai's criterion and Wilks' Λ calculated by a MANOVA is high, as $p < 0.05$ and at least the values of the F-statistic of Wilks' Λ are below the corresponding table value.

However, fine fabrics such as Fabric 1A and Fabric 1B tend to have higher aluminium, niobium and yttrium, but also lower calcium values, with Fabric 1A also showing higher nickel concentrations. In Fabric 1B, the lower calcium values are likely due to the removal of calcite through levigation. Fabric 3A tempered with chaff shows comparatively high iron, but low potassium and rubidium values, with a relatively dense clustering of all related samples. Fabric 2 tends to have higher calcium, potassium and rubidium but lower aluminium concentrations. Fabrics 2C, 3B and 5 are quite distinct in both multivariate analyses (Fig. E2.4).

In summary, all the fabrics and chemical groups might have a local origin according to the compositional characteristics of the samples, and they fit well with the local geology dominated by sedimentary rock formations and alluvial sediments transported and deposited by the activity of the Tigris.¹⁴⁰ Ceramic petrographic and chemical analyses show that most of the variability is

connected to different ways of processing the original raw materials through cleaning and tempering. Main tempering agents include mineral tempering (Fabric 4) and chaff tempering (Fabric 3). The use of chaff is unclear in correlation to Fabrics 1, 2 and 4, where sometimes small to medium-sized, elongated voids might suggest the addition of organic material that combusted during the firing process. However, this organic material may have occurred naturally in the original clay. Therefore, further knowledge of the local sources is necessary before raising a conclusion on this point.

Fabric 5 deserves a separate discussion. The addition of calcite as a temper in cooking pots has a long tradition in

the Near East from prehistory and cooking pots tempered with calcite might have been the output of specialised production centres.¹⁴¹

In conclusion, our work, albeit still based on a limited dataset, has started to shed light on the complexity of pottery traditions at the archaeological site of Assur. Further sampling of both archaeological materials and raw sources for pottery making would be necessary to better monitor the variability observed. This preliminary pilot study helps to create the base for a systematic sampling that will certainly improve our knowledge of pottery production and consumption at this site over its long lifespan.

¹⁴¹ Franken/Kalsbeek 1969; 1974; Beynon *et al.* 1986; London 1991; Vilders 1991; Franken 1992; Shoval *et al.* 1993; Mason/Cooper 1999; Daszkiewicz/Bobryk/Schneider 2000; Schneider 2006; London/Shuster 2021.

F. Small finds from Assur, 2023

Andrea Squitieri

F1. Introduction

During the 2023 campaign at Assur, 381 small finds were collected and registered, most of which were in fragmentary conditions.¹⁴² The finds from the trench NT1 2023 are described in a stratigraphic order in §F2-§F10, starting from the topsoil/trench surface down to NT1 2023 Phase 1. These finds are discussed according to categories, i.e., stone tools, loom weights, personal ornaments, and figurines, in §F11.1-5. The finds found in the sondage next to the 2002 SBAH trench and those unearthed while cleaning the western section of the SBAH trench are presented in §F12 and §F13, respectively. The chapter closes with a discussion of the surface finds collected in 2023 in §F14.

The finds are presented in tables, which report the catalogue number (No.), the item registration number (AS number) and the object descriptions. In the latter, the following abbreviations are used: L. for length, W. for width, H. for height, Th. for thickness, D. for diameter, and Wt. for weight. Their raw materials have been identified by the naked eye. Following each table, the most remarkable finds (if any) are described in detail and comparisons are offered.

The table below summarises the stratigraphic sequence of trench NT1 2023 and indicates the sections in this chapter where the relative finds are discussed.

Stratigraphic phase	Sections
Trench surface/topsoil	§F2
NT1 2023 Phase 9	§F3
NT1 2023 Phase 8	§F4
NT1 2023 Phase 6	§F5; §G2
NT1 2023 Phase 5	§F6
NT1 2023 Phase 4	§F7
NT1 2023 Phase 3	§F8

¹⁴² Note that small finds that share similar characteristics are grouped together under the same catalogue number. The small finds were registered and their descriptions prepared by Andrea Squitieri, while the stamp seal in §F6.1 is discussed by Veronica Hinterhuber. The finds were cleaned and restored by Akam Omar Qaradaghi. The epigraphic finds are discussed in §G.

Stratigraphic phase	Sections
NT1 2023 Phase 2	§F9
NT1 2023 Phase 1	§F10
Finds from the sondage in the 2002 SBAH trench	§F12
Surface finds without stratigraphic context	§F13; §G1.2

F2. Finds from the trench surface and the topsoil

Nine small finds of ancient origin were collected from the trench surface and the topsoil. Among them, only the rotary quern fragment (no. 5) from the topsoil holds chronological significance as this type of quern was used across the Middle East from the second to third centuries AD until the advent of the industrial era.¹⁴³

No.	AS number	Description
1	AS 262432:003:004	Fragment of an iron bar, badly preserved. L. 4.1 cm; W. 1.4 cm.
2	AS 261433:002:003	Iron item with the shape of a button, with two opposite tiny protrusions from the sides. The upper surface is curved while the underside is flat. It is not very corroded, hence it may be modern. Th. 0.4 cm; D. 1.8 cm.
3	AS 262432:012:003	Irregularly shaped bronze fragment, corroded. L. 1.4 cm; W. 0.8 cm.
4	AS 261432:006:002	Bronze fragment, possibly part of a nail or pin shaft. L. 2.2 cm; Th. 0.5 cm.
5	AS 262432:012:004	Rotary quern fragment. The working surface is very flat and smooth, while the dorsal side is rough. The edges are damaged. The centre is not preserved. Made of semi-porous basalt. Th. 3 cm; Reconstructed D. 25 cm.

¹⁴³ Alonso/Frankel 2017.

No.	AS number	Description
6	AS 262432:012:005	Fragment of a grinding stone with a flat working surface and a convex dorsal side. It may belong to a lower grinding stone or a hand-stone. Made of semi-porous basalt. L. 10 cm; W. 7 cm; Th. 6 cm.
7	AS 262432:011:002	Rim fragment of a stone vessel with a rounded shape. The curvature of the rim suggests it may belong to a large plate. The stone is a medium-grained stone, pinkish in colour with some darker and shiny minerals visible. L. 4.8 cm; W. 4.2 cm; Th. 1.5 cm.
8	AS 262432:012:006	Slightly curved glass shard, with a bluish-greenish, whitish and reddish-violet iridescence. The surface is rough due to weathering. L. 2.5 cm; W. 2 cm; Th. 0.2 cm.
9	AS 261433:002:004	Shapeless pottery slag, greenish colour. L. 3.5 cm; W. 3 cm.

F3. Finds from NT1 2023 Phase 9

NT1 2023 Phase 9 comprises a looting pit which seems to have damaged Grave 2. Several small finds were collected from the pit fill, including several beads in various materials which likely belonged to the disturbed grave.¹⁴⁴



Fig. F3.1: Bronze ring: AS 261432:015:034 (18). Photo by Andrea Squitieri.

No.	AS number	Description
10	AS 261432:015:035 AS 261432:015:037 AS 261432:015:038 AS 261432:015:039 AS 261432:015:040 AS 261432:015:041 AS 261432:015:042 AS 261432:015:043 AS 261432:015:044 AS 261432:015:045 AS 261432:015:046 AS 261432:015:047 AS 261432:015:048 AS 261432:015:049 AS 261432:015:050 AS 261432:015:051 AS 261432:015:052 AS 261432:015:053 AS 261432:015:054 AS 261432:015:055 AS 261432:015:056 AS 261432:015:057 AS 261432:015:058 AS 261432:015:059 AS 261432:015:060 AS 261432:015:061 AS 261432:015:062 AS 261432:015:063 AS 261432:015:064 AS 261432:015:065 AS 261432:015:066 AS 261432:015:067 AS 261432:015:068 AS 261432:015:069 AS 261432:015:070 AS 261432:015:071 AS 261432:015:072 AS 261432:015:073 AS 261432:015:074 AS 261432:015:075 AS 261432:015:076 AS 261432:015:077 AS 261432:015:078 AS 261432:015:079 AS 261432:015:080 AS 261432:015:081	46 whitish ring beads made of glass or frit. Diameters c. 0.2 cm.
11	AS 261432:015:005 AS 261432:015:018 AS 261432:015:019 AS 261432:015:020 AS 261432:015:022 AS 261432:015:029 AS 261432:015:036	7 glass/frit spherical beads. Diameters c. 0.5 cm.
12	AS 261432:015:017 AS 261432:015:014 AS 261432:015:016 AS 261432:015:013	4 metal beads made of three or five ring beads glued together to form a cylinder. L. < 1 cm.
13	AS 261432:015:025	Bronze oblate bead. D. 0.3 cm.

¹⁴⁴ For the bead shape terminology used throughout this chapter, see Beck 1928.

No.	AS number	Description
14	AS 261432:015:031	Cowrie shell bead. L. 1.2 cm.
15	AS 261432:015:008 AS 261432:015:010	Two barrel beads possibly made of coral. L. 0.5-0.6 cm.
16	AS 261432:015:026 AS 261432:015:033 AS 261432:015:027 AS 261432:015:015 AS 261432:015:021 AS 261432:015:030 AS 261432:015:009 AS 261432:015:006 AS 261432:015:007 AS 261432:015:011 AS 261432:015:028 AS 261432:015:032 AS 261432:015:012 AS 261432:015:024 AS 261432:015:023	15 beads possibly made of carnelian in spherical, barrel, cylindrical, or conical shapes. Diameters and lengths < 1 cm.
17	AS 261432:015:004	Two fragments of a bronze nail with a pointed tip. L. 2.5 cm.
18	AS 261432:015:034	Flat bronze ring with overlapping ends. D. 1.5 cm (Fig. F3.1)
19	AS 261432:015:003	Shapeless iron fragment, highly corroded. Max. D. 4.8 cm.
20	AS 261432:016:004	Squarish mudbrick, partially preserved, with a rounded depression in the centre of one face which has a diameter of 4.5 cm and is 1.8 cm deep. No circular signs are visible in the depression. L. 15 cm; W. 11 cm; Th. 5.5 cm.
21	AS 261432:016:005	Squarish mudbrick with three corners preserved. At the centre of one face there is a rounded depression, about 6.5 cm in diameter and 2 cm deep. No circular signs are visible in the depression. L. 18 cm; W. 17 cm; Th. 5 cm.
22	AS 261432:016:003	Broken lower grinding stone that originally had a saddle shape. The working surface is slightly concave and polished towards the centre, the edges are slightly pointed, the dorsal side is very rough. Made of semi-porous basalt. L. 30 cm; W. 21 cm; Th. 6 cm.
23	AS 261432:013:003	Broken lower grinding stone, whose one end is preserved. The working surface is flat with polished zones. The dorsal side is convex and very rough. Made of porous basalt. L. 22 cm; W. 18 cm; H. 9 cm.

No.	AS number	Description
24	AS 261432:013:004	Elongated and thick stone possibly used as a pestle as it shows pecking marks on the rounded extremities. The shaft looks unworked. L. 28 cm; D. 8 cm.

F4. Finds from the NT1 2023 Phase 8 (chamber tomb = Grave 1)

The finds retrieved from the chamber tomb, dated to the Parthian period (**§D1.3**), are arranged in the following order:

- finds from within the tomb's walls;
- finds from the floor deposits of the northern chamber and the main corridor;
- finds from the floor deposits of the southern chamber;
- finds from the tomb's upper deposits.

F4.1 Finds from inside the walls of the chamber tomb

While removing the chamber tomb's walls in order to investigate the older phases, we found the following items:

No.	AS number	Description
25	AS 262433:049:002	Cuneiform inscribed brick (§G1)
26	AS 262433:049:003	Cuneiform inscribed brick (§G1)
27	AS 262433:049:004	Two thin metal sheets made of leaded-copper alloy with a higher percentage of lead. ¹⁴⁵ The colour of the outer surface is grey. The larger piece: L. 3.5 cm; W. 2.5 cm; Th. 0.4 cm; Wt. 3.5 g.
28	AS 262433:003:003	Cuneiform inscribed brick (§G1)
29	AS 262433:003:002	Bronze fibula (Fig. F4.1)

(29)

AS number: AS 262433:003:002

Material: Bronze

Dimensions: L. 3 cm; Th. 0.5 cm.

Description: Bronze fibula with a triangular body. One end is folded while the other, where the spiral should be, is not preserved. The surface presents heavy damage, hence it is not clear whether the arms were originally decorated.

¹⁴⁵ The raw material was identified by the restorer Akam Omar Qaradaghi upon cleaning.

Comparisons: Due to its bad state of preservation, it is not easy to find exact parallels. Its small size may indicate it belongs to type C8 in Pedde's classification, dating from the 7th to the beginning of the 6th century BC.¹⁴⁶ However, it is not clear if this fibula has a decoration on the arms as C8 type fibulae do. Undecorated triangular fibulae do exist, though they have not been found in Assur. They belong to Pedde's type C6 and are dated to the 8th-6th century BC.¹⁴⁷ The present fibula clearly represents an older find which ended up in a younger context.



Fig. F4.1: Fibula: AS 262433:003:002 (29). Photo by Andrea Squitieri.

F4.2 Finds from the northern chamber and the main corridor

In the floor deposits of Subdivisions 5, 7, and 8 of the northern chamber, as well as the main corridor, we collected the following items:

No.	AS number	Description	Location
30	AS 262433:021:007	Fully preserved four-handled ceramic vessel with honey-comb decoration (§E1.2)	Subdivision 5
31	AS 262433:023:006	Glass shard, white with a bluish iridescence. L. 2.5 cm; W. 1.3 cm; Th. 0.2 cm.	Subdivision 7
32	AS 262433:023:007	Glass shard, slightly curved, covered by a dark grey patina. L. 2.2 cm; W. 0.8 cm; Th. 0.1 cm.	Subdivision 7

No.	AS number	Description	Location
33	AS 262433:023:008	Bronze fragment, slightly curved, perhaps originally from a ring. L. 1.5 cm; Th. 0.4 cm.	Subdivision 7
34	AS 262433:023:009	Tiny spherical bronze item, perhaps the head of a pin. D. 0.3 cm.	Subdivision 7
35	AS 262433:023:010	Fragment of a glass bowl with a dark grey colour. The flat base and part of the concave body are preserved. The wall is 0.4 cm thick. On the base underside a small and shallow rounded depression is visible and on the inner side of the base a small bump is present. The shape of the fragment is reminiscent of a deep saucer. H. 5.5 cm.	Subdivision 7
36	AS 262433:023:011	Glass rim fragment 0.4 cm wide, with the body slightly curved and 0.3 cm thick. The outer side of the shard is covered by a whitish fluorescent patina, with darker spots, the inner side is bluish transparent. L. 2.5 cm; W. 2 cm.	Subdivision 7
37	AS 262433:023:012	Small ceramic ball, colour beige. D. 2 cm. See also nos. 100-101 from the southern chamber.	Subdivision 7
38	AS 262433:023:013	Convex biconic item with two flat ends and smoothed mid-point. It has no perforations. Possibly a weight. The stone is hard, mottled dark greenish-black. L. 1.6 cm; D. 0.8 cm; Wt. 1.27 g.	Subdivision 7

¹⁴⁶ Pedde 2000, 245-246.

¹⁴⁷ Pedde 2000, 239-242.

No.	AS number	Description	Location
39	AS 262433:023:014	A fragment of a glass handle with the attachment to the vessel body preserved. The handle has a rounded section (0.4 cm diameter) and a curved end; two ridges are visible on its surface. The handle tip looks as if it was folded up upon finishing. L. 3.5 cm; D. 0.4 cm.	Subdivision 7
40	AS 262433:023:015	Cylindrical neck fragment of a bottle with a flaring rim. At the bottom of the neck shaft the beginning of the vessel body is visible. The glass is covered by a dark grey patina under which a bluish fluorescence is visible. It is possibly the neck of an unguentarium. Rim W. 2.5 cm, shaft D. 1.4 cm, L. 3.5 cm. (Fig. F4.2)	Subdivision 7
41	AS 262433:023:016	Bronze shaft with a curved end, the other end is broken. Possibly a needle or a pin. L. 1.5 cm; Th. 0.2 cm.	Subdivision 7
42	AS 262433:023:017	Bronze fragment, L. 0.8 cm.	Subdivision 7
43	AS 262433:023:018	Two small bronze sheet fragments, slightly curved. Both have a thickness of 0.1 cm, and measure about 1 × 1 cm.	Subdivision 7
44	AS 262433:023:019	Half preserved cylinder bead, broken on one end. Made of red carnelian. L. 1.5 cm; D. 1 cm.	Subdivision 7

No.	AS number	Description	Location
45	AS 262433:024:003	Broken lower grinding stone, made of porous basalt. The working surface is flat. The dorsal side is uneven and slightly pointed. The edges are not completely preserved. L. 24 cm; W. 15 cm; Th. 5 cm.	Subdivision 8
46	AS 262433:025:003	Glass shard covered with a whitish patina. In the section a dark green colour is visible. L. 2.8 cm; W. 1.8 cm.	Northern corridor
47	AS 262433:026:001	Rectangular ceramic item, one short side is slightly curved. Several tiny striations are visible on the surface. Possibly used as a polisher. L. 4.7 cm; W. 3 cm; Th. 1 cm.	Main corridor
48	AS 262433:026:003 AS 262433:026:004 AS 262433:026:005 AS 262433:026:006	4 thin and flat iron fragments, L. < 7 cm.	



Fig. F4.2: Glass neck fragment: AS 262433:023:015 (40). Photo by Andrea Squitieri.

F4.3 Finds from the southern chamber

In the floor deposits of Subdivisions 1, 2 and 3, we collected the following items:

No.	AS number	Description	Location
49	AS 262432:019:003	Tiny bronze fragment which may be the end of a pin or a nail. L. 0.5 cm; D. 0.3 cm.	Subdivision 1
50	AS 262432:019:004	Thin bronze needle shaft. L. 4 cm; D. 0.2 cm.	Subdivision 1
51	AS 262432:019:005	Very thin glass fragment broken into two parts, covered by a dark patina. In the break a whitish iridescence can be seen. L. 1 cm; W. 0.5 cm; Th. 0.1 cm.	Subdivision 1
52	AS 262432:020:004	Item composed of a bone part attached to an iron shaft. Possibly it was the handle of a small knife. L. 3.8 cm; D. 0.5 cm.	Subdivision 2
53	AS 262432:020:005	Pointed object with a circular section and a blunt point, 0.2 cm thick. Made of a beige stone whose surface shows blackish stains and several longitudinal striations. Broken in two pieces. Perhaps used as a stylus for alphabetic writing, or as an awl to make perforations. L. 9 cm; D. 1 cm (Fig. F4.3)	Subdivision 2
54	AS 262432:020:006	Thin glass shard covered with a dark patina. L. 1.5 cm; W. 1 cm; Th. 0.1 cm.	Subdivision 2



Fig. F4.3: Stylus or awl made of stone: AS 262432:020:005 (53). Photo by Andrea Squitieri.

No.	AS number	Description	Location
55	AS 262432:020:007	Disc-shaped ceramic object, with irregular edges, and a central perforation 0.6 cm wide. It is a broken sherd that was possibly reused as a loom weight. Th. 1.1 cm; D. 6.2 cm; Wt. 48.40 g.	Subdivision 2
56	G01-S02-V01	Rectangular sarcophagus (Figs. D2.13b; F4.4)	Subdivision 2
57	AS 262432:021:003	Carnelian oblate bead, red translucent. D. 0.9 cm.	Subdivision 3
58	AS 262432:021:006	Fragment of a light red, translucent carnelian bead. L. 0.4 cm.	Subdivision 3
59	AS 262432:021:007	Small tridacna shell with no sign of decoration or perforation. Partially broken. L. 9.5 cm; W. 6 cm (Fig. F4.5)	Subdivision 3
60	AS 262432:021:008	Rim fragment of a basalt bowl or mortar bowl. The body is 2 cm thick, the rim is flat and 1 cm wide. The inner surface is very smooth, while the outer surface is rough. Made of semi-porous basalt. Reconstructed D. 35 cm.	Subdivision 3

(56)

Registration number: G01-S02-V01, from the collection AS 262432:020:001.

Material: ceramics

Dimensions: L. 186 cm, W. 59 cm, H. outside 44 cm, H. inside 41 cm, rim width 6.0 cm, wall width 2.1-2.5 cm

Description: Sarcophagus in the shape of a rectangular basin with a flat base; the longer sides are straight and the shorter sides are curved. The sarcophagus was found in a fragmentary state of preservation, with some of its sherds found scattered in Subdivisions 1 and 2 and the northern corridor (§D2.3.4.3). Its fill did not contain any finds.

The sarcophagus' walls are smoothed on the outer surface whereas the inner surface is rougher and shows horizontal grooves. The rim was formed by adding and



Fig. F4.4: Sarcophagus found in the chamber tomb's Subdivision 2: G01-S02-V01 (56). Photo by Ellen Coster.

modelling clay onto the outer surface of the wall. It was decorated with two parallel grooves with a central ridge between them. The latter is decorated with rounded impressions. About 14 cm below the rim, a decorative band runs around the outer surface, made with a clay coil with an original width of about 1 cm into which round finger/thumb impressions were applied directly next to each other. The colours of both the inner and outer surfaces differ from sherd to sherd, ranging from beige to brown, which could reflect different post-depositional conditions.

Comparisons: Sarcophagi with the same shape as no. 56, in some cases with decorative motifs, were found in Assur during Andrae's excavations in Parthian-period tombs and also in some of the trenches excavated across the city.¹⁴⁸

The floor deposit of Subdivision 4 yielded 56 items. In the tables below, they are arranged by material, except for the beads, which are arranged by shape.



Fig. F4.5: Tridacna shell: AS 262432:021:007 (59). Photo by Andrea Squitieri.

Floor deposit of Subdivision 4: beads		
No.	AS number	Description
61	AS 262432:022:018 AS 262432:022:019 AS 262432:022:021 AS 262432:022:022 AS 262432:022:023 AS 262432:022:025 AS 262432:022:026 AS 262432:022:030 AS 262432:022:032 AS 262432:022:056 AS 262432:022:058	11 cylinder beads, partially broken, made of glass/frit. Whitish with black stains. L. 0.5 to 1.6 cm; D. 0.5-0.6 cm.
62	AS 262432:022:043	Oblate disc bead, whitish colour. Made of glass/frit. The perforation is slightly off-centre and irregular. D. 0.5 cm.
63	AS 262432:022:048	Spherical bead broken in two halves. The outer surface is brilliant blue with some iridescence. Inside the break, it is possible to see a whitish paste below the blue layer that is visible on the outside. Possibly made of faience. D. 1 cm.
64	AS 262432:022:050	Spherical bead, broken in two halves. White colour. D. 0.5 cm.
65	AS 262432:022:044	Triangular bead made of glass/frit. Broken in two fragments. In the section, the surface appears lucent white with some iridescence. The outer surface of the bead is smooth and darkened. The perforation goes through the longest side. L. 2.2 cm; W. 1.5 cm; Th. 0.5 cm.

¹⁴⁸ Andrae/Lenzen 1933, pls. 45a-c, 47i, 490.

Floor deposit of Subdivision 4: beads		
No.	AS number	Description
66	AS 262432:022:051	Oblate disc bead with the perforation running longitudinally, slightly off-centre. The stone is dark red with a white band running transversally. L. 1.5 cm; W. 1.2 cm; Th. 0.6 cm.
67	AS 262432:022:008	Truncated cone bead with flat sides. The perforation is on the lateral side (transversal). The stone is hard and of dark grey colour. L. 1.3 cm; W. 1 cm; Th. 0.5 cm.
68	AS 262432:022:027	Convex truncated cone bead, with a polished surface, made of hard, dark blue stone, possibly steatite. The perforation has a 0.3 cm diameter. L. 1.6 cm; D. 1.7 cm (Fig. F4.6)
69	AS 262432:022:013	Red oblate bead, with some damage on the surface. Likely made of carnelian. D. 2 cm (Fig. F4.7)
70	AS 262432:022:016	Oblate bead. The perforation is slightly off-centre. The colour is dark red, likely made of carnelian. D. 1 cm.
71	AS 262432:022:020	Oblate bead, partially broken and with a damaged surface. Its colour is light red, likely made of carnelian. D. 0.9 cm.
72	AS 262432:022:054	Short truncated convex, bicone bead. Blackish-grey colour. D. 1 cm.
73	AS 262432:022:028	Small pendant with a rectangular-shaped hook, a rounded faceted body and the start of a cylinder base (broken). The colour is light translucent red, likely carnelian. L. 1 cm; W. 0.5 cm.
74	AS 262432:022:024	Spherical bead, made of dark blue-grey stone, with brighter stains. D. 0.7 cm.
75	AS 262432:022:041	Spherical bead, black colour. D. 0.8 cm.



Fig. F4.6: Bead: AS 262432:022:027 (68). Photo by Andrea Squitieri.



Fig. F4.7: Bead: AS 262432:022:013 (69). Photo by Andrea Squitieri.

Floor deposit of Subdivision 4: glass		
No.	AS number	Description
76	AS 262432:022:017	Concave fragment of a bowl or a deep saucer. The glass is covered with a dark patina under which a whitish-bluish iridescence is visible. L. 5 cm; W. 3 cm; Th. 0.2 cm.
77	AS 262432:022:011	Glass shard covered by a bluish-greyish patina. L. 1.5 cm; W. 1.2 cm; Th. 0.05 cm.
78	AS 262432:022:052	Glass shard with a rectangular shape, broken into two parts. The colour is whitish with some black spots. L. 1.4 cm; W. 1 cm; Th. 0.2 cm.
79	AS 262432:022:057	Glass shard, slightly curved, translucent with a hint of a light bluish colour. L. 3 cm; W. 2.1 cm; H. 0.2 cm.

Floor deposit of Subdivision 4: bronze		
No.	AS number	Description
80	AS 262432:022:003	Shapeless bronze fragment. L. 1.8 cm; W. 0.8 cm; Th. 0.6 cm.
81	AS 262432:022:034	Small bronze fragment, one end looks complete and rounded. Possibly the end shaft of a nail or a pin. L. 1.4 cm; D. 0.3 cm.
82	AS 262432:022:035	Roughly spherical bronze fragment, highly corroded. D. 1 cm.
83	AS 262432:022:053	Long bronze fragment, perhaps the shaft of a needle or nail. L. 2 cm; D. 0.3 cm.
84	AS 262432:022:061	Shapeless bronze fragment. L. 2 cm.
85	AS 262432:022:059	Two small shapeless bronze fragments that were found together. L. 1.4 cm each.

Floor deposit of Subdivision 4: bronze		
No.	AS number	Description
86	AS 262432:022:012	Bronze item made of a 1.5 cm long thin shaft (Th. 0.2 cm) characterised by a braid pattern attached to a thin (Th. 0.2 cm) loop, with a diameter of about 1.5 cm, set at a 90-degree angle to the shaft. L. 2 cm (Fig. F4.8)
87	AS 262432:022:014	Bronze item made of a 1.1 cm long thin shaft (Th. 0.2 cm) characterised by a braid pattern attached to a thin (Th. 0.2 cm) loop (about 1.4 cm in diameter) at a 90 degree angle to the shaft. L. 1.1 cm.
88	AS 262432:022:033	Fragment of a bronze pin, about 0.4 cm thick, with a curved head, while the opposite end is broken. L. 2 cm.
89	AS 262432:022:036	Bronze ring with overlapping ends. A tiny ridge runs along the surface. D. 2.5 cm.
90	AS 262432:022:015	Crescent shape earring, the thickest part measures 0.4 cm. At the centre of the crescent, a tiny bump is visible. L. 1.5 cm; W. 1.4 cm (Fig. F4.9)
91	AS 262432:022:042	Rectangular bronze item, broken at one end. The edges are sharp and the surface shows some weathering. L. 3.4 cm; W. 0.8 cm; Th. 0.5 cm.
92	AS 262432:022:031	Bronze fragment with an irregular rounded shape. D. 0.8 cm.
93	AS 262432:022:047	Shapeless bronze fragment with a very corroded surface L. 2 cm.
94	AS 262432:022:049	Shapeless bronze fragment. L. 1.5 cm.



Fig. F4.8: Bronze item: AS 262432:022:012 (86).
Photo by Andrea Squitieri.



Fig. F4.9: Crescent shape earring: AS 262432:022:015 (90).
Photo by Andrea Squitieri.

Floor deposit of Subdivision 4: iron		
No.	AS number	Description
95	AS 262432:022:038	Small curved iron fragment, about 0.5 cm thick. Perhaps part of an earring. L. 1 cm.
96	AS 262432:022:040	Iron fragment with a flat curved end and a thicker part, highly corroded and badly preserved. Perhaps part of an earring or a ring. L. 2 cm; W. 1.8 cm; Th. 0.3 cm.
97	AS 262432:022:037	Two iron fragments caught together. One is curved and resembles a ring or an earring, the other is flattish. Perhaps this item was used as a pendant. L. 1.8 cm.
98	AS 262432:022:039	Iron ring, 0.4 cm thick. A flattish band is wrapped around one end, possibly part of a pendant. L. 2 cm; W. 1.8 cm.
99	AS 262432:022:060	Shapeless iron fragment. L. 2 cm; W. 1 cm; Th. 0.8 cm.

Floor deposit of Subdivision 4: clay, stone and shell		
No.	AS number	Description
100	AS 262432:022:004	Ceramic ball, beige colour. D. 2.5 cm. See also no. 37 .
101	AS 262432:022:006	Ceramic ball, beige colour. D. 2.4 cm. See also no. 37 .
102	AS 262432:022:055	Flint flake. L. 2.5 cm; W. 2 cm; H. 1.5 cm.
103	AS 262432:022:045	Two tiny thin and flat stone fragments, about 0.8 cm wide. The colour is black with whitish stains.
104	AS 262432:022:046	Tiny stone rectangular fragment, blackish colour. L. 1.3 cm; W. 0.9 cm.

Floor deposit of Subdivision 4: clay, stone and shell		
No.	AS number	Description
105	AS 262432:022:029	Concave shell fragment. The outside surface is smooth, beige in colour with some darker banding. The inner part is white, powdery and soft (can be scratched by a fingernail). L. 4 cm; W. 3 cm; Th. 0.5 cm.
106	AS 262432:022:007	Small tridacna shell, with a weathered surface. No sign of decoration or perforation. L. 9 cm; W. 6.5 cm.

F4.4 Finds from the upper deposits

The following tables show the finds collected from the upper deposits of the chamber tomb.

No.	AS number	Description
107	AS 261433:018:003	Possible fragment of a lower grinding stone with a flat surface and a convex dorsal side. Made of porous basalt. L. 10 cm; W. 6 cm; H. 3.5 cm.
108	AS 261433:018:004	Rectangular stone fragment with a concave surface and a slightly pointed edge, while the other side is broken off. Its original shape is unclear. L. 14 cm; W. 12 cm; Th. 2.5 cm.
109	AS 261433:015:002	Fragment of a bronze needle with a curved tip. L. 3 cm; D. 0.3 cm.
110	AS 261433:015:003	Squarish glass fragment, slightly curved. It is whitish with a greyish-bluish patina on the surface that tends to come off. Its surface is iridescent. L. 2.5 cm; W. 2.1 cm.
111	AS 262433:020:002	Fragment of a stone tool with a slightly concave surface, smooth and shiny. The opposite side is rough. It is possibly the fragment of a lower grinding stone. Made of semi-porous basalt. L. 6.5 cm; W. 4.5 cm; Th. 3 cm.
112	AS 262433:020:003	Small bronze shapeless fragment, corroded. D. 0.5 cm.
113	AS 262433:013:002	A fragment of plaster crossed by two ridges longitudinally, on each side of the ridges a line of holes is present, each hole having a diameter of about 0.4 cm and a depth of about 0.5 cm. Possibly they had a practical function or were decorative. L. 14 cm; W. 10 cm; Th. 2.5 cm.

No.	AS number	Description
114	AS 262433:012:003	Badly damaged fragment of a basalt tool with a flat and smooth surface. Possibly belonging to a lower grinding stone. The stone is semi-porous basalt. L. c. 10 cm.
115	AS 262433:017:002	Shapeless bronze fragment. L. 3.5 cm.
116	AS 262433:017:003	Fragment of a bronze shaft, broken at both ends and slightly curved at one end. Th. 0.4 cm; L. 2 cm.
117	AS 262433:015:003	Shapeless iron fragment, highly corroded. L. 4 cm; D. 1.8 cm.
118	AS 262433:015:004	Rectangular object made of stone. One corner is chopped off. The surface is polished and shows some irregular striations. The edges are smoothed. The colour of the surface is light brown while the section is brown-greyish. It is possibly a whetstone. L. 4.8 cm; W. 2.8 cm; Th. 1 cm.
119	AS 262433:005:002	Broken grinding stone. The working surface is flat and rough, with some areas that are smoothed. The dorsal side is convex and very rough. The edges are badly preserved. It may be a fragment of a lower grinding stone with a loaf shape. Made of semi-porous basalt. L. 13 cm; W. 4 cm; Th. 4 cm.
120	AS 262433:005:003	Fragment of a nail or a pin shaft, made of bronze. Highly corroded. L. 3.5 cm; D. 0.5 cm.

No.	AS number	Description
121	AS 262432:007:005	Bronze shaft of a needle or a pin. L. 3 cm; D. 0.3 cm.
122	AS 262432:004:003	Broken grinding stone. Flattish working surface, rough dorsal side. The edges are not preserved. Made of semi-porous basalt. L. 15 cm; W. 11 cm; Th. 3 cm.
123	AS 262432:004:006	Basalt fragment with a trapezoidal shape, two polished flat surfaces at the opposite side while the rest is broken off. It may be the fragment of a bowl handle. L. 5 cm; W. 3.5 cm; Th. 2.5 cm.

No.	AS number	Description
124	AS 262432:004:007	Fragment of a grinding stone, the working surface is flat with some polished zones alternating with rough zones. The dorsal side is convex and very rough. The edges are badly damaged. Made of semi-porous basalt. L. 7.5 cm; W. 4.5 cm; Th. 3.5 cm.
125	AS 262432:004:008	Basalt object with a slightly concave smoothed surface, smooth edges and a flattish base. It has a blunt raised edge on one side. It may have been a grinding stone in origin, reused and reworked to be used for another purpose. L. 14 cm; W. 10 cm; Th. 7 cm.
126	AS 262432:006:002	Half preserved circular earring (Th. 0.3 cm). It has a thicker, grooved section along the shaft. Th. 0.5 cm; L. 1.2 cm.
127	AS 262432:013:003	Tiny fragment of bronze with a cylindrical shape. Corroded. L. 0.6 cm; D. 0.3 cm.
128	AS 262432:013:008	Bronze sheet with rounded edges and a hole (D. 0.1 cm) in the centre. L. 1.5 cm; W. 1 cm; Th. 0.1 cm.
129	AS 262432:013:004	Slightly curved glass fragment, whitish colour with iridescence. L. 2 cm; W. 1.5 cm; Th. 0.2 cm.
130	AS 262432:013:006	Pottery slag, greenish colour, several pores are visible. L. 3.5 cm; W. 3 cm; Th. 1 cm.
131	AS 262432:013:010	Fragment of a basalt tool with a flat surface, slightly smoothed through use. The rest of the tool is broken and damaged. The stone is semi-porous basalt. Probably part of a lower grinding stone. L. 10 cm; W. 9 cm; Th. 3.5 cm.

F5. Finds from NT1 2023 Phase 6: Grave 3 and Grave 4

Grave 3 provided the date 159/158 BC, which was engraved on its sarcophagus (§G2). Grave 4 very likely belongs to the same period though it did not bear any inscription (§D2.5). The tables below list the finds retrieved from each grave, indicating also the location of the finds in relation to the respective skeletons.

Grave 3			
No.	AS number	Description	Location
132	AS 262433:060:001 (also vessel G03-Vo2)	Green glazed amphora (§E1.3)	Near the left arm, at the height of the chest
133	AS 262433:060:003	Highly corroded iron earring, with a flat surface 1.3 cm wide. L. 2 cm; W. 2.5 cm.	Around the left hand's ring finger
134	AS 262433:060:005	Oblate spherical bead made of glass/frit. The colour is brownish. The perforation is 0.2 cm wide. D. 0.4 cm (Fig. I.6)	Among the remains of the hip bone
135	AS 262433:060:006		
136	AS 262433:060:007		
137	AS 262433:060:008	Tiny flat glass piece of whitish colour. L. 0.3 cm.	In between the bones of the right hand
138	AS 262433:060:009	Textile fragments (§I)	On the middle part of the skeleton
139	AS 262433:060:010	Dome-shaped bead made of steatite. The perforation has a diameter of 0.4 cm. H. 1.2 cm; D. 2 cm (Fig. F5.1)	Underneath the skull
140	AS 262433:060:011	Thin fragment of plaster from the sarcophagus' inner surface. L. 5 cm.	On the skeleton
141	AS 262433:060:016	Cylindrical white bead decorated with two transversal grooves about 0.2 cm apart from the bead midpoint. The material could be frit. L. 0.7 cm; D. 0.5 cm (Fig. I.7)	Under the skeleton
142	AS 262433:058:004	Sarcophagus of an ovoid-elliptical shape, with an alphabetic inscription (§G2; Fig. F5.2)	At the bottom of the grave fill
143	AS 262433:058:006 (also Vessel G03-Vo1)	Blue glazed bowl (§E1.3)	Next to the inner edge of the sarcophagus

Grave 3			
No.	AS number	Description	Location
144	AS 262433:056:003	Shapeless glass shard, with a brilliant green colour and iridescence. D. o.6 cm.	In the upper fill of the grave



Fig. F5.1: Dome-shaped bead: AS 262433:060:010 (139). Photo by Andrea Squitieri.

(142)

AS number: AS 262433:058:004

Material: Ceramics

Dimensions: L. 100 cm; W. 76 cm; H. 61 cm.

Description: Completely preserved sarcophagus with an alphabetic inscription incised on its surface, reporting a date in July/August 158 BC, as discussed in §G2. It is made of fired clay and has an elliptical dome shape with a flat everted rim. The colour of the surface is not homogeneous: some parts are light brown, some dark brown. Black spots are also visible, which are the remains of bitumen. On the flat side of the rim, where it touched the ground, a



Fig. F5.2: Sarcophagus from Grave 3, with an alphabetic inscription: AS 262433:058:004 (142). See also §G2. Photo by Ellen Coster.

white powdery plaster is attached. Plaster was also used as a lining for the inner surface, some fragments of which were still attached to the surface when we removed the sarcophagus, while others fell on the skeleton.

Comparisons: Two similar sarcophagi were found at Assur during Andrae's excavations in Square gC9l.¹⁴⁹

Grave 4			
No.	AS number	Description	Location
145	AS 262432:055:003	Leather fragments	Around the feet
146	AS 262432:055:009	Tiny snail shell. No visible perforation. D. o.8 cm.	Near the skeleton
147	AS 262432:055:011	Bronze fragment, L. < 1 cm.	Near the skeleton
148	AS 262432:055:012	Bronze fragment, L. 2.2 cm.	Near the skeleton
149	AS 262432:055:013	Thick fragment of plaster from the sarcophagus' inner surface. L. 4 cm; W. 2.5 cm; Th. 1.5 cm.	On the skeleton
150	AS 62432:054:003	Bead with a convex cone disc shape. Perforation is 0.4 cm wide. The stone is dark blue and highly polished. D. 2.1 cm.	Near the skeleton
151	AS 62432:054:005	Tiny plaster fragments from the sarcophagus' inner surface. L. 3 cm.	Near the skeleton
152	AS 62432:054:004	Sarcophagus of ovoid-elliptic shape (Fig. F5.3)	At the bottom of the fill
153	AS 262432:053:003	Bronze fragment, L. 0.6 cm.	In the upper grave fill

(152)

AS number: AS 262432:054:004

Material: Ceramics

Dimensions: L. 130 cm; W. 76 cm; H. 61 cm.

Description: Completely preserved sarcophagus, with an ovoid-elliptic shape. It is very similar to no. 142, but about 30 cm longer and without an incised inscription. The colour on the outside is brown with large reddish spots. A square hole on the top, measuring 2.7 × 1 cm, was caused when the sarcophagus was struck with a pick during the excavation. This provided us with the oppor-

¹⁴⁹ Andrae/Lenzen 1933, pl. 44e (Ass 14722) and pl. 47g (Ass 14705).

tunity to measure its thickness, which is only about 0.4 cm. The rim surface as well as the inner surface of the sarcophagus were lined with plaster fragments, some of which were also found on the skeleton.

Comparisons: see no. 142.

F6. Finds from NT1 2023 Phase 5

The tables below list the finds collected from Rooms 1, 2 and 3 of Building A, dated to the Hellenistic period, with an indication of their contexts, either floor deposits or room fills (§D2.6).

Building A Room 1			
No.	AS number	Description	Context
154	AS 261433:005:005	Disc-shaped stone item with two opposite polished surfaces and rounded edges. Made of brownish limestone. It may have been a river pebble used as a polisher. L. 9.5 cm; W. 8 cm; Th. 2.4 cm.	Floor
155	AS 261433:005:009	Disc-shaped object, of which $\frac{1}{2}$ is preserved. It has a smooth surface and rounded edges. It may have been used as a polisher. The stone is greyish, fine-grained, with some black-brown areas maybe from contact with fire. Th. 1.5 cm; D. 6 cm.	Floor
156	AS 261433:005:006	Fragment of a shell, possibly from a pendant, but no perforation or other marks are visible. L. 5.1 cm; W. 2.2 cm.	Floor
157	AS 261433:005:008	Shapeless pottery slag of a greenish colour. L 2.1 cm; Width: 1.1 cm.	Floor
158	AS 261433:004:003	Cone shell (<i>Conidae</i> family) with red dots on its surface, and a natural perforation on the flat top. L. 1.5 cm; W. 1 cm.	Room fill



Fig. F5.3: Sarcophagus from Grave 4: AS 262432:054:004 (152). Photo by Ellen Coster.

Building A Room 2			
No.	AS number	Description	Context
159	AS 261432:011:028	Stamp seal made of lapis lazuli (§F6.1; Fig. F6.1)	Floor
160	AS 261432:011:034	Iron fragment, L. 3 cm.	Floor
161	AS 261433:020:026	Bronze fragments, L. < 2 cm.	Floor
162	AS 261433:020:028		
163	AS 261433:020:030	Fragment of a ceramic stilt. Only the end of one leg is partially preserved. L. 2.4 cm; W. 2 cm; Th. 1.8 cm.	Floor
164	AS 261433:020:037	Bronze fragment, L. < 1 cm.	Floor
165	AS 62433:068:004	Terminal end of a lower grinding stone, with irregular edges, very rough dorsal side and a flat working surface smoothed through use. Made of semi-porous basalt. L. 16 cm; W. 10 cm; H. 4 cm.	Floor
166	AS 261432:007:003	Chunk of mud with a curved shape and several striations visible on its surface that may be reed marks. This indicates it may be part of the collapsed roof. L. 17 cm; W. 15 cm; H. 7 cm.	Room fill

Building A Room 2			
No.	AS number	Description	Context
167	AS 261432:007:004	Flat and thin bone object with a pointed extremity. Possibly used as a tool to perforate. Broken in two fragments: the larger is 5.1 cm long, the smaller is 2.1 cm, both are 2 cm wide (max. width). Th. 0.1 cm.	Room fill
168	AS 261433:017:004	Small and shapeless bronze fragment attached to a pottery body sherd. L. 1.8 cm; W. 1 cm.	Room fill
169	AS 262433:065:003	Two small pottery slag fragments.	Room fill
170	AS 262433:065:004	Small bronze fragment with a roughly rectangular section. L. 1 cm; Th. 0.4 cm.	Room fill

Building A Room 3			
No.	AS number	Description	Context
171	AS 262432:058:032	Flattened spherical clay loom weight with a perforation 0.5 cm wide. H. 2.7 cm; D. 3.7 cm; Wt. 28.35 g (Fig. F6.2)	Floor
172	AS 262432:058:034	Small disc made of lead, roughly cut to shape. Th. 0.4 cm; D. 1.4 cm.	Floor
173	AS 262432:058:044	Iron slag. L. 3.5 cm; W. 2.5 cm; Wt. 42.57 g.	Floor
174	AS 262432:051:003 AS 262432:051:005	Bronze fragments, L. < 1.5 cm.	Room fill
175	AS 262432:051:004	Bent bronze nail with a thicker end. L. 6.4 cm; Th. 0.4 cm.	Room fill



Fig. F6.2: Loom weight: AS 262432:058:032 (171). Photo by Andrea Squitieri.

F6.1 The stamp seal AS 261432:011:028

Veronica Hinterhuber

The small lapis lazuli stamp seal (AS 261432:011:028) was found right on the floor of Room 2 (deposit Locus:261432:011 of NT1 2023 Phase 5) in the western part of Building A.

(159)

AS number: AS 261432:011:028

Measurements: L. 1.6 cm, W. 1 cm, H. 0.6 cm, Wt. 2.00 g.
Material and colour: lapis lazuli, blue.

Description: Nearly rectangular stamp seal, perforated lengthwise for suspension. The flat, wide surface shows a roughly engraved scene of a quadruped turning to the right towards a seated figure, the reverse is executed with chamfered edges.

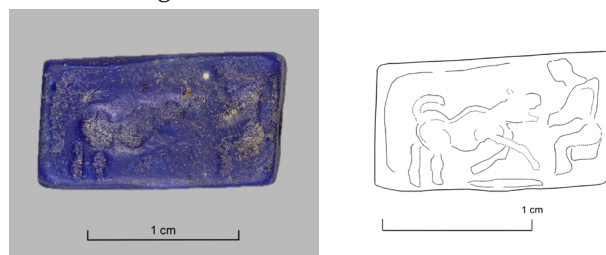


Fig. F6.1: Stamp seal made of lapis lazuli (159). Photo by Andrea Squitieri, drawing by Veronica Hinterhuber.

Comparisons: Lot 346 in Bonhams Antiquities auction catalogue, London, 21 April 2005.¹⁵⁰

Discussion: Our seal shows a quadruped, likely a bull, in front of a seated figure. The animal closely resembles the bull depicted on a rectangular chalcedony stamp seal, or bezel, kept in the British Museum (BM 119800; acquired 1867),¹⁵¹ suggesting that it too should be identified as a bovine. A less close parallel is attested in the depiction of a bull on a round lapis lazuli stamp seal kept in the Penn Museum (registration no. B9405; Babylonian Expedition Purchase, 1891).¹⁵² As they originate from the art market, neither the British Museum nor the Penn Museum examples can be safely dated.

However, an exact duplicate in shape, material and decoration was sold in 2005 in an antiquities auction at Bonhams London as part of a large collection of seals and

¹⁵⁰ <https://www.bonhams.com/auctions/11597/lot/346/> [accessed 26 August 2023]. All objects are said to originate from a German private collection, mainly acquired between 1974 and 1977. For references, see Göbl 1973; Brunner 1978; Gignoux 1978.

¹⁵¹ Bivar 1969, pl. 15: EM 13; see also https://www.britishmuseum.org/collection/object/W_1867-0323-6 [accessed 26 August 2023].

¹⁵² Legrain 1925, no. 794; see also <https://www.penn.museum/collections/object/116377> [accessed 26 August 2023].

seal rings “from a German private collection.” Apart from dating all these objects to the 4th–6th centuries AD, i.e. the Sasanian period, without specifying any chronological criteria, the catalogue provides only a photo of the entire group of objects and no individual information; the present whereabouts of the collection are unknown.

The find from Assur raises serious doubts about the dating of the duplicate seal to the Sasanian period. The most popular shape of Sasanian-period seals was a globular form with flat bases, although rectangular or lozenge shapes sometimes occur.¹⁵³ Examples of rectangular seals or bezels and their impressions were found in the excavation of the Sasanian site of Qasr-i Abu Nasr in the Fars Province of Iran, all with animal figures and without inscriptions.¹⁵⁴ None of these, however, are direct parallels to our seal in either shape or iconography. Our seal and its duplicate in the collection sold in 2005 by Bonhams should therefore not be described as Sasanian, as the find context of our seal, for which a radiocarbon date is available (floor: Locus:261432:011, see §D1.3), clearly indicates a Hellenistic dating.

F7. Finds from NT1 2023 Phase 4: Building B

The finds retrieved from the Unroofed Area 4 of Building B are presented in the following order:

- finds from the substructure of the floor;
- finds from the occupation level; and
- finds from upper deposits.

¹⁵³ Niknami/Naderi 2016, 7; von der Osten 1934, 10. For the different forms and shapes of Sasanian seals, see Göbl 1973, pl. 40.

¹⁵⁴ For rectangular Sasanian seal impressions/seals from Qasr i-Nasr, see Harper 1973, 101: D.304 (lioness), D.311–312 (feline, wolf). For a rectangular example with rounded edges, see Harper 1973, 103: D.398 (bull walking to the right). For other examples of seal impressions, see Gyselen 2007, 22, 162: I/59c (lion). Another comparison is the rectangular chalcedony stamp seal, or bezel, showing a reclining bull that was acquired by Charles Masson in Kabul in the 1830s and that dates either to the Sasanian or the Kushano-Sasanian period; it is now in the British Museum (BM 1880.3581); see Callieri 1997, 64–65, pl. 5: no.2.22 and also https://www.britishmuseum.org/collection/object/A_1880-3581 [accessed 26 August 2023].

Unroofed Area 4: floor substructure		
No.	AS number	Description
176	AS 262432:073:002	Base to rim fragment of a mortar bowl. The base is flat, the wall straight and the rim is rounded with some parts broken off. The inner cavity surface was smoothed through prolonged use. The maximum thickness is 4 cm at the point where the wall meets the base. The base is 1.5 cm thick, the rim about 2 cm. The cavity originally had a triangular section, as the inner and outer profiles do not match. The material is compact basalt. L. 12 cm, reconstructed D. 30 cm
177	AS 262432:073:004	Fragment of a possible lower grinding stone. The dorsal side is flattish and rough, the working surface is flat and not so smooth. The material is porous basalt. L. 14.5 cm; W. 8 cm; H. 5 cm.
178	AS 262432:061:003	Thin and long bronze fragment, slightly wider at one end. L. 1.5 cm; Th. 0.2 cm.
179	AS 262432:061:004	Six tiny glassy fragments, the largest being 1.8 cm long. They are covered by a brownish-grey patina and show a greenish colour in the break with some iridescence.
180	AS 262432:061:005	Shell fragment. L. 2.8 cm; W. 1.2 cm; H. 0.2 cm
181	AS 262432:061:006	Two shapeless bronze fragments that were found together. The larger is 1.5 cm long.
182	AS 262432:061:007	Ovoid-shaped stone showing several pits on one rounded end, while the other end and the rest of the surface are very smooth. It can be interpreted as a pounder. The stone is beige with darker greyish veins, possibly limestone. L. 11.6 cm; W. 7.4 cm; H. 6.5 cm.
183	AS 262432:061:008	Flat and small bronze sheet, found attached to a baked brick fragment. L. 2 cm; W. 1 cm; H. 0.1 cm.
184	AS 262432:061:009	Door socket made of gypsum with broken edges, possibly rectangular in origin. At the centre is a shallow rounded depression 1.1 cm deep and with a diameter of 3.5 cm. Inside the depression, the surface is very smooth and shows tiny circular grooves. L. 17 cm; W. 11 cm; H. 3.5 cm.
185	AS 262432:061:010	Flint flake fragment with ripple marks visible on both surfaces L. 1.6 cm; W. 1 cm; H. 0.4 cm.

Unroofed Area 4: floor substructure		
No.	AS number	Description
186	AS 262432:061:011	Terracotta figurine fragment (Fig. F7.1)
187	AS 262432:061:012	Bronze slag. L. 3.6 cm; W. 3.2 cm; Wt. 37.32 g.
188	AS 262432:061:013	Rounded pebble with a polished surface. It may have been a weight. The stone is greyish-brown, perhaps limestone. L. 2.4 cm; W. 2.2 cm.
189	AS 262432:061:014	Long iron fragment, highly corroded. L. 2.8 cm; H. 0.8 cm.

(186)

AS number: AS 262432:061:011

Material: Terracotta

Dimensions: L. 4.2 cm; W. 3.5 cm; Th. 3.2 cm.

Description: Figurine fragment of a male head, showing a helmet (or hat) with a (broken) ridge on the top, and one wide flap covering the left ear (the right side is broken off). The eyes are represented by two tiny bumps very close to the nose. Below, it seems like a long beard is visible with a triangular shape. The neck is broken.

Comparisons: Figurine fragments representing male heads with a beard and hat were previously found in As-sur.¹⁵⁵



Fig. F7.1: Figurine fragment of a male head: AS 262432:061:011 (186). Photo by Andrea Squitieri.

Unroofed Area 4: occupation level				
No.	AS number	Description	Context	
190	AS 262432:049:003	Shapeless and corroded iron fragment. L. 1.6 cm.	Fill of pit Locus: 262432:048	
191	AS 262432:049:004	Long fragment of bronze, with a flattish section. Maybe from a nail shaft. Highly corroded. L. 4 cm; Th. 0.8 cm.		
192	AS 262432:049:006	Loom weight (Fig. F7.2)		
193	AS 262432:049:007	Loom weight		
194	AS 262432:049:005	Figurine fragment (Fig. F7.3)	Fill covering installation Locus: 262433:071	
195	AS 262433:070:003	Long bronze fragment, slightly curved. Possibly part of a nail or a pin shaft. L. 1.5 cm; Th. 0.4 cm.		
196	AS 262432:063:005	Flat bronze object with a T shape, slightly curved. Three small shapeless bronze fragments were found next to it. L. 3.8 cm; W. 4.1 cm; H. 0.3 cm.		Fill of pit Locus: 262432:062
197	AS 262432:063:007	Squarish bronze sheet. L. 1.2 cm; W. 1.1 cm; Th. 0.1 cm.		
198	AS 262432:063:008	Tiny bronze sheet fragment, slightly curved. L. 0.6 cm; Th. 0.1 cm.		
199	AS 262432:063:003	Shell with a wide perforation on its side. L. 1.4 cm; W. 0.9 cm.		
200	AS 262432:063:004	Broken shell fragment, possibly part of a large cowrie shell (see AS 262432:063:006). L. 4.4 cm; W. 2.6 cm; H. 1.7 cm.		
201	AS 262432:063:006	Half fragment of a long shell with indentation and smooth surface. It looks like a large cowrie shell. L. 7.4 cm; W. 1.5 cm; H. 2 cm.		

¹⁵⁵ Klengel-Brandt/Onasch 2020, cat. nos. 782-825.

Unroofed Area 4: occupation level			
No.	AS number	Description	Context
202	AS 262433:063:003	Fragment of a tripod stilt (also called kiln support). Only the end of one arm is preserved, with a T shape. L. 4.4 cm; W. 2.8 cm; H. 1.8 cm.	Fill covering the previous features
203	AS 262433:063:004	Unworked shell. L. 1.8 cm; W. 2 cm; H. 0.4 cm.	
204	AS 262433:063:005	Flat whetstone broken at both ends. The edges are rounded, and its surface is polished and shows tiny striations. The stone is fine-grained and of grey colour. L. 3.5 cm; W. 2.8 cm; H. 1 cm.	
205	AS 262433:063:006	Stone vessel rim, flat, 1 cm wide. The body is curved and 1 cm thick. It possibly belongs to a bowl. At the rim level, a ledge handle is present: 3.5 cm long and 0.5 cm wide. The inner and outer surfaces are polished. The stone is beige with some dark spots, possibly hard limestone. L. 6 cm; W. 3.5 cm; reconstructed D. 17 cm.	
206	AS 262432:050:006	Biconical bead, with a diameter of 0.6-0.9 cm. The perforation has a 0.2 cm diameter. The stone is dark red, mottled black. L. 1.5 cm; Wt. 1.41 g.	
207	AS 262433:063:007 AS 262432:050:004 AS 262432:050:005 AS 262432:050:009	Iron fragments with a L. < 2.8 cm.	
208	AS 262432:050:003 AS 262432:050:007 AS 262432:050:008 AS 262432:050:010 AS 262432:064:003	Bronze fragments with a L. < 2.2 cm.	
209	AS 262433:062:003	Fragment of a bronze pin with a curved tip. L. 3 cm; D. 0.5 cm.	

Unroofed Area 4: occupation level			
No.	AS number	Description	Context
210	AS 262433:055:003	Broken whetstone with two corners preserved. The surface is polished and shiny. Made of compact basalt. L. 6.2 cm; W. 4.2 cm; H. 2.2 cm.	Fill of pit Locus: 262433:059
211	AS 262433:055:004	Long bronze fragment with a squarish section, maybe part of a nail shaft. Corroded L. 2.7 cm; D. 0.5 cm.	
212	AS 262433:055:005	Loom weight	
213	AS 262433:055:006	Thin bronze fragment L. 0.9 cm; W. 0.6 cm; H. 0.1 cm.	
214	AS 262433:055:007	Baked brick secondarily reused and cut to shape to serve as a rectangular door socket. On the top side, there is an off-centre circular depression, 4.5 cm in diameter and 1.5 cm deep, that displays circular grooves inside. L. 15.5 cm; W. 9.5 cm; H. 4 cm.	
215	AS 262433:055:008	Loom weight (Fig. F7.4)	
216	AS 262433:053:002	Loom weight (Fig. F7.5)	Fill of pit Locus: 262433:052

(192, 193, 212, 215, and 216)

AS numbers: (192) AS 262432:049:006; (193) AS 262432:049:007; (212) AS 262433:055:008; (215) AS 262433:055:005; (216) AS 262433:053:002

Material: Clay

Dimensions: (192) H. 3 cm; D. 4.9 cm; Wt. 43.59 g; (193) L. 4 cm; W. 3.4 cm; H. 3 cm; (212) H. 2.8 cm; D. 3.2 cm; Wt. 22.63 g.; (215) L. 3 cm; W. 2.4 cm (216) H. 3.5 cm; D. 3.9 cm; Wt. 44 g.

Description: (192) Flattened spherical loom weight. The perforation is 0.9 cm wide. (193) Damaged loom weight whose original measurements could not be reconstructed. Only the central part is preserved, with the perforation measuring 0.5 cm in diameter. (212) Biconical loom weight with a slightly off-centre perforation which has a diameter of 0.9 cm. (215) Fragment of a spherical loom weight, with a perforation of 0.5 cm in diameter. (216) Flattened spherical loom weight, damaged on one side. The perforation is 0.5 cm wide.



Fig. F7.2: Loom weight: AS 262432:049:006 (192). Photo by Andrea Squitieri.



Fig. F7.4: Loom weight: AS 262433:055:008 (215). Photo by Andrea Squitieri.



Fig. F7.5: Loom weight: AS 262433:053:002 (216). Photo by Andrea Squitieri.

(194)

AS number: AS 262432:049:005

Material: Terracotta

Dimensions: L. 3.1 cm; W. 3 cm; Th. 1.2 cm.

Description: Fragment of a terracotta figurine showing a male torso with an accentuated waist curve. Parts of the neck, arms, legs, and male genitalia are preserved.

Comparisons: This fragment may belong to a figurine depicting a horseman. Similar figurines have been previously found in Assur.¹⁵⁶



Fig. F7.3: Fragment of a terracotta figurine of a male torso: AS 262432:049:005 (194). Photo by Andrea Squitieri.

Unroofed Area 4: upper deposits		
No.	AS number	Description
217	AS 262432:059:005 AS 262432:059:006 AS 262432:059:009	Bronze fragments with L. < 1 cm.
218	AS 262432:059:008	Two highly corroded iron fragments found together, though they do not attach. L. 3.2; D. 0.8 cm.
219	AS 262432:059:002	Flat sheet made of lead, with irregular edges and surfaces. A perforation is visible off-centre. L. 1.9 cm; W. 1.2 cm; Th. 0.2 cm; Wt. 4.65 g.
220	AS 262432:059:004	Blackish glass fragment. L. 0.7 cm.
221	AS 262432:059:007	Terminal end of a lower grinding stone with irregular edges, a flat and rough dorsal side, and a flat working surface. Made of porous basalt. L. 12 cm; W. 11 cm; H. 4 cm.
222	AS 262433:051:002	Rectangular stone fragment, broken on both ends. The surface is polished and the edges are rounded. Along the edges, the stone is very polished and shiny. Likely used as a whetstone. L. 7.5 cm; W. 4 cm; H 2.4 cm.
223	AS 262433:051:004	Small bronze fragment that looks like the terminal part of a larger item. L. 1.5 cm; W. 1 cm.
224	AS 262433:051:005	Perforated pottery sherd, roughly cut into a disc shape with irregular edges and surfaces. The perforation is in the centre and has a diameter of about 0.4 cm. H. 1.6 cm; D. 6.5 cm; Wt. 64 g.

¹⁵⁶ Klengel-Brandt/Onasch 2020, cat. nos. 646-675.

Unroofed Area 4: upper deposits		
No.	AS number	Description
225	AS 262433:051:006	Small bronze ring with overlapping ends. The surface is molded into a spiral pattern. D. 1.3 cm (Fig. F7.6)
226	AS 262433:051:007	Three-legged stilt (also called kiln support), with only one preserved leg. L. 4.5 cm; W. 4 cm; H. 3 cm.
227	AS 262433:051:009	Thin bone tool with rounded edges and a pointed end, possibly used as a tool to perforate something (e.g., textile). It is broken into two fragments. L. 6 cm; W. 1.5 cm; H. 0.2 cm.
228	AS 262433:051:011	Reworked brick fragment with a flattish surface on which a small circular depression was carved off-centre, having a 0.6 cm diameter and a conic section. The other side of the object is curved. L. 4.1 cm; W. 4 cm; H. 3 cm.
229	AS 262433:051:012	Thick glass fragment with a slight depression on one side that may indicate the inner side of a base vessel. Not much of it is preserved to allow identification of the shape. The item is covered by a whitish patina with darker spots. L. 3 cm; W. 1.8 cm; H. 0.9 cm.
230	AS 262433:051:013	Flint flake of triangular shape, with some tiny ripple marks visible on one side. L. 1.8 cm; W. 0.8 cm; H. 0.2 cm.
231	AS 262432:032:002	Rim fragment of a basalt vessel, flat with a curved profile, likely belonging to a bowl/mortar bowl. The outer surface is rough while the inner surface is very smooth. L. 5 cm; W. 5 cm; H. 1 cm; D. 35 cm.
232	AS 262432:032:003	Bronze fragment, perhaps of a nail or pin shaft. L. 2 cm; D. 0.4 cm.
233	AS 262432:047:002 (also Vessel B-04-V01)	Ceramic beaker with a nipple base (§E1.4)



Fig. F7.6: Bronze ring:
AS 262433:051:006 (**225**).
Photo by Andrea Squitieri.

Unroofed Area 4: upper deposits		
No.	AS number	Description
234	AS 262432:047:005	Fragment of a flat bronze disc, highly corroded. L. 2.5 cm; Th. 0.9 cm.
235	AS 262433:032:002	Chunk of soil with a 5 cm wide green mark, left by the contact with a bronze item. L. 6.5 cm; W. 5 cm.

F8. Finds from NT1 2023 Phase 3: Grave 5

Grave 5 was radiocarbon dated to 770-542 calBC and 775-545 calBC (95.4 % probability; **§D1.3**). The finds retrieved from the grave are listed in the table below.

No.	AS number	Description	Context
236	AS 262432:071:003	Bronze fibula (Fig. F8.1)	Lower grave fill
237	AS 262432:071:004	Bronze fragment. L. 1.2 cm.	
238	AS 262432:070:005 (also Vessel G05-V01)	Miniature glazed jar (§E1.5)	Upper grave fill

(**236**)

AS number: AS 262432:071:003

Material: Bronze

Dimensions: L: 4.5 cm; W: 3.4 cm.

Description: Bronze fibula whose bow is preserved while the pin is missing. The latter was attached to a terminal segment folded as a spiral at one end of the bow, on the opposite side the pin was accommodated into a folded end. The top of the bow is 0.4 cm thick; it is bent but not pointed. On both sides, the bow is decorated with two hatched block segments. The latter are both 0.6 cm wide, while one is 1.2 cm long and the other 1 cm long.

Comparisons: In the classification proposed by Friedhelm Pedde, this fibula belongs to type C8, which he dates



Fig. F8.1: Bronze fibula:
AS 262432:071:003 (**236**).
Photo by Andrea Squitieri.

to the 7th and the beginning of the 6th century BC.¹⁵⁷ Eight fibulae of this type have been found in Assur in Andrae's excavations; other parallels come from Dur-Shar-ruken (Khorsabad), Kalhu (Nimrud) and Dur-Katlimmu (Tell Sheikh Hamad).¹⁵⁸ This type is also found in the Levant, specifically at Tell Sweyhat, Deve Höyük, Byblos, Sarepta and Megiddo.¹⁵⁹

F9. Finds from NT1 2023 Phase 2

The finds listed below come from the fills covering the walls and the installation of NT1 2023 Phase 2.

No.	AS number	Description	Context
239	AS 262432:074:004	Base to rim fragment of a small basalt mortar bowl. The rim is rounded, the base is flat and 2 cm thick, and the outer profile is curved. The cavity is 2.4 cm deep and has a flat base. Reconstructed D. 12 cm. L. 7 cm; Th. 3 cm.	Fills covering the walls
240	AS 262432:074:005	Corner fragment of a possible square stone bowl, with a flat base and upright wall, which is 1.5 cm thick. The stone is fine-grained and compact. Its colour is greyish with some reddish discolourations. L. 5.2 cm; W. 3 cm; H. 3.5 cm.	
241	AS 262432:074:003	Elongated bronze fragment. L. 1.4 cm; Th. 0.4 cm.	
242	AS 262432:067:003	Shapeless bronze fragment with dimensions < 1 cm.	
243	AS 262433:075:002	Cylindrical bead fragment, broken longitudinally. Light blue colour, possibly Egyptian blue. L. 0.6 cm; D. 0.2 cm.	Fills covering the drain installation Locus: 262433:074

No.	AS number	Description	Context
244	AS 262433:075:003	Disc-shaped bronze object with a perforation of 0.2 cm in diameter. L. 1.8 cm; W. 1.5 cm; Th. 0.6 cm.	Fills covering the drain installation Locus: 262433:074
245	AS 262433:076:003	Shapeless bronze fragment. L. 2 cm	
246	AS 262433:076:004	Elongated bronze fragment. L. 1.4 cm; Th. 0.4 cm.	
247	AS 262433:076:005	Shapeless iron fragment. L. 1.5 cm.	
248	AS 262433:072:003	Flattened spherical pebble with a smooth surface showing some weathering. Possibly made of limestone. D. 4.5 cm.	
249	AS 262433:072:004	Unworked shell fragment. L. 3.6 cm; W. 2.8 cm.	

F10. Finds from the NT1 2023 Phase 1

NT1 2023 Phase 1 was identified within a deep sounding that reached the virgin soil. From the fill of a pit cutting the virgin soil, a piece of charcoal was collected and radiocarbon dated to 1506-1440 calBC (95.4 % probability; §D1.3).

No.	AS number	Description	Context
250	AS 262432:086:001	Flint flake with traces of retouching. L. and W. 1.5 cm; Th. 0.5 cm.	On the floor Locus: 262432:086 (visible in the section)
251	AS 262432:079:002	Limestone sphere covered with patina. D. 1.8 cm.	Fill of pit cutting the virgin soil
252	AS 262432:076:004	Shell fragment with perforation. L. 1.3 cm; W. 1 cm; H. 0.6 cm.	Fill of the deep sounding
253	AS 262432:076:006	Shell bead with cylindrical shape. L. 1.2 cm; Th. 0.6 cm.	
254	AS 262432:076:005	Carnelian bead fragment. L. 1.8 cm.	

¹⁵⁷ Pedde 2000, 245-250.

¹⁵⁸ Pedde 2000, pls. 55-56.

¹⁵⁹ Pedde 2000, pls. 55-56.

No.	AS number	Description	Context
255	AS 262432:076:007	Elongated bronze fragment with squared section, maybe the shaft of a pin. L. 2.4 cm; Th. 0.4 cm.	Fill of the deep sounding

F11. Finds from NT1 2023 arranged by main categories

F11.1 Stone tools

32 stone tools were collected, all in fragmentary conditions, ranging from grinding devices, mortars, stone vessels, pestles, whetstones, pounders, and polishers. The fragments collected are made of basalt, except for five which are made of limestone. Assur lies in a geological zone rich in carbonates, marl limestone and gypsum, conglomerates and clastics, whereas igneous rocks such as basalt can be found further to the north and north-east, towards the mountains.¹⁶⁰ Though the sample is quite small, it seems that it was not a problem for the inhabitants of Assur to acquire basalt from the sources located in the mountains. The highest number of tools came from the upper deposits of the chamber tomb (10 out of 32), which may indicate that they had been reused in the tomb's walls as building material.

F11.2 Loom weights

Six clay loom weights were found, which have a flattened spherical shape,¹⁶¹ that is sometimes also called a "doughnut shape". Their weights vary from 22.63 g to 44.00 g. Five (192, 193, 212, 215, 216) came from the occupation level of Unroofed Area 4 (NT1 2023 Phase 4). One (171) was found on the floor of Room 3 (Building A) (NT1 2023 Phase 5).

F11.3 Personal ornaments

Several bronze and iron fragments have been collected which could not be assigned to a specific object type. Others, which were in better condition, could be identified as earrings, rings and fibulae. These finds are all mostly

connected to funerary contexts. Four out of five earrings came from the chamber tomb, and one from Grave 3. Three rings derive from the chamber tomb, one from the looted Grave 2 and one from Unroofed Area 4. Finally, one bronze fibula (29) was found inside the chamber tomb's walls, while another (236) came from the fill of Grave 5.

Among the personal ornaments, beads constitute by far the largest group. The two largest concentrations came from the looting pit that destroyed Grave 2 (76 beads, 10-16) and from the floor of Subdivision 4 of the chamber tomb (22 beads, 61-75). Additionally, four beads were found in Grave 3 (134-6, 139), and one in Grave 4 (150). Overall, the beads are made of glass/frit, faience, stone (mostly carnelian, though agate and steatite are also attested), bronze, coral and shell. They are in such shapes as ring, spherical, oblate, cylindrical, barrel, truncated conic, convex conic, dome, and triangular. Shapes and raw materials do now show any chronological pattern.

F11.4 Figurines

Two figurine fragments were collected: a male head (186) with a hat (or helmet) and beard, coming from the floor substructure of Unroofed Area 4; and a male torso (194) with an accentuated waist curve from the occupation level of Unroofed Area 4. They both belong to figurine types that have been found in Assur in previous excavations.

F12. Finds from the sondage linked to the 2002 SBAH trench

In the sondage opened in the baulk between NT1 2023 trench and the 2002 SBAH trench, "Room 5" and "Room 6" were excavated down to the floors (SD3). The finds collected from these rooms are described in the table below.

F12.1 "Room 5"

No.	AS number	Description	Context
259	AS 262432:066:007 AS 262432:066:009	Two bronze fragments, L. < 1 cm.	Floor deposit
260	AS 262432:066:011	Snail shell, no perforation visible. D. 1.1 cm.	Floor deposit
261	AS 262432:056:002	Cylindrical bronze item made of a sheet wrapped on itself. One end is open, while the other end is folded. L. 6.2 cm; D. 0.6 cm.	Lower fill

¹⁶⁰ Sissakian/Saeed 2012, fig. 8.

¹⁶¹ For the loom weight shape terminology, see Mårtensson/Nosch/Strand 2009, fig. 2.

No.	AS number	Description	Context
262	AS 262432:056:005	Long bronze fragment with a circular section, one end is rounded, the other is broken. Possibly belonging to a nail. L. 2.1 cm; D. 0.3 cm.	Lower fill
263	AS 262432:056:006	Bent iron filament, in a shape that resembles modern hair tweezers. Possibly modern. L. 4 cm; W. 1 cm; Th. 0.2 cm.	
264	AS 262432:056:007	Bent iron filament, roughly circular and very thin. No signs of heavy corrosion, hence possibly modern. Th. 0.2 cm; D. 2.5 cm.	
265	AS 262432:056:008	Bronze ring, 0.3 cm thick, broken in two fragments. D. 1.5 cm.	
266	AS 262432:056:009	Bent and thin iron filament with no signs of heavy corrosion, hence possibly modern. L. 2 cm, W. 1.8 cm; Th. 0.2 cm.	
267	AS 262432:056:010	Bent iron filament with no signs of heavy corrosion, hence possibly modern. L. 2.5 cm; W. 2 cm.	
268	AS 262432:056:011	Metal slag. L. 4 cm; W. 2.7 cm; Th. 1.3 cm; Wt. 15.22 g.	
269	AS 262432:056:013	Sub-spherical bronze fragment, corroded. D. 1.5 cm.	
270	AS 262432:056:014	Iron slag, L. 2 cm.	
271	AS 262432:056:015	Bronze fragment with a slightly oval shape. L. 2 cm; W. 1.1 cm; Th. 0.5 cm.	
272	AS 262432:056:016	Long and thin bronze fragment, likely part of a needle shaft. Corroded. L. 3.2 cm; Th. 0.2 cm.	
273	AS 262432:056:018	Long bronze fragment, maybe the shaft of a nail or pin L. 1.7 cm; Th. 0.3 cm.	

No.	AS number	Description	Context
274	AS 262432:056:004	Long and thick cylindrical bead with one preserved pointed end, the other is broken off. The perforation is 0.4 cm wide. The stone is whitish with black discolouration and banded. L. 5.3 cm; D. 1.4 cm.	Lower fill
275	AS 262432:056:017	Unworked shell. L. 2.5 cm; W. 1.5 cm; Th. 0.2 cm.	
276	AS 263432:004:002	White glazed miniature amphora (§E1.8)	
277	AS 262432:010:003	Half preserved bone item with a cylindrical shape and a ridge protruding from the mid-point. The upper and lower extremities look finished and the item's surface is smoothed and darkened. Perhaps used as a token. Th. 1.1 cm; D. 1.6 cm.	Upper fill
278	AS 262432:010:004	Spherical bronze fragment, highly corroded. D. 0.4 cm.	
279	AS 262432:010:005	Shapeless fragment showing a mixed iron (red) and bronze (green) corrosion. L. 1.3 cm; W. 2.8; Wt. 11 g.	
280	AS 262432:010:006	Terracotta figurine fragment (Fig. F12.1)	

(280)**AS number:** AS 262432:010:006**Material:** Terracotta**Dimensions:** L. 3.6 cm; W. 1.5 cm.**Description:** Fragment of a figurine in the shape of a horse's head and neck. The hair along the neck and on the head as well as the ears are preserved, while the nose is partially broken. The details of the eyes are not visible. No details of the harness are present.**Comparisons:** Similar figurines have been previously found in Assur.¹⁶²

162 Klengel-Brandt/Onasch 2020, cat. nos. 1207-1210.



Fig. F12.1: Fragment of a figurine in the shape of a horse's head and neck: AS 262432:010:006 (280). Photo by Andrea Squitieri.

F12.2 "Room 6"

No.	AS number	Description	Context
281	AS 263432:005:003	Bronze fragment, L. 0.5 cm.	Fill in between lower and upper floor
282	AS 263432:005:004	Bitumen fragments	Fill in between lower and upper floor
283	AS 263432:002:004	Flattened spherical loom weight made of clay. H. 3.5 cm; D. 4.8 cm; Wt. 67 g.	On the upper floor

F13. Finds from cleaning the 2002 SBAH trench

During the cleaning of the western section of the 2002 SBAH trench and of some of the excavated rooms, we collected seven small finds, described in the table below.

No.	AS number	Description
284	AS 263433:001:001 AS 263433:001:003	2 clay loom weights (Fig. F13.1)
285	AS 263433:001:005	Fragment of a lower grinding stone, with a convex dorsal side, a flattish working surface slightly concave and smoothed through use, and rounded edges. It is made of semi-porous basalt. L. 13.5 cm; W. 15 cm; Th. 4.5 cm.
286	AS 263433:001:006	Long iron fragment with a circular section, highly corroded. L. 5.8 cm; D. 0.7 cm.
287	AS 263433:001:007	Shapeless bronze fragment, L. 1.3 cm.
288	AS 263433:001:008	Ceramic miniature wheel (Fig. F13.2)
289	AS 263433:001:009	Half preserved door socket cover stone (Fig. F13.3)

(284)

AS numbers: (1) AS 263433:001:001; (2) AS 263433:001:003

Material: Clay

Dimensions: (1) H. 2.80 cm; D. 5.2 cm; Wt. 87 g; (2) H. 4 cm; D. 5.5 cm; Wt. 102 g

Description: Flattened spherical loom weights. The perforation of both measures 1.5 cm on one side and 0.8 cm on the other. Both are partially damaged.



Fig. F13.1: Loom weight: AS 263433:001:001 (284). Photo by Andrea Squitieri.

(288)

AS number: AS 263433:001:008**Material:** Ceramics**Dimensions:** D. 5 cm; Th. 0.5 cm (edges) - 2 cm (centre).**Description:** Ceramic miniature wheel with perforation in the centre. At the edges, it is 0.5 cm thick, while around the perforation it reaches a thickness of 2 cm.**Comparisons:** Such wheels, already found in Assur, were originally parts of miniature wagons.¹⁶³

Fig. F13.2: Ceramic miniature wheel:
AS 263433:001:008 (288).

Photo by Andrea Squitieri.

(289)

AS number: AS 263433:001:009**Material:** Gypsum**Dimensions:** L. 56 cm; W. 40 cm; Th. 8 cm.**Description:** Half preserved door socket cover stone, with a rectangular shape, made of gypsum. The edges are slightly damaged. The hole in the centre has a diameter of 23 cm and it is surrounded by a profile made of three flat steps. It was found lying in one of the excavated rooms of the SBAH trench and was already visible upon our arrival in early February 2023.**Comparisons:** This type of door socket cover is typically Assyrian. Larger examples were found at Dur-Sharruken (Khorsabad),¹⁶⁴ Kalhu (Nimrud),¹⁶⁵ Dur-Katlimmu on the Khabur (Tell Sheikh Hamad),¹⁶⁶ Tepe Giyan in western Iran,¹⁶⁷ and Dor on the Mediterranean coast.¹⁶⁸

Fig. F13.3: Half preserved door socket cover
stone: AS 263433:001:009 (289).

Photo by Andrea Squitieri.

F14. Surface finds without stratigraphic context

The following finds were collected outside the excavation area, on the surface of Assur New Town during the magnetometer survey (§C2). They were assigned to the generic Locus:000001:001.

No.	AS number	Description
290	AS 000001:001:001 AS 000001:001:002 AS 000001:001:003 AS 000001:001:006 AS 000001:001:007 AS 000001:001:008	Bricks and brick fragments with cuneiform inscriptions of various Assyrian kings (§G1.2)
291	AS 000001:001:004	Brick with an incised game board (§G1.4)
292	AS 000001:001:005	Highly corroded iron arrowhead. L. 7 cm; W. 0.5 cm.

¹⁶³ Klengel-Brandt/Onasch 2020, cat. nos. 1808-1877.

¹⁶⁴ Loud 1936, figs. 101, 120; Loud/Altman 1938, pl. 20.

¹⁶⁵ Oates/Oates 2001, fig. 97.

¹⁶⁶ Kreppner/Schmidt 2013, 281, fig. 294.

¹⁶⁷ Reade 1995, 40, pl. IIa.

¹⁶⁸ Gilboa/Sharon 2016, 244, fig. 22.2.

G. Epigraphic finds from Assur, 2023

G1. Cuneiform finds from Assur, 2023

Karen Radner

Most of the cuneiform texts presented here are bricks, some complete and some fragmentary, with the inscriptions of various kings of Assyria from the 13th to the 8th century BC (namely Adad-nerari I, Shalmaneser I, Shalmaneser III and Tiglath-pileser III) that were collected from the surface (Texts 4-9). Three small brick fragments (Texts 1-3) were unearthed during the 2023 excavation but in a much later building context: around one and a half millennia separate the creation of these bricks in the 13th century BC under Adad-nerari I (1305-1274 BC) from their reuse as part of the walls constructed for a chamber tomb in the early centuries AD. How and when a large stone block from the Aššur temple with the inscription of Sennacherib (704-681 BC) ended up in front of the excavation house is unclear but as it does not seem to have been published before, we include it here as Text 10.

The three appendices to this chapter present a brick with an incised gameboard found on the surface that may or may not be an ancient artefact; a hitherto unpublished brick from Assur with an inscription of the mid-second-millennium-BC ruler Aššur-nerari I that was taken to Germany in 1918 and is now in a private collection in Munich; and a brick from Kar-Tukulti-Ninurta with an inscription of Tukulti-Ninurta I (1243-1207 BC) that was found on the surface during the team's visit to that site and is now stored in the excavation house.

G1.1 Bricks with royal inscriptions unearthed during the 2023 excavations

Three brick fragments with cuneiform inscriptions were found in a secondary position within the walls of the Parthian chamber tomb (§D2.3). All these small pieces can be attributed to Adad-nerari I of Assyria (1305-1274 BC), and we can assign two of the fragments with certainty to bricks commemorating his construction of the quay wall of Assur (Texts 1 and 2).

All of these bricks were originally between 5-6 cm thick and have a greenish colour that indicates an unusually

high firing temperature of more than 1000° C,¹⁶⁹ requiring the use of a substantial amount of fuel. The fragments share these notable material qualities with three other Adad-nerari bricks that were found in 2023 on the surface of various areas of Assur (Texts 4-5).

Is this high firing temperature typical for bricks created under Adad-nerari I, or more generally perhaps in the Middle Assyrian period? An autopsy of all relevant bricks from Andrae's excavations at Assur stored in the Vorderasiatisches Museum Berlin in October 2023¹⁷⁰ showed conclusively that this is not the case. Most Assyrian bricks from Assur, regardless of their date, exhibit a pinkish-red colour that indicates a firing temperature of around 700° C or a beige colour indicative of a firing temperature in the range of 750-950° C.¹⁷¹

On the other hand, the autopsy of the Berlin material demonstrated that the green colouring of the fabric is a characteristic of the bricks from the quay wall constructed by Adad-nerari I along the Tigris. The inscriptions of Text 1 (AS 262433:003:003), Text 2 (AS 262433:049:002) and Text 4 (AS 000001:001:008) mention the quay wall explicitly.

This huge building project, of which much is in place even today, was built to protect Assur against the river's spring flood. To ensure that the wall would better withstand the water, the layers of its bricks were glued together with bitumen. For the same reason, it was sensible to choose a higher firing temperature as it produces a much harder brick that would stand a better chance of bearing up against the Tigris' water masses. Such durability is not necessary for bricks used anywhere else in Assur.

¹⁶⁹ Kreppner 2006, 99; Schneider 2006, 404.

¹⁷⁰ This work was undertaken in the context of the *Royal Inscriptions of Assyria* project, headed by myself and Grant Frame. The team consisted of Jana Richter, Poppy Tushingham and myself. My thanks are due to Barbara Hellwing, the VAM's director, to Helen Gries, the curator in charge, and their staff for graciously facilitating and supporting our work from 9-13 October 2023.

¹⁷¹ Kreppner 2006, 99; Schneider 2006, 404.

Text 1: AS 262433:003:003. Brick fragment with a cuneiform inscription of Adad-nerari I of Assyria (1305-1274 BC). Measurements: *8.6 × *11.2 × 5.8 cm (**Fig. G1.1**)

This is a new example of Adad-nerari's brick inscription from the quay wall of Assur (RIMA 1 A.o.76.40). The text is stamped and arranged in a frame inscribed with four lines of well-shaped cuneiform script, of which only the final signs are preserved. There are no horizontal line divisions. The height of the lines is 2.5 cm.



Fig. G1.1: AS 262433:003:003 = Text 1. Brick fragment with a stamped inscription of Adad-nerari I (1305-1274 BC). Photo by Karen Radner.

- 1 [É.GAL ^m10-ERIM.TÁH UG]ULA
- 2 [A GÍD-DI-DINGIR UG]ULA-*ma*
- 3 [šá *ki-si-ir-ti*]
- 4 [šá IGI] ÍD

(1) “[Palace of Adad-nerari, over]seer, (2) [son of Arik-deni-ili], also [over]seer. (3) [(Brick) belonging to the faci]ng (of the quay wall) (4) [which fronts onto] the river (Tigris).”

Text 2: AS 262433:049:002. Brick fragment with a cuneiform inscription of Adad-nerari I of Assyria (1305-1274 BC). Measurements: *11.0 × *21.8 × 5.2 cm (**Fig. G1.2**)

This is another new example of Adad-nerari's brick inscription from the quay wall of Assur (RIMA 1 A.o.76.40), of which only the final sign of the second line and parts of the final sign of lines 3-4 are preserved. The text is stamped, but not with the same stamp as AS 262433:003:003 as the spacing between the signs is different. Also, this text has

horizontal rulings separating the individual lines while AS 262433:003:003 lacks this feature. The stamp has been impressed only lightly, at least on the preserved right-hand side, as the cuneiform characters are very shallow in depth and the stamp frame has not left any discernible impression. The height of the lines is 2.6 cm.

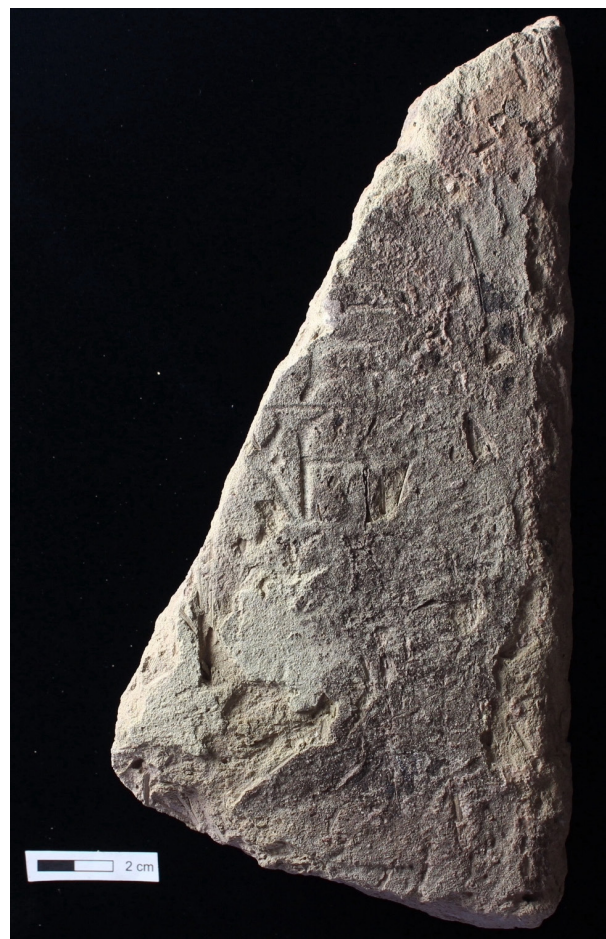


Fig. G1.2: AS 262433:049:002 = Text 2. Brick fragment with a stamped inscription of Adad-nerari I (1305-1274 BC). Photo by Karen Radner.

- 1 [É.GAL ^m10-ERIM.TÁH UG]ULA]
- 2 [A GÍD-DI-DINGIR UG]ULA]-*ma*
- 3 [šá *ki-si-ir-ti*]
- 4 [šá IGI] ÍD

(1) “[Palace of Adad-nerari, overseer, (2) son of Arik-deni-ili], also [over]seer. (3) [(Brick) belonging to the faci]ng (of the quay wall) (4) [which fronts onto the river (Tigris)].”

An autopsy of the material in the Vorderasiatisches Museum Berlin has allowed us to identify five distinct stamps that were used for Adad-nerari's brick inscription from the

VA 3135 Stamp 5



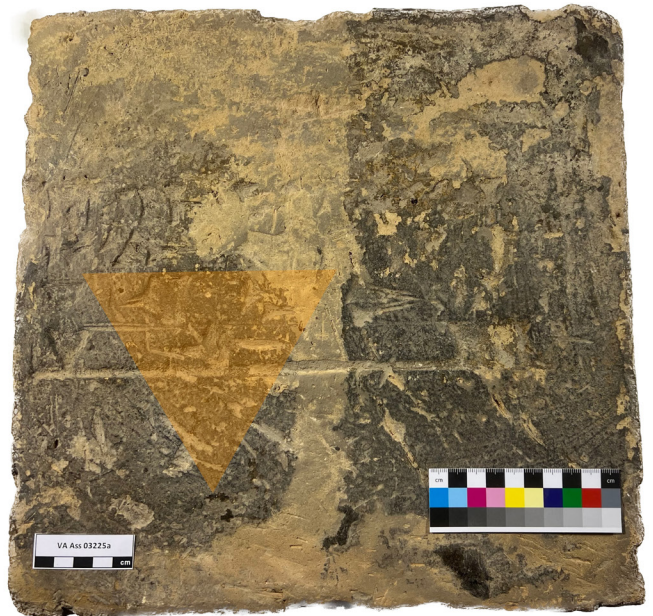
VA 6932

Stamp 1



VA Ass 3225b

Stamp 2



VA Ass 3225c

Stamp 3

VA Ass 3225a

Stamp 4

Fig. G1.3: Adad-nerari's stamped brick from the quay wall of Assur (RIMA 1 A.0.76.40): exemplars of the five different stamps currently known. Photos and composite by Karen Radner.

quay wall of Assur. Four of these stamps are impressed on bricks that survive intact: VA 6932 (RIMA 1 A.o.76.40 ex. 10); VA Ass 3225a (ex. 15); VA Ass 3225b (ex. 11); and VA Ass 3225c (ex. 16). Another stamp is attested as a partial impression on a fragmentary brick, VA 3135 (ex. 5). The most prominent diagnostic is the distribution of the signs KI and SI in line 3 and of the sign IGI in line 4 relative to each other (**Fig. G1.3**).

Three of these stamps can be shown to have been impressed on other bricks. The stamp on VA 6932 was used to create the fragmentarily preserved impressions on VA 2970 (ex. 3), VA 3140 (ex. 8) and VA Ass 3225d (ex. 19); moreover, the fragments VA 2970 and VA 3140 are most likely parts of the same brick. The stamp used for VA Ass 3225a was also impressed on the fragmentary brick VA 3137 (ex. 6), as well as AS 262433:049:002 (Text 2). The stamp of VA Ass 3225b is the same one used on the brick fragments VA 3133 (ex. 4) and AS 262433:003:003 (Text 1), as well as probably also VA 3138 (ex. 7).

Text 3: AS 262433:049:003. Brick fragment with a cuneiform inscription of Adad-nerari I of Assyria (1305-1274 BC). Measurements: *8.0 × *8.1 × 6.0 cm (**Fig. G1.4**)

This is another stamped inscription. The height of the lines is 2.7 cm, and there are no visible horizontal rulings. The stamp frame has not left any discernible impression.

It is unclear whether this inscription had only two lines or more. In the latter case, the building for which the brick had been created would have been mentioned. Whatever the case, our brick likely originated from the quay wall, like the other two pieces found in a secondary position during the 2023 excavations with which it shares the characteristic green colour.



Fig. G1.4: AS 262433:049:003 = Text 3. Brick fragment with a stamped inscription of Adad-nerari I (1305-1274 BC). Photo by Karen Radner.

The spacing of the preserved signs suggests that the inscription did not start with É.GAL. While this is rare among Adad-nerari's bricks from Assur, it is a feature of a series of bricks from the courtyard of the Aššur temple (RIMA 1 A.o.76.35). The spelling with ^dIM for the divine element in the king's name is another relatively rare occurrence in the Assur brick material and attested in bricks from the Courtyard of the Divine Emblems (RIMA 1 A.o.76.38) and the House of the Red *šudutinnu* (RIMA 1 A.o.76.33-34).

1 [ṁ^d]M-ER[IM.TÁH ...]
2 [A G]ÍD-[DI-DINGIR ...]

(1) “[Ad]ad-ne[rari, ...], (2) [son of A]rik-[den-ili, ...]”

G1.2 Bricks with royal inscriptions found on the surface

Text 4: AS 000001:001:008. Brick with two cuneiform inscriptions of Adad-nerari I of Assyria (1305-1274 BC). Measurements: 33.5 × 33.5 × 6.4 cm (**Fig. G1.5**)

This brick was found by members of the Sherqat Directorate of Antiquities and Heritage. It is the fourth attested exemplar of a series of bricks from the northern quay wall of Adad-nerari I to feature two stamped inscriptions.¹⁷² The five-line inscription is stamped into the front of the brick (RIMA 1 A.o.76.39) while the one-line inscription is stamped on one of its sides (RIMA 1 A.o.76.46). In the



Fig. G1.5: AS 000001:001:008 = Text 4. Complete brick with two stamped inscriptions of Adad-nerari I (1305-1274 BC). Photo by Karen Radner.

¹⁷² The other ones being RIMA 1 A.o.76.39 ex. 2 (VA 6921), ex. 8 (EŠ 9217) and ex. 10 (VA Ass 3238b).

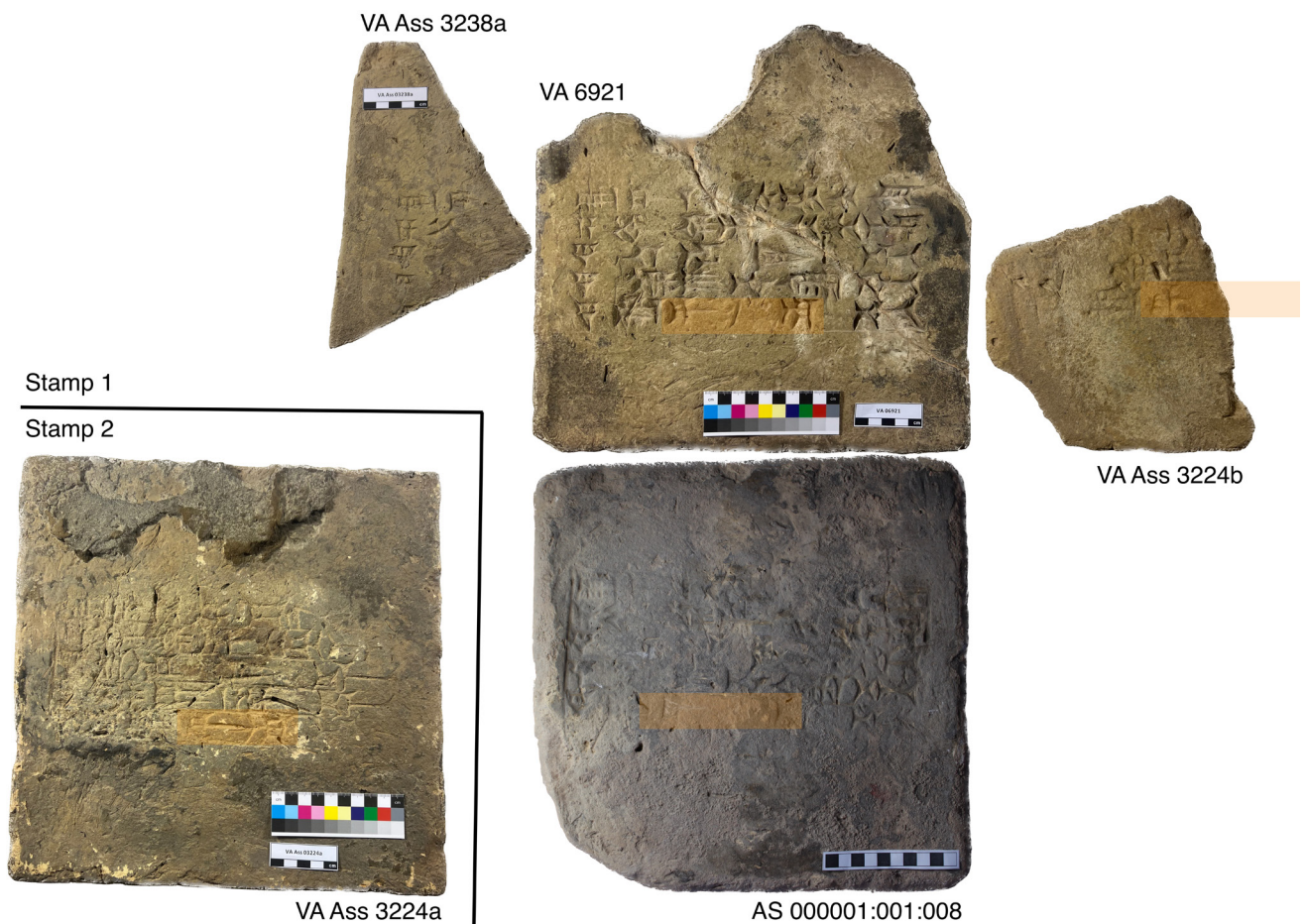


Fig. G1.6: Adad-nerari's stamped brick from the northern part of the quay wall of Assur (RIMA 1 A.0.76.39): five exemplars impressed with two different stamps. Photos and composite by Karen Radner.

case of our example, the height of the lines of both inscriptions is 2.5 cm. The inscription on the side would be upside-down if the brick was laid in a way that made the inscription on the front visible.

Front:

- 1 É.GAL¹ m₁₀-ERIM.TÁH¹ MAN KIŠ
- 2 A G¹ÍD¹-DI-DINGIR MAN KUR.Aš-šur
- 3 šá ki-¹sí¹-ir-ti
- 4 šá¹ KA¹-i na-ar-ti
- 5 šá¹ É¹.GAL-la-ti

(1) "Palace of Adad-nerari (I), king of the universe, (2) son of Arik-den-ili, king of Assyria. (3) (Brick) belonging to the facing (of the quay wall) (4) at the mouth of the canal (5) of the palace complex."

An autopsy of the material in the Vorderasiatisches Museum Berlin has allowed us to identify two distinct stamps that were used for the inscription of the northern part of Adad-nerari's quay wall. The spacing of the signs GAL and

LA in the fifth line offers a clear diagnostic indication (**Fig. G1.6**). The stamp used on the front of our example was also used for VA 6921 (RIMA 1 A.0.76.39 ex. 2, complete), VA Ass 3224b (ex. 11, fragmentary) and VA Ass 3238b (ex. 10, fragmentary) whereas another stamp was used for VA Ass 3238a (ex. 3, complete).

Side:

- 1 É.GAL¹ m₁₀-ERIM.TÁH¹ MAN KIŠ¹

"Palace of Adad-nerari (I), king of the universe."

Text 5: AS 000001:001:003. Brick fragment with a cuneiform inscription of Adad-nerari I of Assyria (1305-1274 BC). Measurements: *14.0 × *15.5 × 6.2 cm (**Fig. G1.7**)

This brick fragment was discovered by Jörg Fassbinder during the geophysical prospection of Assur, in the area between the Parthian Palace and the excavation house. The text is stamped and neatly arranged inside a rectangular

frame in two lines of very well-formed cuneiform, of which only the first few signs are preserved. The width of the stamp frame is 5.5 cm, and the height of the lines is 2.7 cm.

This is a new exemplar of a short two-line brick inscription of Adad-nerari I from Assur that does not explicitly mention the building for which it was produced (RIMA 1 A.o.76.44). However, two bricks can be demonstrated to come from the quay wall.¹⁷³ The restorations of the royal titles for the king and his father follow the better-preserved examples.



Fig. G1.7: AS 000001:001:003 = Text 5. Brick fragment with a stamped inscription of Adad-nerari I (1305-1274 BC). Photo by Karen Radner.

- 1 É.GAL ^m10-[ERIM.TÁH MAN ŠĀR]
- 2 A GĪD-D[I-DINGIR MAN KUR.Aš-šur]

(1) “Palace of Adad-[nerari, king of the universe], (2) son of Arik-de[n-ili, king of Assyria]”.

Text 6: AS 000001:001:006. Brick fragment with a cuneiform inscription of Adad-nerari I of Assyria (1305-1274 BC). Measurements: *25.5 × *19.5 × 6.2 cm (**Fig. G1.8**)

Hero Salih Ahmed (Sulaymaniyah Directorate of Antiquities and Heritage) found this brick fragment during a walk across the site, in the area southwest of the excava-

tion house. It bears the remains of a stamped inscription. The stamp was applied in such a way that the signs on the right-hand side are impressed more deeply than those on the left. The stamp frame, too, has only left its impression on the right-hand side. The height of the lines is 2.6 cm, and there are rulings between them. The bulk of the inscription’s first and second lines are preserved, but only traces of a few wedges from the top of the third line remain.

The text is most likely another new example of Adad-nerari’s brick inscription from the quay wall of Assur (RIMA 1 A.o.76.40). This is the only inscription with more than two lines where Adad-nerari and his father Arik-denili are identified with the title “overseer”, the most likely reading of the final sign preserved in the second line as the father’s title. This title is also used in two inscriptions that are only known from one specimen each (RIMA 1 A.o.76.43 and RIMA 1 A.o.76.45 ex. 1) but it is certain that our text is not a new exemplar for either of these. What little remains of the third line can easily be interpreted to accommodate the expected sequence *šá ki-si-ir-ti*. It is worth emphasising that the distribution of the signs in the surviving lines excludes identification with any of the four stamps known from the complete exemplars of the quay inscription (there is not enough overlap with the preserved portion on the fragmentary stamp impression of VA 3135, representing the fifth known stamp, to argue one way or another).

However, unlike the previously discussed green-coloured bricks that can be associated with the quay wall of Assur with certainty (Texts 1, 2 and 4), the present piece has a pinkish-reddish colour that indicates a lower firing temperature of around 700° C.¹⁷⁴

This brick is less hard and therefore less durable than the green specimens that were manufactured to create a barrier against the Tigris spring flood, and one might thus prefer to interpret it as a brick made for another of Adad-nerari’s buildings. But as will become clear in the following there are no plausible alternatives. Some of Adad-nerari’s inscriptions use the title LUGAL for *šar-ru* “king”, namely those on bricks for the Red *šudutinnu* Building (RIMA 1 A.o.76.33 and 34) and the Courtyard of Emblems (RIMA 1 A.o.76.38), and the surviving wedges of the last sign in the second line could easily be seen as the beginning of that sign. But these inscriptions always spread the names and titles of son and father across four lines, not two. These remaining wedges could also stand for the start of the sign ŠID, the logographic writing for *iššiakku* “vice-regent” which is followed by the divine name Aššur. There is only one series of bricks that uses

¹⁷³ Grayson 1987, 175.

¹⁷⁴ Kreppner 2006, 99; Schneider 2006, 404.

this title for Adad-nerari and his father Arik-den-ili: it was created to commemorate the building work undertaken on a facade of the courtyard of the Aššur temple (RIMA 1 A.o.76.35). However, all exemplars of this five-line inscription start with the royal name, and not with É.GAL, as our specimen does. Moreover, it is impossible to reconcile the remains of our third line with the expected *mu-ta-li-ik-ta* “facing” of that text. We can therefore confidently exclude that our text is a version of any of these inscriptions.

In conclusion, even though the brick was not fired at the high temperature we have come to expect from other examples, I still consider it a new exemplar of a brick bearing the quay wall inscription of Adad-nerari I (RIMA 1 A.o.76.40).



Fig. G1.8: AS 000001:001:006 = Text 6. Brick fragment with a stamped inscription of Adad-nerari I (1305-1274 BC). Photo by Karen Radner.

- 1 É.GAL ^m10-ERIM.TÁH [UGULA]
- 2 [A G]ÍD-DI-DINGIR UG[ULA-*ma*]
- 3 [šá k]rⁱ-sī^r-[ir-ti]
- 4 [šá IGI ÍD]

(i) “Palace of Adad-nerari, [overseer, (2) son of A]rik-den-ili, [also] over[seer]. (3) [(Brick) belonging to the f]ac[ing (of the quay wall) (4) which fronts onto the river (Tigris)].”

Text 7: AS 000001:001:007. Brick fragment with two cuneiform inscriptions of Shalmaneser I of Assyria (1273-1244 BC). Measurements: 33.5 × *25.5 × 5.5 cm (**Fig. G1.9**)

Members of the Sherqat Directorate of Antiquities and Heritage found this large brick fragment in the northern part of the site. The beige colour of its fabric indicates a firing temperature in the range of 750-950° C.¹⁷⁵

Like the brick of Adad-nerari I from the northern quay wall (AS 000001:001:008 = Text 4), this brick of Shalmaneser I features two stamped inscriptions. The text on the obverse is a new exemplar of the four-line brick inscription known from several bricks found in the Aššur temple, which Shalmaneser renovated (RIMA 1 A.o.77.31). There are no horizontal lines between the individual lines, and the line height is 3.3 cm. Note that, unlike the other known examples, the king’s name is not written with the vertical wedge introducing a personal name (*Personenkeil*).

Our brick also features a further one-line inscription, again with a height of 3.3 cm, mentioning the king with the title “king of the universe”, which was stamped on one of the brick’s sides. If the brick were laid so that the inscription on the front was visible, the text on the side would also be oriented correctly.

This is the first known exemplar of Shalmaneser’s bricks from the Aššur temple to feature inscriptions on two sides. However, as most of the hitherto attested bricks stamped with the text of RIMA 1 A.o.77.31 are only fragmentarily preserved, other pieces of this series may well have shared this characteristic.



Fig. G1.9: AS 000001:001:007 = Text 7. Brick fragment with two stamped inscriptions of Shalmaneser I (1273-1244 BC). Photo by Karen Radner.

Front:

- 1 É.GAL
- 2 ^dDI-*ma-nu*-MAŠ
- 3 MAN KIŠ A 10-[ERIM.TÁH]
- 4 [MAN] KIŠ-*ma*

(i) “Palace of (2) Shalmaneser (I), (3) king of the universe, son of Adad-nerari (I) (4) also king of the universe.”

¹⁷⁵ Kreppner 2006, 99; Schneider 2006, 404.

Side:

1 𐎠DI-*ma-nu*-MAŠ MAN KIŠ

“Shalmaneser (I), king of the universe.”

Text 8: AS 000001:001:002. Brick fragment with a cuneiform inscription of Shalmaneser III of Assyria (858-824 BC). Measurements: *15.0 × *11.0 × 5.6 cm (**Fig. G1.10**)

This brick fragment was discovered during the geophysical prospection of Assur, in the area between the Parthian Palace and the excavation house. The beige colour of its fabric indicates a medium firing temperature in the range of 750-950° C.¹⁷⁶

The brick inscription is written by hand, with a line height of 2.5 cm. Although no trace remains on this brick fragment of a third line of cuneiform script, it is most likely a new exemplar of Shalmaneser’s three-line brick inscription from Assur (RIMA 3 A.o.102.109), and the text has been reconstructed in this way.



Fig. G1.10: AS 000001:001:002 = Text 8. Brick fragment with a hand-written inscription of Shalmaneser III (858-824 BC). Photo by Karen Radner.

- 1 É.GAL 𐎠DI-*m*[*a-nu*-MAŠ MAN KUR.AŠ]
- 2 𐎠A 𐎠[AŠ-PAB]-𐎠A 𐎠[MAN KUR.AŠ]
- 3 [A 𐎠TUKUL-MAŠ MAN KUR.AŠ-*ma*]

(1) “Palace of Shalm[aneser (III), king of Assyria], (2) son of [Ashurnasirpal (II), king of Assyria, (3) son of Tukulti-Ninurta (I), also king of Assyria].”

Text 9: AS 000001:001:001. Brick fragment with the cuneiform inscription of an Assyrian king, most likely Tiglath-pileser III (744-727 BC). Measurements: *14.0 × *15.0 × 9.8 cm (**Fig. G1.11**)

This unusually thick brick fragment was discovered during the geophysical prospection of Assur, in the area between the Parthian Palace and the excavation house. The fabric of this brick has a reddish colour that indicates a low firing temperature of around 700° C.¹⁷⁷

A frame surrounds the brick’s hand-written inscription, of which only a few signs of the first line are preserved. While traces of the top parts of the second line can be made out, they are illegible. The height of the one preserved line is 3.8 cm. The first preserved sign is GAL, which is not followed by the single vertical wedge that generally introduces the name of the king responsible for the creation of the brick in all examples from Assur.

The sign GAL could therefore be taken to stand for the adjective *rabû* “great” and the subsequent sign read as the initial wedges of the sign *ú*, forming part of the epithet *šarru rabû* “great king”. This is not only epigraphically difficult but rendered unlikely by two further factors. Firstly, in bricks, the shorter spelling GAL-*u* is generally preferred to the one with the much longer sign *ú*. Secondly, in the known bricks from Assur, the epithet *šarru rabû* is extremely rare and attested only in the brick inscriptions of Sin-šarru-iškun (626-612 BC), commemorating his rebuilding the Nabû temple (RINAP 5/3: Sin-šarra-iškun 13, also Sin-šarra-iškun 14). This is a very long text written in relatively small cuneiform signs that do not match the size of the characters on our brick.

If GAL is therefore taken as the second component of É.GAL = *ekallu* “palace” after all, then the royal name would have been written without the personal name indicator – perhaps best seen as a mere omission. In this case, the subsequent wedges are to be read as GIŠ.tu[kul-ti] or GIŠ.TU[KUL] = *tukultu* “help; support; trust”, which is epigraphically without difficulties. This is the first element of the royal names Tukulti-Ninurta and Tukulti-apil-Ešarra (“Tiglath-pileser”).

Attested on bricks at Assur are the kings Tukulti-Ninurtas I and II and Tiglath-pileser I and III. Tukulti-Ninurta I (1243-1207 BC) has his name written with GIŠ.tukul-ti as

¹⁷⁶ Kreppner 2006, 99; Schneider 2006, 404.

¹⁷⁷ Kreppner 2006, 99; Schneider 2006, 404.

the first component, but crucially, all his Assur bricks (RIMA 1 A.o.78.30–33) are stamped, which ours is not; we can therefore confidently exclude this option. Tukulti-Ninurta II (890–884 BC) is also excluded as his name is written ^mGISKIM–^dMAŠ in all his known bricks from Assur (RIMA 2 A.o.100.14–16).

This leaves us with the Tiglath-pileasers. Only one brick inscription of Tiglath-pileser I (1114–1076 BC) from Assur begins with *ekallu* (RIMA 2 A.o.87.28), of which at least one exemplar features the spelling ^mGIŠ.tukul-ti-A-É-šár-ra (VA Ass 4306a = ex. 4; collated on 12 October 2023). However, a much better option is to assign our brick to Tiglath-pileser III (744–727 BC). The main argument for this is that our fragment is unusually thick for a brick (9.8 cm) and that only one series of bricks with a hand-written inscription attested in Assur matches this thickness. These are the bricks that Tiglath-pileser III had made for the platform of the Aššur temple (RINAP 1: Tiglath-pileser 58). Of these, VA Ass 3252 (= ex. 1) is 10 cm thick, and VA Ass 4306b (= ex. 6) is 11 cm thick, and the texts on both these bricks are inscribed within frames, as is ours. Therefore, I propose to see this piece as an additional, if very fragmentary, exemplar of this very important text, which is the only inscription of Tiglath-pileser III to mention his parentage, as the son of Adad-nerari (III).

- 1 [É].GAL ^{<m>}GIŠ.t[ukul-ti-A-É-šar-ra]
- 2 [MAN KUR.Aš-šur A ^m10-ERIM.TÁH MAN KUR.Aš-šur]
- 3 [ša ki-gal-li ša É Aš-šur]

(1) “[Pal]ace of Tig[lath-pileser (III)], (2) king of Assyria, son of Adad-nerari (III), king of Assyria: (3) (This brick) belongs to the platform of the temple of (the god) Aššur.”

G1.3 An inscribed stone block from the Aššur temple

Text 10: A stone block with a cuneiform inscription of Sennacherib of Assyria (704–681 BC). Measurements: 100 × 60 × 56 cm (**Fig. G1.12**)

As of 2023, this stone block sits just outside of the excavation house, in front of its southern wall. It is unclear when and from where it was brought there. The block does not bear a find or inventory number.

An exemplar of Sennacherib’s “Stone Block Inscription” (RINAP 3/2: Sennacherib 170), the text on the fully preserved block is complete as it is, with three lines. It demonstrates the basic accuracy of the flawed copy of Ex. 1 = Ass 3798a, which was published by Leopold Messer-



Fig. G1.11: AS 000001:001:001 = Text 9. Brick fragment with a hand-written inscription, most likely of Tiglath-pileser III (744–727 BC). Photo by Karen Radner.

schmidt in the first volume of *Keilschrifttexte aus Assur historischen Inhalts* (1911: no. 74) after the on-the-spot copy (“Fundkopie”) of Walter Andrae. F.H. Weissbach (1934: 229) suggested that this piece was a further exemplar of a series of blocks with a five-line inscription (last edition: RINAP 3/2: Sennacherib 171), with the final lines of the inscription broken off. Eckart Frahm (1997: 168: T135) treated this suggestion with scepticism and saw the inscription as a separate item, but cautiously allowed for the possibility that the text might have continued on a hypothetical adjoining block. For the present case, this too can be excluded as the three lines of the inscription sit in the middle of the block and are clearly meant to be appreciated as a complete text.

- 1 ^{md}30-PAB.MEŠ-SU MAN ŠÚ
- 2 MAN KUR.Aš-šur.‘KI’ e-piš
- 3 ša-lam AN.ŠÁR DINGIR.MEŠ GAL.MEŠ

(1) “Sennacherib, king of the world, (2) king of Assyria, the one who fashioned (3) image(s) of (the god) Aššur (and) the great gods.”

The sign KI in the third line is damaged but the final wedge and the basic outline of the sign are clear.



Fig. G1.12: Text 10: Stone block with an inscription of Sennacherib (704-681 BC). Photo by Karen Radner.



Fig. G1.13: AS 000001:001:004: Brick fragment with an incised board of Nine Men's Morris. Photo by Karen Radner.

G1.4 Appendix A: A brick with an incised gaming board

AS 000001:001:004: Brick fragment with an incised board of Nine Men's Morris. Measurements: *15.6 × *27.5 × 7.5 cm (**Fig. G1.13**)

This brick fragment was discovered during the geophysical prospection of the New Town of Assur. Its fabric has a beige colour that indicates a medium firing temperature in the range of 750-950° C. The brick was not fired long enough for the heat to penetrate it completely, resulting in patches of a different, reddish colour on the inside.¹⁷⁸

A gaming board is incised into the square brick. It consists of three boxes set inside each other. Only the innermost box is square, measuring 7 × 7 cm. The second and third frames are rectangular, and their sides measure 13 × 11 cm and 20 × 15 cm. The two lines dividing the sides of the three boxes intersect in the centre of the gaming board at a right angle.



Fig. G1.14: A gameboard for playing Nine Men's Morris incised in the ground next to the excavation trench in March 2023. Photo by Karen Radner.

In the Middle East, the board game Nine Men's Morris is well attested from Roman times onwards. The best evidence is available for Palestine, where gameboards incised in rock are known from Nessana, Elousa, Jerusalem, and Capernaum.¹⁷⁹ As Assur was a flourishing settlement in the contemporary Parthian period, the brick might date to that time, or later. There is no reason to assign the brick to an earlier period in the city's long history.

On the other hand, the gameboard may not date to antiquity at all, as playing Nine Men's Morris has remained locally popular right up to the present day. This was demonstrated by the fact that during the 2023 excavations, the workers occasionally cut a gameboard into the dry ground to play the game during their breaks (**Fig. G1.14**).

G1.5 Appendix B: A brick with an inscription of Aššur-nerari I, now in Munich

Complete brick of Aššur-nerari I from Assur. Measurements: 32.5 × 32.5 × 7.5 cm (**Fig. G1.15**)

- 1 ^dA-šūr-né-ra-ri
- 2 ÉNSI ^dA-šūr
- 3 DUMU lš-me-^dDa-gan
- 4 ÉNSI ^dA-šūr-ma
- 5 ba-ni É ^dBe-li-ib-ri-e

(1) "Aššur-nerari (I), vice-regent of the god Aššur, (3) son of lšme-Dagan (II), vice-regent of the god Aššur, (5) builder of the shrine of the god Bel-ibriya."

Aššur-nerari I is the father and predecessor of Puzur-Aššur III who first built the New Town of Assur according to the inscriptions on two fragmentary clay cones.¹⁸⁰ When precisely in the mid-second millennium BC Aššur-nerari I ruled at Assur is unclear but according to the Assyrian King List his reign lasted for 26 years.¹⁸¹

This brick was originally set into a floor pavement. It is a new exemplar of a hand-written brick inscription of Aššur-nerari I (RIMA 1 A.o.60.1) and features the variant spelling *-e* instead of *-a* at the end of line 5.

Acquired by Walter Klingspor during his service with the Brennstoffkommando Arabien in Northern Iraq in 1918, the brick is today in the possession of his grandson

179 Hübner 1992, 77, 224, figs. 34-37.

180 For IM 57822 and Ass 2065 = Ist A 3369, see Miglus 2010, 236-237. For the historical context, see also Miglus 2011.

181 Grayson 1980-83, 107-108: Assyrian King List §28.

178 Kreppner 2006, 99; Schneider 2006, 404.

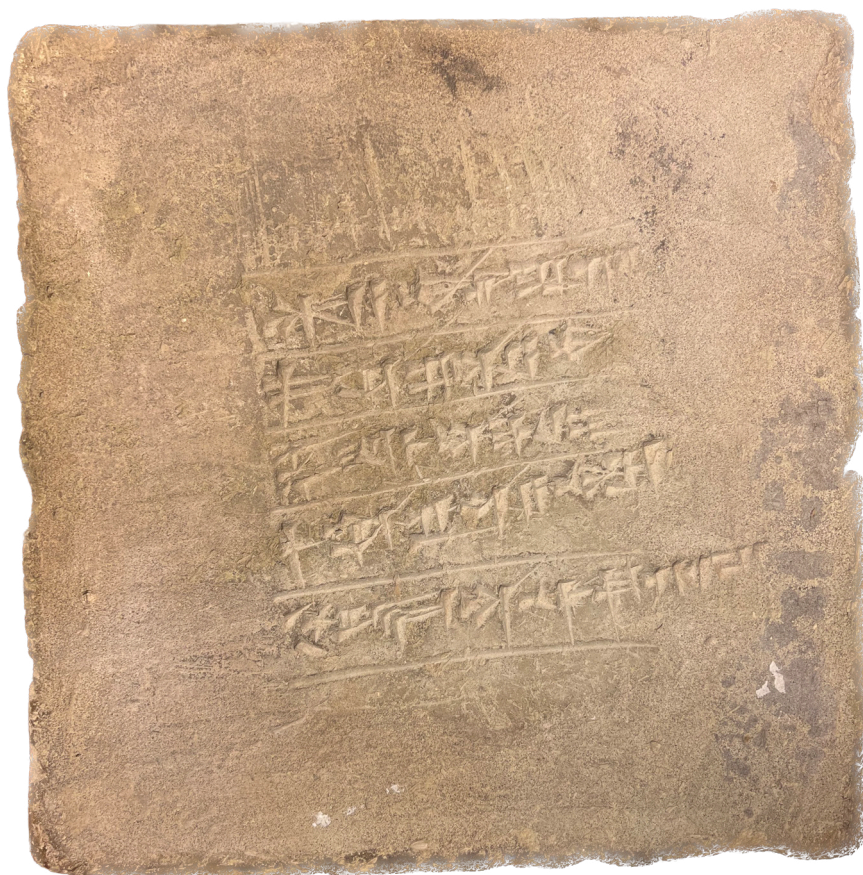


Fig. G1.15: Brick with a hand-written inscription of Aššur-nerari I in a private collection in Munich. Photo by Karen Radner.

Walter F. Kalthoff (Munich), to whom I am grateful for his kind permission to publish the piece. After it was brought to my attention by its owner, the original brick was examined on 28 November 2023.

G1.6 Appendix C: A brick with an inscription of Tukulti-Ninurta from Kar-Tukulti-Ninurta

KTN 2023: Brick fragment with a cuneiform inscription of Tukulti-Ninurta I of Assyria (1243-1207 BC) from Kar-Tukulti-Ninurta. Measurements: *19,5 × *21,5 × 6,3 cm (**Fig. G1.16**)

This fragmentary brick was found by Jens Rohde in the northern part of the palace of Kar-Tukulti-Ninurta near the bank of the Tigris during a visit on 17 March 2023. The SBAH representatives brought it to the Assur excavation house, where it is presently stored. In order to prevent confusion with material from Assur, it has been marked “KTN 2023”.

It is a new exemplar of a well-attested brick inscription of Tukulti-Ninurta I (1243-1207 BC) that is known from Kar-Tukulti-Ninurta, like our piece, but also from Assur, Nineveh, and Šibaniba / Tell Billa (RIMA 1 A.o.78,38). The text was produced with a stamp. While the horizontal rulings separating the individual lines are well visible, the stamp frame has left no discernible impression. The height of the lines is 2.7 cm.



Fig. G1.16: Brick fragment from Kar-Tukulti-Ninurta with a stamped inscription of Tukulti-Ninurta I (1243-1207 BC). Photo by Karen Radner.

- 1 [É.GAL ^mGIŠ].^rtukulⁿ-ti-
 2 [^dNin-urta] MAN KIŠ
 3 [A ^dDI-ma-nu-MAŠ] MAN KIŠ-ma

(i) “Palace of Tukulti-Ninurta, king of the universe, (3) son of Shalmaneser (I), (4) also king of the universe.”

G2. The Aramaic inscription on the sarcophagus of Grave 3 from Assur

Holger Gzella

G2.1 Script and language

The inscription has been scratched on the surface of the sarcophagus AS 262433:058:004, found in Grave 3 (§D2.5.1), with a sharp instrument and only consists of a brief dating formula without any accompanying personal name or mention of an event (Figs. G2.1, G2.2). A relative homogeneity of the letterforms and cipher numbers as well as their stance, despite the uneven surface of the object, may point to a hand that was not entirely unskilled. There are no orthographic, grammatical, or lexical peculiarities. As a result, the text can be easily read. While the four words it contains, i.e., the two prepositions *b-* and *l-*, the name of the month ^ʿ*b* “Ab”, and the feminine singular noun *šnt* “year of”, are common to all Semitic idioms of ancient Syria-Palestine, the script supports an identification of the underlying language as Aramaic. In particular, the opening of the head of the letter *b*, which occurs twice in the text, is an early distinctive trait of the Aramaic tradition of the West Semitic linear alphabet as opposed to Phoenician, Hebrew, or the regional alphabets of the Transjordan area.¹⁸² Aramaic is also the language one would expect at Assur in this period for historical-linguistic reasons, as it had spread quickly throughout Mesopotamia since the 8th century BC and is particularly well-documented again during the second and third centuries AD in inscriptions from the same area that reflect Aramaic’s continuous spoken use.¹⁸³

Even so, the letterforms, while evidently Aramaic, cannot be subsumed under any of the established post-Achaemenid varieties of the Aramaic script family that emerged in Palmyra, Edessa, Assur, Hatra, and other places in Eastern Mesopotamia from the latter half of the first century BC onwards. Only the letter ^ʿ – with its two slanted vertical strokes, on an almost straight horizontal line, that do not extend below the baseline – displays a

characteristic feature of the North Mesopotamian ductus. The North Mesopotamian ductus is best attested in the Eastern Mesopotamian Aramaic inscriptions from Assur and Hatra between the mid-first century BC and the mid-third century AD, but also in a few others from further afield.¹⁸⁴ A somewhat similar shape of the letter ^ʿ moreover appears in the first-century-BC Parthian ostraca from Nisa, although their script is not normally considered to be part of the North Mesopotamian branch.¹⁸⁵ Lastly, it occurs in at least one of a handful of badly-preserved Aramaic inscriptions that were only discovered in the winter of 2021, painted on the walls of a cave in the western central Zagros Mountains on the Iraqi-Iranian border area; the one in question is dated to the fourth or early third century BC by the editors.¹⁸⁶ This form no doubt evolved from an Achaemenid cursive variant of the ^ʿ sign.¹⁸⁷ The other letters of the newly-found inscription from Assur, however, all correspond to the more archaic shapes of the Old and Achaemenid Aramaic lapidary script, which is attested until the first quarter of the second century BC,¹⁸⁸ and do not yet foreshadow the innovations of the later, decisively more cursive scripts. The numerical ciphers for 1, 10, 20, and 100 appear in their customary forms as well.¹⁸⁹

The scarcity of post-Achaemenid Aramaic written evidence from before the late first century BC that has been unearthed up to now in Syria-Mesopotamia obscures the connections between the various new Aramaic scripts that subsequently cropped up in the region. Nonetheless, this inscription seems to belong to an older local, and perhaps still low-profile, writing tradition of Aramaic. It may have continued in use for simple domestic and basic administrative purposes in parts of Eastern Mesopotamia, before a fresh sense of regional autonomy and self-consciousness, reinforced by the demise of Seleucid hegemony, washed over several emerging vassal states at some point in the late second or early first century BC. A subsequent process of consolidation and standardisation

184 Naveh 1972 provides a summary of the evidence.

185 See the script tables in Klugkist 1982, 92 and 113, and also Bertolino 2008, 25.

186 No. 3 in Alibaigi *et al.* 2023, 424-426, in particular the initial letters of the first two lines on the photograph on p. 426. The other inscriptions are not accompanied by photographs, but, judging from the drawings, the shape of the ^ʿ there seems to correspond to the older Achaemenid form instead, which may suggest a slightly later date for no. 3.

187 Klugkist 1982, 92.

188 Healey/Bin Seray 1999-2000, 6.

189 They are generally stable in the post-Achaemenid material from Syria and Mesopotamia (with the exception of later Eastern Mesopotamian, on which see below), as pointed out by Klugkist 1982, 112.

182 Naveh 1970, 19; Millard 2011, 21.

183 Gzella 2021, 73-82 and 151-186.



Fig. G2.1: Detail of the inscription on the sarcophagus AS 262433:058:004. Photo by Karen Radner.



Fig. G2.2: Detail of the inscription on the sarcophagus AS 262433:058:004. Photo by Karen Radner.

brought about the rise of several new and highly visible Aramaic chancellery languages in these principalities. They came to be widely employed for local law, public display, and private *memoria* for some time, but most of them disappeared again during the Roman-Sasanian conflict of the mid-third century AD.

G2.2 Text, translation, and notes

Reading and interpreting the text is completely unproblematic thanks to the clear writing and the adherence to a known formula:

b 10+1+1+1+1+1 *l*'*b* *šnt* 1x100+20+20+10+1+1+1

Reconstructed vocalisation of the purely consonantal writing according to the pronunciation of Aramaic around 150 BC:

ba-15 *la*-*ʾAb* *šana**t* 153

Translation:

“On the 15th of the month Ab (i.e., the eleventh month, corresponding to July/August) of the year 153 (i.e., according to the Seleucid reckoning, hence 159/158 BC).”

The numbering of years counting from the first regnal year of Seleucus Nicator (312/311 BC) was presumably installed as a means of promoting unity and stability in a culturally diverse area with a rich history of its own and remained the dominant system for centuries in territories formerly under Seleucid rule. In all likelihood, then, it is the point of reference that also underlies the date specified here.¹⁹⁰ However, dating formulae in Aramaic inscriptions from the Hellenistic and Roman periods conform to different patterns in terms of syntax and order of constituents. Those that include the day in addition to the month and the year are by and large less frequent than other templates, but the specific form *bD lM šnt Y* (with D being the day of the month, M being the name of the month, and Y being the year), as it appears here, is evidently a remnant from Achaemenid Official Aramaic

legalese.¹⁹¹ It had completely fallen out of fashion by the time the new administrative and representational forms of Aramaic from Palmyra, Edessa, and Eastern Mesopotamia were standardised and has only left traces in the highly conservative diction of Nabataean and Jewish legal documents of the first century AD that were discovered in the Dead Sea region. The later Eastern Mesopotamian Aramaic inscriptions from Assur, by contrast, consistently employ the formula *bywm D bM (b)šnt Y* (“on day D in the month M (in) the year Y”, with the rare variant *dšnt* “of the year”).¹⁹² Consequently, the epigraph under discussion here still attests to an unbroken use of an older Achaemenid Aramaic clerical practice in early Parthian Assur despite the innovative shape of the letter ʾ and the adoption of a new continuous counting of years, as elsewhere in post-Achaemenid Syria and Mesopotamia. This is, in fact, its wider historical significance.

G2.3 Historical implications

Terse and mundane though it seems, the new epigraphic discovery offers a rare glimpse into writing at Assur before the rise of the Eastern Mesopotamian scribal tradition that eventually spread to Hatra and other adjacent areas and is now attested in some 660 inscriptions in total. Although the presence of Aramaic in Mesopotamia during the Seleucid and early Parthian periods continues to be badly documented in general, the characteristically Achaemenid pattern of the dating formula demonstrates the ongoing use of at least some Achaemenid bureaucratic conventions in northern Mesopotamia until at least the mid-second century BC. At the same time, as elsewhere in the former Achaemenid territory, the script gradually developed regional traits after the collapse of the imperial chancellery and the waning of its standardising effect on Aramaic writing.

Yet its scope seems to have been limited at first. A new written idiom that was more closely patterned after the Aramaic vernacular employed a more innovative spelling practice with a fuller indication of short vowels than before, and displays but little influence from Achaemenid Official Aramaic diction and legalese only became firmly

190 It has been proposed in the past that the dates in Parthian-period Aramaic inscriptions may relate to other forms of era-counting, but the Seleucid one is now generally accepted, see Naveh 1972, 300–302.

191 Brock 1992 provides a very useful synopsis; the formula encountered in the newly-found inscription from Assur belongs to type “3h” according to his classification (Brock 1992, 254 and 260).

192 The standard edition is Beyer 1998, 11–25. Those that bear a date are all from the second and, more frequently, from the third century AD.

established in Eastern Mesopotamia by the first century AD.

This piece of evidence for the use of Aramaic writing at Assur in the mid-second century BC now adds further support to the hypothesis that the later Eastern Mesopotamian Aramaic chancellery language did not originate at Hatra, where the lion's share of the evidence was discovered, but at Assur.¹⁹³ The refounding of the Aššur temple and the probable resettlement of the place in Achaemenid times¹⁹⁴ could provide a suitable historical context for the concomitant reappearance of Aramaic writing there.

¹⁹³ The most recent analysis of the evidence is Gzella 2023, 273-282.

¹⁹⁴ Radner 2017, 85-90.

H. Plant remains from Assur, 2023

H1. Introducing the contexts and periods concerned

Karen Radner & Andrea Squitieri

To obtain more information about Assur's ancient vegetation and plant use, charcoal, paleobotanical remains and phytoliths were collected. Whereas the latter will be analysed at a later stage, both the charcoal and the paleobotanical remains were handed over to specialists as soon as they reached Germany. We are grateful to Katleen Deckers (University of Tübingen) and Claudia Sarkady (Archaeobotanical Laboratory in Eggstätt) for analysing the material within the very tight time frame of only six months stipulated by the State Board of Antiquities and Heritage.

During the 2023 excavations at Assur in the NT1 2023 trench, 21 charcoal samples were collected and submitted for wood analysis. In order of their chronological sequence, one sample was collected from the chamber tomb, specifically the floor of Subdivision 6; a molar provided a radiocarbon dating range of 83-215 calAD (95.4% probability; see §D1.3 and §D2.3.3.2). 17 samples came from the floors of Rooms 2 and 3 of Building A, which can be dated to the second century BC (§D1.3). One sample was collected from Grave 3 and two from Grave 4, which were

both cut down from the floors of Rooms 2 and 3 of Building A; an inscription dates Grave 3 to July/August 158 BC (§G2).

Furthermore, in the sondage opened in the baulk between the NT1 2023 trench and the 2002 SBAH trench (§D3), one additional charcoal sample was collected from the lower floor of "Room 6". That same charcoal yielded a radiocarbon dating range of 751-422 calBC (95.4% probability; see §D1.3 and §D3.2).

Katleen Deckers presents the preliminary results of her wood analysis of these 22 charcoal samples in §H2 and in Table H1.1.

In the course of the excavation of the NT1 2023 trench, 27 soil samples were taken for flotation from the gridded floor deposits of Rooms 1, 2 and 3 of Building A. These samples were collected according to the protocol described in §D1.2.1. One more flotation sample came from the fill of a complete vessel (G01-S05-V01) that was found on the floor of Subdivision 5 in the chamber tomb (§D2.3.3.3). While the chamber tomb's construction and first use can be dated to the early centuries AD (§D1.3), the vessel itself belongs to the late Sasanian / Early Islamic period based on its shape and decoration (§E1.2).

In the sondage between the NT1 2023 trench and the 2002 SBAH trench, two further soil samples were collected for flotation from a floor unearthed in "Room 5"

Sample no.	Unit	Subunit	Context	Tamarix	Populus/Salix	Populus	Salix	Abies/Cedrus	Taxus	Juglans	Lycium	Dicotyledon	Ringp. Dicot.	Notes
NT1 2023 trench														
AS 262433:022:004	Chamber tomb (= Grave 1)	Subdivision 6	Floor deposit									5		Small shrubby plant with thick rays
AS 261432:007:005	Building A	Room 2	Room fill					4						2 fragments with diameter >10 cm
AS 261432:011:031	Building A	Room 2	Floor deposit		1									
AS 261432:011:033	Building A	Room 2	Floor deposit								1			
AS 261433:020:031	Building A	Room 2	Floor deposit	2	2					2		2		
AS 261433:020:032	Building A	Room 2	Floor deposit	2						1				
AS 261433:020:033	Building A	Room 2	Floor deposit	1	3									1 <i>Pop/Sal.</i> fragment with animal borehole
AS 261433:020:034	Building A	Room 2	Floor deposit	1	4	2								
AS 261433:020:035	Building A	Room 2	Floor deposit	6										
AS 261433:020:036	Building A	Room 2	Floor deposit	6	7							4	2	
AS 262432:058:035	Building A	Room 3	Floor deposit	3	1						7			
AS 262432:058:037	Building A	Room 3	Floor deposit	1								2		Dicots from shrubby plants
AS 262432:058:036	Building A	Room 3	Floor deposit								3			
AS 262432:058:038	Building A	Room 3	Floor deposit	3	2									
AS 262432:058:039	Building A	Room 3	Floor deposit								1			
AS 262432:058:040	Building A	Room 3	Floor deposit	6						3				
AS 262432:058:042	Building A	Room 3	Floor deposit	10			1					1		1 <i>Tamarix</i> fragment with bark attached
AS 262432:058:043	Building A	Room 3	Floor deposit	3										
AS 262433:060:004	Grave 3	/	Near the skeleton	1										
AS 262432:055:010	Grave 4	/	Near the skeleton		3	1								
AS 262432:055:002	Grave 4	/	Near the skeleton						3			3		
Sondage linked to 2002 SBAH trench														
AS 263432:006:003	/	Room 6	Lower floor		17									1 with fungal hyphae

Table H1.1: Results of the wood analysis by context. Prepared by Katleen Deckers.

Sample ID	Unit	Context
From NT1 2023 trench		
AS 261433:005:002	Building A Room 1	Floor deposit
AS 261432:011:001	Building A Room 2	Floor deposit
AS 261432:011:002	Building A Room 2	Floor deposit
AS 261432:011:003	Building A Room 2	Floor deposit
AS 261432:011:004	Building A Room 2	Floor deposit
AS 261432:011:005	Building A Room 2	Floor deposit
AS 261432:011:006	Building A Room 2	Floor deposit
AS 261432:011:007	Building A Room 2	Floor deposit
AS 261432:011:008	Building A Room 2	Floor deposit
AS 261432:011:009	Building A Room 2	Floor deposit
AS 261433:020:001	Building A Room 2	Floor deposit
AS 261433:020:002	Building A Room 2	Floor deposit
AS 261433:020:003	Building A Room 2	Floor deposit
AS 261433:020:004	Building A Room 2	Floor deposit
AS 261433:020:005	Building A Room 2	Floor deposit
AS 261433:020:006	Building A Room 2	Floor deposit
AS 261433:020:007	Building A Room 2	Floor deposit
AS 261433:020:008	Building A Room 2	Floor deposit
AS 262433:068:002	Building A Room 2	Floor deposit
AS 261432:007:006	Building A Room 2	Room fill
AS 262432:058:001	Building A Room 3	Floor deposit
AS 262432:058:003	Building A Room 3	Floor deposit
AS 262432:058:004	Building A Room 3	Floor deposit
AS 262432:058:005	Building A Room 3	Floor deposit
AS 262432:058:006	Building A Room 3	Floor deposit
AS 262432:058:007	Building A Room 3	Floor deposit
AS 262432:058:008	Building A Room 3	Floor deposit
AS 262433:021:004	Chamber tomb	Fill of vessel G01-S05-V01 in the chamber tomb
From the sondage linked to the 2002 SBAH trench		
AS 262432:066:001	Room 5	Floor deposit
AS 262432:066:002	Room 5	Floor deposit
AS 263432:006:002	Room 6	Lower floor deposit
AS 263432:002:001	Room 6	Upper floor deposit

Table H1.2: List of flotation samples arranged by context. Prepared by Andrea Squitieri.

(which was collected from two excavation squares, hence in two samples), and one more sample each from the two floors exposed in “Room 6”. Both these rooms belong to the monumental Assyrian residence excavated in 2002 by a team of the State Board of Antiquities and Heritage. “Room 5” yielded a piece of charcoal (too small for wood analysis), taken directly from the floor, that was radiocarbon dated to 1416-1278 calBC (95.4% probability; see §D1.3 and §D3.2, also for the modified sampling protocol). In “Room 6”, two floors were exposed one above the other. A charcoal sample from the younger produced a radiocarbon dating range of 755-482 calBC (95.4% probability), whereas the older floor is dated to 751-422 calBC (95.4% probability; see above).

The light fractions of these 32 flotation samples in total (**Table H1.2**) were exported from Iraq to Munich in May 2023 and handed over to Claudia Sarkady who examined them and isolated and identified all plant remains. She presents her methodology and the preliminary results of her identifications in §H3.

H2. Wood identification from charcoal remains

Katleen Deckers

Little is known about the wood use and the vegetation along the Tigris in antiquity so far. The new charcoal samples from Assur therefore deliver important new insights into wood use and the former vegetation in that region.

The site of Assur is located on the western bank of the Tigris and today receives only approximately 250 mm of rainfall annually. Therefore, woody vegetation is mainly confined to the Tigris alluvial zone near the river that consists of poplar (*Populus*), willow (*Salix*), and tamarisk (*Tamarix*), with the latter extending also further away from the river into more arid zones, comparable to buckthorn (*Lycium*).¹⁹⁵

For this first study of charcoal from Assur, 22 samples from various occupation periods have been investigated. From these samples, 133 charcoal fragments in total have been identified by analysing transversal, tangential and radial sections for diagnostic characteristics, with magnifications varying between 60× and 500× and using the reference collection of the University of Tübingen as well as identification literature.¹⁹⁶

From the floor of Subdivision 6 of the Parthian chamber tomb (= Grave 1; §D2.3), five charcoal fragments were investigated that could not be precisely identified. They were likely from a small shrubby plant with thick rays.

From Rooms 2 and 3 of Building A (§D2.6), 17 charcoal samples were extracted for identification (**Table H1.1**). The function of this building is unclear at the current stage of excavation since the artefacts found offer only limited insights into the purpose of the building. In total, 100 charcoal fragments were identified from this building and at least nine taxa were detected. *Tamarix* and *Populus/Salix* were strongly represented, but also *Lycium* is in evidence, as well as walnut (*Juglans*) and fir/cedar (*Abies/Cedrus*) and some indeterminate Dicotyledoneae. While *Tamarix*, *Populus* and *Salix* as well as *Lycium* were in all likelihood locally available,¹⁹⁷ *Abies/Cedrus* (most likely *Abies* since no scalloped tori were visible)¹⁹⁸ probably represents imported wood since these species occur naturally in the mountainous regions of Turkey and Lebanon.¹⁹⁹ The

¹⁹⁵ Handel-Mazzetti 1914.

¹⁹⁶ Such as e.g., Fahn/Werker/Baas 1986; Gale/Cutler 2000; Schweingruber 1990; Crivellaro/Schweingruber 2013.

¹⁹⁷ Handel-Mazzetti 1914.

¹⁹⁸ Romagnoli *et al.* 2007.

¹⁹⁹ López-Tirado *et al.* 2023; López-Tirado *et al.* 2021.

use of imported wood originating from further away may be indicative of an elite or official building.²⁰⁰

Additionally, the *Juglans* charcoal in the samples may represent a cultivated taxon. Little is known as of yet about the domestication history of the walnut, but pollen data from Iran suggest its expansion of cultivation already by c. 2500 BC to zones where it previously was not present.²⁰¹ Also, at Tell Jerablus in the Middle Euphrates region of Syria, *Juglans* charcoal was found in layers dating to 2900–2650 BC, perhaps indicative of the expansion of its cultivation.²⁰² *Juglans* cultivation appears to also have spread to the Levant and Cyprus, by at least 1500 and 1000 BC, respectively.²⁰³ A stronger boom in *Juglans* cultivation however appears to have occurred from around 500 BC onwards, in many areas of the Middle East,²⁰⁴ and the presence of its wood in Assur in the second century BC may align with this pattern.

With regards to spatial differences in wood use within Building A, there are similarities between the attested wood use within Rooms 2 and 3, but also differences (Fig. H2.1). In both rooms, *Tamarix*, *Populus/Salix*, *Juglans* and *Lycium* were present, but there was less *Populus/Salix* and more *Lycium* in Room 3 and in addition, *Abies/Cedrus* (most likely *Abies*) was found that was so far not detected in Room 2.

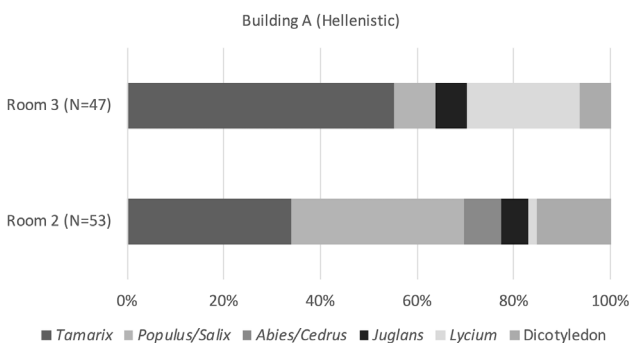


Fig. H2.1: Proportions of charcoal fragments of the different taxa for Rooms 2 and 3 of Building A, dated to the second century BC. Prepared by Katleen Deckers.

The charcoal samples from Graves 3 and 4 (§D2.5), which date to the mid-second century BC, were derived from near the skeletons of these burials although it is unclear whether they were associated with burial rites or whether they were only part of the fill of the grave. In

total, eleven fragments were identified from these grave contexts. The two graves each contained taxa that were likely locally available: *Tamarix* in the case of Grave 3 and *Populus/Salix* in the case of Grave 4. In addition, Grave 4 also had charcoal of yew (*Taxus*), which must have been imported from further afield since it typically grows within the Middle East in mountainous regions, with the nearest habitats today located more than 500 km away from Assur on the Caspian Sea, and other habitats over 600 km away in the Amanus and the Caucasus.²⁰⁵

“Room 6” (§D3.1), whose function is currently unclear and which was partially unearthed in the sondage in the baulk of the 2002 SBAH trench, yielded one sample from the lower floor, consisting of 17 fragments of *Populus/Salix* and likely representing local vegetation (Table H2.1). One of these fragments had fungal hyphae, which may indicate that the wood was collected as deadwood.

In conclusion, these first charcoal results from Assur provide important new data for a region, for which until now little is known about its former vegetation and wood use. While some of the material likely captures local vegetation, some taxa were identified that were imported and thus indicate long-distance connections.

H3. Plant identification from light fraction flotation samples

Claudia Sarkady

H3.1 Methodology: collection and preparation of the samples in the lab

Karen Radner, Jana Richter and Andrea Squitieri processed the 32 soil samples collected from floor contexts on site in the excavation house at Assur using a flotation machine (§D1.2.1) and thus separated the charred plant remains from the heavy mineral sediments.²⁰⁶ As they were taken according to the different find contexts, the volume of the processed soil samples varied from 1 to 44 litres. The light fractions were air-dried in their flotation bags on a clothesline, before being bagged in plastic bags for export. The heavy fractions stayed in Assur and are not available to the present author. According to Radner, Richter and Squitieri, these remains are very well-cleaned and should no longer contain any plant remains.

The present author carried out laboratory preparation and plant identification in the Archaeobotanical Laborato-

200 Deckers 2011.

201 Djamali *et al.* 2011.

202 Wilkinson/Deckers 2015.

203 Pound/Hazell/Hockin 2023 (with references).

204 See e.g., Djamali *et al.* 2011; Potts 2018; Pound/Hazell/Hockin 2023.

205 Caudullo/Welk/San-Miguel-Ayanz 2017.

206 This section was language edited by Karen Radner.

ry in Eggstätt (Germany), following standard procedures. The 32 light fraction samples had a total weight of 431.2 g. All specimens were picked out using a stereomicroscope manufactured by Helmut Hund GmbH in Wetzlar (Germany) with 6.7 to 45× magnification. No random sampling was done and all plant remains were recorded fully quantitatively. A total of 8,665 predominantly charred plant remains were collected from the samples, of which 5,207 were crop plants and 3,458 were wild plants.

For their identification, a reference collection of modern seeds as well as specific seed atlases and archaeobotanical studies of archaeological sites in Syria were available to the present author.²⁰⁷ The reference collection was adequate for the identification of cultivated plants, but the representation of the wild flora of the Middle East proved insufficient for detailed determinations down to the species level. Therefore, taxa were identified as species only in cases of good preservation, and otherwise determined to genus or family level. In some cases, taxa with uncertain identification are listed with the abbreviation cf. (for Latin *confer* “compare”) before the botanical name, which is meant to indicate a very close determination. In certain cases, the abbreviation sp. (for Latin *species*) is used to indicate that the determination of the exact species was not possible.²⁰⁸ Many plant remains are moderately or poorly preserved or are highly fragmented and thus cannot be more closely determined, not even to the next classification level of the family; in that case, the abbreviation indet. (for Latin *indeterminata* “indeterminates”) is used.

To gain deeper insights, it would be highly desirable to obtain a more precise species identification of Middle Eastern wild plants, which would mean assembling a modern comparative collection of plant species. It is almost 25 years since Hansjörg Küster, who then studied the archaeobotanical remains from Tall Munbaqa on the Middle Euphrates, emphasised the importance of collecting such materials and suggested that this could take place during ongoing excavation projects.²⁰⁹

In only 431.2 g light fraction, a total amount of 8,665 plant remains were collected, of which 5,207 are cultivated plants and 3,458 are wild plants. All taxa identified from Assur are listed in **Table H3.1**, arranged by context. The nomenclature and classification of taxa that follow

207 Cappers/Bekker/Jans 2012; Beijerinck 1976; Oberdorfer 1990; van Zeist/Bakker-Heeres 1982; 1984a; 1984b; 1985. The descriptions and illustrations in the works of van Zeist and Bakker-Heeres were especially useful.

208 Following the conventions used by van Zeist and Bakker-Heeres in their afore-mentioned works.

209 Küster 1989, 85.

the traditional names according to recent ecology and sociology are based on Erich Oberdorfer’s work.²¹⁰

The results are subdivided first into cultivated plants (§H3.2-4), followed by wild plants – weeds in the broadest sense. From each group, all complete seeds and fragments were counted and these numbers are summarised in the table. In addition to plant remains (seeds, fruits, stems), the samples contained other classes of materials including charcoal fragments and animal remains (bones, insect remains, snail shells). These are summarised as “varia” at the end of the table, but have not been further analysed for this study.

To avoid further damage, the identified material is conserved in gelatin capsules that are placed in small rectangular plastic boxes. While these remain in Munich, the remainder of the sampled material (chiefly sediments) was returned to the State Board of Antiquities and Heritage of Iraq in late October 2023.

Total seeds	8,665
Total cultivar count	5,207
Total wild plants	3,458
Total cereal chaff	54
Cultivated plants : wild plants	1.5

H3.2 Cereals

H3.2.1 Barley (*Hordeum vulgare*)

Domesticated barley (*Hordeum vulgare*) belongs to the founder crops of Old World Neolithic agriculture and is thus one of the oldest cultivated cereals of mankind. Barley belongs to the grass family (Poaceae) and is a summer crop.²¹¹ It adapts very well and grows everywhere where cereals can be grown at all. It withstands poor and dry soils and can cope with some salinity. Whereas wheat does not tolerate higher salt content in the soil, barley can be grown on artificially irrigated – and therefore over time salinised – arable soils and still produce the most satisfactory yields.²¹² The cultivation of barley can also take place in higher mountainous areas.

During its long history of cultivation, several forms of barley have developed. There are two principal morphological types: two-row barley and multi-row barley. In both, there are hulled barley and naked-grained

210 Oberdorfer 1990.

211 Miedaner 2014, 92-97.

212 Helbaek 1960, 186-196.

(free-threshing) forms. Today, the hulled grains are called pearl barley and are used as an ingredient in dishes cooked on the fire or in the oven. The use of barley is varied, as groats (porridge), semolina, flour, or fodder plant.²¹³ Barley is also significant for brewing beer. Due to its lack of gluten, it is not suitable for baking conventional bread, but rather for preparing flatbread.

At Assur, 134 grains of *Hordeum vulgare* were found in 24 of the 32 samples, and there were also 14 presumptive barley grains (designated as cf. *Hordeum vulgare*) in five samples. Therefore, barley is the most frequent cereal currently attested at Assur. It was identified in all contexts sampled in 2023 but there are so far no threshing residues.

Except for a few grains, the state of preservation is moderate. Most of the grains are eroded, fragmented or deformed, which makes their identification difficult or impossible; they are then classified as *Cerealia indet.* (*Cerealia indeterminata* “undetermined cereal”). The husks enclose the grains tightly in the form of small siliceous shells and cannot be easily separated from the grains. They are often missing in charred finds. However, the husks often leave impressions on the grains, which is why the husked grain can be recognised in archaeobotanical finds. The grains must be dehusked before consumption, as the husks are hard and inedible for humans. Ethnographic comparisons of grain processing in Turkey have shown that numerous work steps are required to achieve this.²¹⁴ The Assur samples have a different degree of purity depending on which step was reached when the grains were charred.

Archaeobotanically, it is often possible to recognise whether the crop was contaminated by weeds, roughly cleaned or well cleaned. During threshing, the stalk breaks down into spikelets. Dehusking requires the grain to be completely dry. This time-consuming first step in the preparation process is done in a mortar or on a millstone. Subsequently, the grains are separated from the chaff and weed residues by sieving and winnowing. During the winnowing process, portions of the crop are thrown into the wind to separate the heavy grains from the lighter chaff. Only then can the grains be stored until it is needed for food preparation and ground into flour.²¹⁵ Barley grains are found charred when they got too close to the fire in the run-up to the preparation of a meal.

H3.2.2 Wheat

Also two wheat species, namely emmer and einkorn, belong to the first species to be domesticated by humans (“founder crops”). Like barley, wheat belongs to the grass family (*Poaceae*). The grains are rich in starch, minerals and vitamins. Wheat species are not as frugal and adaptable as barley and prefer nutrient-rich soils. They cannot be grown on the same field every year, as this would reduce their yield. Therefore, longer crop rotations are necessary. Wheat is primarily a bread grain, but also suitable for porridge or groats.

A distinction is made between the hulled wheat emmer (*Triticum dicoccum*), einkorn (*Triticum monococcum*), spelt (*Triticum spelta*) and the naked, or free-threshing, wheat such as bread wheat (*Triticum aestivum*), hard wheat (*Triticum durum*), and club wheat (*Triticum compactum*). The grains of free-threshing wheat are easier to process than emmer, and einkorn wheat. For the palaeobotanist, free-threshing weeds are difficult to keep apart, if not indistinguishable, as they are very similar.²¹⁶ A distinguishing criterion is the number of chromosomes: bread wheat and club wheat are hexaploid, and durum wheat is tetraploid.

H3.2.2.1 Emmer (*Triticum dicoccum*)

The grains of emmer (*Triticum dicoccum*) are enclosed in husks. They are easily recognisable by their distinctive drop-shaped form and the hump-like curved back line. With moderately preserved grains, it is not always possible to clearly distinguish them from spelt (*Triticum spelta*). However, spelt was of no importance in the Middle East in antiquity and, except for the Caucasus, is not found anywhere in ancient finds there.²¹⁷ Emmer is a summer crop. It is sown in spring, grows quickly, has a short ripening period and can be harvested early. Due to the high gluten content, it is a good bread grain.²¹⁸

Among the 2023 Assur samples, *Triticum dicoccum* is represented by only one single grain and some threshing residues (four glume bases in three samples and 15 rachis segments in eight samples). Based on these few records, it is not possible to assess the importance of emmer, which may have been significant. Currently, the available sam-

213 Kroll/Reed 2016, 84.

214 Hillman 1984, 114-152.

215 Küster 1989, 89; 2013, 56.

216 This is why in archaeobotanical literature one finds often terms such as *Triticum aestivum-compactum*, *Triticum aestivum-durum*, etc.

217 Körber-Grohne 1988, 82; Miedaner 2014, 40.

218 Körber-Grohne 1988, 326-330

ples provide no evidence for the local cultivation of emmer in Assur.

H3.2.2.2 Einkorn (*Triticum monococcum*)

The grain of the einkorn (*Triticum monococcum*) has a characteristic shape with a high arched back and flat sides. It is the most delicate cereal, but also the most resistant. It can adapt to many ecological conditions and is also tolerant of the cold, which is why einkorn is known as a winter crop. It is sown in the fall and grows until the onset of frost as the seedlings can withstand frost. It then has a growth advantage over summer cereals, which are only sown in the spring.²¹⁹ Each ear contains only one grain. *Triticum monococcum* is more suitable for cooked dishes than for baked goods, as it is only a moderate bread cereal. It was also used to make groats and flour.²²⁰

Triticum monococcum was found in seven samples collected at Assur in 2023, with only one single grain and additional threshing residues (three spikelet forks, five glume bases, and one internode). The samples currently available provide no evidence for the local cultivation of einkorn at Assur.

H3.2.2.3 Bread wheat (*Triticum aestivum*)

Bread wheat (*Triticum aestivum*) was never as important as emmer and einkorn in the early agricultural societies of southwest Asia and Europe, even though it was more productive. It is, however, more sensitive to both drought and waterlogging and therefore needs to grow on well-drained, fertile soils. Bread wheat belongs to the group of naked, or free-threshing, grains. The name is misleading, because here too the grains are enclosed in husks, but these are loose and the grains fall out easily from the husks during threshing.²²¹ This has advantages, as the preparation of meals is considerably faster, especially when demand increases with a growing population. There are also disadvantages, however, because naked grain is more difficult to store and more susceptible to fungal infestation, pests or bird damage.²²²

Naked wheat grains are generally more difficult to detect than hulled wheat grains among archaeobotanical samples, as the hard husk shells of hulled wheat protect

the caryopses and therefore the grains' chances of survival are higher. Among the Assur 2023 samples, bread wheat is documented with six grains in three samples, and probably with one more grain (designated as cf. *Triticum aestivum*). The grains are moderately preserved and eroded. Whether bread wheat was cultivated in its own fields, or whether it was grown in the barley fields, cannot be determined at present due to the small number of finds.

H3.2.3 Threshing residues ("chaff")

Threshing residues such as rachis internodes, spikelet forks and glume bases of emmer and einkorn are by-products or waste produced during grain processing. It can be assumed that the threshing areas were located outside the settlement near the arable fields, possibly close to the river Tigris.

The threshing remains found in the 2023 samples were most likely blown in by the wind, or washed in by the rain. However, the presence of chaff cannot definitively prove that emmer and einkorn were cultivated.

H3.2.4 Indeterminate wheat

56 fragments from 14 of the 2023 Assur samples were identified as indeterminate wheat (*Triticum* sp.). This category mainly includes wheat grains that cannot be further identified as emmer, einkorn or bread wheat, but only to genus level. The reason for this is that the remains are either fragments without distinctive identification features or because the grains are very poorly preserved, porous or deformed.

H3.2.5 Indeterminate cereals

In addition to the indeterminate wheat, a large number of cereal fragments were isolated. Indeterminate cereals (*Cerealia indeterminata*) are grains that cannot be further identified, i.e. neither designated as barley nor as wheat, as they are present as deformed grains that have no characteristic features or are very corroded and completely unrecognisable.

Due to the comparatively high proportion of barley grains compared to wheat grains, it can be assumed that the majority of indeterminate grains (4,893 fragments from all 32 samples) constitute barley fragments.

219 Küster 2013, 55.

220 Körber-Grohne 1988, 322.

221 Küster 2013, 57.

222 Miedaner 2014, 45.

H3.3 Cultivated pulses

Cultivated legumes such as lentils and peas have been found in minimal quantities among the 2023 samples from Assur, but this is to be expected as the chances of preservation for these crops are nearly as good as those of cereals. By their very nature, pulses have fewer chances of coming into contact with fire than cereal grains. They do not necessarily have to be roasted to be consumed, as the semi-ripe and ripe seeds of pulses can be eaten raw, such as the tasty sugar snap peas. Therefore, there is already a certain degree of selection by humans.

Moreover, pulses can also be cultivated on small garden-like plots of land, rather than in large areas, which makes them harder to verify archaeologically as it is not worthwhile to harvest or thresh small quantities. During harvesting, the pods are picked, and the seeds are split out by hand, resulting in hardly any losses. This further limits their occurrence, as only a few seeds fall to the ground and end up in archaeological samples. Only ripe seeds that are charred dry remain preserved.²²³

However, lentils and peas were certainly cultivated regularly and on a large scale in antiquity. Since the beginning of agriculture, these crops have been among the most important cultivated plants and constituted staple foods for humans due to their high protein content. Plant protein is no substitute for animal protein, but that can be obtained from dairy products.²²⁴ Moreover, legumes live in symbiosis with nodule bacteria on their roots, which can bind nitrogen from the air. These nitrogen compounds enriched the soil, increasing soil fertility. Legumes may grow as a spontaneous addition to cereal fields or be grown intentionally together with cereals, which means that no further fertilisation is required. The same applies if one alternates between cereals and pulses.²²⁵ In modern agriculture, a crop specifically cultivated to be incorporated into the soil while still green is called “green manure”.²²⁶

What little evidence there is currently of legumes among the samples from Assur is therefore highly significant, representing the manifestation of a potentially much more extensive phenomenon.

223 Kroll 1983, 127-128.

224 Kroll 1983, 124-125.

225 Küster 2013, 65.

226 Pieters 1927.

H3.3.1 Lentil (*Lens culinaris*)

The lentil (*Lens culinaris*) is another founder crop and among the oldest cultivated useful plants. Its plants are tender and require a supporting plant, as they cannot grow upright themselves. This is the reason why lentil is often sown together with cereals, as its plants can climb up the cereal ears. When they grow as an admixture in cereal fields lentils are harvested by hand and threshed separately. Lentil growing is laborious because weeds generally grow faster than lentil plants, which therefore require weeding and tending. However, dried lentils can be stored well, and lentil dishes are popular and tasty.²²⁷

The seeds of the lentil can be easily recognised by their relatively sharp edges. In Assur, this legume is currently only present in the form of three seed halves in two samples, which are moderately preserved (*Lens* sp.). The few finds of lentils in Assur so far are likely to be classified as admixture in cereal fields. There is currently no evidence for their cultivation in dedicated vegetable patches.

H3.3.2 Pea (*Pisum sativum*)

Peas (*Pisum sativum*) are also a founder crop. The seeds are spherical and can be flattened or very small, depending on their place in the pod.²²⁸ The plants are vigorous with thick, seed-rich pods but like lentil plants, they too need support for climbing. Peas are nutritious, tasty, easy to grow and can be stored well.²²⁹

The most important criterion for the identification of the seed is the typical navel. If this is missing, peas are difficult to classify. In Assur, there is one seed half in each of two samples. These should be marked with a question mark, as the determination is uncertain (cf. *Pisum* sp.). The few finds likely should be interpreted as an admixture in cereal fields. Generally, it is not possible to prove local cultivation in dedicated vegetable patches archaeobotanically.²³⁰

H3.3.3 Indeterminate legumes

This collective category includes 23 indeterminate fragments of legumes from seven samples. They are more or less spherical, but otherwise featureless.

227 Kroll 2016, 116.

228 Kroll 1983, 54.

229 Kroll 2016, 118.

230 Kroll 1983, 54.

H3.4 Olive

One small angular fragment each was found in three samples. It is unclear whether these are the remains of olive stones (hence classified as cf. *Olea* sp.). Due to this uncertainty, we will refrain from discussing here the undoubted economic importance of olives in antiquity.

H3.5 Wild plants

In the following, the families of wild plants are listed in alphabetical order.

H3.5.1 Aizoaceae, noon flower family

The Aizoaceae are a family in the order of the Caryophyllales. The name means “always alive” (from Greek *aeí* “always” and *zôon* “the living”),²³¹ and this is based on the assumption that these plants are indefinitely perennial. The plants have a succulent character and their crown resembles a daisy.

24 seeds of the Spanish Aizoon (*Aizoon hispanicum*) were identified in six samples. The seeds are almost round, laterally compressed. Their characteristic feature is concentric ribs on the surface.²³² This plant is annual, herbaceous and native to the Middle East, North Africa and the Mediterranean region. It grows on compacted dry sandy soil in desert plains and saline areas.²³³

H3.5.2 Amaranthaceae, foxtail family

The spherical and flattened seeds of the genus *Suaeda* are difficult to identify as they have hardly any morphological characteristics that could serve for their classification. Nevertheless, *Suaeda* is attested in the form of ten seeds in nine of the 2023 samples from Assur.

The plants are common all over the world, and some species colonize wetlands with saline and alkaline soils, especially near the coast.²³⁴ The English name “seablite” refers to the fact that they grow in salt marshes and along sea shores, while the German designation “Sode” refers to the former use in the extraction of potash and soda, as

the plants contain sodium carbonate.²³⁵ The young succulent leaves and also the seeds of the plants can be eaten as fresh vegetables.

H3.5.3 Asteraceae or Compositae, sunflower family

The knapweed (*Centaurea* sp.) of the Asteraceae (or Compositae) family is native to Europe, the Mediterranean and the Middle East. In Assur, it is present in six samples, each with one achene, that is, a nut-like cluster. The achenes have fine hairs, but these are no longer preserved in charred finds.

These plants grow on loose loamy soils and sandy or stony soils and are thermophilic.²³⁶ The botanical genus name *Centaurea* is borrowed from the centaurs of Greek mythology, as dwellers of forests and mountains.²³⁷

H3.5.4 Boraginaceae, forget-me-not family

Among the Assur material, a great number of fruitlets from the forget-me-not family were identified as gromwell (*Lithospermum arvense*): 1,828 pieces are attested in 31 samples. Furthermore, the prophet flower (*Arnebia linearifolia*) is in evidence with one seed each in two samples.

Gromwell (*Lithospermum arvense*) is a desert steppe plant that prefers sandy-loamy and slightly calcareous soils and grows in the fields of winter cereals, alongside roads and on rubble.²³⁸ This ancient medicinal plant can be used as a tea.²³⁹ The fruitlets of *Lithospermum arvense* have a triangular base and a rough, verrucose surface, with prominent humps.

The prophet flower (*Arnebia linearifolia*) is another desert steppe plant common in the Middle East. Its seeds are similar to those of *Lithospermum arvense*, only larger.²⁴⁰

When in contact with high temperature and carbonised, the surfaces of seeds from the family Boraginaceae turn whitish or greyish rather than black because of the high silica content.²⁴¹ In this form of preservation, members of this family occur commonly in archaeological sites in the Middle East. But they also can survive uncarbonised even in poor conditions, which is likely the reason

231 Genaust 1996, 47.

232 van Zeist/Bakker-Heeres 1982, 212.

233 Klak/Hanáček/Bruyins 2017.

234 van Zeist/Bakker-Heeres 1982, 214; Oberdorfer 1990, 352.

235 Genaust 1996, 617.

236 Oberdorfer 1990, 970–971.

237 Genaust 1996, 138.

238 Oberdorfer 1990, 779.

239 Kroll 1983, 81.

240 van Zeist/Bakker-Heeres 1982, 212; 1984b, 180.

241 van Zeist/Bakker-Heeres 1982, 212.

why they are often overrepresented in archaeobotanical assemblages.

Because boraginaceous seeds often survive in an uncharred state in archaeological contexts there is frequently a problem regarding their date.²⁴² It is often difficult to determine whether or not the seeds have been in contact with fire, as they do not turn black on burning. For this reason, some uncertainty will always remain about whether these seeds are of the same age as the deposit or whether they are due to a later intrusion (e.g. from seed-collecting animals).

The fruitlets of *Lithospermum arvense* recovered in Assur in 2023 are very fragile. Whether this can be taken as an indication that they date from the same period as the archaeological contexts in which they have been found cannot be securely determined at this time. The question of whether this many seeds arrived in the buildings through collecting activity or in some other way remains open.

H3.5.5 Brassicaceae, mustard family

Gold-of-pleasure (*Camelina sativa*), also known as oil-seed, from the *Camelina* genus within the mustard or cabbage family, has long been used as a crop as the plants were cultivated for their oily seeds, which serve human nutrition.²⁴³ One seed each was identified in two samples in Assur. Whether gold-of-pleasure was grown locally cannot be determined from this limited evidence.

Camelina sativa grows preferably on sandy and loamy soils. It thrives in grain fields (also of summer cereals), alongside roads or on rubble and wasteland, as it finds its best development opportunities in human-cultivated areas.²⁴⁴ It can therefore also be seen as a weed in the broadest sense and as ruderal plant.

The seeds of cabbage (genus *Brassica*) are small black spherical seeds of different sizes. The plant's parts such as beets, leaves and seeds can be used in various ways. Since ancient times, many cabbage species have been cultivated as vegetables or as fodder plants. Some species, such as black mustard, have oily seeds.

Cabbage prefers sandy and loamy soils and grows as a debris weed (*Sisymbrium*, annual ruderal vegetation) and as a field weed (*Polygono-Chenopodietalia*, root crop weed communities).

At Assur, 27 *Brassica* seeds were found in nine samples, which cannot be further identified to species level due to the lack of characteristic features on the seed surface. In general, indeterminate seeds of cabbage (*Brassica* sp.) frequently occur in archaeobotanical assemblages but their intended use is unclear.²⁴⁵

H3.5.6 Caryophyllaceae, carnation or pink family

At Assur, seeds of white campion, also known as catchfly flower (*Silene latifolia* ssp.²⁴⁶ *alba*), from the carnation or pink family are represented in ten samples by 23 seeds.

Silene species are annual or biennial herbaceous plants that grow to a height of 30-120 cm. They are widespread as they grow in cereal weed communities alongside paths and field edges and on rubble.²⁴⁷ Known as "white soapwort", its roots were once used as for washing due to their saponin content. The Latin genus name *Silene* refers to Silenus, the fat-bellied drunkard companion of Dionysos, god of wine in Greek mythology, and the comparison is aimed at the inflated, grape-shaped calyx of the bladder campion (*Silene vulgaris*).²⁴⁸

Cowherb (*Vaccaria pyramidata*) also belongs to this family. This is a winter annual and a characteristic weed in winter cereal fields because its seeds survive in the cold; in dry conditions and in the sun, the plants wither and die.²⁴⁹

The cowherb seeds are more or less spherical and when charred, severely deformed, usually splitting into two halves whereas parts of the typical seed coat typically remain intact. One seed each was found in three samples from Assur.

H3.5.7 Cistaceae, cistus family

The sunflower takes its name from its sunny location and the bright yellow flowers. The botanical genus name *Helianthemum* is composed of the Greek words *helios* "sun" and *ánthemon* "blossom, flower". The plants orient their blooms according to the position of the sun.²⁵⁰

Some species such as *Helianthemum ledifolium* grow in steppes and deserts.²⁵¹ One seed each was found in two

242 These seeds can also be collected by ants, see van Zeist/Bakker-Heeres 1982, 212.

243 van Zeist/Bakker-Heeres 1985, 254.

244 Oberdorfer 1990, 477.

245 Kroll 2016, 139.

246 Ssp. = subspecies.

247 Oberdorfer 1990, 365.

248 Genaust 1996, 584.

249 van Zeist/Bakker-Heeres 1982, 214.

250 Genaust 1996, 282.

251 van Zeist/Bakker-Heeres 1982, 215.

samples from Assur, but could not be identified at the species level (hence designated as *Helianthemum* sp.).

H3.5.8 Hyacinthaceae, hyacinth family

Hyacinthaceae are a subfamily within the asparagus family (Asparagaceae). The seeds of the hyacinth (*Bellevalia* sp.) are irregularly roundish with a typical hole on the underside where carbonisation caused the thin seed coat to disappear. The plants grow as weeds in cereal fields.²⁵² *Bellevalia* is present in Assur with a single seed.

H3.5.9 Fabaceae, wild legume family

Legumes are among the most species-rich plant families. In contrast to the family's cultivated species with their large seeds (pea and lentil, see §H3.3), which are hardly documented in Assur, the small-seeded wild legumes (Fabaceae)²⁵³ are very well documented among the 2023 samples. Small-fruited species such as those of the genera *Coronilla*, *Melilotus*, *Medicago*, *Trigonella*, *Lotus*, *Onobrychis*, *Prosopis* and *Trifolium*, as well as other taxa that cannot be further identified, are moderately common.

Scorpion vetches (*Coronilla*) are lushly growing shrubs. Among the Assur material, they are documented with 17 seeds in twelve samples. Their functions in these samples is not clear. An origin from the grain harvest is rather unlikely. On the other hand, *Coronilla* species have a high protein content and are valuable fodder plants for sheep and goats, which are insensitive to the poisonous glycoside coronillin they contain. The seeds may therefore have reached the vicinity of fire as dung that was used as fuel after having travelled through the digestive system of these animals, which they survive unscathed.²⁵⁴ The use as a medicinal plant is also conceivable.²⁵⁵

Melilot or sweet clover (*Melilotus*) prefers sandy soils and occurs in weed plant communities.²⁵⁶ It was detected in the form of 24 seeds in ten samples from Assur. Due to the charring process, some seeds are deformed or burst open so that they cannot be assigned to a specific species.

Medick or burclover (*Medicago*) is in evidence with 51 seeds in 18 samples. The seeds are small, elongated and

bean-shaped and are similar in size to numerous species of other genera of the Papilionaceae, a subfamily of the legume family. A reliable classification is only possible if at least parts of the fruit pods are preserved as these are characteristically snail-like, with a spiky edge.²⁵⁷ Unfortunately, these fruit pods are missing in Assur so that the *Medicago* seeds cannot be assigned to any particular species.

The determination of legumes is generally made more difficult by the large diversity of species and the strong shape variability within the species. The Arabian clover (*Medicago* cf. *arabica*) may occur with 13 seeds in two samples, and the sickle clover (*Medicago* cf. *falcata*) may be represented by a single seed at Assur, but the identification of these two species is not entirely certain.

Fenugreek (*Trigonella* sp.) is another small-seeded legume, with 38 seeds identified in ten samples, and so is clover (*Trifolium* sp.) with three seeds in one sample. Both taxa are species of steppe vegetation and also grow in fields.²⁵⁸

Bird's foot trefoil (*Lotus*) is another clover species detected at Assur, moderately well recorded with 21 seeds from nine samples, which were not further identified as species identification is still problematic.²⁵⁹ Three seeds in one sample may represent *Lotus* cf. *corniculatus* although this identification is uncertain due to moderate preservation. These plants are annuals and grow on pastures, alongside paths, in quarries, in saline clay soils and on damp sites such as springs or ditches.²⁶⁰

A single seed is presumably evidence for the caterpillar plant (cf. *Scorpiurus* sp.), again with uncertain determination due to moderate preservation. The legumes of this species are curved and covered with spines so that they resemble a scorpion's tail, hence the Latin name. There are only two thorny or prickly shrubby *Scorpiurus* species attested in the Mediterranean and the Middle East.²⁶¹

Sainforn is another genus within the legume family and represented by 41 seeds in eight samples at Assur that could not be further identified (hence classified as *Onobrychis* sp.). They grow on warm, moderately dry and loose soils.²⁶² Known to be excellent animal fodder plants,²⁶³ like all legumes they also greatly improve soil conditions (see §H3.3).

252 van Zeist/Bakker-Heeres 1982, 227.

253 The term Leguminosae is outdated but is still used as a synonym for Fabaceae in archaeobotanical literature.

254 Miller 1984, 71-79.

255 Riehl 2000, 233.

256 Oberdorfer 1990, 586-587.

257 Kroll 1983, 78.

258 van Zeist/Bakker-Heeres 1982, 210.

259 van Zeist/Bakker-Heeres 1985, 259.

260 Oberdorfer 1990, 598-599.

261 Genaust 1996, 571; Erhardt 2008, 1731.

262 Oberdorfer 1990, 606-607.

263 Genaust 1996, 436.

The wild legume finds from Assur are difficult to interpret but *Medicago* in particular appears to be attested quite regularly. Beyond an origin as a weed in cereal fields, it was perhaps used as animal fodder. Among the small-seeded legumes, there are some valuable fodder plants such as alfalfa and *Medicago* cf. *falcata* as horse feed or as concentrated livestock fodder. Therefore, the intentional cultivation of such plants is conceivable. They survive the hot summer period well because their richly branched, deep roots supply them with water and can then be harvested.²⁶⁴ A common feature of these wild legume plants is also that their small seeds are not only edible, but sweet and tasty. *Lotus* species especially do not merely serve as animal feed, but their sweet pods were eaten raw by people around the Mediterranean, e.g. on Crete. Ancient authors identify some species such as the North African lotus with the food of the Lotophages, the lotus-eating people in Homer's *Odyssey* whose land was identified in antiquity with the Lesser Syrtis, that is the island of Djerba.²⁶⁵

The deep-rooted poisonous weed mesquite (*Prosopis*)²⁶⁶ belongs to the mimosa subfamily (Mimosoidiaceae) within the legume family. The prickly shrubs grow very well in dry locations. The seeds are recognisable by a horse-shoe-shaped line on both sides. They ripen in pods and are often eaten by sheep and goats.²⁶⁷ At Assur, one single seed (*Prosopis* cf. *farcta*) was collected but the identification of the species is uncertain.

In addition, ten fragments of leguminous plants were collected, but could not be further identified.

H3.5.10 Lamiaceae, labiate family

Ground pine or yellow bugle (*Ajuga chamaepitys*) is a member of the bugle genus (*Ajuga*). Many species are ground-cover plants. The yellow bugle grows on and along paths, on walls and in fallow land as well as as a weed in winter cereal fields and also in vineyards.²⁶⁸ The plant is used for medicinal purposes. Only one seed was found in Assur, and the evidence is therefore much too limited to draw any conclusions.

Germander (*Teucrium*) also belongs to the labiate family. These plants are woody and semi-shrubby. They grow

on stony, gravelly, fallow land, but also in dry grassland.²⁶⁹ Germander is another medicinal plant.²⁷⁰ At Assur, it is recorded with one seed (*Teucrium* sp.).

Also the genus *Stachys* is part of the labiate family. The plants grow upright, are herbaceous and have an unpleasant odour. They are undemanding as far as their location is concerned, but prefer sunny spots. They grow in open weed communities, fields and fallow land. Most species require dry soils. The Greek botanical name *Stachys* means "ear of grain" and this refers to the pseudo-ears that these plants produce.²⁷¹ The genus is probably represented by one seed each in three samples, but the determination is uncertain (cf. *Stachys* sp.).

H3.5.11 Malvaceae, mallow family

Members of the mallow family are very often found in synanthropic plant communities that have adapted close to human settlements so that their natural habitat can no longer be reconstructed.²⁷² Many mallow species prefer sandy and loamy soils and grow ruderal on rubble or in fields.²⁷³

Mallows occur moderately constantly and in small numbers at Assur: 50 seeds of a species of mallow (*Malva* sp.) were found in 19 samples. Typically, the outside of the kidney-shaped sub-fruits has a net-like structure, making identification easy. If this is no longer preserved, as in Assur, the seeds are naked. Due to this missing morphological feature, they cannot be identified as species, especially as related species of *Althaea* (such as marshmallow or hollyhock) may also occur.

Mallows were already known as medicinal plants in ancient times, and the flowers and leaves were used.²⁷⁴ The leaves can be used to make a spinach-like porridge, which becomes sticky due to the plant mucilage. The cheese-shaped fruits are called cheese.²⁷⁵ The question of whether the mallow was collected from its wild habitats or cultivated at Assur cannot be answered at present. However, if the latter applied it would suggest that the mallows were not only used as medicinal plants but also for food.

264 Kroll 1983, 78.

265 Genaust 1996, 350.

266 Erhardt *et al.* 2008, 1656.

267 Van Zeist/Bakker-Heeres 1985, 261.

268 Oberdorfer 1990, 794.

269 Willerding 1986, 265; Oberdorfer 1990, 806-808.

270 Kroll 1983, 82.

271 Genaust 1996, 607.

272 Kroll 1983, 79, 872-873.

273 Oberdorfer 1990, 658-659.

274 Wichtl 2009, 413.

275 Kroll 2016, 137.

H3.5.12 Papaveraceae, poppy family

The horned poppy (*Glaucium*) from the poppy family is represented by seven seeds in three samples at Assur. The identification is uncertain due to the moderate form of preservation (hence classified as cf. *Glaucium* sp.). Annual or perennial herbs with bluish shimmering leaves and milky sap,²⁷⁶ the plants grow on salty sandy soils and ruderal meadows, in cereal fields and on rubble sites.²⁷⁷

H3.5.13 Plantaginaceae, plantain family

Plantago species colonise grassland, grow along paths, between stones and in fields and prefer sandy-loamy soils.²⁷⁸ They belong to special plant communities that can tolerate high levels of stress due to trampling, which other plants do not tolerate; hence their name that is derived from Latin *planta* “sole of the foot”.²⁷⁹ Vegetative parts of the plant are used medicinally but are also eaten as wild vegetables.²⁸⁰

In Assur, one seed each of hare’s foot plantain (*Plantago lagopus*) was identified in three samples, and also one seed each of psyllium plantain (*Plantago psyllium*), again in three samples. As plantains often grows on fields in the vicinity of settlements, they may have come into the settlement in small quantities with grain that had not yet been cleaned. It is also possible that the plants grew within the settlement in moist locations.

H3.5.14 Poaceae, grass family

Grasses (Poaceae, also called Gramineae) are among the most numerous and constant wild plants currently attested among the Assur samples, with 253 finds isolated in 24 samples. Most of these probably grew as weeds in barley and wheat fields. The grasses arrived at the settlement together with the harvested crop and most likely originate from cereal processing.

As the narrow fruits often break, essential characteristics are not available for identification and they cannot be reliably separated according to species. Therefore, they were only identified up to the genus classification level. Genera such as brome (*Bromus*), goat grass (*Aegilops*), fes-

cue (*Festuca*) and ryegrass (*Lolium*) are present, of which only *Aegilops* occurs reasonably consistently in the Assur finds.

Bromus species have a wide ecological range.²⁸¹ They can be found on meadows, fields and rubble. They grow along paths and walls and prefer loose, sandy and gravelly soils.²⁸² *Bromus* species (*Bromus* sp.) are present with 21 seeds in eight samples; it is quite possible that several species are attested as there are long-fruited and short-fruited seeds, but they cannot be separated and identified with any certainty. Furthermore, twelve seeds in four samples are assigned to the barren brome or poverty brome (*Bromus sterilis*).

Ryegrass (*Lolium*) is another characteristic cereal weed. At Assur, eight seeds were found in two samples, which could not be further identified (*Lolium* sp.). When this plant procreates too successfully this can be highly problematic, especially if it is darnel ryegrass (*Lolium temulentum*). Its consumption is dangerous for humans, as this can lead to severe poisoning that may end fatally with respiratory arrest. Symptoms are dizziness, apathy, headache, confusion of the senses and speech, anxiety, vomiting, pain and trembling. *Lolium temulentum* can be affected by a poisonous fungus that grows within the plant without damaging it. The fungus penetrates the seeds and lives on in them. When these seeds are sown, the germinating new plants are also infected by the fungus. As *Lolium* seeds resemble cereal grains, they are often harvested by mistake and not necessarily recognised during grain cleaning. The present author found the contamination in a grain storage with several thousand grains at Bronze Age Ebla in northwestern Syria to be very high as every tenth grain was identified as *Lolium temulentum*. Today, *Lolium temulentum* is of no significance today as a weed in agricultural contexts.²⁸³

Goat grass (*Aegilops*) is another cereal weed and mainly grows in barley fields.²⁸⁴ Tausch’s goatgrass, also known as rough-spike hard grass (*Aegilops tauschii*), is the ancestor of wheat (*Triticum aestivum*), which was created by crossing it with emmer (*Triticum dicoccum*), whereas spelt (*Triticum spelta*) was created by crossing emmer (*Triticum dicoccum*) with another *Aegilops* species.²⁸⁵ At Assur, 84 seeds of *Aegilops* sp. were found in 19 samples.

Fescue (*Festuca*) is very species-rich genus that occurs worldwide. Fescue species grow along paths, and while

276 Genaust 1996, 267.

277 Oberdorfer 1990, 425.

278 Oberdorfer 1990.

279 Genaust 1990, 491.

280 Genaust 1996, 491.

281 Kroll 1983, 93.

282 Oberdorfer 1990, 206.

283 Kroll 1983, 85.

284 Genaust 1996, 40.

285 Oberdorfer 1990, 235.

some species prefer sandy soils, others like locations along streams and wet places.²⁸⁶ At Assur, only one seed was found.

H3.5.15 Polygonaceae, knotweed family

This family includes dock (*Rumex*), which prefers sites with a moderate water balance. The plants grow on rubble and along paths.²⁸⁷ At Assur, only one seed of fiddle dock (*Rumex pulcher*) was found.

H3.5.16 Rosaceae, rose family

Hawthorn (*Crataegus* sp.) is a white-flowering shrub with thorns and often used as a hedge plant. Its fruits are edible, and the stone cores are thick-walled. This deep-rooting plant is part of the steppe vegetation and grows on stony, loamy and calcareous soils.²⁸⁸ It is a medicinal plant that can be used to treat heart problems.

At Assur, one seed each of thorny hawthorn (*Crataegus monogyna*) was found in two samples. Two further seeds from another sample could not be further identified as they were only preserved as fragments (hence designated as *Crataegus* sp.). It is conceivable that the berries were collected near the settlement.

H3.5.17 Rubiaceae, bedstraw family

Bedstraw (*Galium*) grows in perennial weed and fringe communities as well as as a weed in cereal fields. It needs another plant to attach itself to in order to grow diagonally upwards. Its fruits are small hollow balls with a hole on the ventral side and barbs or bristles on the pericarp, which are generally not preserved in charred material. With these, the bedstraw seeds adhere to animal fur or textiles and are spread in this way.²⁸⁹

The name *Galium* comes from Greek *gala* “milk”, and the German name “Labkraut” refers to the beneficial properties of the plant that causes the coagulation of milk.²⁹⁰ It is used in traditional medicine for the treatment

of ulcers, festering glands and skin rashes as well as bladder problems.²⁹¹

Common *Galium* species are stickwilly or false cleaver (*Galium spurium*) and goosegrass (*Galium aparine*), which has larger fruits. The distinguishing features of the seeds are the fine net-like structures on the surface, which could not be observed in the specimens found at Assur. Bedstraw occurs moderately constantly in small numbers in Assur: 27 seeds from fifteen samples were identified, but could not be assigned to a specific species (hence designated as *Galium* sp.).

Another member of the bedstraw family is blue wood-raft (*Asperula arvensis*). It is a typical weed in cereal fields and thrives best on warm, dry and calcareous loamy soils.²⁹² At Assur, two seeds were found in one sample, but their determination is uncertain (cf. *Asperula arvensis*).

Species of the genus *Crucianella* also belong to the bedstraw family. These are annual herbs that are native to the Mediterranean, the Arabian Peninsula and Central Asia.²⁹³ The exact species attested in one seed from Assur could not be determined, especially as charred seeds are very similar to *Plantago* seeds.²⁹⁴

H3.5.18 Scrophulariaceae, figwort family

The species takes its name from the throat-like shape of its flowers, which was thought to cure mycobacterial cervical lymphadenitis, formerly known as scrofula. This disease mainly affects domestic animals such as horses and pigs as an inflammation of the pharyngeal mucosa, palate and tonsils (hence *scrofulae* “neck glands”, which in turn is probably derived from *scrofa* “sow, female pig”).²⁹⁵

A figwort species (cf. *Scrophularia* sp.) is probably represented by one seed from Assur. The determination is uncertain, as it is only moderately preserved. Some species of this family prefer dry locations, but they can also be found on river banks or in wetlands.²⁹⁶

H3.5.19 Thymelaeaceae, daphne family

Sparrow weed (*Thymelaea passerina*) is a weed characteristic for nutrient-rich, calcareous soils that are ideal for

286 Oberdorfer 1990, 212.

287 van Zeist/Bakker-Heeres 1982, 229.

288 Oberdorfer 1990, 508.

289 Willerding 1986, 134-135.

290 Kroll 1983, 87.

291 Melzig/Hiller 2010, 254.

292 Oberdorfer 1990, 762.

293 Erhardt *et al.* 2008, 1338.

294 van Zeist/Bakker-Heeres 1985, 263.

295 Genaust 1996, 572.

296 Oberdorfer 1990, 832.

cereal cultivation.²⁹⁷ The small seeds look like bird heads with beaks, hence the plant's name. The fruits are poisonous. At Assur, sparrow weed is represented with four seeds in two samples. One of these seeds is soft and might therefore be of modern date.

H3.5.20 Valerianaceae, valerian family

Corn salad (*Valerianella*) is the best-known representative of the Valerian family. The members of the *Valerianella* species are common cereal weeds. The leaves grow in rosettes, are easy to collect and make a tasty salad. Wild lettuces and their use is difficult to prove archaeobotanically, as the tender leaves do not normally survive. However, storage of seeds may indicate intentional cultivation, but this is not presently in evidence at Assur, and therefore corn salad is listed here with the wild plants.²⁹⁸ One single seed of bladder cornsalad (*Valerianella vesicaria*) was identified.

H3.6 Vitaceae, grape family

Generally speaking, grape seeds have an unmistakable shape and are so easy to recognise that even fragments can be reliably identified. However, finds of vine seeds from archaeological contexts always raise the question of whether they are to be interpreted as cultivated wine (*Vitis vinifera sativa*) or wild wine (*Vitis vinifera sylvestris*). Wild vines are very diverse in form and so is the cultivated vine, which developed from the wild vine. This diversity affects the shape and dimensions of the seeds, and it is therefore the seed morphology that serves as the key to identification; cultivated wine has slender, narrow grape pips and wild wine plump, roundish pips. The number of individual finds can also be used as an indicator for or against cultivation.²⁹⁹

It is important to assess whether the finds are the result of collecting wild grapes or of harvesting cultivated vineyards. If an archaeological context produces only few vine seeds that do not occur continuously this can be more likely attributed to wild grape collecting, especially if the seeds are of roundish and plump. If grape seeds are routinely found in permanent settlements, this tends to be

indicative of cultivated vines, although the collection of wild grapes cannot be ruled out.³⁰⁰

In eight samples from Assur, one grape seed each was found of the roundish, plump type that can be classified as wild vine (*Vitis sylvestris*). At present, nothing can be said about their specific use, whether that was a raw food, dried as raisins, for wine, or for vinegar. Two grape seeds of the elongated, slender type can be classified as cultivated (*Vitis vinifera sativa*). In addition, five grape peduncles that cannot be assigned to either cultivated or wild vine were found in three samples (*Vitis* sp.). As larger accumulations of grape seeds are missing, it would be premature to speculate if or to what extent wine may have been cultivated locally in Assur.

H3.7 Zygophyllaeae, caltrop family

One seed of steppe rue (*Peganum harmala*) was found at Assur. This low shrub grows upright to a height of up to 50 cm tall and has cream-coloured flowers. It thrives in the deserts and steppes of the Mediterranean and the Middle East. A toxic plant with many uses, all its parts contain harmaline alkaloids, which affect the central nervous system and can cause antispasmodic and analgesic, but also euphoric and hallucinogenic reactions.³⁰¹ An ancient medicinal plant, steppe rue is used both internally to treat stomach pains and externally to treat wounds and skin rashes. In Central Asia, it is traditionally used as a smoking agent and aphrodisiac.³⁰²

H3.8 Indeterminate seeds

This category includes 598 fragments from 29 samples that cannot be determined precisely because the seeds have too few preserved characteristics due to their moderate or poor state of preservation.

H3.9 Indeterminate stems

21 stems have been identified in ten samples that cannot be attributed with any certainty to specific plants.

297 Oberdorfer 1990, 661.

298 Kroll 1983, 96.

299 Riehl 2001, 160.

300 Kroll 1983, 61-62.

301 Rättsch 2004, 425; Andreozzi/Sarkady 2022, 155.

302 van Wyk/Wink/Wink 2004, 230.

H3.10 Indeterminate husk fragments

167 seed shell fragments were isolated from 16 samples. As they have no recognisable surface structure they cannot be assigned to a certain species.

H3.11 Varia

This group include charcoal, bone fragments, snail shells, insect remains and artefacts that are not analysed in the present study.

There are also amorphous objects that could represent the remains of cereal porridge, as the charred mass exhibits a characteristic bubbly structure that is the result of grain being crushed and processed into bulgur. Some of these fragments have a smooth side, which could be explained as parts of the porridge that stuck to the inside of a vessel.

H3.12 Preliminary overall assessment

From the 32 samples retrieved during the 2023 excavations at Assur, a total of 8,655 plant remains were identified, of which 5,207 can be attributed to cultivated plants and 3,458 to wild plants. In total, this material consists of the comparatively small total amount of 431.2 g. Across the samples, the frequency of finds varies, but mostly small numbers occur. While the attested taxa are very homogeneous across the samples from various stratigraphic contexts, the continuity and ubiquity varies (§H3.12).

The range of attested cultivated plants is still rather small, and the finds of cereals include both grains and chaff. No mass finds or evidence for grain storage has been identified so far. Multi-row barley (*Hordeum vulgare*) is the most common and constant cereal attested in the 2023 material, even if it is found only in small numbers in most of the samples. Its role as an important crop can be considered certain. Barley is far better attested than emmer (*Triticum dicoccum*) and einkorn (*Triticum monococcum*), both of which are represented by only one single grain each. At Assur, these cereals are currently mainly attested in the form of threshing remains (spikelet forks, husk and rachis fragments), but these do not constitute proof of local cultivation. Barley is also much better attested than free-threshing wheat (*Triticum aestivum*), which is currently present at Assur in the form of six grains.

But although the local cultivation of emmer, einkorn and free-threshing wheat cannot be considered certain due to the sparse finds, it is rather unlikely that no other cereals than barley were grown at Assur. However, in

contrast to the various types of wheat, barley has an undemanding and resistant nature, and this may well have led to its preferential cultivation. Without precautionary protective measures, intensive farming leads to leaching of the soil and increased cereal diseases, and this may be reasons why the frugal yet high-yielding barley was preferred.

At present, there is limited evidence for other cultivated plants. Only a few cultivated pulses such as lentils (*Lens culinaris*) and peas (*Pisum sativum*) have been detected among the Assur samples. But as these can also be eaten raw, pulses generally come into less contact with fire than cereals. The evidence for olive (*Olea europaea*) must be viewed with a question mark, as the identification of the fragments found is uncertain. Cultivated wine (*Vitis vinifera sativa*) is currently documented with one grape seed whereas wild wine (*Vitis vinifera sylvestris*) is in evidence with eight grape seeds, and five peduncle remains cannot be assigned to one species or the other.

Wild plants are represented by numerous species and with the high number of 3,458 finds overall. However, it is striking that the quantity per species is relatively low. The plants occur only sporadically, or in quantities of fewer than ten seeds. Most of the attested grasses (*Bromus*, *Aegilops*, *Lolium*) prefer dry locations. However, there are also some wild plants in evidence that prefer moist or occasionally wet sites (clovers, dock species); as these occur in small numbers their significance cannot yet be clarified. Small-seeded wild legumes (Fabaceae) are documented with several species, but in terms of finds not as numerous as the grasses. At present, the spectrum of wild plants does not yet provide any clear information about the ecological conditions around the settlement in antiquity. The grasses certainly played an important role in the steppe vegetation, and the small-seeded legumes may have been used as animal fodder.

Table H3.2 shows the botanical calendar for Assur based on the flowering and fruiting period for each plant species identified from the flotation samples in 2023.

H3.13 Evaluation according to stratigraphic contexts

Andrea Squitieri & Karen Radner

In this section, we briefly discuss the identified plant remains from contexts excavated in 2023 that can be safely assumed not to be contaminated with older material.

In the first instance, these are the two floors of “Room 6” that both date to the late Neo-Assyrian period, almost certainly to the 7th century BC (§D1.3). **Table H3.3** gives

Taxon	Flowering/fruiting period	Land use designation
<i>Aegilops</i> sp.	April-June	Wheat fields
<i>Aizoon hispanicum</i>	July-August	Desert plains, saline areas
<i>Ajuga</i> cf. <i>chamaepithys</i>	May-September	Cereal fields, along paths, walls, fallow land, winter cereal fields, vineyards
<i>Althaea officinalis</i>	June/July-August	Fields, rubble
<i>Arnebia linearifolia</i>	June-July	Fields, alongside roads, rubble
cf. <i>Asperula arvensis</i>	May-August	Cereal fields, fallows, vineyards
<i>Bellevalia</i> sp.	May-June	Cereal fields
<i>Brassica</i> sp.	February-June	Grain fields, alongside roads, rubble, wasteland
<i>Bromus sterilis</i> / <i>Bromus</i> sp.	February-August	Meadows, fields, roadsides, paths, walls, waste grounds
<i>Centaurea</i> sp.	June-August	Grassland, ruderal places, roadsides, fields
<i>Coronilla</i> sp.	May-July	Woodland margins, scrubland, dams, roadsides
<i>Crataegus monogyna</i>	May-June	Hedges, forest edges
<i>Crucianella</i> sp.	June-August	Forest, grassland
<i>Festuca</i> sp.	June-July	Paths, along streams, grassland
<i>Galium</i> sp.	March-September	Grain fields, steppe, forest edges
cf. <i>Glaucium</i> sp.	May-August	Ruderal meadows, cereal fields, rubble sites
<i>Helianthemum</i> sp.	May-July/August	Steppes, deserts
<i>Hippocrepis</i> sp.	April/May-September	Grassland, roadsides, dams, forest edges
<i>Lithospermum arvense</i>	May-June	Deserts, steppe, grain fields, alongside roads, rubble
<i>Lolium</i> sp.	March-June	Grain fields, steppe
<i>Lotus</i> sp./ <i>Lotus</i> cf. <i>corniculatus</i>	May-August/September	Pasture, alongside paths, in quarries, springs, ditches
<i>Malva</i> sp.	July-September	Fields, ruderal places
<i>Medicago</i> sp.	March-September	Fields, steppe, forest, grassland
<i>Medicago</i> cf. <i>arabica</i>	April-June	Grassland, sideroads, dams
<i>Medicago</i> cf. <i>falcata</i>	May/June-October	Forest, fields, sideroads, waste ground, grassland
<i>Melilotus</i> sp.	July-September	Weed plant communities, grassland
cf. <i>Olea</i> sp.	April-June	Steppe, semi-deserts
cf. <i>Onobrychis</i>	May-July	Grassland, hedges, sideroads, embankments
<i>Peganum harmala</i>	April-June	Steppe, deserts, semi-deserts
<i>Plantago lagopus</i>	March/April-June	Fields near settlements, sideroads, grassland, meadows
<i>Plantago</i> cf. <i>ovata</i>	January-April	Fields near settlements, sideroads, grassland, meadows
<i>Plantago psyllium</i>	March-July	Fields, grassland, ruderal places, sideroads, meadows, moist places
<i>Plantago squarrosa</i>	March/April-June	Grassland
<i>Prosopis</i> cf. <i>farcta</i>	April-September	Along irrigation channels, water courses, waste places, roadsides, fields
<i>Rumex pulcher</i>	June-August	Paths, rubble, moist places
cf. <i>Scorpiurus</i> sp.	June-September	Fallow land, cultivated fields, ruderal places
cf. <i>Scrophularia</i>	June-August	Forests edges, river banks, wetland
<i>Silene latifolia</i> ssp. <i>alba</i>	June-September	Alongside paths, field edges, rubble
cf. <i>Stachys</i> sp.	June-July/August	Forests, fields, fallow land roadsides
<i>Suaeda</i>	July-September	Wetland near coasts, salt marshes, seashores
<i>Teucrium</i> sp.	June-October	Stony fellow land, grassland
<i>Thymelaea passerina</i>	July-September	Cereal fields, grassland
<i>Trifolium</i> sp.	May-October	Steppe, fields, grassland, sideroads
<i>Trigonella</i> sp.	April-June	Steppe, fields, grassland, sideroads
<i>Vaccaria pyramidatata</i>	June-September	Winter cereal fields, ruderal places
<i>Valerianella vesicaria</i>	April-May	Cereal fields, grassland, along sideroads
<i>Vitis vinifera sylvestris</i>	May-June	Forest edges, forest clearings
<i>Hordeum vulgare</i>	March-May	Fields
<i>Triticum aestivum</i>	April-June	Fields
<i>Triticum dicoccum</i>	May	Fields
<i>Triticum monococcum</i>	June-July	Fields
cf. <i>Lens</i> sp.	March-June	Fields
cf. <i>Pisum</i> sp.	April-May	Fields
<i>Vitis vinifera</i>	June-August	Vineyards, hedges, floodplain forest, riversides

Table H3.2: Botanical calendar for Assur based on the flowering and fruiting period for each plant species identified from the flotation samples in 2023. Prepared by Claudia Sarkady.

a survey of the identified plants. The material from these floors yielded a mix of cultivated and wild plants. Attested are the cereals barley (*Hordeum vulgare*), emmer wheat (*Triticum dicoccum*) and einkorn wheat (*Triticum monococcum*), with barley by far the most common (see the frequency graph: Fig. H3.1). Note that free-threshing wheat (*Triticum aestivum*) is not attested. Only a few other domesticated food plants are in evidence, namely grape (*Vitis sp.*; §H3.6) and probably pea (*cf. Pisum sp.*; §H3.3.2). A fairly wide range of wild plants is attested, among which field gromwell (*Lithospermum arvense*, see §H3.5.4), found uncharred, is by far the most common, followed by grasses (Poaceae; §H3.5.14). The wild plants *Althaea officinalis* (§H3.5.11), *Rumex pulcher* (§H3.5.15), *cf. Asperula arvensis* (§1.3.5.17), and *Bellevalia sp.* (§H3.5.8) are attested in this assemblage, but not in any of the other samples taken in 2023.

Secondly, the soil sample taken from within the late Sasanian / early Islamic water jug (G01-S05-V01, §E1), which was deposited at a later stage in the chamber tomb (§D2.3), contained two indeterminate cereal seeds and three taxa of wild plants (*Aizoon hispanicum*, see §H3.5.1; *Lithospermum arvense*, see §H3.5.4; *Medicago sp.*, see §H3.5.9) as well as a small bone fragment (Table H3.4).

Radiocarbon-dating of randomly chosen barley seeds from Building A demonstrated that older material survived on the floors of Room 2 and 3, for whatever reason (§D1.3). Because of this, the assemblage can not be taken as representative of the time when the building was in use. Similarly, because of the way the deposits above the floor of “Room 5” were excavated, it is not justified at the moment to see them as representative of the Late Bronze Age: while a charcoal piece found directly on the floor produced the radiocarbon dating range of 1416-1278 calBC, a randomly chosen barley seed was dated to 771-545 calBC (both 94.5 % probability; §D1.3); we will further investigate this important context in 2024.

Archaeobotanical Laboratory CS Claudia Sarkady					
Assur 2023, Archaeobotanical Investigations, Room 6					
Sample no. (AS)		263432:002:001 Upper floor	263432:006:002 Lower floor	Sum	
Volume of samples (l)		6	12	18	
Weight incl. packaging (g)		5.4	11.0	16.4	
Net weight (g)		1.4	7.0	8.4	
TAXA	TAXA				Nm*
CEREALS	CEREALS				
<i>Hordeum vulgare</i>	barley	7	14	21	2
<i>Triticum dicoccum</i>	emmer wheat, rachis	4		4	1
<i>Triticum monococcum</i>	einkorn wheat, glume base		1	1	1
<i>Triticum sp.</i>	wheat, indeterminate		7	7	1
Cerealia indet.	cereal grains indeterminate	208	438	646	2
Cerealia indet.	cereal glume base		1	1	1
Cerealia indet.	cereal rachis internodes		3	3	1
OTHER FOOD PLANTS	OTHER FOOD PLANTS				
Fabaceae	legumes		2	2	1
<i>cf. Pisum sp.</i>	prob. pea		1	1	1
<i>Vitis sp.</i>	grape, pedicle		2	2	1
WILD PLANTS	WILD PLANTS				
<i>Aegilops sp.</i>	goat grass	1	6	7	2
<i>Althaea officinalis</i>	marsh mallow	1		1	1
<i>cf. Asperula arvensis</i>	woodruff		2	2	1
<i>Bellevalia sp.</i>	roman hyacinth	1		1	1
<i>Camelina sativa</i>	gold-of-pleasure	1		1	1
<i>Centaurea sp.</i>	knapweed	1	1	2	2
<i>Coronilla sp.</i>	scorpion vetch	3	1	4	2
<i>Crataegus monogyna</i>	common hawthorn		1	1	1
<i>Galium sp.</i>	bedstraw	3	1	4	2
<i>cf. Glaucium sp.</i>	horned poppy	2		2	1
<i>Helianthemum sp.</i>	rock rose		1	1	1
<i>Lithospermum arvense</i>	field gromwell	74	31	105	2
<i>Lotus sp.</i>	trefoil	2		2	1
<i>Malva sp.</i>	mallow	2	1	3	2
<i>Medicago sp.</i>	bur clover	4	8	12	2
<i>cf. Onobrychis sp.</i>	prob. sainfoin	5		5	1
Poaceae	grass family	51	11	62	2
<i>Rumex pulcher</i>	fiddle dock		1	1	1
<i>Silene latifolia ssp. alba</i>	white campion	10	1	11	2
<i>Vitis sylvestris</i>	wild grape, kernels		1	1	1
Indet., seeds	Indeterminate seeds	28	30	58	2
Indet. stem	Indeterminate stem	1	5	6	2
Indet., seed shell frg.	Indeterminate seed shell		18	18	1
	Sum			998	
	Total	409	589	998	
	Seed frequency (seeds/litre)	68.2	49.1	54.4	
Varia	Varia				
	Wood charcoal (pieces)	52	94	146	
	Amorphous objects	18	25	43	
	Bone fragments (pieces)		15	15	
	Insect remains	1		1	
	Snail shells	9	2	11	
	Other finds		mouse dropping		
	Number of samples	1	1	2	

Table H3.3: List of plant species recovered from both subsequent floors of “Room 6”, dated to the Iron Age. Abbreviations: cf. = confer (lat), compare; sp. = species (lat.). Prepared by Claudia Sarkady.

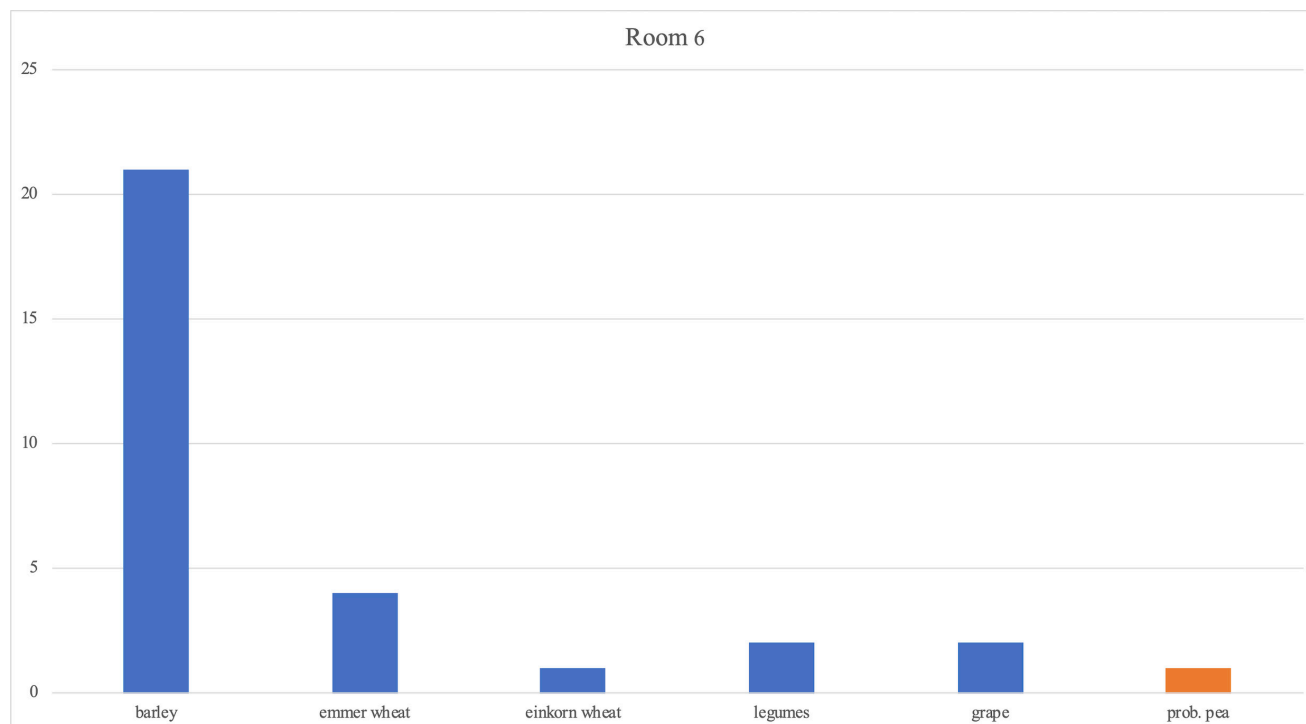


Fig. H3.1: Frequency of cultivated plant remains identified in “Room 6”, dated to the Iron Age. Probable identifications are in orange colour. Indeterminate finds are not shown. Prepared by Andrea Squitieri.

Archaeobotanical Laboratory CS Claudia Sarkady				
Assur 2023, Archaeobotanical Investigations, vessel fill G01-S05-V01				
Sample no. (AS)		262433:021:004	Sum	
Volume of samples (l)		5	5	
Weight incl. packaging (g)		4.3	4.3	
Net weight (g)		0.3	0.3	
TAXA	TAXA			Nm*
CEREALS	CEREALS		Sum	
Cerealia indet.	cereal grain indeterminate	2	2	1
WILD PLANTS	WILD PLANTS			
<i>Aizoon hispanicum</i>	Spanisch aizoon	1	1	1
<i>Lithospermum arvense</i> : uncharred	field gromwell	2	2	1
<i>Medicago</i> sp.	bur-clover	1	1	1
	Sum		6	
	Total	6	6	
	Seed frequency (seeds/litre)	1.2	1.2	
Varia	Varia			
	Bone fragments (pcs.)	1	1	
	Number of samples	1	1	

Table H3.4: List of plant species recovered from the fill of vessel G01-S05-V01, dated to the late Sasanian / Early Islamic period. Abbreviations: cf. = confer (lat), compare; sp. = species (lat.). Prepared by Claudia Sarkady.

I. Calcinated textile fragments from Grave 3: a preliminary report

Annette Paetz gen. Schieck

After the excavations at Assur in spring 2023, permission was granted in May 2023 to export 54 very small calcinated textile fragments from Grave 3 (§D2.5.1) and 33 tiny pieces of leather from Grave 4 (§D2.5.2) from Iraq to Munich, which were then brought to the Deutsches Textilmuseum Krefeld for analyses.³⁰³ There, the author investigated all objects with the help of a Dino-Lite USB microscope. In October 2023, the objects were returned to Iraq, except for a few samples that remain in Krefeld for further examination.

This contribution focuses on the textile remains. It is a preliminary first report, and a catalogue presenting each fragment in detail will follow at a later date.

I.1 Preservation conditions

The textile fragments (sample number AS 262433:060:009) were collected on 13 March 2023 from Grave 3 (§D2.5.1) where they were found scattered around the torso of the skeleton. The deceased was buried in a crouching position, lying on one side beneath a clay sarcophagus of an elliptical dome shape (§F5: no. 142). This sarcophagus bears an incised alphabetic inscription that provides the date of July/August 158 BC (§G2), which provides a *terminus ante quem* for the production of the textiles with which the deceased was buried.

The textile fragments are preserved as three-dimensional, calcinated structures whereas the organic fibres have decomposed (Fig. I.1). The fragments are very brittle and break and pulverize easily even though they were treated with a consolidating substance (PVB 5%) during excavation.

The term “calcination” describes a natural phenomenon that occurs when several premises are met. The find context, in this case, the burial was flooded shortly after being installed, and this must have happened at a time when the organic materials had not yet disintegrated. The water breaking in contained a high quantity of dissolved lime or plaster. While the humidity slowly vanished, the lime settled on the textile fibres, thereby creating casts that are exact copies of the textile structures, while the organic substances dispersed.

These calcinated “copies” preserve and transmit all information and characteristics of the lost textiles, such as the weaving structures and techniques (which cast a light on the technology, density, quality, and decoration of the textiles), spinning directions of threads (S or Z), structures and features of the fibres (plant or animal origin), condition of the fibres when deposited (worn or new) and any traces of wear. However, such calcinated copies do not preserve the textile’s former colours and dyestuffs.³⁰⁴



Fig. I.1: Debris containing tiny textile fragments of various structures and qualities. Photo by Annette Paetz gen. Schieck, DTM Krefeld.

³⁰³ My thanks go to Professors Karen Radner and F. Janoscha Kreppner for sharing this remarkable material with me. I also thank Dr Andrea Squitieri and Dr Jana Richter for providing me with information on the site and the excavation details, and again to Dr Richter for transporting the objects to and from Krefeld.

³⁰⁴ The only exception would be murex purple, which is not attested among the finds of Grave 3.

They also do not permit radiocarbon dating. Today, the fragments show monochrome shades of off-white, beige, greyish brown, and dark brown, and these are possibly reflections of their former materials and their differing colouring.

When interpreting the textile finds of Grave 3, a unique feature can be traced. 18 out of the 54 objects, many of them twined cords, are coated with a hard substance that sits on top of the woven structures (**Fig. I.2b** and **Fig. I.5**). This is a very fine sediment of a light greyish colour with fine blackish sprinkles that seems to have been viscous when attached, solidifying to a hard cast when drying. This coating most likely derives from dissolved soil drawn in by water that seeped into the burial, whereas larger particles were kept out by the lid of the sarcophagus. The sections covered with this sediment are very narrow and are found only along one side of the cords (**Fig. I.2b**) or



Fig. I.2a: Finishing border of a weave, twined cord deriving from the edge of a cloth, 19 mm in length. Photo by Annette Paetz gen. Schieck, DTM Krefeld.



Fig. I.2b: Reverse of the finishing border depicted in **Fig. I.2a** with adhesive sediment. Photo by Annette Paetz gen. Schieck, DTM Krefeld.



Fig. I.3: Textile fragments bearing a whitish crystal substance on one side of the weave, 12 mm in length. Photo by Annette Paetz gen. Schieck, DTM Krefeld.

the elevated areas of some folds. It is most likely that the water covered the ground of the burial to a height of just a few millimetres, thus affecting only those parts of the textiles that touched the ground as they hung down from the deceased's body. Therefore, also the calcination process only affected these small sections of the textiles.

Other weaves bear white crystals of salt. Some objects show them as scattered individual crystals; others show a compact layer on just one side of the textile (**Fig. I.3**). Again, this process was caused by the ingress of water that transmitted salt into the weave, and this is likely also the explanation for the skeleton's comparatively poor state of preservation.

I.2 Textile qualities

42 of the fragments from Grave 3 derive from woven textiles of various qualities in terms of thickness, stiffness, density, and thread count. 12 fragments consist of plied cords, of which at least 7 served as twined finishing borders of a woven textile; the weaves that were formerly attached are lost (**Figs. I.2a-b**). Since the preserved weaves themselves neither provide starting or finishing borders, nor turning edges, neither the warp nor the weft can be determined for certain. They are therefore referred to as "System 1" and "System 2".

All these textiles are woven in tabby with a rep-like structure. Plain tabby or other weaving techniques such as basket-weave have not been detected. All threads are spun in S-direction, which is the dominant spinning direction in archaeologically preserved textiles from the Ancient Near East, in various strengths, tensions and

spinning angles. No plies have been found. Most of the weaves show thicker threads in greater distances in one weaving system, and thinner threads in a higher density in the other, causing a ribbed structure.

Even though very small in size, at least six different qualities of weaves are attested among the textile fragments from Grave 3. To name the two extremes:

1. System 1 is composed of 4 threads per centimetre, hard spun, while System 2 consists of 12 threads per centimetre that are thick, voluminous, and very little spun (**Fig. I.4**). The resulting textile was very dense, thick, and stiff.
2. Other textiles are made of thin, little spun threads. In System 1, we count 11 threads per half a centimetre (= about 22 per centimetre), and in System 2, 27 threads per half a centimetre (= about 54 threads per centimetre).



Fig. I.4: Fragment of a thick, dense, and formerly stiff textile, 20 mm in length. Photo by Annette Paetz gen. Schieck, DTM Krefeld.



Fig. I.5: Light and open weave, folded in several layers, 5 mm in length, covered with sediment on the upper edge and bearing the hole of a sewing needle (0.7 mm in diameter). Photo by A. Paetz gen. Schieck, DTM Krefeld.

metre). This created a very light, open, and gauze-like weave (**Fig. I.5**).

This second quality can be found several times among the fragments. 6 of these fragments preserve two other unique features that provide evidence for the processing of the woven textiles. They are deliberately folded into tiny square-shaped packages of up to 7 layers of cloth, bearing a circular hole of about 0.5–0.7 mm in diameter. This hole was driven through the textile stack with a sewing needle, inserting a sewing thread, which is still preserved in some of the fragments. When the needle pushed through the textiles from one side, its pressure created a depression, and when it stepped out on the other side, it produced a rim consisting of tiny fibre fragments.

These 6 fragments, therefore, document sewing activity, most likely in order to attach appliqué decorative elements such as the beads that were also found in Grave 3, namely three spherical glass or frit beads of a diameter of 4 mm (AS 262433:060:005–007: **§F5 nos. 134–136**; see **Fig. I.6**) and a cylindrical white bead with a diameter of 5 mm (AS 262433:060:16: **§F5 no. 141**; **Fig. I.7**). Just as the textile remains, those beads were found in the area of the deceased's hip.



Fig. I.6: Oblate spherical bead made of glass/frit, with a diameter of 4 mm and a perforation of a width of 2 mm: AS 262433:060:006 (**§F5 no. 135**). Photo by Andrea Squitieri.



Fig. I.7: Cylindrical bead likely made of frit, with a length of 7 mm, a diameter of 5 mm and a perforation of a width of 3 mm: AS 262433:060:016 (**§F5 no. 141**). Photo by Andrea Squitieri.

No other traces of sewing stitches, mending, inwoven decoration or embroidery can be detected in the attested fragments.

I.3 First conclusions

The six different textile qualities observed among the calcinated textile remains from Grave 3 suggest that the burial was equipped with at least six different textile objects. At this point of the investigation, we must state that the preserved textile fragments are too small to indicate whether they once formed a burial shroud, a loincloth, a garment, or a blanket. It also is not possible to tell whether the textiles were produced especially for burial purposes or whether they have been used and worn before being positioned in the burial.

Still, the textile fragments from Grave 3 are amazing in terms of their variety and fineness, their quality, and their early date. It is worth pointing out that they are older than the date mentioned in the inscription of the sarcophagus, since the harvesting of the fibres as well as the weaving processes were carried out before that *terminus ante quem*, and the textiles may well have been kept or used for years before they were used in the burial ceremony.

Further investigations will concentrate on the weaves. For instance, technical data will be collected on thread counts, in order to group the objects according to their textile quality. Microscopic observations will be used to try to identify the fibres, the crystalline substance as well as the sediment. Finally, comparable finds and find contexts will be searched for in the published literature.

J. First conclusions

Karen Radner & F. Janoscha Kreppner

Our first fieldwork campaign in February and March 2023 represented the resumption of any sort of archaeological excavation work at Assur since the Iraqi State Board of Antiquities and Heritage (SBAH) last dug there in 2002. Challenging as it was to live and work within a community that had experienced great trauma and loss in the past decades, we were able to achieve significant results and produce data that is in many cases the first of its kind available for the site and its region.

As a first step, the severely damaged excavation house, which is part of the Unesco World Heritage portfolio and was first built by Robert Koldewey and Walter Andrae from 1903 onwards, was restored in the last third of 2022 (§B) and then served as a base for our work in spring and autumn of 2023. As a second step, at the very beginning of the field season in February 2023, the archaeological site of Assur was mapped by drone flight and fixed points were established. Of the points created by Barthel Hrouda's team in 1989, five could be relocated and were integrated into the new map (§C1).

The magnetometer prospection that Barthel Hrouda had initiated in 1989 was continued under the leadership of Jörg Fassbinder who had been part of the original team (§C2). He now added electric resistivity tomography (ERT) to the geophysical prospection programme. During ten days of fieldwork, a large-scale and high-resolution magnetometer survey was conducted in the entire area of the New Town of Assur (ca. 250 × 500 m) as well as in further parts of the city's residential area while the ERT measurements provide details on the depth of selected archaeological features.

This spring campaign also saw the very first geoarchaeological coring ever undertaken at Assur, led by Mark Al-taweel (§C3 and §C4). Most significantly, this brought to light evidence of a paved street in the New Town that seems to be connected to the gate that leads southwards through the city's fortification wall. During the SBAH excavations undertaken in 1979-80 in the western area of the New Town, the archive of a man called Aššur-matu-taqin from the second half of the 7th century BC was

found in the residential building unearthed there. One of its documents contains the description of a house:³⁰⁵

“A built house with its beams and with its doors. The main house with its walls, the side house, the courtyard, the workshop (*kurhu*) (are) within. A lot 15 (cubits long and) 20 cubits wide, adjoining the house of Uninu, adjoining the King's Road, adjoining the house of [PN], adjoining the alley, [adjoining the house of] Nabû-šallim-ahhe.”

According to this description, the house in question adjoined the Royal Road, and this may well have been the stretch of the road leading through the New Town that was revealed by Core 7. We intend to open a trench in this area in 2024.

In the course of the excavation of the trench NT1 2023 in 2023 (§D2), a total area of 120 square metres was investigated, and our work yielded a stratigraphic sequence from the site surface (162.97 m above sea level) to the virgin soil (159.08 m above sea level), which means that the beginning of the settlement history of the New Town of Assur can be further investigated in the future.

A piece of charcoal (sample AS 262432:079:003) taken from the fill of a pit cutting into the bedrock at the bottom of our deep sounding yielded a radiocarbon dating range of 1506-1440 calBC (95.4% probability). This date corresponds well with the oldest mention of the construction of the wall and the gates of the New Town in the inscriptions on two fragmentary clay cones of Puzur-Aššur III, an Assyrian ruler of the mid-second millennium BC conventionally dated to 1521-1498 BC (cf. §G1.5):

“For his life and the well-being of his city, he (i.e. Puzur-Aššur III) built the great wall and the gates of the New City (*ālu eššu*) from the great wall of the

305 Ahmad 1996, 234-237, 281: no. 10: ll. 5-13 (eponym year of Šamaš-šar-ru-ibni, commander-in-chief); for an edition of this passage, see Radner 1997, 290 (no. 71).

Inner City (*Libbi-āli*) as far as the river, in its entirety from its foundations to its crest.”³⁰⁶

This seems to imply that the New Town was added to the area of the city of Assur under Puzur-Aššur III. Given the radiocarbon date, the pit could represent the result of human activity at the time of the founding of the New Town, and this is an important puzzle piece for understanding the beginnings of settlement in this part of Assur. However, it is worth emphasising that as of yet, no architecture belonging to this period has been identified in the very limited context of our sounding. As only a few diagnostic pieces were recovered from the pit fill, not one of which is a rim fragment, the significance of this material is severely limited. In the soil deposit (Locus:262432:076) above the pit fill, we encountered pottery types that are known well from reference sites in the Assyrian heartland and the Syrian Jazirah in the 13th century BC, including fragments of carinated bowls and beakers with elongated bodies and nipple bases (§E1.6).

In general, good archaeological contexts dating to such early times are hitherto lacking in the New Town. Although Walter Andrae reached the bedrock in several of his sections (iA12I to iB12I,³⁰⁷ iE12I,³⁰⁸ iC14I and iD14I,³⁰⁹ mC14I / mC13V,³¹⁰ kC15I to kE15I,³¹¹ and mB15I to mC15I³¹²) Middle Assyrian features were only found in the northernmost part of the New Town in the sections ID11I³¹³ and iA13I.³¹⁴ Therefore, to excavate on a larger scale the oldest phase that we encountered in this first campaign (“NT1 2023 Phase 1”; §D2.10) promises exciting new insights into the occupational history of Assur for a time that is practically unknown at this site.

Above this, we encountered architectural remains that were assigned to “NT1 2023 Phase 2” (§D2.9). What little has been excavated of these so far indicates that there was a northern wall complex, which already existed at the time when a southern wall complex was added. This observa-

tion raises several questions that cannot be answered based on the limited data presently available: whether the northern and southern wall complexes represent construction phases of the same building that were built in quick succession; or whether there was a time gap between constructing the northern and southern wall complexes; or whether they each represent components of independent buildings erected directly next to each other.

As the southern wall complex respects the northern one, both must have existed simultaneously from a certain point in time onwards before all the walls were levelled to a uniform level. There are no preserved floors adjoining the walls, which is why the date of construction and the length of time when this architecture was in use can only be narrowed down by the chronological classification of the older and younger stratigraphic phases. Due to the ceramic material identified in the aforementioned deposit (Locus:262432:076), it seems plausible that the building ground was prepared and the structures erected in the 13th century BC, although a later construction date cannot be ruled out.

A *terminus ante quem* for the end of the use of this building results from the radiocarbon dating of two molars from Grave 5 (§D2.8) to 770–542 calBC and 775–545 calBC, respectively (both 95.4% probability). As the burial cuts into two walls of the earlier building (Locus:262432:082 and Locus:262432:083), that architectural unit was no longer in use at the time when the grave pit was cut. This means that the building’s construction and use fall into the hitherto archaeologically poorly-known time from the Middle Assyrian to the early Neo-Assyrian period. The fact that its walls (Locus:262432:080 to Locus:262432:085) were levelled at some point represents a significant change in the use of space and thus a discontinuity in the development of settlement in the area under investigation. Further exploration of these structures promises intriguing insights into the Assyrian city from the late second to the early first millennium BC.

The walls of this early occupation phase are sealed by a floor of the Unroofed Area 4 that belongs to what we dubbed Building B (NT1 2023 Phase 4; §D2.7). Also sealed by this floor was the already-mentioned Grave 5, and it was therefore assigned its own stratigraphic phase (NT1 2023 Phase 3; §D2.8). This burial is of late Neo-Assyrian date because it contained a partially preserved bronze fibula of Friedhelm Pedde’s C8 type (7th / early 6th century BC; §F8 no. 236) and a glazed miniature vessel (§E1.5; Vessel G05-V01) that is closely comparable to another piece from Assur found by Walter Andrae in a late Neo-Assyrian tomb.

The grave and its radiocarbon dating ranges provide a *terminus post quem* for the use of the floor of the Unroofed

306 IM 57822, ll. 6–9a: *a-na ba-lá-ti-šu u ša-lá-am a-li-šu* (6) BĀD ṚGAL [ū] ṚKĀ.GAL.MEŠ *ša URU.KI iš-še* (7) Ṛiš-tū [BĀD] GAL *ša li-ib-bi-URU.KI* (8) *a-[di ID a-na si-ḫi-ir]-Ṛti-šu iš-tù uš-še-šu* (9) *a-[di ša-ap-ti]-Ṛšū e-pu-uš*. For this text and the worse preserved parallel Ass 2065 = Ist A 3369, see Miglus 2010, 236–237.

307 Miglus 1996, 322.

308 Miglus 1996, 324.

309 Miglus 1996, 339–340.

310 Miglus 1996, 345.

311 Miglus 1996, 345–346.

312 Miglus 1996, 348.

313 Miglus 1996, 321.

314 Miglus 1996, 331.

Area 4, which is abutted by the walls Locus:262433:054 in the north and Locus:262432:075 in the southeast. While the dates fall firmly into the Hallstadt Plateau of the radiocarbon calibration curve (§D1.3), the substantial dimensions of the walls alone (Locus:262433:054 is three mudbricks = c. 1.3 m wide) and the high economic investment they imply strongly suggest that Building B was built before the fall of Assur in 614 BC, and not after. Moreover, the pottery that was found on the floor of the Unroofed Area 4 can be easily connected in terms of quality and typology to Neo-Assyrian pieces from the 7th century BC. What brought the occupation of Building B to an end and whether the abandonment was sudden or gradual is hitherto uncertain. We can state with some confidence that it was not caused by fire since no burnt debris has been found in the Unroofed Area 4.

In the absence of burnt debris, we can exclude destruction by fire in this specific area when the Medes conquered Assur in 614 BC. However, it remains unclear whether the end of Building B was sudden or whether it was gradually abandoned. Be that as it may, it was subsequently exposed to erosion, as characterised by fills consisting of mudbrick debris in the overlying earth deposits (Locus:262432:065, Locus:262432:059, and Locus:262432:057). After the building's use had come to an end, the northern wall Locus:262433:054 remained standing only up to a height of c. 161.25 metres above sea level and was covered by rubble.

On the other hand, the southeastern wall Locus:262433:075 remained standing up to a level of c. 162.15 metres above sea level and therefore about 90 cm higher than the northern wall. Since the floor levels of the Hellenistic Building A (NT1 2023 Phase 5; §D2.6) were lower-lying (Locus:262432:060 of Room 3 at c. 161.90 metres above sea level and Locus:262433:069 of Room 2 at c. 162.05 metres above sea level), remains of the southeastern wall of Building B were perhaps still visible when the much later architecture was in use. If this were the case, this wall would represent an architectural element that connects these two phases of Assur's occupational history.

The remains of Building A were unearthed closely below the site surface and currently consist of three rooms. The floor of Room 2 is cut by the pit of Grave 3 (NT1 2003 Phase 6; §D2.5), whose sarcophagus is incised with an alphabetic inscription dated to July/August 158 BC, thus providing the stratigraphic sequence with a chronologically absolute fixpoint in the Hellenistic period (§G2). A second such sarcophagus found nearby in Grave 4 was without an inscription. Remarkably, Grave 3 contained calcinated textile fragments of at least six different types of cloth (§I). Further exploring this phase is particularly exciting, as the dating to a *terminus ante quem* 158 BC

guarantees new insights into Assur's material culture and history during the barely known time between the Neo-Assyrian and Parthian periods, both of which the work of Andrae brought so vividly to light.

At Kalhu, remains dating to the Hellenistic period were unearthed in the form of a small village on top of the southeastern corner of the citadel mound during the excavations led by Max Mallowan in 1957, published by Joan and David Oates,³¹⁵ and further analysed by David Oates,³¹⁶ who described them as representing "a period of insecurity when the citadel was reoccupied on a small scale."³¹⁷ After briefly summing up the limited evidence from Nineveh,³¹⁸ Oates states that for Assur on the other hand "no traces of Seleucid occupation were identified,"³¹⁹ and goes on to say: "Andrae remarks that the period from the fall of Assur in 614 BC to the appearance of Parthian buildings, which he dates to the first century BC, has no history."³²⁰ The new evidence for the Hellenistic period from the New Town of Assur in the form of Building A and the two burials Graves 3 and Grave 4 is therefore highly significant.

Building A was cut by a large Parthian-period vaulted chamber tomb that covered a surface of 46 square metres (§D2.3). We completely exposed the tomb whose vaults, walls and floors had been damaged already in antiquity. Over a dozen skeletons were found piled up in different parts of the structure. Analysis of these and the human remains from the earlier burials will provide new insights into the identity of Assur's inhabitants across time; the radiocarbon dates provided by the analysis of two molars date the deposition of these bodies in the tomb to the beginning of the common era. Three brick fragments of Adad-nerari I of Assyria (1305-1274 BC) were found in a secondary position within the walls of the tomb (§G1.1), two of which can be assigned with certainty to bricks commemorating his building the nearby quay wall of Assur. Inside the tomb, a water jar of the late Sasanian / early Islamic date (§E1.2: G01-S05-V01) presumably attests to the looting of the tomb in or around the 7th century AD.³²¹

315 Oates/Oates 1958. The coins, which were crucial in establishing the chronology of the six levels observed, were published by Jenkins 1958.

316 Oates 1968, 59, 63-66, 122-144 (pottery).

317 Oates 1968, 62.

318 Oates 1968, 61.

319 Oates 1968, 61.

320 Oates 1968, 62, summing up Andrae 1938, 169.

321 At that time, Assur would have been part of the district of Tīrhān, on which see Morony 1982, 15-16 (with regional maps for the late Sasanian period on p. 11 fig. 4 and for the early Islamic period on p. 12 fig. 5).

This too extends our knowledge of Assur's history into a largely unknown time.

In addition to the excavations in trench NTo1 2023, some small-scale work was undertaken in the baulk that separates this trench from the large area excavated by the Iraqi State Board of Antiquities and Heritage in 2002 (§D3). The corners of two adjoining rooms dubbed "Room 5" (in the north) and "Room" 6 (in the south) were uncovered so that we would reach floor levels that could provide material suitable for radiocarbon dating. In "Room 6", two floors, one directly above the other, were exposed in an area of 1.4 square metres. The lower one was situated 160.94 metres above sea level and the deposit directly above it contained fragments of a Palace Ware goblet with dimple decoration (§E1.7: Vessel 00-06-J01) as well as a piece of charcoal that was radiocarbon dated to 751-422 calBC (95.4% probability). The younger floor lay at an altitude of 161.17 m above sea level, and a piece of charcoal found on top of it yielded a radiocarbon dating range of 755-482 calBC (95.4% probability). The radiocarbon analysis of two carbonised seeds produced supporting dating ranges. These floors are positioned substantially higher than the floors exposed in the Iraqi trench of 2002. In "Room 5", a charcoal piece was retrieved directly from a floor level that lay at an altitude of 160.05 metres above sea level, which broadly matches the altitude of the SBAH-excavated floors, and this was radiocarbon dated to 1416-1278 calBC (95.4% probability). On the other hand, a carbonised seed from the deposit above the floor yielded a dating range of 771-545 calBC (95.4% probability). We will further investigate this room context, as the 2023 findings at least open up the possibility that the large Assyrian building unearthed in 2002 dates back to a Late Bronze Age foundation and was used until the late 7th century BC when Assur was conquered by the Medes. The characteristic door socket cover found within this house certainly dates to a late phase of its building history (§F13, no. 289).

In total, our excavations have produced 17 radiocarbon dating ranges derived from the analysis of charcoal, seeds and human teeth: these are the very first ¹⁴C dates available from Assur (§D1.3).

Already during the excavation, good progress was achieved in processing the ceramic finds and further inroads were made in October / November 2023 during a two-week study season (§E1) when parts of the database interface had been translated into Arabic so that the SBAH members could participate in all stages of the registration process. Both in spring and in autumn, the use of a Laser Aided Profiler was instrumental in recording vessel shapes and establishing first typologies; we have since purchased a second such instrument. In addition,

the possibility of exporting ceramic samples allowed us to commission the first thin section and XRF analyses of the fabrics of the newly excavated pottery assemblages (§E2), continuing the longstanding collaboration with Silvia Amicone and her colleagues in Tübingen and involving now also our LMU colleague Michaela Schauer.

We have already indicated the chronologically most relevant vessels when discussing the excavation results. In addition, some chronologically significant small finds are worth mentioning here again. The small rectangular lapis lazuli stamp seal, for which an exact duplicate is known from the art market that had been assigned to the Sasanian period, has a secure archaeological context in the second century BC, i.e. the Hellenistic period, that renders a later dating impossible (§F6.1 no. 159). The find context of a partially preserved bronze fibula of Friedhelm Pedde's C8 type in the disturbed Grave 5 confirms the dating of this type to the late Neo-Assyrian period (§F8 no. 236). A similar, albeit more damaged bronze fibula was found in a much later, secondary context within the walls of the chamber tomb from the early centuries AD (§F4.1 no. 29).

The 2023 campaign cannot boast any hugely impressive cuneiform finds (§G1) although it is interesting to note that in these same tomb walls, brick fragments turned up from Adad-nerari I's quay wall that had been constructed a millennium and a half earlier. Further Assyrian royal inscriptions on various bricks and brick fragments were found on the surface, in particular during the magnetometer survey, and a stone block from the Aššur temple with an inscription of Sennacherib unexpectedly turned up just outside the excavation house. But the most important epigraphic find made during the 2023 excavations is, without doubt, the sarcophagus incised with an alphabetic inscription dated to July/August 158 BC (= Month Ab in the year 153 of the Seleucid era; Fig. J1). Brief as this text



Fig. J1: Star find: the sarcophagus from Grave 3, with an alphabetic inscription (see §D2.5.1, §F5 and §G2). Photo by Ali Saad.

is, as Holger Gzella's careful analysis shows (§G2), it provides precious insights into writing and dating practices at Assur after the end of local cuneiform writing and before the rise of the Eastern Mesopotamian scribal tradition that would eventually spread to Hatra and other areas.

A key aspect of our work is the attempt to retrieve organic materials from the excavation that can be used both for radiocarbon dating (in addition to human teeth from burials) and for plant identification (§D1.2). We have been able to recover 22 charcoal samples, from which Katleen Deckers could isolate 133 charred wood fragments that she then analysed (§H2). Some of the material represents local vegetation, in particular poplar (*Populus*), willow (*Salix*), and tamarisk (*Tamarix*) from the alluvial zone along the Tigris, and buckthorn (*Lycium*) from the nearby more arid environments. While the wood of the cedar (*Abies/Cedrus*) and of the yew (*Taxus*) must have been imported, the presence of walnut (*Juglans*) raises the intriguing question of whether the tree may have been locally cultivated.

Although establishing the necessary water and power supply for running the flotation machine was a substantial challenge, we were successful in retrieving 431.2 g of

paleobotanical plant remains from the light fraction of the 32 soil samples taken (§H3). The vast majority of the material stems from the floors of the three rooms exposed in Building A, which dates to the second century BC. Further material comes from the floors exposed of "Room 5" and "Room 6" in the sondage on the western section of the 2002 SBAH excavation. In total, Claudia Sarkady isolated 8,655 plant remains, of which she attributed 5,207 to cultivated plants and 3,458 to wild plants. Multi-row barley (*Hordeum vulgare*) emerges as the most important cultivated cereal but emmer (*Triticum dicoccum*), einkorn (*Triticum monococcum*) and free-threshing wheat (*Triticum aestivum*) are also attested. Both cultivated wine (*Vitis vinifera sativa*) and wild wine (*Vitis vinifera sylvestris*) are documented, albeit in small numbers, as well as lentils (*Lens culinaris*) and peas (*Pisum sativum*). Most of the attested wild grasses (*Bromus*, *Aegilops*, *Lolium*) prefer dry locations but there are also wild plants in evidence that prefer moist conditions, which they would presumably have found down near the Tigris. At present, the observed range of plants does not yet provide clear information about the past ecology of Assur but the work undertaken in this first year is certainly a promising start.

Bibliography

Bibliographic abbreviations

RIMA 1 = Grayson 1987

RIMA 2 = Grayson 1991

RIMA 3 = Grayson 1996

RINAP 1 = Tadmor/Yamada 2011

RINAP 3/2 = Grayson/Novotny 2014

RINAP 5/3 = Novotny/Jeffers/Frame 2023

Ad-hoc-AG Boden 2005

Ad-hoc-AG Boden, *Bodenkundliche Kartieranleitung*, Stuttgart 2005 (5th edition).

Ahmad 1996

A.Y. Ahmad, "The archive of Aššur-matu-taqin in the New Town of Assur." *Al-Rafidan* 17 (1996), pp. 207–288.

Aimers/Farthing/Shugar 2014

J.J. Aimers, D.J. Farthing, and A.N. Shugar, "Handheld XRF analysis of Maya ceramics: A pilot study representing issues related to quantification and calibration." In: A.N. Shugar and J.L. Mass (eds.), *Handheld XRF for Art and Archaeology*, Ithaca 2014, pp. 423–448.

Aitken 1958

M.J. Aitken, "Archaeology without digging. Or: How a bottle of water — and 150 transistors — can detect underground features: The proton magnetometer." *The Illustrated London News*, 4 October 1958, pp. 560–561.

Aitken 1961

M.J. Aitken, *Physics and Archaeology*, New York 1961.

Alibaigi et al. 2023

S. Alibaigi, I. Rezaei, F. Moradi, S. Haruta, J. MacGinnis, N. Aminikhah, and S. Khosravi, "Daya Cave: a place of worship of Mesopotamian and Persian gods in the west central Zagros Mountains, Iran." *American Journal of Archaeology* 127 (2023), pp. 419–435.

Alonso/Frankel 2017

N. Alonso and R. Frankel 2017, "A survey of ancient grain milling systems in the Mediterranean." *Revue Archéologique de l'Est* 43 (2017), pp. 461–478.

Altaweel 2008

M. Altaweel, *The Imperial Landscape of Ashur: Settlement and Land Use in the Assyrian Heartland*, Heidelberg 2008.

Altaweel/Eckmeier 2019

M. Altaweel and E. Eckmeier, "Geoarchaeological work at the Dinka Settlement Complex, 2018." In: K. Radner, F.J. Kreppner, and A. Squitieri (eds.), *The Dinka Settlement Complex 2018: Continuing the Excavations at Qalat-i Dinka and the Lower Town* (Peshdar Plain Project Publications 4), Gladbeck 2019, pp. 25–31.

Anastasio 2010

S. Anastasio, *Atlas of the Assyrian Pottery of the Iron Age*, Turnhout 2010.

Andrae 1904a

W. Andrae, "Aus zwölf Briefen von W. Andrae (Assur)." *Mitteilungen der Deutschen Orient-Gesellschaft zu Berlin* 21 (1904), pp. 10–38.

Andrae 1904b

W. Andrae, "Ein Privatbrief von W. Andrae." *Mitteilungen der Deutschen Orient-Gesellschaft zu Berlin* 21 (1904), pp. 43–48.

Andrae 1904c

W. Andrae, "Aus den Berichten von W. Andrae aus Assur." *Mitteilungen der Deutschen Orient-Gesellschaft zu Berlin* 22 (1904), pp. 12–38.

Andrae 1904d

W. Andrae, "Zwei Privatbriefe W. Andrae's (Assur)." *Mitteilungen der Deutschen Orient-Gesellschaft zu Berlin* 22 (1904), pp. 61–72.

Andrae 1904e

W. Andrae, "Aus einundzwanzig Berichten W. Andraes aus Assur." *Mitteilungen der Deutschen Orient-Gesellschaft zu Berlin* 25 (1904), pp. 16–73.

Andrae 1904f

W. Andrae, "Ein Privatbrief von W. Andrae." *Mitteilungen der Deutschen Orient-Gesellschaft zu Berlin* 25 (1904), pp. 73–77.

Andrae 1905

W. Andrae, "Aus den Berichten W. Andraes aus Assur von Oktober 1904 bis März 1905." *Mitteilungen der Deutschen Orient-Gesellschaft zu Berlin* 26 (1905), pp. 19–64.

Andrae 1908a

W. Andrae, "Aus den Berichten W. Andraes aus Assur von Mai 1907 bis Januar 1908." *Mitteilungen der Deutschen Orient-Gesellschaft zu Berlin* 36 (1908), pp. 16–38.

Andrae 1908b

W. Andrae, "Aus den Berichten aus Assur. A) Von W. Andrae: Februar und März 1908." *Mitteilungen der Deutschen Orient-Gesellschaft zu Berlin* 38 (1908), pp. 21–25.

Andrae 1909a

W. Andrae, "Aus den Grabungsberichten aus Assur: April bis Ende Juni 1909." *Mitteilungen der Deutschen Orient-Gesellschaft zu Berlin* 42 (1909), pp. 32–39.

Andrae 1909b

W. Andrae, "Aus den Grabungsberichten aus Assur: August bis November 1909." *Mitteilungen der Deutschen Orient-Gesellschaft zu Berlin* 42 (1909), pp. 45–53.

Andrae 1911

W. Andrae, "Aus zwei Privatbriefen Dr. Andraes (Assur)." *Mitteilungen der Deutschen Orient-Gesellschaft zu Berlin* 45 (1911), pp. 50–64.

Andrae 1913

W. Andrae, "Aus den Grabungsberichten aus Assur. September 1912 bis März 1913." *Mitteilungen der Deutschen Orient-Gesellschaft zu Berlin* 51 (1913), pp. 43–47.

Andrae 1938

W. Andrae, *Das wiedererstandene Assur*, Leipzig 1938.

Andrae 1988

W. Andrae, *Lebenserinnerungen eines Ausgräbers*, Stuttgart 1988 (2nd edition).

Andrae/Boehmer 1989

E.W. Andrae and R.M. Boehmer, *Bilder eines Ausgräbers / Sketches by an Excavator: Walter Andrae im Orient, 1898–1919.*, Berlin 1989.

Andrae/Lenzen 1933

W. Andrae and H. Lenzen, *Die Partherstadt Assur*, Leipzig 1933.

Andreozzi/Sarkady 2022

R. Andreozzi and C. Sarkady, "Forbidden at Philae: procription of aphrodisiac and psychoactive plants in Ptolemaic Egypt." In: D. Stein, S.K. Costello, and K.P. Foster (eds.), *The Routledge Companion to Ecstatic Experience in the Ancient World*, London 2022, pp. 152–172.

Beck 1928

H.C. Beck, "Classification and nomenclature of beads and pendants." *Archaeologia* 77 (1928), pp. 1–76.

Becker 1991

H. Becker, "Zur magnetischen Prospektion in Assur: Testmessung 1989." *Mitteilungen der Deutschen Orient-Gesellschaft zu Berlin* 123 (1991), pp. 123–131.

Beijerinck 1976

W. Beijerinck, *Zadenatlas der Nederlandsche Flora*, Amsterdam 1976.

Belshé 1957

J.C. Belshé, "Recent magnetic investigations at Cambridge University." *Advances in Physics* 6 (1957), pp. 192–193.

Bertolino 2008

R. Bertolino, *Manuel d'Épigraphie Hatréenne*, Paris 2008.

Beyer 1998

K. Beyer, *Die aramäischen Inschriften aus Assur, Hatra und dem übrigen Ostmesopotamien (datiert 44 v. Chr. bis 238 n. Chr.)*, Göttingen 1998.

Beynon et al. 1986

D.E. Beynon, J. Donahue, R.T. Schaub, and R.A. Johnston, "Tempering types and sources for Early Bronze Age ceramics from Bab edh-Dhra' and Numeira, Jordan." *Journal of Field Archaeology* 13 (1986), pp. 297–305.

Bezur/Lee/Loubster 2020

A. Bezur, L. Lee, and M. Loubster, *Handheld XRF in Cultural Heritage: A Practical Workbook for Conservators*, Los Angeles 2020.

Bilardello 2020

D. Bilardello, "Practical magnetism, II: Humps and a bump, the maghemite song." *The IRM Quarterly* 30 (2020), pp. 1–16.

Bivar 1969

A.D.H. Bivar, *Catalogue of the Western Asiatic Seals in the British Museum: Stamp Seals, II: the Sassanian Dynasty*, London 1969.

Blume et al. 2010

H.-P. Blume, G.W. Brümmer, R. Horn, E. Kandeler, I. Kögel-Knabner, R. Kretzschmar, K. Stahr, and B.-M. Wilke, *Scheffer/Schachtschabel: Lehrbuch der Bodenkunde*, Heidelberg 2010 (16th edition).

Brock 1992

S.P. Brock, "Some notes on dating formulae in Middle Aramaic inscriptions and in Early Syriac manuscripts." In: Z.J. Kapera (ed.), *Intertestamental Essays in Honour of Józef Tadeusz Milik*, Cracow 1992, pp. 253–264.

Brunner 1978

C.J. Brunner, *Sasanian Stamp Seals in the Metropolitan Museum of Art*, New York 1978.

Callieri 1997

P. Callieri, *Seals and Sealings from the North-West of the Indian Subcontinent and Afghanistan*, Naples 1997.

Camargo 2022

A. Camargo, "PCAtest: Testing the statistical significance of Principal Component Analysis in R." *PeerJ* 10 (2022), 12967. doi: 10.7717/peerj.12967.

Cappers/Bekker/Jans 2012

R.T.J. Cappers, R.M. Bekker, and J.E.A. Jans, *Digitale Zadenatlas van Nederland*, Groningen 2012.

Caudullo/Welk/San-Miguel-Ayanz 2017

G. Caudullo, E. Welk, and J. San-Miguel-Ayanz, "Chronological maps for the main European woody species." *Data in Brief* 12 (2017), pp. 662–666.

Crivellaro/Schweingruber 2013

A. Crivellaro and F.H. Schweingruber, *Atlas of Wood, Bark and Pith Anatomy of Eastern Mediterranean Trees and Shrubs, with a Special Focus on Cyprus*, Heidelberg 2013.

Daszkiewicz/Bobryk/Schneider 2000

M. Daszkiewicz, E. Bobryk, and G. Schneider, "Water permeability and thermal shock resistance of 6th–3rd millennium cooking pots from north Mesopotamia." In: G. Schulze and I. Horn (eds.), *Archäometrie und Denkmalpflege: Kurzberichte 2000*, Berlin 2000, pp. 98–101.

Dearing 1999

J.A. Dearing, *Environmental Magnetic Susceptibility Using the Bartington MS2 System*, Kenilworth 1999 (2nd edition).

Dearing et al. 1996

J.A. Dearing, R. Dann, K.L. Hay, J. Lees, P.J. Loveland, B.A.

Maier, and K. O'Grady, "Frequency-dependent susceptibility measurements of environmental materials." *Geophysical Journal International* 124 (1996), pp. 228–240. DOI: 10.1111/j.1365-246x.1996.tb06366.x.

Deckers 2011

K. Deckers, "Wood use in the palace of Qatna." In: K. Deckers (ed.), *Holocene Landscapes through Time in the Fertile Crescent*, Turnhout 2011, pp. 157–172.

Demján/Pavúk/Roosevelt 2022

P. Demján, P. Pavúk, and C.H. Roosevelt, "Laser-Aided Profile Measurement and Cluster Analysis of Ceramic Shapes." *Journal of Field Archaeology* 48 (2022), pp. 1–18.

Denis 2015

D.J. Denis, *Applied Univariate, Bivariate and Multivariate Statistics*, New York 2015.

Dittmann 1990

R. Dittmann, "Ausgrabungen der Freien Universität Berlin in Assur und Kār-Tukultī-Ninurta in den Jahren 1986–89." *Mitteilungen der Deutschen Orient-Gesellschaft zu Berlin* 122 (1990), pp. 157–171.

Djamali et al. 2011

M. Djamali, N.F. Miller, E. Ramezani, V. Andrieu-Ponel, J.-L. de Beaulieu, M. Berberian, F. Guibal, H. Lahijani, R. Lak, and P. Ponel, "Notes on arboricultural and agricultural practices in ancient Iran based on new pollen evidence." *Paléorient* 36 (2011), pp. 175–188.

Drennan 2010

R.D. Drennan, *Statistics for Archaeologists: A Common Sense Approach*, London/Heidelberg 2010.

Duri/Rasheed/Hamze 2011

R. Duri, Q.H. Rasheed, and H.A. Hamze, "The Iraqi excavations in the city of Ashur (1999–2002)." *Sumer* 56 (2011), pp. 111–150.

Duri/Rasheed/Hamze 2013

R. Duri, Q.H. Rasheed, and H.A. Hamze, "Iraqi investigation in the public district of Ashur during the 2002 season." In: D. Kertai and P.A. Miglus (eds.), *New Research on Late Assyrian Palaces*, Heidelberg 2013, pp. 83–90.

Erhardt et al. 2008

W. Erhardt, E. Götz, N. Bödeker, and S. Seybold, *Der große Zander: Enzyklopädie der Pflanzennamen*, Stuttgart 2008.

Eslami/Wicke/Rajabi 2020

M. Eslami, D. Wicke, and N. Rajabi, "Geochemical analyses result of prehistoric pottery from the site of Tol-e Kamin (Fars, Iran) by pXRF." *Science & Technology of Archaeological Research* 6 (2020), pp. 61–71.

Fabian/Shcherbakov/McEnroe 2013

K. Fabian, V.P. Shcherbakov, and S.A. McEnroe, "Measuring the Curie temperature." *Geochemistry, Geophysics, Geosystems* 14 (2013), pp. 947–961. DOI: 10.1029/2012GC004440.

Fahn/Werker/Baas 1986

A. Fahn, E. Werker, and P. Baas, *Wood Anatomy and Identification of Trees and Shrubs from Israel and Adjacent Regions*, Jerusalem 1986.

Fassbinder 1994

J.W.E. Fassbinder, *Die magnetischen Eigenschaften und die Genese ferrimagnetischer Minerale in Böden im Hinblick auf die magnetische Prospektion archäologischer Bodendenkmäler*, Rahden 1994.

Fassbinder 2017

J.W.E. Fassbinder, "Magnetische Eigenschaften der archäologischen Schichten von Qantir (Ägypten)." In: E.B. Pusch and H. Becker (eds.), *Fenster in die Vergangenheit: Einblicke in die Struktur der Ramses-Stadt durch magnetische Prospektion und Grabung* (Forschungen in der Ramses-Stadt 9), Hildesheim 2017, pp. 327–350.

Fassbinder 2023

J.W.E. Fassbinder, "Magnetometry for archaeology." In: A.S. Gilbert, P. Goldberg, R.D. Mandel, and V. Aldeias (eds.), *Encyclopedia of Geoarchaeology*, Cham 2023. DOI: 10.1007/978-3-030-44600-0_169-1

Fassbinder/Ašandulesei 2016

J.W.E. Fassbinder and A. Ašandulesei, "The magnetometer survey of Qalat-i Dinka and Gird-i Bazar, 2015." In: K. Radner, F.J. Kreppner and A. Squitieri (eds.), *Exploring the Neo-Assyrian Frontier with Western Iran: The 2015 Season at Gird-i Bazar and Qalat-i Dinka* (Peshdar Plain Project Publications 1), Gladbeck 2016, pp. 36–42.

Ferguson 2014

J.R. Ferguson, "X-Ray-Fluorescence of obsidian: approaches to calibration and the analysis of small samples." In: A.N. Shugar and J.L. Mass (eds.), *Handheld XRF for Art and Archaeology*, Ithaca 2014, pp. 401–422.

Frahm 1997

E. Frahm, *Einleitung in die Sanherib-Inschriften*, Vienna 1997.

Frahm/Doonan 2013

E. Frahm and R.C.P. Doonan, "The technological versus methodological revolution of portable XRF in Archaeology," *Journal of Archaeological Science* 40 (2013), pp. 1425–1434.

Franken 1992

H.J. Franken, *Excavations at Tell Deir 'Alla: the Late Bronze Age Sanctuary*, Leuven 1992.

Franken/Kalsbeek 1969

H.J. Franken and J. Kalsbeek, *Excavations at Tell Deir 'Alla: A Stratigraphical and Analytical Study of the Iron Age Pottery*, Leiden 1969.

Franken/Kalsbeek 1974

H.J. Franken and J. Kalsbeek, *In Search of the Jericho Pottery: Ceramics from the Iron Age and from the Neolithicum*, Amsterdam/Oxford 1974.

Gale/Cutler 2000

R. Gale and D. Cutler, *Plants in Archaeology: Identification Manual of Vegetative Plant Materials Used in Europe and the Southern Mediterranean to c. 1500*, Otley 2000.

Gavagnin/Iamoni/Palermo 2016

K. Gavagnin, M. Iamoni, and R. Palermo, "The Land of Nineveh Archaeological Project: the ceramic repertoire from the Early Pottery Neolithic to the Sasanian Period." *Bulletin of the American Schools of Oriental Research* 375 (2016), pp. 119–169.

Genaust 1996

H. Genaust, *Etymologisches Wörterbuch der botanischen Pflanzennamen*, Hamburg 1996.

Gignoux 1978

P. Gignoux, *Catalogue des Sceaux, Camées et Bulles Sasanides de la Bibliothèque Nationale et du Musée du Louvre, II: Les Sceaux et Bulles Inscrits*, Paris 1978.

Gilboa/Sharon 2016

A. Gilboa and I. Sharon, "The Assyrian *kāru* at Dor (ancient Du'ru)." In J. MacGinnis, D. Wicke, and T. Greenfield (eds.), *The Provincial Archaeology of the Assyrian Empire*, Cambridge 2016, pp. 241–252.

Gilder/Chen/Şen 2001

S. Gilder, Y. Chen, and Ş. Şen, "Oligo-Miocene magnetostratigraphy and rock magnetism of the Xishuigou section, Subei (Gansu Province, Western China) and implications for shallow inclinations in Central Asia." *Journal of Geophysical Research* 106 (B12) (2001), pp. 30505–30521. DOI: 10.1029/2001jb000325.

Göbl 1973

R. Göbl, *Der sāsānidische Siegelkanon* (Handbücher der mittelasiatischen Numismatik 4), Braunschweig 1973.

Golitko 2011

M. Golitko, "Provenience investigations of ceramic and obsidian samples using laser ablation inductively coupled plasma mass spectrometry and portable X-Ray fluorescence." *Fieldiana Anthropology* 42 (2011), pp. 251–287.

Grayson 1980-83

A.K. Grayson, "Königslisten und Chroniken. B. Akkadisch." *Reallexikon der Assyriologie und Vorderasiatische Archäologie* 6 (1980-83), pp. 86–135.

Grayson 1987

A.K. Grayson, *Assyrian Rulers of the Third and Second Millennia BC (to 115 BC)* (Royal Inscriptions of Mesopotamia: Assyrian Periods 1), Toronto 1987.

Grayson 1991

A.K. Grayson, *Assyrian Rulers of the Early First Millennium BC (114-859 BC)* (Royal Inscriptions of Mesopotamia: Assyrian Periods 2), Toronto 1991.

Grayson 1996

A.K. Grayson, *Assyrian Rulers of the Early First Millennium BC (858-745 BC)* (Royal Inscriptions of Mesopotamia: Assyrian Periods 3), Toronto 1996.

Grayson/Novotny 2014

A.K. Grayson and J. Novotny, *The Royal Inscriptions of Sennacherib, King of Assyria (704-681 BC), part 2* (Royal Inscriptions of the Neo-Assyrian Period 3/2), Winona Lake IN 2014.

Gyselen 1993

R. Gyselen, *Catalogue des Sceaux, Camées et Bulles Sassanides de la Bibliothèque Nationale et du Musée du Louvre, I: Collection Générale*, Paris 1993.

Gyselen 2007

R. Gyselen, *Sasanian Seals and Sealings in the A. Saeedi Collection* (Acta Iranica 44), Leuven 2007.

Gzella 2021

H. Gzella, *Aramaic: A History of the First World Language*, Grand Rapids 2001.

Gzella 2023

H. Gzella, *Aramäisch: Weltsprache des Altertums*, Munich 2023.

Hahn et al. 2022

S.E. Hahn, J.W.E. Fassbinder, A. Otto, B. Einwag, and A.A. Al-Hussainy, "Revisiting Fara: comparison of merged prospection results of diverse magnetometers with the earliest excavations in ancient Şuruppak from 120 years ago." *Archaeological Prospection* 29 (2022), pp. 1–13. DOI: 10.1002/arp.1878.

Hair et al. 2014

J.F. Hair, W.C. Black, B.J. Babin, and R.E. Anderson, *Multivariate Data Analysis*, Harlow 2014.

Handel-Mazzetti 1914

H. von Handel-Mazzetti, "Die Vegetationsverhältnisse von Mesopotamien und Kurdistan." *Annalen des Naturhistorischen Museums in Wien* 28 (1914), pp. 48–111.

Hanesch/Stanjek/Petersen 2006

M. Hanesch, H. Stanjek, and N. Petersen, "Thermomagnetic measurements of soil iron minerals: The role of organic carbon." *Geophysical Journal International* 165 (2006), pp. 53–61. DOI: 10.1111/j.1365-246X.2006.02933.x.

Harper 1973

P.O. Harper, "Descriptions of the drawings of impressions." In: R.N. Frye (ed.), *Sasanian Remains from Qasr-i Abu Nasr: Seals, Sealings, and Coins*, Cambridge MA 1973, pp. 96–104.

Hauser 1996

S.R. Hauser, "The production of pottery in Arsacid Ashur." In: K. Bartl and S.R. Hauser (eds.), *Continuity and Change in Mesopotamia from the Hellenistic to the Early Islamic Period*, Berlin 1996, pp. 55–85.

Hauser 2012

S.R. Hauser, *Status, Tod und Ritual: Stadt- und Sozialstruktur Assurs in neuassyrischer Zeit*, Wiesbaden 2012.

Hausleiter 2010

A. Hausleiter, *Neuassyrische Keramik im Kerngebiet Assurs*, Wiesbaden 2010.

Healey/Bin Seray 1999-2000

J.F. Healey and H. Bin Seray, "Aramaic in the Gulf: towards a corpus." *ARAM* 11/12 (1999-2000), pp. 1-13.

Helbaek 1960

H. Helbaek, "Ecological effects of irrigation in ancient Mesopotamia." *Iraq* 12 (1960), pp. 186-196.

Helfert 2013

M. Helfert, "Die portable energiedispersive Röntgenfluoreszenzanalyse (P-ED-RFA): Studie zu methodischen und analytischen Grundlagen ihrer Anwendung in der archäologischen Keramikforschung." In: B. Ramminger, O. Stilborg, and M. Helfert (eds.), *Naturwissenschaftliche Analysen vor- und frühgeschichtlicher Keramik, III: Methoden, Anwendungsbereiche, Auswertungsmöglichkeiten*, Bonn 2013, pp. 13-47.

Hillman 1984

G. Hillman, "Traditional husbandry and processing of archaic cereals in modern times, part 1: the glume wheats." *Bulletin on Sumerian Agriculture* 1 (1984), pp. 114-152.

Hrouda 1991

B. Hrouda, "Vorläufiger Bericht über die neuen Ausgrabungen in Assur Frühjahr 1990." *Mitteilungen der Deutschen Orient-Gesellschaft zu Berlin* 123 (1991), pp. 95-109.

Hübner 1992

U. Hübner, *Spiele und Spielzeug im antiken Palästina*, Freiburg 1992.

Jarjis 2020

M.A. Jarjis, *Qaṣr Andrayh: maqarr bi'ta at-tanqib al-almāniya fi Āšūr*, Mosul 2020.

Jenkins 1958

G.K. Jenkins, "Hellenistic coins from Nimrud." *Iraq* 20 (1958), pp. 158-168.

Johnson 2014

J. Johnson, "Accurate measurements of low Z elements in sediments and archaeological ceramics using portable X-Ray fluorescence (PXRF)." *Journal of Archaeological Method and Theory* 21 (2014), pp. 563-588.

Jordan 1909

J. Jordan, "Aus den Grabungsberichten aus Assur: Ende Juni bis Ende Juli 1909." *Mitteilungen der Deutschen Orient-Gesellschaft zu Berlin* 42 (1909), pp. 40-44.

Jordan 1912

J. Jordan, "Aus den Grabungsberichten aus Assur. November 1911 bis April 1912." *Mitteilungen der Deutschen Orient-Gesellschaft zu Berlin* 48 (1912), pp. 25-28.

Jordanova 2016

N. Jordanova, *Soil Magnetism: Applications in Pedology, Environmental Science and Agriculture*, Amsterdam 2016.

Jordanova/Jordanova 2016

D. Jordanova and N. Jordanova, "Thermomagnetic behavior of magnetic susceptibility: Heating rate and sample size effects." *Frontiers in Earth Science* 3 (2016), p. 90. DOI: 10.3389/feart.2015.00090.

Klak/Hanáček/Bruyns 2017

C. Klak, P. Hanáček, and P.V. Bruyns, "Disentangling the Aizoioideae: new generic concepts and a new subfamily in Aizoaceae." *Taxon* 66 (2017), pp. 1147-1170.

Klengel-Brandt/Onasch 2020

E. Klengel-Brandt and H.U. Onasch, *Die Terrakotten aus Assur im Vorderasiatischen Museum Berlin*, Wiesbaden 2020.

Klugkist 1982

A.C. Klugkist, *Midden-Aramese Schriften in Syrië, Mesopotamië, Perzië en Aangrenzende Gebieden*, PhD dissertation, Groningen 1982.

Koldewey 1903

R. Koldewey, "Aus fünf weiteren Briefen R. Koldewey's (Assur)." *Mitteilungen der Deutschen Orient-Gesellschaft zu Berlin* 20 (1903), pp. 17-30.

Koldewey 1909

R. Koldewey, "Aus den Berichten aus Assur 16. A) Von Julius Jordan: November und Dezember 1908." *Mitteilungen der Deutschen Orient-Gesellschaft zu Berlin* 40 (1909), pp. 16-17.

Körber-Grohne 1988

U. Körber-Grohne, *Nutzpflanzen in Deutschland: Kulturgeschichte und Biologie*, Stuttgart 1988.

Kostadinova-Avramova/Kovacheva 2013

M. Kostadinova-Avramova and M. Kovacheva, "The magnetic properties of baked clays and their implications for past geomagnetic field intensity determinations." *Geophysical Journal International* 195 (2013), pp. 1534-1550. DOI: 10.1093/gji/ggt329.

Kreppner 2006

F.J. Kreppner, *Die Keramik des „Roten Hauses“ von Tall Šēḥ Ḥamad / Dūr-Katlimmu. Eine Betrachtung der Keramik Nordmesopotamiens aus der zweiten Hälfte des 7. und aus dem 6. Jahrhundert v. Chr.* (Berichte der Ausgrabungen von Tall Šēḥ Ḥamad / Dūr-Katlimmu 7), Wiesbaden 2006.

Kreppner/Schmidt 2013

F.J. Kreppner and J. Schmidt, *Die Stratigraphie und Architektur des „Roten Hauses“ von Tall Šēḥ Ḥamad / Dūr-Katlimmu* (Berichte der Ausgrabungen von Tall Šēḥ Ḥamad / Dūr-Katlimmu 11), Wiesbaden 2013.

Kroll 1983

H.J. Kroll, *Kastanas – Ausgrabungen in einem Siedlungshügel der Bronze- und Eisenzeit Makedoniens, 1975–1979: Die Pflanzenfunde* (Prähistorische Archäologie in Südosteuropa 2), Berlin 1983.

Kroll/Reed 2016

H.J. Kroll and K. Reed, *Die Archäobotanik*. (Feudvar: Ausgrabungen und Forschungen in einer Mikroregion am Zusammenfluss von Donau und Theiß 3), Würzburg 2016.

Krotkoff 1972

G. Krotkoff, “Bagdader Studien.” *Zeitschrift der Deutschen Morgenländischen Gesellschaft* 122 (1972), pp. 93–101.

Küster 1989

H.J. Küster, “Bronzezeitliche Pflanzenreste aus Tall Munbāqa.” *Mitteilungen der Deutschen Orient-Gesellschaft zu Berlin* 121 (1989), pp. 85–91.

Küster 2013

H.J. Küster, *Am Anfang war das Korn: eine andere Geschichte der Menschheit*, München 2013.

Lanza/Mancini/Ratti 1972

R. Lanza, A. Mancini, and G. Ratti, “Geophysical surveys at Seleucia.” *Mesopotamia* 7 (1972), pp. 27–41.

Legendre/Legendre 2012

P. Legendre and L. Legendre, *Numerical Ecology*, Amsterdam 2012.

Legrain 1925

L. Legrain, *The Culture of the Babylonians* (Publications of the Babylonian Section 14), Philadelphia 1925.

Linford et al. 2007

N. Linford, P. Linford, L. Martin, and A. Payne, “Recent results from the English Heritage caesium magnetometer

system in comparison with recent fluxgate gradiometers.” *Archaeological Prospection* 14 (2007), pp. 151–166. DOI: 10.1002/arp.313

Liritzis/Zacharias 2011

I. Liritzis and N. Zacharias, “Portable XRF of archaeological artefacts: current research, potential and limitations.” In: M.S. Shackley (eds.), *X-Ray Fluorescence Spectrometry (XRF) in Geoarchaeology*, New York 2011, pp. 109–131.

London 1991

G.A. London, “Aspects of Early Bronze and late Iron Age ceramic technology at Tell el-Umeiri.” In: L.G. Herr, L.T. Geraty, O.S. La Bianca, and R.W. Younker (eds.), *Madaba Plains Project 2: The 1987 Season at Tell el-Umeiri and Vicinity and Subsequent Studies*, Berrien Spring 1991, pp. 383–419.

London/Shuster 2021

G.A. London and R. Shuster, “Calcite: a hard habit to break.” In: M.S. Chesson (ed.), *Daily Life, Materiality, and Complexity in Early Urban Communities of the Southern Levant: Papers in Honor of Walter E. Rast and R. Thomas Schaub*, Cambridge MA 2021, pp. 233–246.

López-Tirado et al. 2021

J. López-Tirado, F. Vessella, J. Stephan, S. Ayan, B. Schirone, and P.J. Hidalgo, “Effect of climate change on potential distribution of *Cedrus libani* A. Rich in the twenty-first century: an Ecological Niche Modelling assessment.” *New Forests* 52 (2021), pp. 363–376.

López-Tirado et al. 2023

J. López-Tirado, M. Moreno-García, D. Romera-Romera, V. Zarco, and P.J. Hidalgo, “Forecasting the circum-Mediterranean firs (*Abies* spp., Pinaceae) distribution: an assessment of a threatened conifers’ group facing climate change in the twenty-first century.” *New Forests* (2023), DOI: 10.1007/s11056-023-09972-y.

Loud 1936

G. Loud, *Khorsabad, I: Excavation in the Palace and at a City Gate*, Chicago 1936.

Loud/Altman 1938

G. Loud and C.B. Altman, *Khorsabad, II: The Citadel and the Town*, Chicago 1938.

Marsh/Altaweel 2020

A. Marsh and M. Altaweel, “The search for hidden landscapes in the Shahrizor: Holocene land use and climate in northeastern Iraqi Kurdistan.” In: D. Lawrence, M. Altaweel, and G. Philipp (eds), *New Agendas in Remote Sens-*

ing and Landscape Archaeology: Studies in Honour of Tony J. Wilkinson, Oxford 2020, pp. 7–25.

Mårtensson/Nosch/Strand 2009

L. Mårtensson, M.L. Nosch, and E.A. Strand, “Shape of things: understanding a loom weight.” *Oxford Journal of Archaeology* 28 (2009), pp. 373–398.

Marzahn 1998

J. Marzahn, “Farbe in Assur. Frühe Farbdiaspositive in der Archäologie (1909–1910).” *Mitteilungen der Deutschen Orient-Gesellschaft zu Berlin* 130 (1998), pp. 223–239.

Mason/Cooper 1999

R.B. Mason and L. Cooper, “Petrographic analysis of Bronze Age pottery from Tell Hadidi.” *Levant* 31 (1999), pp. 135–147.

Mathé/Lévêque/Druez 2009

V. Mathé, F. Lévêque, and M. Druez, “What interest to use caesium magnetometer instead of fluxgate gradiometer?” *ArcheoSciences: Revue d’Archéométrie* 33 (suppl.) (2009), pp. 325–327. DOI: 10.4000/archeosciences.1781.

Maxbauer 2020

D.P. Maxbauer, “Rock magnetic properties of Paleocene-Eocene sediments from the Piceance Creek Basin, western Colorado.” *The IRM Quarterly* 30 (2020), pp. 5–8.

Melzig/Hiller 2010

M.F. Melzig and K. Hiller, *Lexikon der Arzneipflanzen und Drogen*, Heidelberg 2010.

Meschede 2015

D. Meschede, *Gerthsen Physik*, Berlin/Heidelberg 2015.

Messerschmidt 1911

L. Messerschmidt, *Keilschrifttexte aus Assur historischen Inhalts, erstes Heft: Autographien*, Leipzig 1911.

Miedaner 2014

T. Miedaner, *Kulturpflanzen: Botanik – Geschichte – Perspektiven*, Berlin 2014.

Miglus 1996

P.A. Miglus, *Das Wohngebiet von Assur: Stratigraphie und Architektur*, Berlin 1996.

Miglus 2000

P.A. Miglus, with contributions by J. Bär, A. Hausleiter, F.M. Stepniowski, Z.R. Abdallah, and H.A. Hamze, “Assur

– Frühjahrskampagne 2000.” *Mitteilungen der Deutschen Orient-Gesellschaft zu Berlin* 132 (2000), pp. 13–54.

Miglus 2010

P.A. Miglus, “Festungswerke von Assur im 2. Jahrtausend v. Chr.” In: S.M. Maul and N. Heeßel (eds.), *Assur-Forschungen*, Wiesbaden 2010, pp. 229–243.

Miglus 2011

P.A. Miglus, “Middle Assyrian settlement in the south.” In: P.A. Miglus and S. Mühl (eds.), *Between the Cultures: The Central Tigris Region from the 3rd to the 1st Millennium BC*, Heidelberg 2011, pp. 217–225.

Millard 2011

A.R. Millard, “The alphabet.” In: H. Gzella (ed.), *Languages from the World of the Bible*, Berlin/New York 2011, pp. 14–27.

Miller 1984

N.F. Miller, “The use of dung as fuel: an ethnographic model and an archaeological example.” *Paléorient* 10 (1984), pp. 71–79.

Morony 1982

M.G. Morony, “Continuity and change in the administrative geography of late Sasanian and early Islamic al-‘Irāq.” *Iran* 20 (1982), pp. 1–49.

Naveh 1970

J. Naveh, “The development of the Aramaic script.” *Proceedings of the Israel Academy of Sciences and Humanities* 5 (1970), pp. 1–69.

Naveh 1972

J. Naveh, “The North-Mesopotamian Aramaic script-type in the late Parthian period.” *Israel Oriental Studies* 2 (1972), pp. 293–304.

Neff/Voorhies/Umaña 2014

H. Neff, B. Voorhies, and F.P. Umaña, “Handheld XRF elemental analysis of archaeological sediments: some examples from Mesoamerica.” In: A.N. Shugar and J.L. Mass (eds.), *Handheld XRF for Art and Archaeology*, Ithaca 2014, pp. 379–399.

Niknami/Naderi 2016

K.A. Niknami and S. Naderi, *Sasanian Clay Sealings in the Bandar Abbas Museum*, Oxford 2016.

Nováček et al. 2016

K. Nováček, M. Melcak, L. Starkova, and N.A.M. Amin,

Medieval Urban Landscape in Northeastern Mesopotamia, Oxford 2016.

Novotny/Jeffer/Frame 2023

J. Novotny, J. Jeffer, and G. Frame, *The Royal Inscriptions of Ashurbanipal (668–631 BC), Aššur-etel-ilāni (630–627 BC) and Sîn-šarra-iškun (626–612 BC), Kings of Assyria, part 3* (Royal Inscriptions of the Neo-Assyrian Period 5/3), University Park PA 2023.

Oates 1968

D. Oates, *Studies in the Ancient History of Northern Iraq*, Oxford 1968.

Oates/Oates 1958

D. Oates and J. Oates, “Nimrud 1957: the Hellenistic settlement.” *Iraq* 20 (1958), pp. 114–157.

Oates/Oates 2001

D. Oates and J. Oates, *Nimrud: An Assyrian Imperial City Revealed*, London 2001.

Oberdorfer 1990

E. Oberdorfer, *Pflanzensoziologische Exkursionsflora*, Stuttgart 1990 (6th edition).

Orlando et al. 2021

L. Orlando, R. Alibi, P. Skoglund, C. Der Sarkissian, P.W. Stochhammer, M.C. Avila-Arcos, Q. Fu, J. Krause, E. Willerslev, A.C. Stone, and C. Warinner, “Ancient DNA analysis.” *Nature Reviews Methods Primers* 1 (2021), DOI: 10.1038/s43586-020-00011-0.

Parsi et al. 2023

M. Parsi, S. Hahn, J.W.E. Fassbinder, K. Kaniuth, M. Wolf, A. Aşandulesei, and C. Brasoveanu, “Illuminating traces of an Achaemenid’s monumental complex in the Southern Caucasus by electrical resistivity tomography.” *Journal of Applied Geophysics* 209 (2023), 104886. DOI: 10.1016/j.jap-geo.2022.104886.

Peacock 1970

D.P.S. Peacock, “The scientific analysis of ancient ceramics: a review.” *World Archaeology* 1 (1970), pp. 375–389.

Pedde 2000

F. Pedde, *Vorderasiatische Fibeln von der Levante bis Iran*, Saarbrücken 2000.

Pfälzner 1995

P. Pfälzner, *Mittanische und mittelassyrische Keramik: eine chronologische, funktionale und produktionsökonomische*

Analyse (Berichte der Ausgrabungen von Tall Šēḫ Ḥamad / Dūr-Katlimmu 3), Berlin 1995.

Pieters 1927

A.J. Pieters, *Green Manuring: Principles and Practice*, London 1927.

Pillay et al. 2000

A.E. Pillay, C. Punyadeera, L. Jacobson, and J. Eriksen, “Analysis of ancient pottery and ceramic objects using X-Ray fluorescence spectrometry.” *X-Ray Spectrometry* 29 (2000), pp. 53–62.

Pollard et al. 2007

M. Pollard, C. Batt, B. Stern, and S.M.M. Young, *Analytical Chemistry in Archaeology*, Cambridge 2007.

Potts 2008

P.J. Potts, “Introduction, analytical instrumentation and application overview” In: P.J. Potts and M. West (eds.), *Portable X-Ray Fluorescence Spectrometry: Capabilities for in situ Analysis*, Cambridge 2008, pp. 1–12.

Potts 2018

D.T. Potts. “Arboriculture in ancient Iran: walnut (*Juglans regia*), plane (*Platanus orientalis*) and the ‘*Radde dictum*’.” *DABIR: Digital Archive of Brief Notes & Iran Review* 6 (2018), pp. 101–109.

Pound/Hazell/Hockin 2023

M. Pound, C.J. Hazell, and E.P. Hockin, “The Late Holocene introduction of *Juglans regia* (walnut) to Cyprus.” *Vegetation History and Archaeobotany* 32 (2023), pp. 125–131.

Quinn 2022

P.S. Quinn, *Thin Section Petrography, Geochemistry and Scanning Electron Microscopy of Archaeological Ceramics*, Oxford 2022.

Radner 1997

K. Radner, *Die neuassyrischen Privatrechtsurkunden als Quelle für Mensch und Umwelt*, Helsinki 1997.

Radner 2017

K. Radner, “Assur’s ‘Second Temple Period’: the restoration of the cult of Aššur, c. 538 BCE.” In: C. Levin and R. Müller (eds.), *Herrschaftslegitimation in vorderorientalischen Reichen der Eisenzeit*, Tübingen 2017, pp. 77–96.

Ralph 1964

E. Ralph, “Comparison of a proton and a rubidium mag-

netometer for archaeological prospecting.” *Archaeometry* 7 (1964), pp. 20–27. DOI: 10.1111/j.1475-4754.1964.tb00590.x.

Rätsch 2004

C. Rätsch, *Enzyklopädie der psychoaktiven Pflanzen: Botanik, Ethnopharmakologie und Anwendung*, Aarau/Munich 2004 (7th edition).

Ratti 1971

G. Ratti, “Applicazione di metodi geofisici per ricerche archeologiche in Iraq.” *Bollettino Associazione Mineraria Subalpina* 8 (1971), pp. 3–4.

Reade 1995

J.E. Reade, “Iran in the Neo-Assyrian period.” In: M. Liverani (ed.), *Neo-Assyrian geography*, Rome 1995, pp. 31–42.

Reuther 1910

O. Reuther, *Das Wohnhaus in Bagdad und anderen Städten des Irak*, Berlin 1910.

Riehl 2000

S. Riehl, “Erste Ergebnisse der archäobotanischen Untersuchungen in der zentralen Oberstadt von Tall Mozan/Urkes im Rahmen der DOG-IIMAS-Kooperation.” *Mitteilungen der Deutschen Orient-Gesellschaft zu Berlin* 132 (2000), pp. 229–238.

Riehl 2001

S. Riehl, “Vorbericht der archäobotanischen Bestandsaufnahme in Emar.” *Baghdader Mitteilungen* 32 (2001), pp. 157–173.

Romagnoli et al. 2007

M. Romagnoli, M. Sarlatto, F. Terranova, E. Bizzarri, and S. Cessetti, “Wood identification in the Cappella Palatina ceiling (12th century) in Palermo (Sicily, Italy).” *IAWA Journal* 28/2 (2007), pp. 109–123.

Santos et al. 2008

J.O. Santos, C.S. Munita, M.E.G. Valério, C. Vergne, and P.M.S. Oliveira, “Correlations between chemical composition and provenance of Justino site ceramics by INAA.” *Journal of Radioanalytical and Nuclear Chemistry* 278 (2008), pp. 185–190.

Save et al. 2020

S. Save, J. Kovacik, F. Demarly-Cresp, R. Issenmann, S. Poirier, S. Sedlbauer, and Y. Teyssonneyre, “Large-scale geochemical survey by pXRF spectrometry of archaeological settlements and features: new perspectives on the method.” *Archaeological Prospection* 27 (2022), pp. 203–218.

Schauer 2023a

M. Schauer, *La Hoguette – Kultur, Subkultur, Phänomen? Neue archäologische Studien sowie portable, energiedisper-sive Röntgenfluoreszenzanalysen (P-ED-RFA) an Keramik zu einer altbekannten Frage*. PhD dissertation, LMU Munich.

Schauer 2023b

M. Schauer, “R-scripts and data of coefficient corrections developed since 2017 for the Niton XL3t No. 97390 following the Munich Procedure.” *Open Data LMU* (deposited 12 September 2023). DOI: 10.5282/ubm/data.405

Schauer 2024

M. Schauer, “Coefficient corrections for portable X-ray fluorescence data of the Niton XL3t No. 97390 (coefcor I-IV) developed according to the Munich Procedure.” *Data in Brief* (2024, forthcoming).

Scheinost/Schwertmann 1999

A.C. Scheinost and U. Schwertmann, “Color identification of iron oxides and hydroxysulfates.” *Soil Science Society of America Journal* 63 (1999), pp. 1463–1471. DOI: 10.2136/sssaj1999.6351463x.

Schneider 2006

G. Schneider, “Mineralogisch-chemische Untersuchungen der mittel- und neuassyrischen Keramik von Tall Šēḫ Ḥamad.” In: F.J. Kreppner, *Die Keramik des „Roten Hauses“ von Tall Šēḫ Ḥamad / Dür-Katlimmu. Eine Betrachtung der Keramik Nordmesopotamiens aus der zweiten Hälfte des 7. und aus dem 6. Jahrhundert v. Chr.* (Berichte der Ausgrabungen von Tall Šēḫ Ḥamad / Dür-Katlimmu 7), Wiesbaden 2006, pp. 391–420.

Schweingruber 1990

F.H. Schweingruber, *Anatomie europäischer Hölzer: ein Atlas zur Bestimmung europäischer Baum-, Strauch- und Zwergstrauchhölzer*, Bern/Stuttgart 1990.

Scollar/Krückeberg 1966

I. Scollar and F. Krückeberg, “Computer treatment of magnetic measurements from archaeological sites.” *Archaeometry* 9 (1966), pp. 61–71. DOI: 10.1111/j.1475-4754.1966.tb00907.x.

Shackley 2011

M.S. Shackley, “An introduction to X-Ray fluorescence (XRF) analysis in archaeology.” In: M.S. Shackley (ed.), *X-Ray Fluorescence Spectrometry (XRF) in Geoarchaeology*, New York 2011, pp. 7–44.

Shackley 2012

M.S. Shackley, "Portable X-ray fluorescence spectrometry (pXRF): the good, the bad, and the ugly." *Archaeology Southwest Magazine* 26 (2012), pp. 1–8.

Shoval et al. 1993

S. Shoval, M. Gaft, P. Beck, and Y. Kirsh, "Thermal behaviour of limestone and monocrystalline calcite tempers during firing and their use in ancient vessels." *Journal of Thermal Analysis* 40 (1993), pp. 263–273.

Shugar/Mass 2014

A.N. Shugar and J.L. Mass, "Introduction." In: A.N. Shugar and J.L. Mass (eds.), *Handheld XRF for Art and Archaeology*, Ithaca 2014, pp. 17–36.

Simpson 1996

S.J. Simpson, "From Tekrit to the Jaghjagh: Sasanian sites, settlements patterns and material culture in Northern Mesopotamia." In: K. Bartl and S.R. Hauser (eds.), *Continuity and Change in Northern Mesopotamia from the Hellenistic to the Early Islamic Period*, Berlin 1996, pp. 87–126.

Sissakian/Saeed 2012

V.K. Sissakian and Z.B. Saeed, "Lithological map of Iraq, compiled using GIS techniques." *Iraqi Bulletin of Geology and Mining* 8 (2012), pp. 1–13.

Sissakian/Al-Ansari/Knutsson 2014

V.K. Sissakian, N. Al-Ansari, and S. Knutsson, "Origin of some transversal linear features of NE-SW trend in Iraq, and their geological characters." *Natural Science* 6 (2014), pp. 996–1011. DOI: 10.4236/ns.2014.612091.

Sissakian et al. 2016

V.K. Sissakian, A.A. Ahad, N. Al-Ansari, and S. Knutsson, "Geology of the archeological hills and monuments: Examples from Iraq." *Journal of Earth Sciences and Geotechnical Engineering* 6 (2016), pp. 1–28. <http://www.diva-portal.org/smash/record.jsf?pid=diva2:985804>.

Speakman/Little/Creel 2011

R.J. Speakman, N.C. Little, and D. Creel, "Sourcing ceramics with portable XRF spectrometers? A comparison with INAA using mimbres pottery from the American Southwest." *Journal of Archaeological Science* 38 (2011), pp. 3483–3496.

Stele et al. 2019

A. Stele, J.W.E. Fassbinder, J.W. Härtling, J. Bussmann, J. Schmidt, and C. Zielhofer, "Genesis of magnetic anomalies and magnetic properties of archaeological sediments in floodplain wetlands of the Fossa Carolina." *Archaeo-*

logical Prospection 27 (2019), pp. 169–180. DOI: 10.1002/arp.1761.

Stele et al. 2023

A. Stele, L. Kaub, R. Linck, M. Schikorra, and J.W.E. Fassbinder, "Drone-based magnetometer prospection for archaeology." *Journal of Archaeological Science* 158 (2023), 105818. DOI: 10.1016/j.jas.2023.105818.

Stephani 1991

M. Stephani, "Zur topographischen Aufnahme und Geländedarstellung von Assur." *Mitteilungen der Deutschen Orient-Gesellschaft zu Berlin* 123 (1991), pp. 115–122.

Stone 2023

D.L. Stone, "Review of S. Ritter and S. Ben Tahar (eds.), *Studies on the Urban History of Meninx (Djerba): The Meninx Archaeological Project 2015–2019*, Wiesbaden 2022." *American Journal of Archaeology* 127 (2023), pp. E114–E116. DOI: 10.1086/727121.

Tabachnick/Fidell 2013

B.G. Tabachnick and L.S. Fidell, *Using Multivariate Statistics*, Boston 2013.

Tadmor/Yamada 2011

H. Tadmor and S. Yamada, *The Royal Inscriptions of Tiglath-pileser III (744–727 BC) and Shalmaneser V (726–722 BC), Kings of Assyria* (Royal Inscriptions of the Neo-Assyrian Period 1), Winona Lake IN 2011.

Tipler et al. 2019

P.A. Tipler, G. Mosca, P. Kersten, and J. Wagner, *Physik*, Berlin/Heidelberg 2019.

van der Plicht 2004

J. van der Plicht, "Radiocarbon, the calibration curve and Scythian chronology." In: E.M. Scott, A.Y. Alekseev, and G. Zaitseva (eds.), *Impact of the Environment on Human Migration in Eurasia*, Amsterdam 2004, pp. 45–61.

van Wyk/Wink/Wink 2004

B.E. van Wyk, C. Wink, and M. Wink, *Handbuch der Arzneipflanzen: ein illustrierter Leitfaden*, Stuttgart 2004.

van Zeist/Bakker-Heeres 1982

W. van Zeist and J.A.H. Bakker-Heeres, "Archaeobotanical Studies in the Levant, 1: Neolithic sites in the Damascus basin: Aswad, Ghoraife, Ramad." *Palaeohistoria* 24 (1982), pp. 165–256.

van Zeist/Bakker-Heeres 1984a

W. van Zeist and J.A.H. Bakker-Heeres, "Archaeobotanical studies in the Levant, 2: Neolithic and Halaf levels at Ras Shamra." *Palaeohistoria* 26 (1984), pp. 151–170.

van Zeist/Bakker-Heeres 1984b

W. van Zeist and J.A.H. Bakker-Heeres, "Archaeobotanical studies in the Levant, 3: Late-Palaeolithic Mureybit." *Palaeohistoria* 26 (1984), pp. 171–199.

van Zeist/Bakker-Heeres 1985

W. van Zeist and J.A.H. Bakker-Heeres, "Archaeobotanical studies in the Levant, 4: Bronze Age sites on the North Syrian Euphrates." *Palaeohistoria* 27 (1985), pp. 247–316.

Vilders 1991

M. Vilders, "Some technological features of the Late Bronze and Iron Age cooking pots from Tell es-Sa'idiyeh, Jordan." *Newsletter: Department of Pottery Technology* 9/10, pp. 69–81.

von der Osten 1939

H.H. von der Osten, *Ancient Oriental Seals in the Collection of Mr Edward T. Newell*, Chicago 1934.

Weissbach 1934

F.H. Weissbach, "Review of G. Martiny, *Die Kultrichtung*

in Mesopotamien, Berlin 1932." *Orientalistische Literaturzeitung* 37 (1934), pp. 218–232.

Wichtl 2009

M. Wichtl, *Teedrogen und Phytopharmaka*, Stuttgart 2009.

Wilkinson/Deckers 2015

T.J. Wilkinson and K. Deckers, "The regional setting of Jerablus Tahtani." In: E. Peltenburg, D. Bolger, S. Campbell, S. Colledge, and P. Croft (eds.), *Tell Jerablus Tahtani, Syria, I: Mortuary Practices at an Early Bronze Age Fort on the Euphrates River*, Oxford 2015, pp. 13–23.

Wilke/Rauch/Rauch 2016

D. Wilke, D. Rauch, and P. Rauch, "Is non-destructive provenancing of pottery possible with just a few discriminative trace elements?" *Science & Technology of Archaeological Research* 2 (2016), pp. 141–158.

Willerding 1986

U. Willerding, *Zur Geschichte der Unkräuter Mitteleuropas*, Neumünster 1986.

Zar 2010

J.H. Zar, *Biostatistical Analysis*, Upper Saddle River 2010.